

Systematic Palaeontology and Palaeobiogeography of Mamenchisaurid Dinosaurs
in Thailand

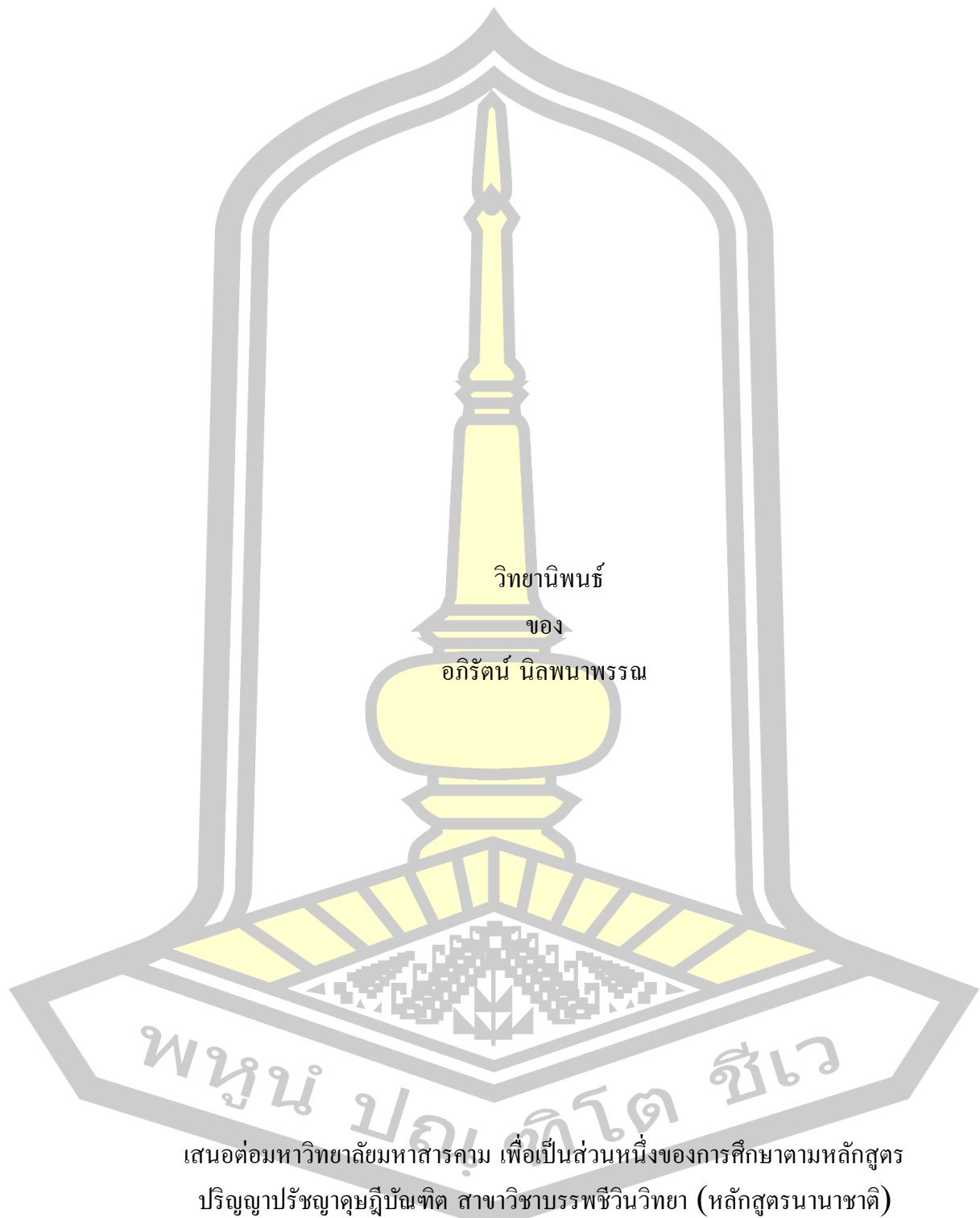
Apirut Nilpanapan

A Thesis Submitted in Partial Fulfillment of Requirements for
degree of Doctor of Philosophy in Palaeontology (International Program)

June 2024

Copyright of Mahasarakham University

ซิสเต็มมาดิกส์และชีวภูมิศาสตร์บรรพกาล ของไดโนเสาร์กลุ่มมาเมนซิซอริคในประเทศไทย



เสนอต่อมหาวิทยาลัยมหาสารคาม เพื่อเป็นส่วนหนึ่งของการศึกษาตามหลักสูตร
ปริญญาปรัชญาดุษฎีบัณฑิต สาขาวิชาบรรพชีวินวิทยา (หลักสูตรนานาชาติ)

มิถุนายน 2567

ลิขสิทธิ์เป็นของมหาวิทยาลัยมหาสารคาม

Systematic Palaeontology and Palaeobiogeography of Mamenchisaurid Dinosaurs
in Thailand

Apirut Nilpanapan

พหุบัณฑิต

A Thesis Submitted in Partial Fulfillment of Requirements
for Doctor of Philosophy (Palaeontology (International Program))

June 2024

Copyright of Mahasarakham University



The examining committee has unanimously approved this Thesis, submitted by Mr. Apirut Nilpanapan , as a partial fulfillment of the requirements for the Doctor of Philosophy Palaeontology (International Program) at Mahasarakham University

Examining Committee

Chairman

(Asst. Prof. Rattanaphorn Hanta ,
Ph.D.)

Advisor

(Assoc. Prof. Komsorn Lauprasert ,
Ph.D.)

Committee

(Asst. Prof. Sakboworn
Tumpeesuwan , Ph.D.)

Committee

(Asst. Prof. Uthumporn Deesri ,
Ph.D.)

External Committee

(Phornphen Chanthasit , Ph.D.)

Mahasarakham University has granted approval to accept this Thesis as a partial fulfillment of the requirements for the Doctor of Philosophy Palaeontology (International Program)

(Prof. Pairot Pramual , Ph.D.)
Dean of The Faculty of Science

(Assoc. Prof. Krit Chaimoon , Ph.D.)
Dean of Graduate School

| | | | |
|-------------------|---|--------------|--|
| TITLE | Systematic Palaeontology and Palaeobiogeography of Mamenchisaurid Dinosaurs in Thailand | | |
| AUTHOR | Apirut Nilpanapan | | |
| ADVISORS | Associate Professor Komsorn Lauprasert , Ph.D. | | |
| DEGREE | Doctor of Philosophy | MAJOR | Palaeontology (International Program) |
| UNIVERSITY | Maharakham University | YEAR | 2024 |

ABSTRACT

Mamenchisauridae constitutes a diverse and widespread sauropod fauna in the Middle to Late Jurassic of East Asia. Recent studies represent the occurrence of the clade in the Southeast Asia and East Africa. The spatiotemporal distribution of the clade to the Early Cretaceous but less diverse in the Jurassic. In Thailand, there are reports of the isolated teeth of Mamenchisauridae sauropods from northeastern and the incomplete dorsal vertebra from Krabi province. Here, the 170 isolated cranial and postcranial specimens of Mamenchisauridae sauropods from the Upper Jurassic assemblage Phu Noi locality, Kalasin Province, Northeastern Thailand, which is interpreted as the part of Lower Phu Kradung Formation has been studied. From the description and comparison, the locality has yielded at least four types of Mamenchisauridae sauropods, which correlated to the Late Jurassic Southwestern and Northwestern China taxa and one distinct taxon from the posterior skull roof and two dorsal vertebrae. Moreover, phylogenetic affinity of Phu Noi taxa is distinct from previously reported Phu Dan Ma taxon from the Upper Phu Kradung locality. Other Phu Noi mamenchisaurid types are resembled to the Lower and Upper Shaximiao Formation which could be interpreted that the Lower Phu Kradung Formation is the Callovian to Oxfordian in spatiotemporal age instead of Tithonian to Berriasian, which previously dated by the key Early Cretaceous palynomorph. The Shaximiao mamenchisaurids dispersed to Indochina terrane and surviving through the temporal time scale to the entire present age of Phu Kradung Formation, which related to Phu Dan Ma taxon, Upper Phu Kradung Formation, Kalasin province.

Keyword : Late Jurassic, Mamenchisauridae, Phu Kradung Formation, Phu Noi locality, Southeast Asia

ACKNOWLEDGEMENTS

I would like to express my deepest gratitude to my advisor, Associate Professor Dr. Komsorn Lauprasert for the guidance, and empathy along the fulfillment of the dissertation. Words cannot express my gratitude to the Chairman, Assistant Professor Dr. Rattanaphorn Hanta for accepting the chairman invitation and quality commentation.

I'm extremely grateful to Dr. Phornphen Chanthasit for empathy, the understanding the struggle along the research and the providing of the Materials from the collection of Sirindhorn Museum.

I would like to extend my sincere thanks to Assistant Professor Dr. Uthumporn Deesri for the instruction in the osteology of vertebrates and suggestion for the research methods in palaeontology, Assistant Professor Dr. Sukboworn Tumpeesuwan for the empathy and the grateful guidance on the thesis.

I am grateful to all staff of the Palaeontological Research and Education Centre of Mahasarakham University, Sirindhorn Museum, Department of Mineral Resources.

I would like to extend my sincere thanks to Dr. Varavudh Suteethorn and all staffs who have taken part in the excavation of the Mesozoic vertebrate in Thailand.

Finally, this thesis is dedicated to my family for their love and supporting me during the long journey of my life.

Apirut Nilpanapan

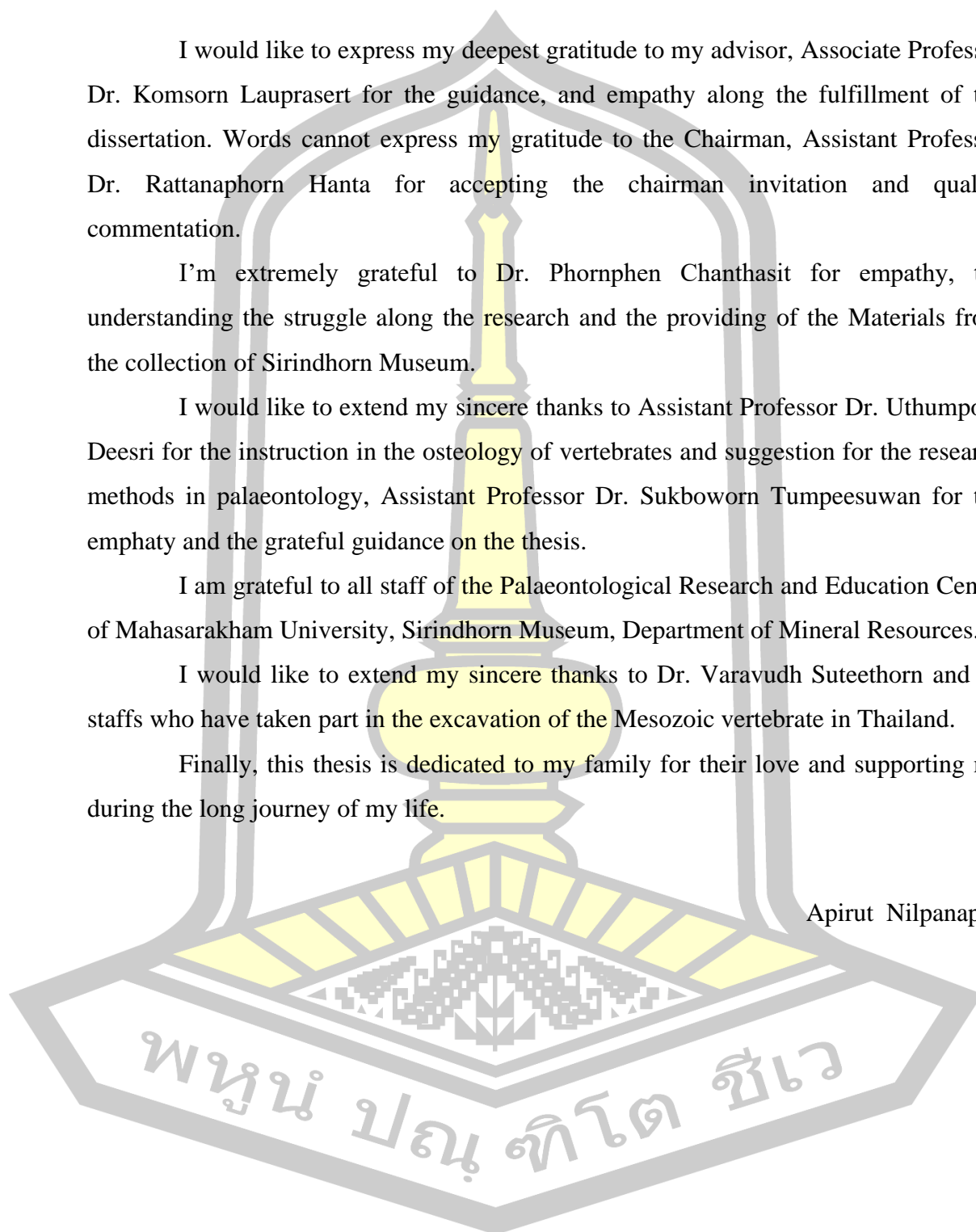


TABLE OF CONTENTS

| | Page |
|--|-------------|
| ABSTRACT..... | D |
| ACKNOWLEDGEMENTS..... | E |
| TABLE OF CONTENTS..... | F |
| LIST OF TABLES..... | I |
| LIST OF FIGURES | J |
| CHAPTER 1 INTRODUCTION | 1 |
| 1.1 Rational of the research | 1 |
| 1.2 Objectives | 2 |
| 1.3 Scope of the research | 2 |
| 1.4 Significance of the research..... | 2 |
| 1.5 plans of the research | 3 |
| CHAPTER 2 LITERATURE REVIEW | 4 |
| 2.1 Introduction to Dinosaurs | 4 |
| 2.2 Introduction to Sauropod | 7 |
| 2.3 Phylogeny of Sauropod..... | 14 |
| 2.4 Mamenchisauridae sauropod | 16 |
| 2.5 The discovery of Mamenchisauridae Sauropods outside China..... | 20 |
| 2.6 The discovery of Sauropod dinosaur in Thailand..... | 27 |
| CHAPTER 3 MATERIAL AND METHOD | 30 |
| 3.1 Geological setting | 30 |
| 3.2 Materials | 32 |
| 3.3 Methods | 32 |
| 3.3.1 Descriptions and comparisons..... | 32 |
| 3.3.2 Preliminary phylogenetic analysis..... | 32 |
| 3.4 Institutional abbreviations..... | 33 |

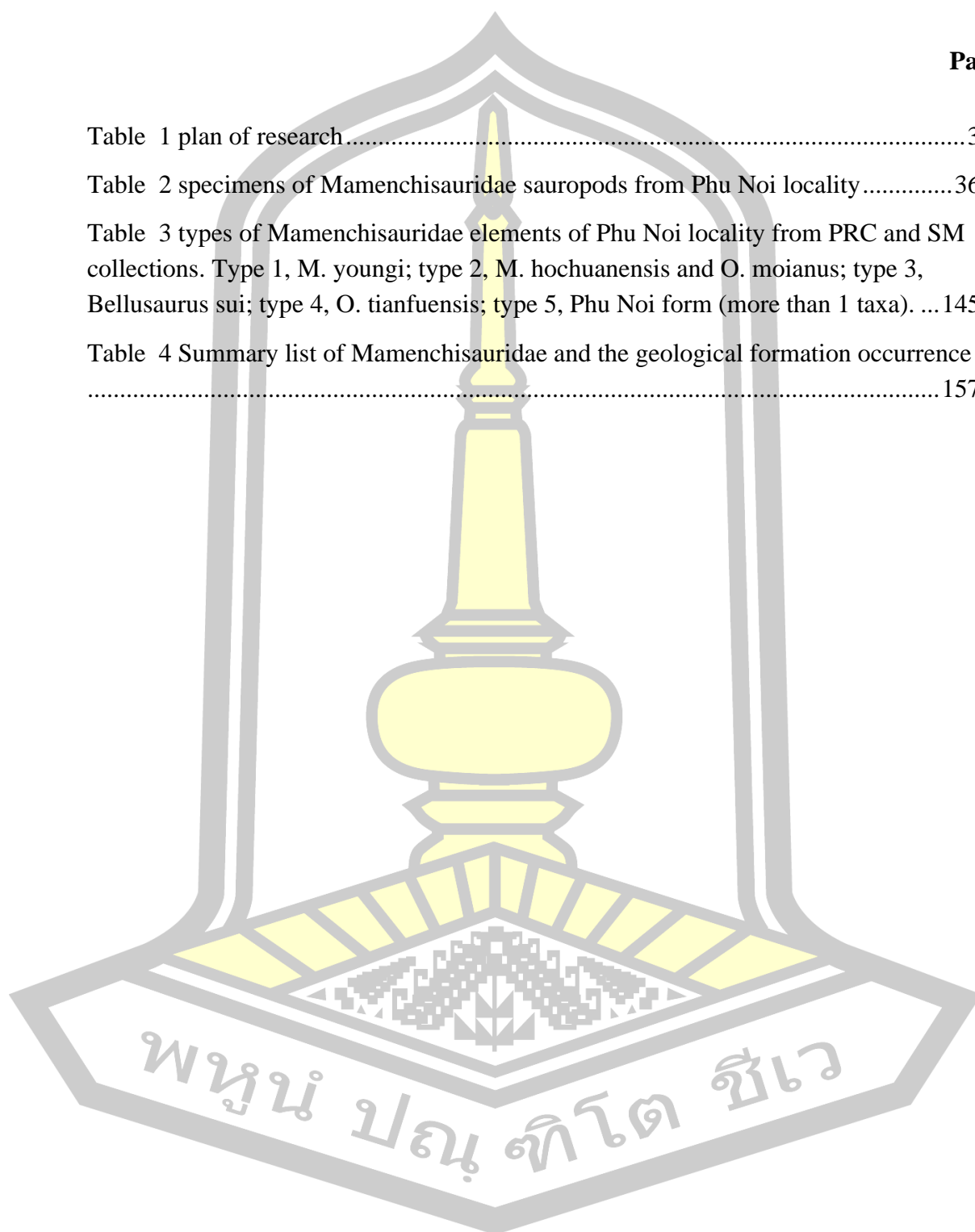
| | |
|--|-----|
| 3.5 Anatomical abbreviation..... | 33 |
| 3.5.1 Cranial element..... | 33 |
| 3.5.2 Axial skeleton..... | 34 |
| 3.3.3 Appendicular skeleton..... | 35 |
| 3.3.4 Other abbreviation..... | 35 |
| CHAPTER 4 RESULTS | 42 |
| 4.1 Descriptions and Comparison..... | 42 |
| 4.1.1 Cranial materials..... | 42 |
| Premaxillae | 42 |
| Nasal 48 | |
| Frontal-parietal | 48 |
| Occipital | 56 |
| Lachrymal..... | 62 |
| Jugal 64 | |
| Postorbitals | 67 |
| Squamosal | 70 |
| Quadratojugal | 74 |
| Dentary | 75 |
| Teeth 82 | |
| 4.1.2 Postcranial Elements | 88 |
| Cervical vertebrae..... | 88 |
| Anterior to middle cervical vertebra..... | 88 |
| Middle cervical vertebrae..... | 90 |
| Posterior cervical vertebrae..... | 94 |
| Cervical ribs..... | 98 |
| Dorsal vertebrae..... | 102 |
| Anterior dorsal vertebrae..... | 103 |
| Middle to posterior dorsal vertebrae | 108 |
| Anterior dorsal ribs..... | 119 |

| | |
|--|-----|
| Caudal vertebrae | 120 |
| Anterior caudal vertebrae | 121 |
| Middle caudal vertebrae | 124 |
| Posterior caudal vertebrae | 128 |
| Distal caudal vertebrae | 129 |
| Chevron (haemal arch) | 130 |
| Pectoral girdle..... | 134 |
| Scapula and scapulocoracoid..... | 134 |
| Forelimb | 137 |
| Humerus | 137 |
| Pubic girdle..... | 139 |
| Ilium 140 | |
| pubis 141 | |
| 4.2 Summary of comparison..... | 142 |
| 4.3 Preliminary phylogenetic analysis and implications | 146 |
| CHAPTER 5 DISCUSSION AND CONCLUSION | 151 |
| 5.1 Diversity of Mamenchisauridae sauropods from the Phu Noi locality..... | 151 |
| 5.2 Systematic palaeontology | 152 |
| 5.3 Palaeobiogeography of Mamenchisauridae sauropods..... | 153 |
| 5.4 Conclusion | 155 |
| REFERENCES | 163 |
| APPENDIX..... | 170 |
| BIOGRAPHY | 233 |

พูน ปณ ทิโต ชีเว

LIST OF TABLES

| | Page |
|---|------|
| Table 1 plan of research | 3 |
| Table 2 specimens of Mamenchisauridae sauropods from Phu Noi locality | 36 |
| Table 3 types of Mamenchisauridae elements of Phu Noi locality from PRC and SM collections. Type 1, <i>M. youngi</i> ; type 2, <i>M. hochuanensis</i> and <i>O. moianus</i> ; type 3, <i>Bellusaurus sui</i> ; type 4, <i>O. tianfuensis</i> ; type 5, Phu Noi form (more than 1 taxa). ... | 145 |
| Table 4 Summary list of Mamenchisauridae and the geological formation occurrence | 157 |



LIST OF FIGURES

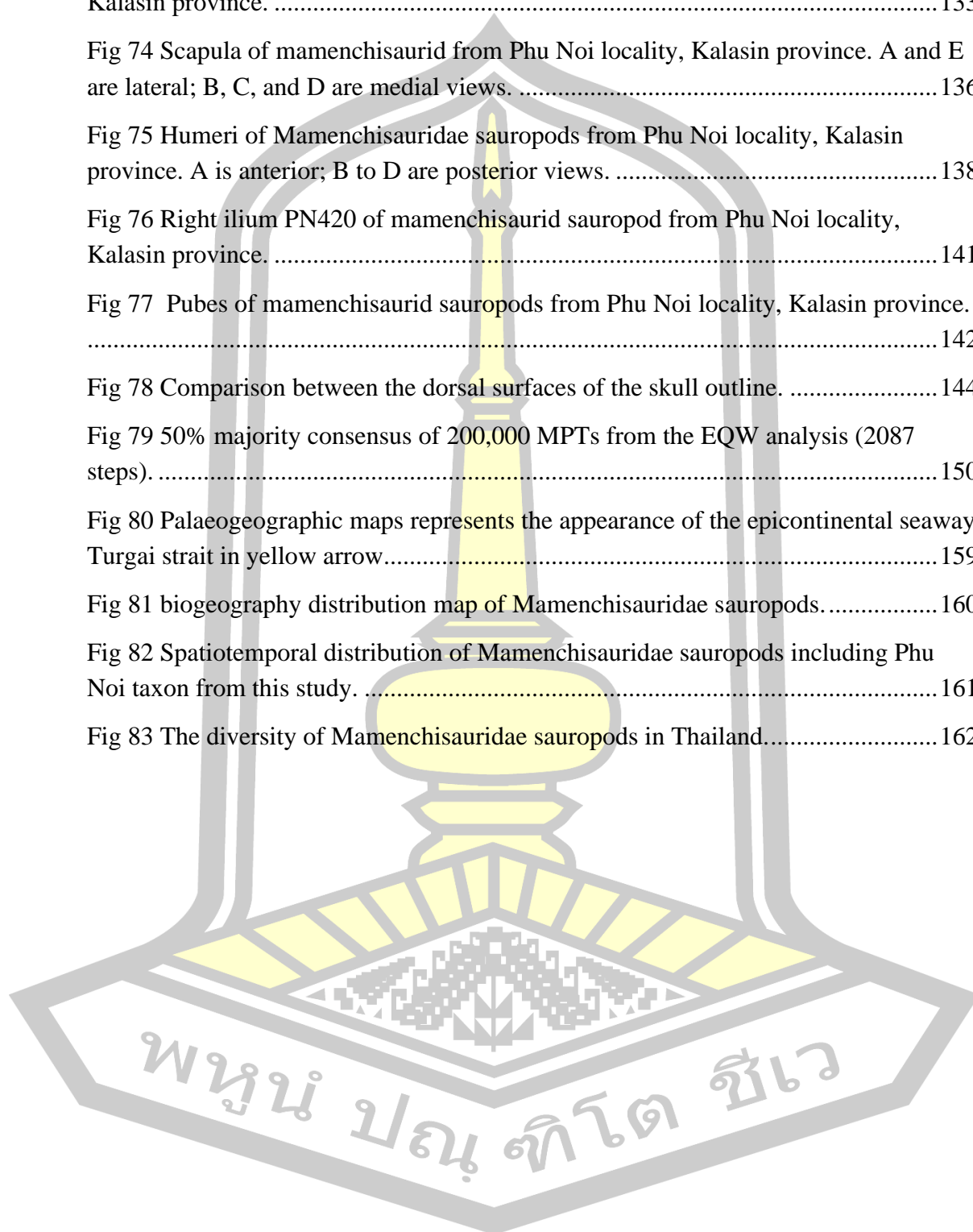
| | Page |
|---|------|
| Fig 1 Skull of reptile. A, Anapsid. B, Synapsid. C, Diapsid. (modified from Fastovsky and Weishampel, 2017) | 4 |
| Fig 2 Ankle bones of reptiles. A, Crurotarsi. B, Ornithodiran. (modified from Fastovsky and Weishampel, 2017) | 5 |
| Fig 3 Characteristics of dinosaurs. A, elongate deltopectoral crest. B, perforate acetabulum. C, fibula contact $\leq 30\%$ of astragalus. D, epiphyses on cervical vertebrae. E, asymmetrical fourth trochanter on femur (modified from Fastovsky and Weishampel 2017) | 6 |
| Fig 4 phylogeny of Diapsid reptiles (modified from Lucas 2016). | 6 |
| Fig 5 size comparison of sauropods dinosaurs with modern mammal (Human, Elephant and Blue whale). (modified from Hallett and Wedel 2016) | 8 |
| Fig 6 the skull of sauropod Giraffatitan brancai and the features of skull. (1) nasal, (2) frontal, (3) quadratojugal, (4) jugal, (5) articular, (6) maxilla, (7) premaxilla, (8) dentary, (9) sclerotic ring, (10) prefrontal, (11) orbital fenestra, (12) external naris, (13) coronoid process, (14) angular, (15) postorbital, (16) parietal, (17) quadrate, (18) pterygoid, (19) basioccipital, (20) lacrimal, (21) surangular, (22) antorbital fenestra, (23) infratemporal fenestra, (24) narial fenestra (modified from Hallett and Wedel 2016) | 9 |
| Fig 7 Skulls of sauropod the left is Diplodocus and the right is Camarasaurus | 10 |
| Fig 8 Dorsal vertebra of Apatosaurus, Diplodocidae sauropod. | 11 |
| Fig 9 Types of centrum joint of Sauropod vertebra. Procoelous, Opisthocoelous and Amphicoelous (Modified from Lucas 2016) | 12 |
| Fig 10 Axial sections of sauropod vertebrae showing pneumatic features. a) Haplocanthosaurus priscus. b), Camarasaurus sp. c), Saltasaurus loricatus | 13 |
| Fig 11 Forefoot and hindfoot of sauropod. (modified from Fastovsky and Weishampel 2017) | 14 |
| Fig 12 phylogeny of dinosaurs. (modified from Baron et al., 2018) | 15 |
| Fig 13 Evolution of vertebral pneumatic structures in sauropods | 16 |
| Fig 14 skeleton reconstruction of Mamenchisaurus youngi.(modified from Paul 2016) | 17 |

| | |
|---|----|
| Fig 15 skull of <i>Mamenchisaurus youngi</i> . (modified from Pi, Ou and Ye 1996) | 18 |
| Fig 16 vertebra of <i>Mamenchisaurus</i> sp. Anterior (top), left lateral (middle), and posterior (bottom) views of anterior cervical (cv 9), posterior cervical (cv 17), anterior dorsal (dv 2), posterior dorsal (dv 8), and anterior caudal (ca 1) vertebrae. (modified from Wilson et al. 2011) | 19 |
| Fig 17 cervical vertebra of mamenchisauridae sauropod from Phu Dan Ma, Kalasin province. (Suteethorn et al., 2013)..... | 22 |
| Fig 18 first caudal vertebra and teeth of mamenchisauridae sauropod from Middle Jurassic Itat Formation of the Berezovsk coal mine, Krasnoyarsk (Averianov et al. 2019) | 23 |
| Fig 19 series of <i>Wamweracaudia keranjei</i> caudal vertebrae. (Mannion et al. 2019)... | 25 |
| Fig 20 Time-calibrated phylogenetic agreement subtree, based on equal weights analysis. Taxon ranges include both true stratigraphic range and uncertainty. (Mannion et al. 2019)..... | 26 |
| Fig 21 Map of northeast Thailand showing the distribution of Khorat group geological strata. (modified from Wongko et al. 2011) | 28 |
| Fig 22 Lithostratigraphic column and dinosaur ichnofauna of the Khorat Group | 29 |
| Fig 23 Bone map of Phu Noi locality, Kham Muang District, Kalasin Province, Thailand. | 31 |
| Fig 24 Premaxillae of Mamenchisauridae sauropods from Phu Noi locality, Kalasin province..... | 44 |
| Fig 25 The left premaxilla KS34-1766. | 45 |
| Fig 26 The right premaxilla KS34-2199..... | 47 |
| Fig 27 Nasals of Mamenchisauridae sauropod from Phu Noi locality, Kalasin province..... | 48 |
| Fig 28 Frontal and frontal-parietals of Mamenchisauridae sauropods from Phu Noi locality, Kalasin province. | 50 |
| Fig 29 Mamenchisauridae sauropod right frontal-parietal PN19-31 from Phu Noi locality, Kalasin province. | 52 |
| Fig 30 The comparison of frontal-parietals from Phu Noi locality, Kalasin province with <i>Bellusaurus sui</i> (V17768.7) and <i>Qijianglong guokr</i> (QJGPM 1001). | 55 |
| Fig 31 Mamenchisauridae occipital PN14-139 from Phu Noi locality, Kalasin province..... | 58 |

| | |
|---|----|
| Fig 32 Comparison of Eusauropoda occipitals to Phu Noi specimens. All of illustrations are posterior view (not to scale)..... | 61 |
| Fig 33 Exoccipitals of Mamenchisauridae sauropods from Phu Noi locality, Kalasin province..... | 62 |
| Fig 34 Left lachrymal KS34-1226. | 63 |
| Fig 35 Jugals of Mamenchisauridae sauropods from Phu Noi locality, Kalasin province..... | 66 |
| Fig 36 Mamenchisaurus youngi like left jugals KS34-1387. | 67 |
| Fig 37 Right postorbital KS34-1492..... | 68 |
| Fig 38 Postorbitals of Mamenchisauridae sauropods from Phu Noi locality, Kalasin province..... | 69 |
| Fig 39 Squamosals of Mamenchisauridae sauropods from Phu Noi locality, Kalasin province..... | 70 |
| Fig 40 Two representatives of the squamosal of Mamenchisauridae sauropods from Phu Noi locality. | 72 |
| Fig 41 Right squamosal of Bellusaurus sui (IVPP V17768.8). Modified from Moore et al., 2018..... | 73 |
| Fig 42 Quadratojugals of Mamenchisauridae sauropods from Phu Noi locality, Kalasin province. | 75 |
| Fig 43 Dentaries of Mamenchisauridae sauropods from SM collection, Phu Noi locality, Kalasin province. | 76 |
| Fig 44 Dentaries of Mamenchisauridae sauropods from PRC collection, Phu Noi locality, Kalasin province. | 78 |
| Fig 45 Representative dentary KS34-1572 (left)..... | 79 |
| Fig 46 The dentary of Mamenchisauridae. | 81 |
| Fig 47 Isolated anterior teeth of Mamenchisauridae sauropods from PRC collection, Phu Noi locality, Kalasin province. | 83 |
| Fig 48 Isolated anterior teeth of Mamenchisauridae sauropods from SM collection, Phu Noi locality, Kalasin province. | 84 |
| Fig 49 Isolated middle teeth of Mamenchisauridae sauropods from PRC collection, Phu Noi locality, Kalasin province. | 85 |
| Fig 50 Isolated middle teeth of Mamenchisauridae sauropods from SM collection, Phu Noi locality, Kalasin province. | 86 |

| | |
|--|-----|
| Fig 51 Isolated posterior teeth of Mamenchisauridae sauropods from SM collection, Phu Noi locality, Kalasin province. | 87 |
| Fig 52 Anterior to middle cervical centrum of Mamenchisauridae sauropod from Phu Noi locality PN17-47. | 90 |
| Fig 53 Middle cervical vertebrae of Mamenchisauridae sauropods from Phu Noi locality, Kalasin province. | 91 |
| Fig 54 No number neural arch from Phu Noi locality. | 93 |
| Fig 55 Middle cervical vertebra from Phu Noi locality PN 602..... | 95 |
| Fig 56 Posterior cervical centrum and neural arch PN15-123..... | 96 |
| Fig 57 No number posterior cervical neural arch. | 97 |
| Fig 58 Three posterior most cervical elements of mamenchisaurid sauropods from Phu Noi locality. | 100 |
| Fig 59 Cervical ribs of mamenchisaurid sauropods from Phu Noi locality..... | 102 |
| Fig 60 three anterior dorsal elements of mamenchisaurid sauropods from Phu Noi locality..... | 106 |
| Fig 61 Anterior cervical vertebra PN581..... | 107 |
| Fig 62 Middle to posterior dorsal elements of mamenchisaurid sauropods from Phu Noi locality..... | 110 |
| Fig 63 Middle dorsal vertebra PN692..... | 112 |
| Fig 64 Posterior dorsal vertebra PN13-23. | 118 |
| Fig 65 Anterior dorsal ribs of Mamenchisauridae sauropods from Phu Noi locality in anterior view. | 119 |
| Fig 66 Caudal vertebrae of mamenchisaurids from Phu Noi locality..... | 120 |
| Fig 67 PRC anterior caudal vertebra in plaster. Scale bar represents 10 cm. | 122 |
| Fig 68 Anterior caudal vertebra PN14-146..... | 123 |
| Fig 69 Middle caudal series PN14-212A to F. | 126 |
| Fig 70 Y-shape anterior chevrons of sauropods from PRC collection in anterior view. | 131 |
| Fig 71 Middle chevron of Mamenchisauridae sauropods from Phu Noi locality, Kalasin province. | 132 |
| Fig 72 Middle chevron of mamenchisaurid sauropods KS34-2240 from Phu Noi locality, Kalasin province. | 133 |

| | |
|--|-----|
| Fig 73 Posterior Chevron of Mamenchisauridae sauropods from Phu Noi locality, Kalasin province. | 133 |
| Fig 74 Scapula of mamenchisaurid from Phu Noi locality, Kalasin province. A and E are lateral; B, C, and D are medial views. | 136 |
| Fig 75 Humeri of Mamenchisauridae sauropods from Phu Noi locality, Kalasin province. A is anterior; B to D are posterior views. | 138 |
| Fig 76 Right ilium PN420 of mamenchisaurid sauropod from Phu Noi locality, Kalasin province. | 141 |
| Fig 77 Pubes of mamenchisaurid sauropods from Phu Noi locality, Kalasin province. | 142 |
| Fig 78 Comparison between the dorsal surfaces of the skull outline. | 144 |
| Fig 79 50% majority consensus of 200,000 MPTs from the EQW analysis (2087 steps). | 150 |
| Fig 80 Palaeogeographic maps represents the appearance of the epicontinental seaway Turgai strait in yellow arrow..... | 159 |
| Fig 81 biogeography distribution map of Mamenchisauridae sauropods..... | 160 |
| Fig 82 Spatiotemporal distribution of Mamenchisauridae sauropods including Phu Noi taxon from this study. | 161 |
| Fig 83 The diversity of Mamenchisauridae sauropods in Thailand..... | 162 |



CHAPTER 1

INTRODUCTION

1.1 Rational of the research

Sauropod is a clade of gigantic, long neck quadrupedal herbivorous dinosaurs which appeared in the late Triassic period (Buffetaut et al. 2000) and remained an important part of dinosaur fauna until their extinction at the end of the Cretaceous. They achieved a global distribution during the middle Jurassic and attained a high generic-level diversity. More than 120 genera have been proposed (Weishampel et al., 2004). In Thailand, Sauropod's fossils can be generally found in the red bed on the facies of the rocks in the area of northeastern part of Thailand called Khorat group, which is in the Mesozoic era including Triassic, Jurassic and Cretaceous periods (Department of mineral resources ministry of natural resources and environment, 2014). Phu Kradung formation, one of the Khorat group's sub-units which is the late Jurassic to early Cretaceous. It has yielded a rich of vertebrate fauna remains. Two localities, Phu Noi and Phu Dan Ma in Kalasin province, were found numerous sauropod specimens such as elements of skull and many vertebrae which are either articulated skeletal components or isolated bones. Some of them showed specific characteristics of the sauropod family called Mamenchisauridae, the family of Sauropod which is commonly found in China. Mamenchisaurid can be characterized by the shape of supraoccipital and foramen magnum on skull, spatula shape teeth, bifurcate neural spine shape including a small pneumatic camellae structure inside cervical vertebrae and procoelous shape of centrum from anterior caudal vertebrae (Suteethorn, Loeuff, Buffetaut, Suteethorn, & Wongko, 2013). Currently, the remains of these Sauropod fossils, including partial skull and skeleton which were found from Phu Noi locality, are housed at the Sirindhorn Museum and the Palaeontological Research and Education Centre (PRC), Mahasarakham University. The recent work aims to analyze distinctive characters of Phu Kradung Formation's sauropod specimens from both localities comparing with other Mamenchisaurid sauropods by phylogenetic analysis method in order to determine whether the sauropod dinosaur from Thailand is a distinct species.

1.2 Objectives

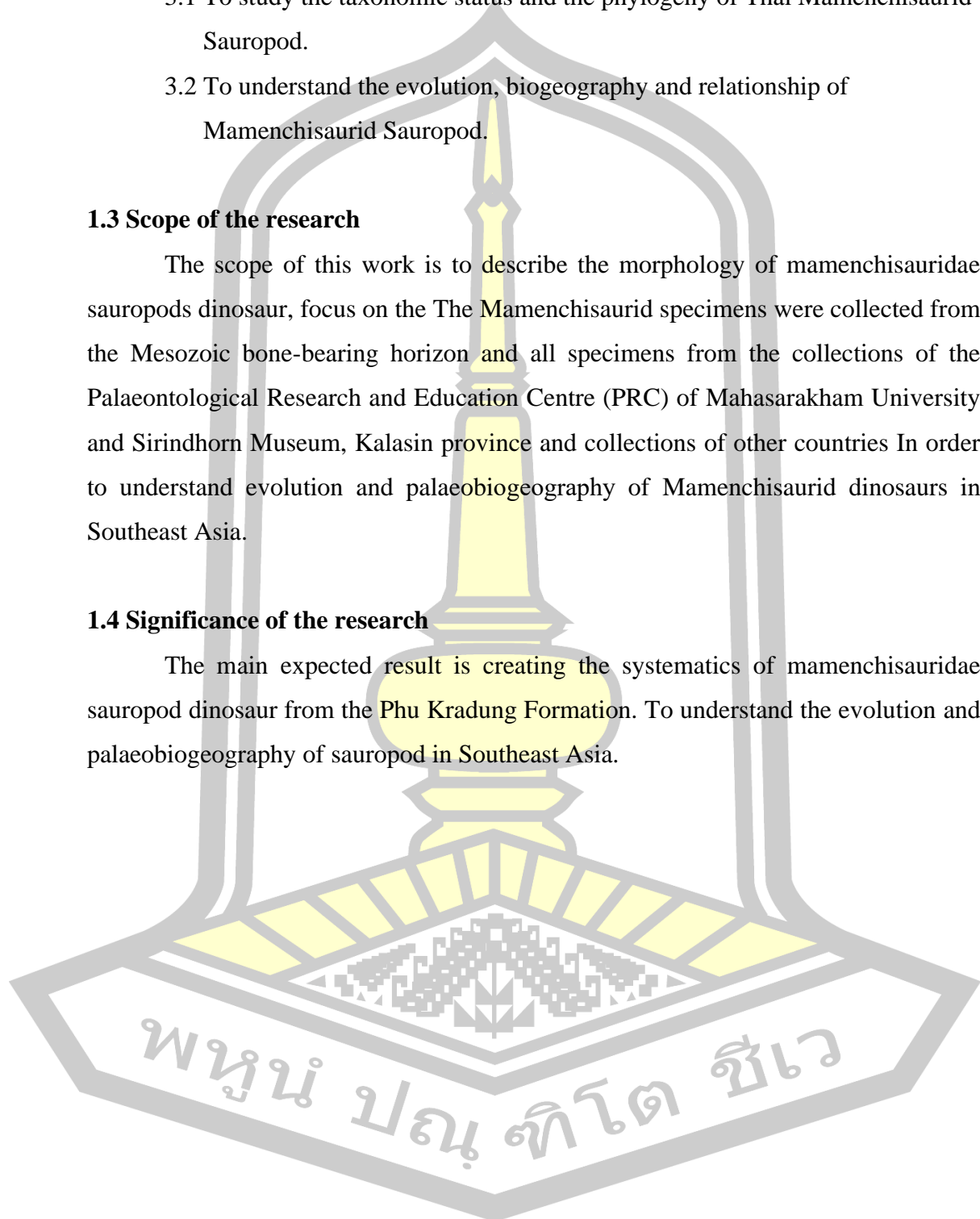
- 3.1 To study the taxonomic status and the phylogeny of Thai Mamenchisaurid Sauropod.
- 3.2 To understand the evolution, biogeography and relationship of Mamenchisaurid Sauropod.

1.3 Scope of the research

The scope of this work is to describe the morphology of mamenchisauridae sauropods dinosaur, focus on the The Mamenchisaurid specimens were collected from the Mesozoic bone-bearing horizon and all specimens from the collections of the Palaeontological Research and Education Centre (PRC) of Mahasarakham University and Sirindhorn Museum, Kalasin province and collections of other countries In order to understand evolution and palaeobiogeography of Mamenchisaurid dinosaurs in Southeast Asia.

1.4 Significance of the research

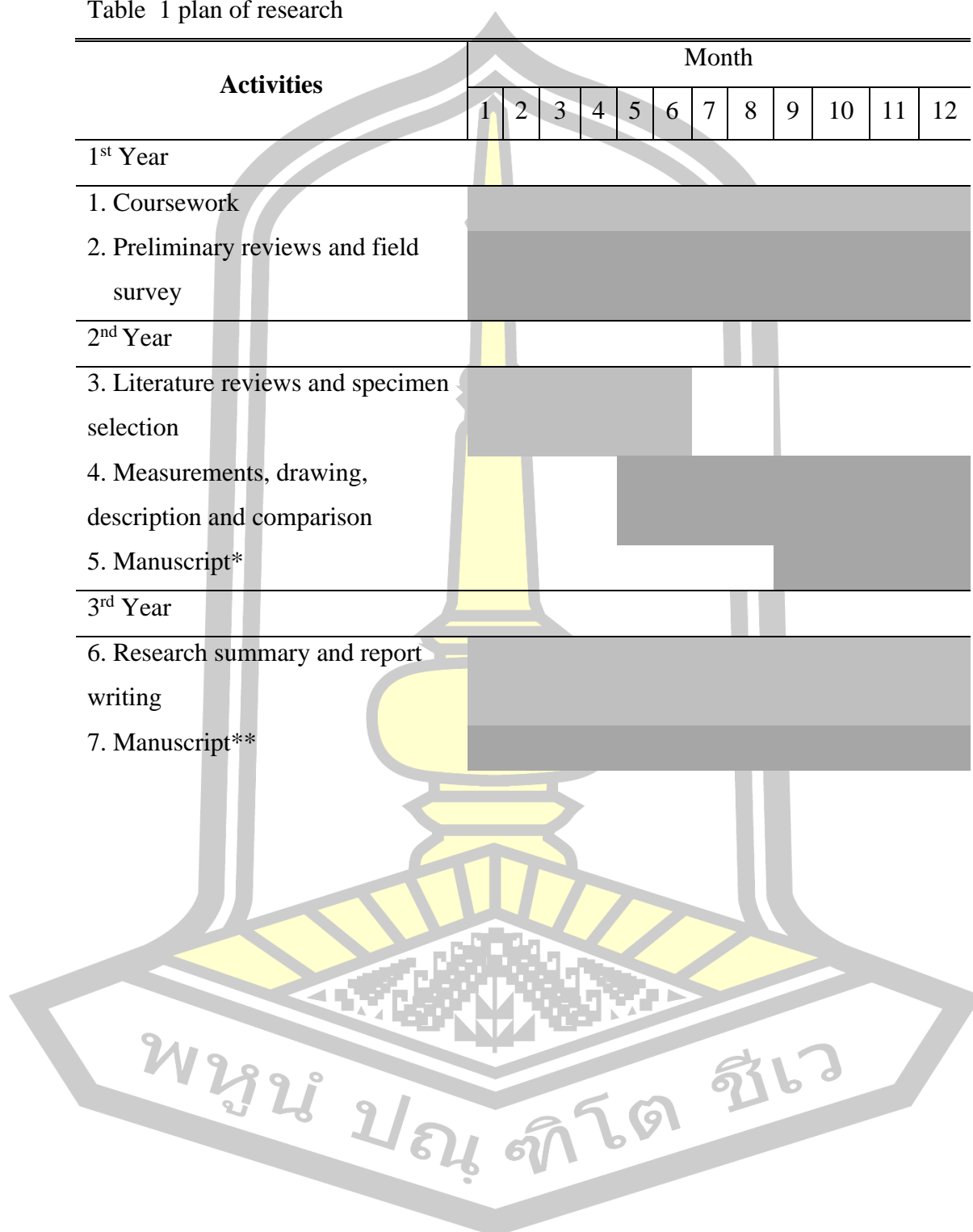
The main expected result is creating the systematics of mamenchisauridae sauropod dinosaur from the Phu Kradung Formation. To understand the evolution and palaeobiogeography of sauropod in Southeast Asia.



1.5 plans of the research

Table 1 plan of research

| Activities | Month | | | | | | | | | | | |
|--|-------|---|---|---|---|---|---|---|---|----|----|----|
| | 1 | 2 | 3 | 4 | 5 | 6 | 7 | 8 | 9 | 10 | 11 | 12 |
| 1 st Year | | | | | | | | | | | | |
| 1. Coursework | | | | | | | | | | | | |
| 2. Preliminary reviews and field survey | | | | | | | | | | | | |
| 2 nd Year | | | | | | | | | | | | |
| 3. Literature reviews and specimen selection | | | | | | | | | | | | |
| 4. Measurements, drawing, description and comparison | | | | | | | | | | | | |
| 5. Manuscript* | | | | | | | | | | | | |
| 3 rd Year | | | | | | | | | | | | |
| 6. Research summary and report writing | | | | | | | | | | | | |
| 7. Manuscript** | | | | | | | | | | | | |



CHAPTER 2

LITERATURE REVIEW

2.1 Introduction to Dinosaurs

Dinosaurs are extinct Diapsid, the subgroup of reptiles classified by the character of two openings on each side of the skull roof behind the orbit called fenestra, consists of Archosaur which has crocodile dinosaur and pterosaur (extinct flying reptile) and Lepidosaur which have Lizard and snake.

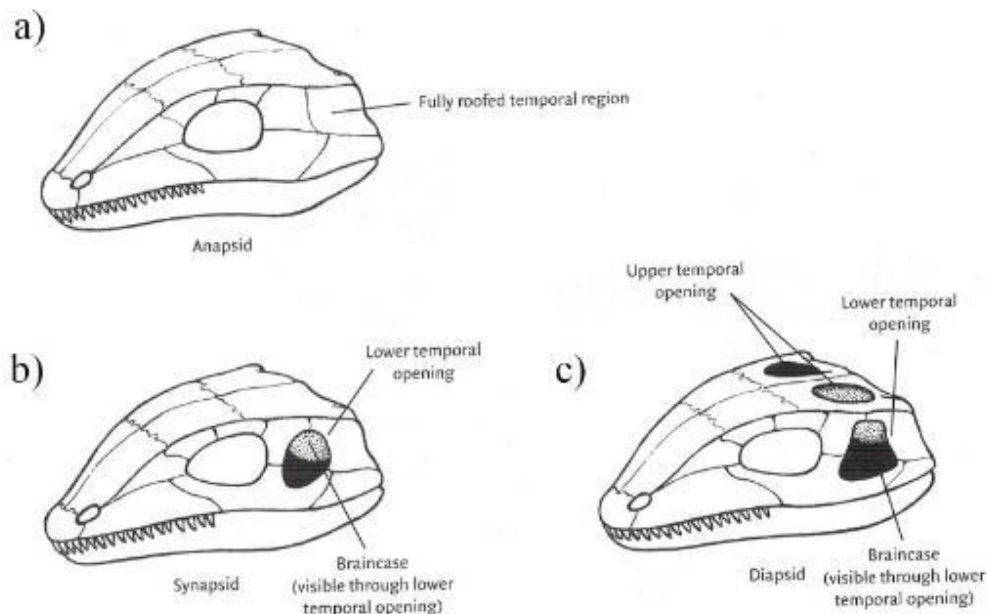


Fig 1 Skull of reptile. A, Anapsid. B, Synapsid. C, Diapsid. (modified from Fastovsky and Weishampel, 2017)

The unique feature that distinguishes dinosaurs from the rest of archosaurs are special type of ankle structure called advanced mesotarsal ankle (AM ankle), the astragalus bone is much larger than the calcaneum and both bones are strictly attached to each other also to the tibia that makes the foot swings backward and forward in a straight line, the subgroup of archosaur which have AM ankle called Ornithodiran.

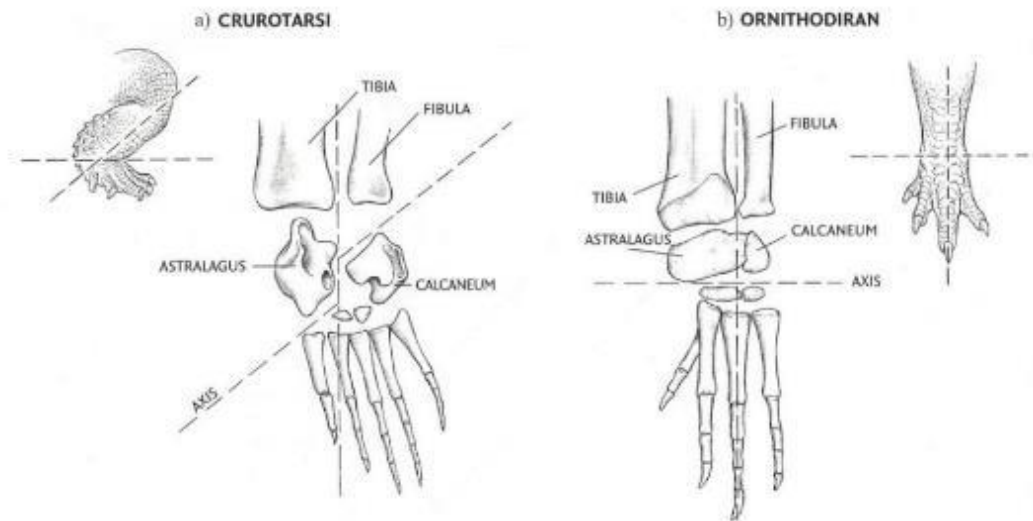


Fig 2 Ankle bones of reptiles. A, Crurotarsi. B, Ornithodiran. (modified from Fastovsky and Weishampel, 2017)

The shapes of dinosaurs pelvis and femur (thigh bone) also contrast with other archosaurs' pelvis, it has the neck-and-ball offset on the barrel-shaped head of the femur attached with the strait pelvis and oriented at approximately 90° made dinosaurs walk in the upright posture while the subgroup of archosaurs called Crurotarsi have crocodile-normal ankle (CN ankle) and broad pelvis that force them to walk in the sprawling posture. Moreover, there are some more derived characters, for instance, the perforate acetabulum (an opening in the hip socket), the present of epiphyses on cervical vertebrae, asymmetrical fourth trochanter on the femur, a well-developed, elongate deltopectoral crest on the humerus (upper arm) nevertheless the oldest dinosaur fossils are of late Triassic age, about 230 to 225 million years old from the Upper Triassic Ischigualasto Formation of Argentina and the last group of dinosaurs were killed by the Asteroid impact and Deccan plateau volcanic eruption about 66 million years ago at the end of Cretaceous period.

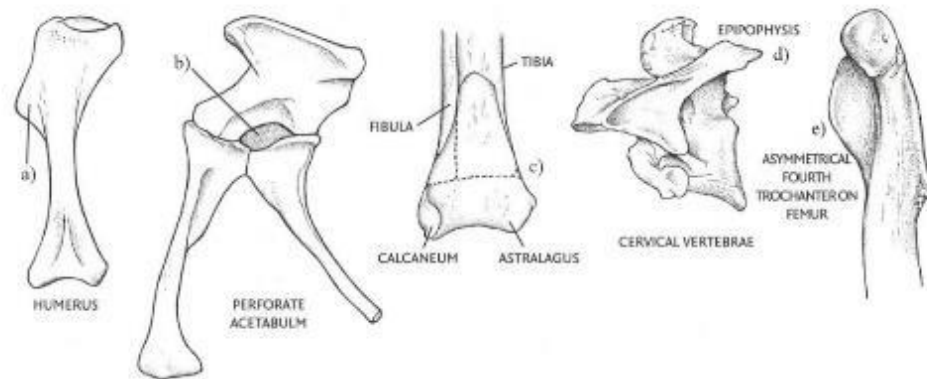


Fig 3 Characteristics of dinosaurs. A, elongate deltopectoral crest. B, perforate acetabulum. C, fibula contact $\leq 30\%$ of astragalus. D, epiphyses on cervical vertebrae. E, asymmetrical fourth trochanter on femur (modified from Fastovsky and Weishampel 2017)

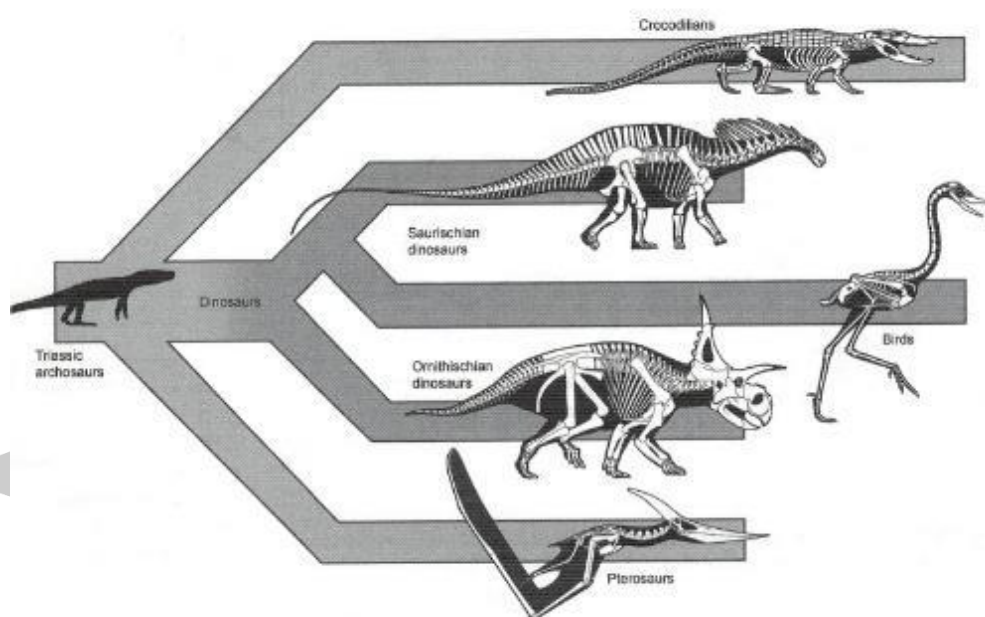
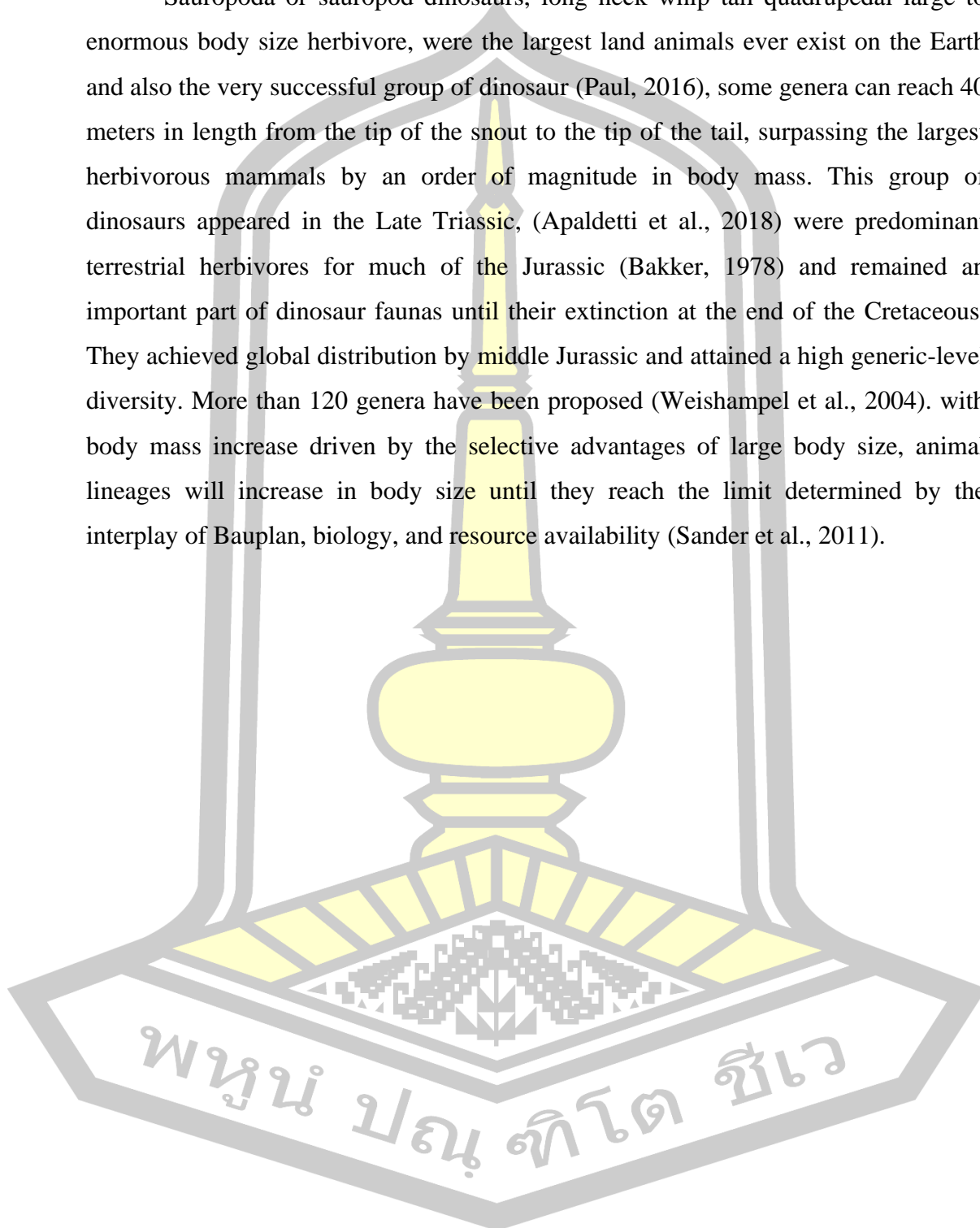


Fig 4 phylogeny of Diapsid reptiles (modified from Lucas 2016).

2.2 Introduction to Sauropod

Sauropoda or sauropod dinosaurs, long neck whip tail quadrupedal large to enormous body size herbivore, were the largest land animals ever exist on the Earth and also the very successful group of dinosaur (Paul, 2016), some genera can reach 40 meters in length from the tip of the snout to the tip of the tail, surpassing the largest herbivorous mammals by an order of magnitude in body mass. This group of dinosaurs appeared in the Late Triassic, (Apaldetti et al., 2018) were predominant terrestrial herbivores for much of the Jurassic (Bakker, 1978) and remained an important part of dinosaur faunas until their extinction at the end of the Cretaceous. They achieved global distribution by middle Jurassic and attained a high generic-level diversity. More than 120 genera have been proposed (Weishampel et al., 2004). with body mass increase driven by the selective advantages of large body size, animal lineages will increase in body size until they reach the limit determined by the interplay of Bauplan, biology, and resource availability (Sander et al., 2011).



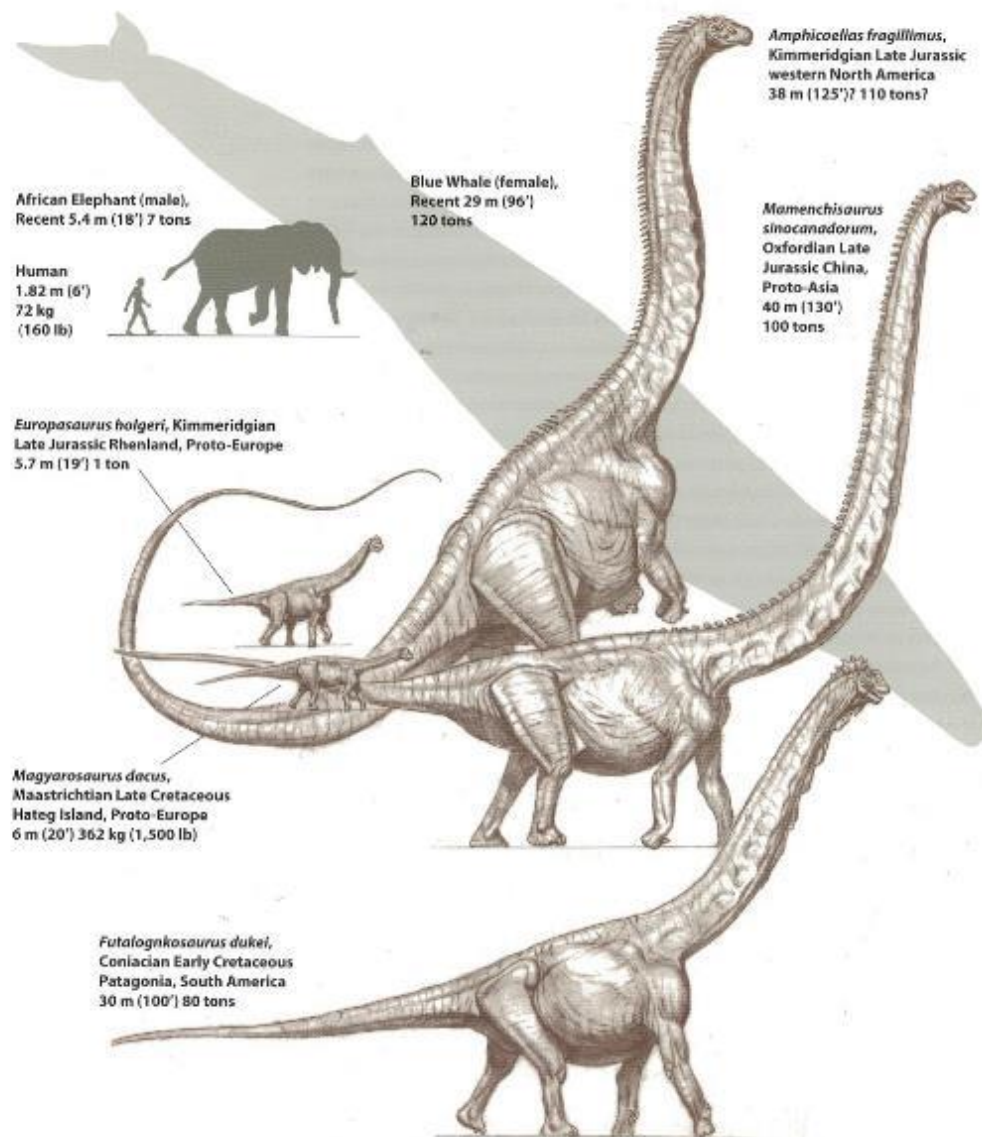


Fig 5 size comparison of sauropod dinosaurs with modern mammal (Human, Elephant and Blue whale). (modified from Hallett and Wedel 2016)

These obligate herbivorous quadrupeds were highly evolved, with many biomechanical adaptations for large size and weight, including four pillar-like limbs and a massive pelvis, a tendency to lighten bones not immediately involved in bodily support functions, and a complex girder-like neck design, tipped by a tiny skull, to increase leverage and decrease weight by the presence of pleurocoels or pneumatic diverticula, hollow space suggestive of avian-style air sacs.

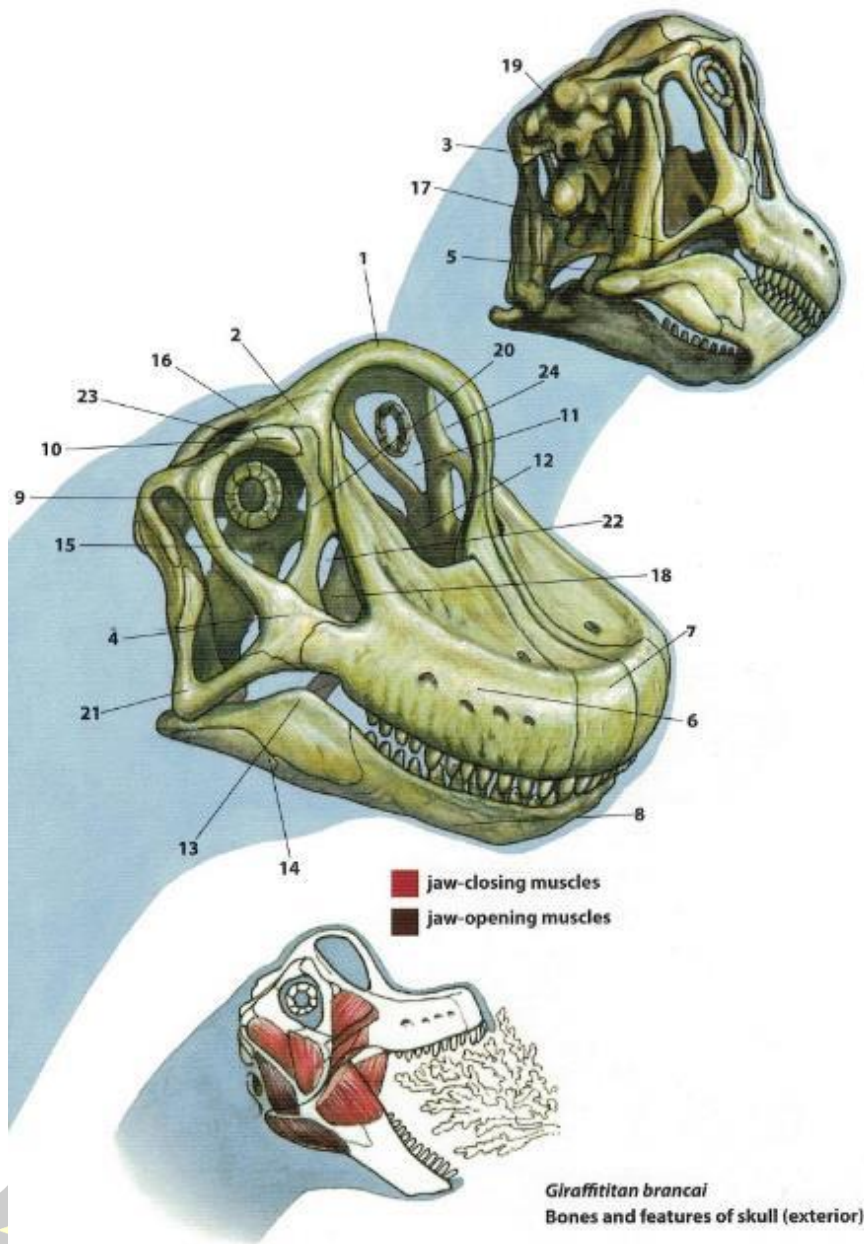


Fig 6 the skull of sauropod *Giraffatitan brancai* and the features of skull. (1) nasal, (2) frontal, (3) quadratojugal, (4) jugal, (5) articular, (6) maxilla, (7) premaxilla, (8) dentary, (9) sclerotic ring, (10) prefrontal, (11) orbital fenestra, (12) external naris, (13) coronoid process, (14) angular, (15) postorbital, (16) parietal, (17) quadrate, (18) pterygoid, (19) basioccipital, (20) lacrimal, (21) surangular, (22) antorbital fenestra, (23) infratemporal fenestra, (24) narial fenestra (modified from Hallett and Wedel 2016)

The skulls of sauropods were relatively small, tended to be delicately built with large opening. The external nares, instead of residing at the tip of the snout, it generally tendency toward migrating the nostrils or nares to the top of the skull and the homodont dentition with the various shape of teeth depend on the type of plant it eats, for instance, leaf-shaped, spatula-shaped, chisel-like shaped and pencil-like shaped restricted to the front of the mouth. There are two type of sauropod that is distinguished by the shape of skull, the first one is Diplodocoids, that have long slender elongate muzzles and jaw with peg-like teeth confine to the front of the mouth. The nostrils are on top of the skull, in front of and above the orbits. The second one is Macronarians, that have short skull with a blunt snout over the orbits. The jaw bore relatively large, spatulate teeth along their entire mouth.

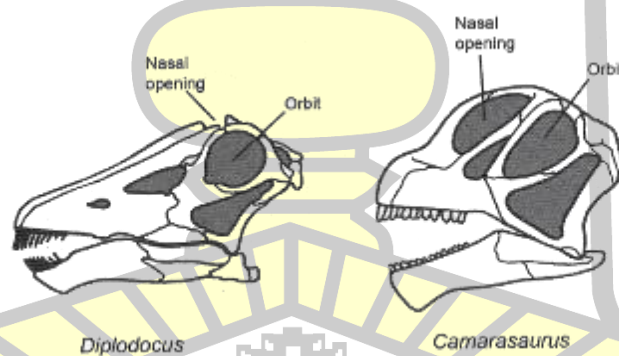


Fig 7 Skulls of sauropod the left is Diplodocus and the right is Camarasaurus

(modified from Lucas 2016)

Skulls of sauropods were small and weakly connected to their vertebral columns easily detached and lost after death, so the paleontologists use other well-preserved part of skeleton, especially their vertebrae, to classify them. The sauropod vertebra consists of a centrum beneath a neural arch. The centrum is the body of the

vertebra and provides a site of attachment for muscles that support the body and also supports the neural arch, a complex structure that encloses the spinal cord and sends out bony struts to which the ribs and other vertebrae are attached. The top of the neural arch is a flange of bone called the neural spine, another site of attachment for tendons, muscles, and ligaments, especially in the shoulder and hip regions.

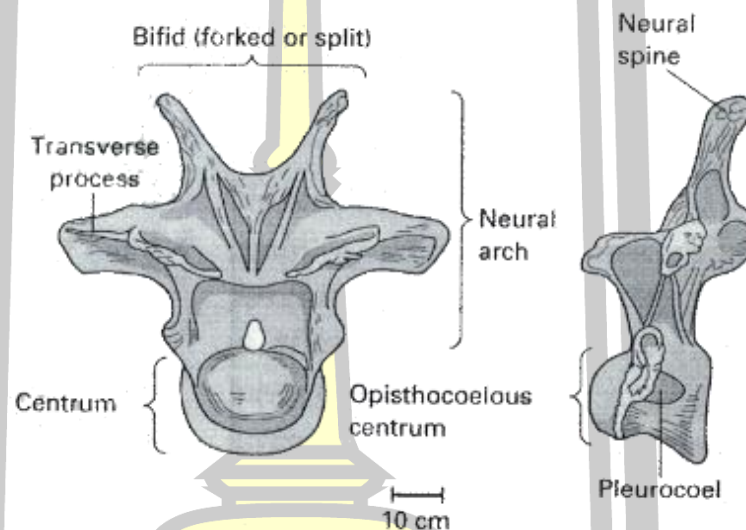


Fig 8 Dorsal vertebra of *Apatosaurus*, *Diplodocidae* sauropod.

(Modified from Lucas 2016)

Vertebra can be divided into four regions: cervical (neck), dorsal (back), sacral (hip), and caudal (tail). In addition, the shapes of the surfaces at which the centra meet each other (articulate) have descriptive names. In sauropods, the centra meet at ball-and-socket joints. In a single centrum, if the socket is anterior and the ball is posterior, the vertebra is termed procoelous, from the Greek words pro, meaning “before,” and koilus (coelos), meaning “hollow” or cavity.” If the situation is reversed—socket posterior and ball anterior—the vertebra is termed opisthocoelous (opisthen is Greek for “behind”). Vertebrae bounded by two cavities are called amphicoelous (amphi is

Greek for "double"). Indeed, one sauropod genus, *Amphicoelias*, takes its name from the amphicoelous nature of some of its vertebral centra.

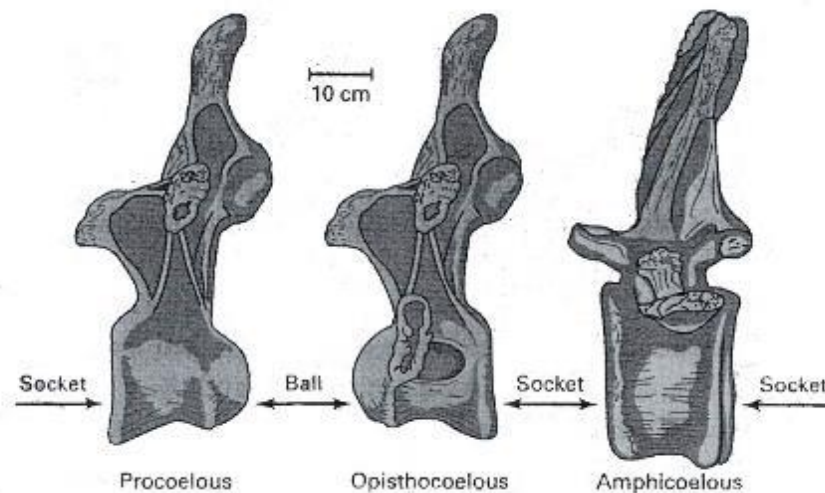


Fig 9 Types of centrum joint of Sauropod vertebra. Procoelous, Opisthocoelous and Amphicoelous

(Modified from Lucas 2016)

The vertebrae of sauropod dinosaurs are characterized by complex architecture involving laminae, fossae, and internal chambers of various shapes and sizes. These structures are interpreted as osteological correlates of an intricate system of air sacs and pneumatic diverticula similar to birds. In basal sauropods pneumatic features are limited to fossae. Camerae and camellae are internalized pneumatic chambers independently acquired in neosauropods and some Chinese forms. The poly camerate and camellate vertebrae of higher neosauropods are characterized by internal pneumatic chambers of considerable complexity. The independent acquisition of these derived morphologies in *Mamenchisaurus*, derived diplodocids, and most titanosauriforms is correlated with increasing size and neck length. The presacral vertebrae of basal sauropods were probably pneumatized by diverticula of cervical air

sacs similar to those of birds. Although pneumatic characters in sauropods are most extensive and complex in presacral vertebrae, the sacrum was also pneumatized in most neosauropods. Pneumatization of the proximal caudal vertebrae was achieved independently in diplodocids and titanosaurids.

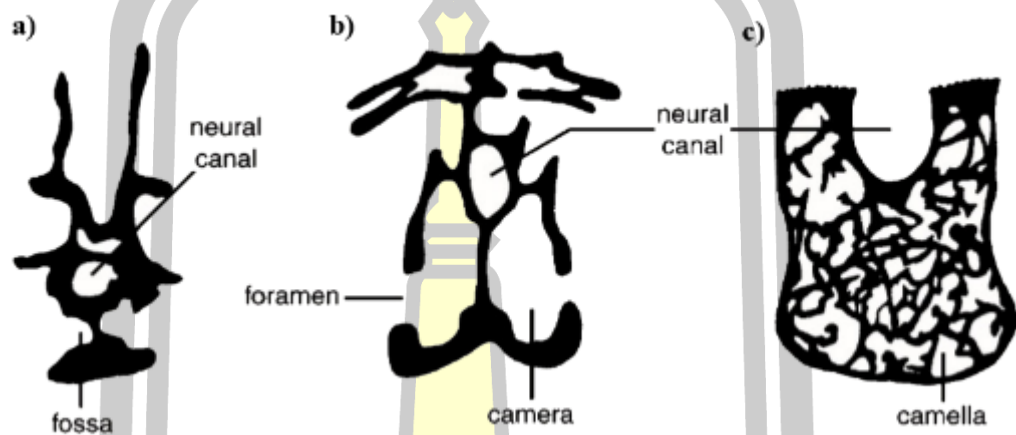


Fig 10 Axial sections of sauropod vertebrae showing pneumatic features.

a) *Haplocanthosaurus priscus*. b), *Camarasaurus* sp. c), *Saltasaurus loricatus*

(Modified from Wedel 2003)

The forefeet were digitigrade, which means that the animals stand on their fingertips. The fingers were arranged in a nearly symmetrical horseshoe-shaped semicircle, and the first digit (thumb) carried a large claw. By contrast, the hindfeet were semi-plantigrade, which means that the Sauropods weight was support along the lengths of its toe bones. The foot was asymmetrical and had three large claws.

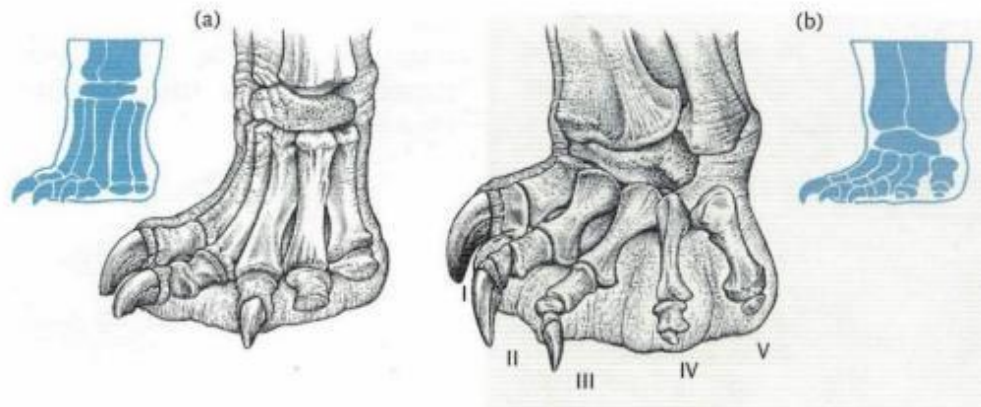


Fig 11 Forefoot and hindfoot of sauropod.

(modified from Fastovsky and Weishampel 2017)

2.3 Phylogeny of Sauropod

Sauropods have a closer relationship with carnivorous dinosaurs group called Theropoda than other herbivore dinosaurs because they are classified in saurischian, the order of dinosaurs that have reptile-like pelvis while other famous plant-eater such as Ankylosaur Ceratopsian Iguanodontid Hadrosaur and Stegosaur are in the ornithischian, the order that has bird-like pelvis (Dixon, 2010). However, some groups of paleontologists discussed to change the clade's division of dinosaurs after referred for 130 years. They found sister group of relationship between Ornithischia and Theropoda then united in the new clade Ornithoscelida and another clade is the redefine Saurischia with Sauropodomorpha and Herrerasauridae in group (Baron et al., 2017) but this theory has not acquiesced to all paleontology community because some of them rejected Baron's hypothesis and suggested that there was currently great uncertainty about early dinosaur relationships and the basic structure of the dinosaur family tree (Langer et al. 2017).

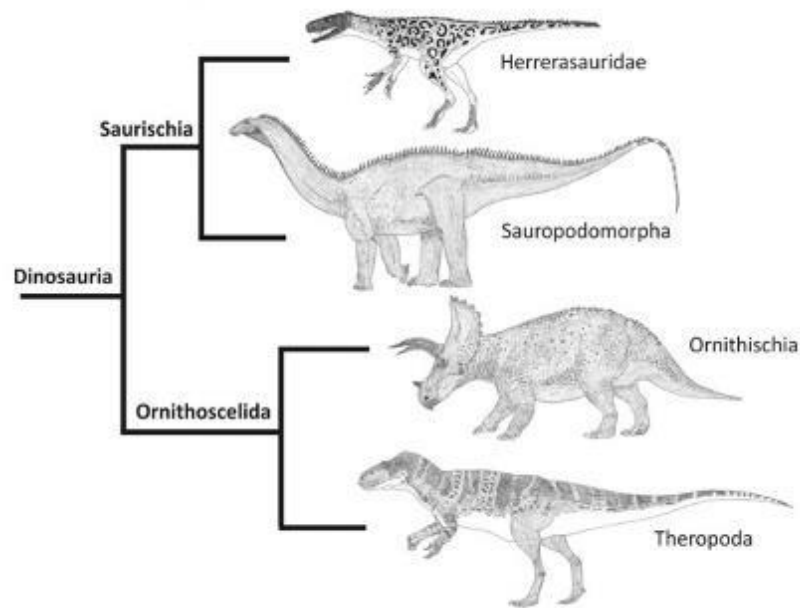


Fig 12 phylogeny of dinosaurs. (modified from Baron et al., 2018)

Due to the classification of pneumatic structure can explain evolution of Sauropod. There are many studies agree on most points, positing Vulcanodon, Barapasaurus, Omeisaurus, the diplodocids, Camarasaurus, and Brachiosauridae as successively closer outgroups to Titanosauria. Mamenchisaurus is the eusauropod which have camellae inside vertebrae. This distribution of taxa requires two independent acquisitions of camerae, once in the Chinese sauropods and once in Neosauropoda. In fact, camerae are synapomorphic for Neosauropoda if this phylogeny is accurate. Camellae also evolved independently a minimum of two times, once in the Chinese sauropods and at least once in Titanosauriformes. However, some titanosauriforms appear to have lacked camellate internal structure. The Jones Ranch sauropod from the Early Cretaceous of Texas is a titanosauriform that lacks camellae (Gomani et al., 1999). As discussed above, the vertebral morphology of Gondwanatitan suggests that it is a camerate titanosaurid. In addition, vertebrae from

the Dalton Wells titanosaurid have large lateral camerae and lack camellae (Britt et al., 1997), demonstrating that at least some titanosaurids had camerate vertebrae (Wedel., 2003).

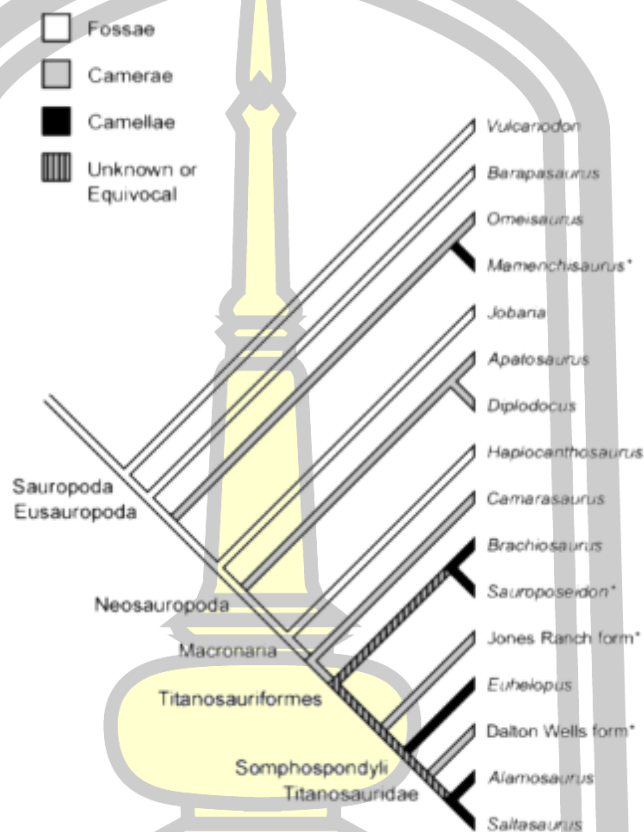


Fig 13 Evolution of vertebral pneumatic structures in sauropods

(Modified from Wilson and Sereno 1998)

2.4 Mamenchisauridae sauropod

Mamenchisauridae is the family of Eusauropods, which used to belong to the family Euhelopodidae and Omeisauridae, have outstanding characteristics such as the extremely long-necked, about the half of their total length, with retroverted hips and sled-shaped chevrons, that may have been adaptations to reach bipedally into the canopy, extending their reach even further. Muzzles are narrow, so despite their large size, they may have been selective high browsers and some taxon had tiny clubs at the

end of their tail like *Mamenchisaurus hochuanensis* and *Omeisaurus tianfuensis* [refs]. The familiar members of the family are *Chuanjiesaurus*, *Eomamenchisaurus*, *Hudiesaurus*, *Mamenchisaurus*, *Qijianglong*, *Tonganosaurus*, *Xinjiangtitan* and *Yuanmousaurus* despite the various genera are already published but the most complete and well-studied specimens are belonging to the genus *Mamenchisaurus*.



Fig 14 skeleton reconstruction of *Mamenchisaurus youngi*.(modified from Paul 2016)

Mamenchisaurus is one of the most well-known members of the family which is discovered in China. C. C. Young proposed *Mamenchisaurus* according to some fossils excavated in Yibin, Sichuan, China in 1954. *M. constructus* was named at that time. In 1972, the new species *M. hochuanensis* was published and described with the nearly complete vertebral column about 23 meters in total length but the skull, teeth, pectoral girdle, and forelimb are missing until 1996 the skeleton with the almost complete skull of new species *Mamenchisaurus youngi* from Shangshaximiao Formation, Late Jurassic; Xinmin village, Zigong city, China was described.

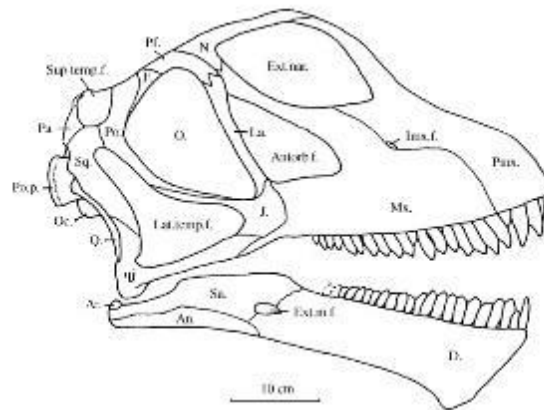


Fig 15 skull of *Mamenchisaurus youngi*. (modified from Pi, Ou and Ye 1996)

The skull of *M. youngi* is small and light, with well-developed openings and thin bones. The brain cavity is very small, only about 60 ml. the orbit is very large, in which the sclerotic rings are well developed. The wear facets of teeth are prominent and V - shaped. The rice - shaped wearfacets are present in external surface of anterior teeth. These features show its food included not only tender plant material, but also rough plant. Meanwhile, the teeth are numerous, and the replacement structure of teeth are well developed.

M. youngi have 18 cervical vertebrae, relatively elongated, with laminal structures and zygapophysial structures well developed. The cervical ribs are extremely slender, there are 3 or 4 rib shafts under a cervical vertebra. These structures strengthen the connection of cervicals enabling it to raise its long neck. The honeycomb structure in cervical and dorsal vertebrae are well developed. Cavity and fossa in the neural arch of cervical are well developed. These structures can reduce its weight and increase its mobility. High and stout neural spines of Anterior caudals, according to other specimens of *Mamenchisaurus* (especially, the new materials of *M. hochuananensis* from Huidong, Zigong), the tail of *M. youngi* should be very long,

and its distal caudals have an expanding appearance. Therefore, its long tail not only balanced its body, but also acted as a defensive weapon and increased its defensive ability. The crest and fossa in the limbs of *M. youngi* are well developed and improve the bearing ability. The limbs indicate some features of walking erectly: the humerus head of *M. youngi* is well developed and strikingly inclined inward; the head of femur is well developed and forms a right angle with the shaft of femur. Meanwhile, the angle between in metacarpals and the axial line of phalanges is nearly 90°. These features are an indication that the animal lived on land. Furthermore, there are at least 4 other species of the genus *Mamenchisaurus*.

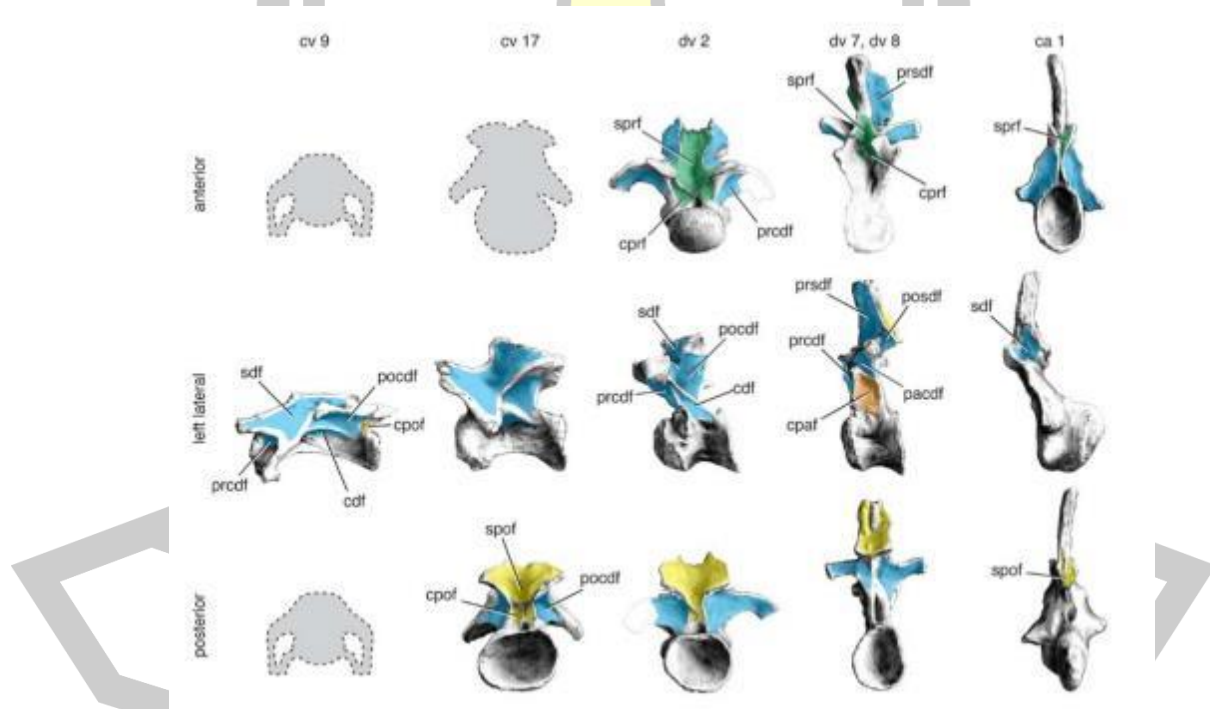


Fig 16 vertebra of *Mamenchisaurus* sp. Anterior (top), left lateral (middle), and posterior (bottom) views of anterior cervical (cv 9), posterior cervical (cv 17), anterior dorsal (dv 2), posterior dorsal (dv 8), and anterior caudal (ca 1) vertebrae.

(modified from Wilson et al. 2011)

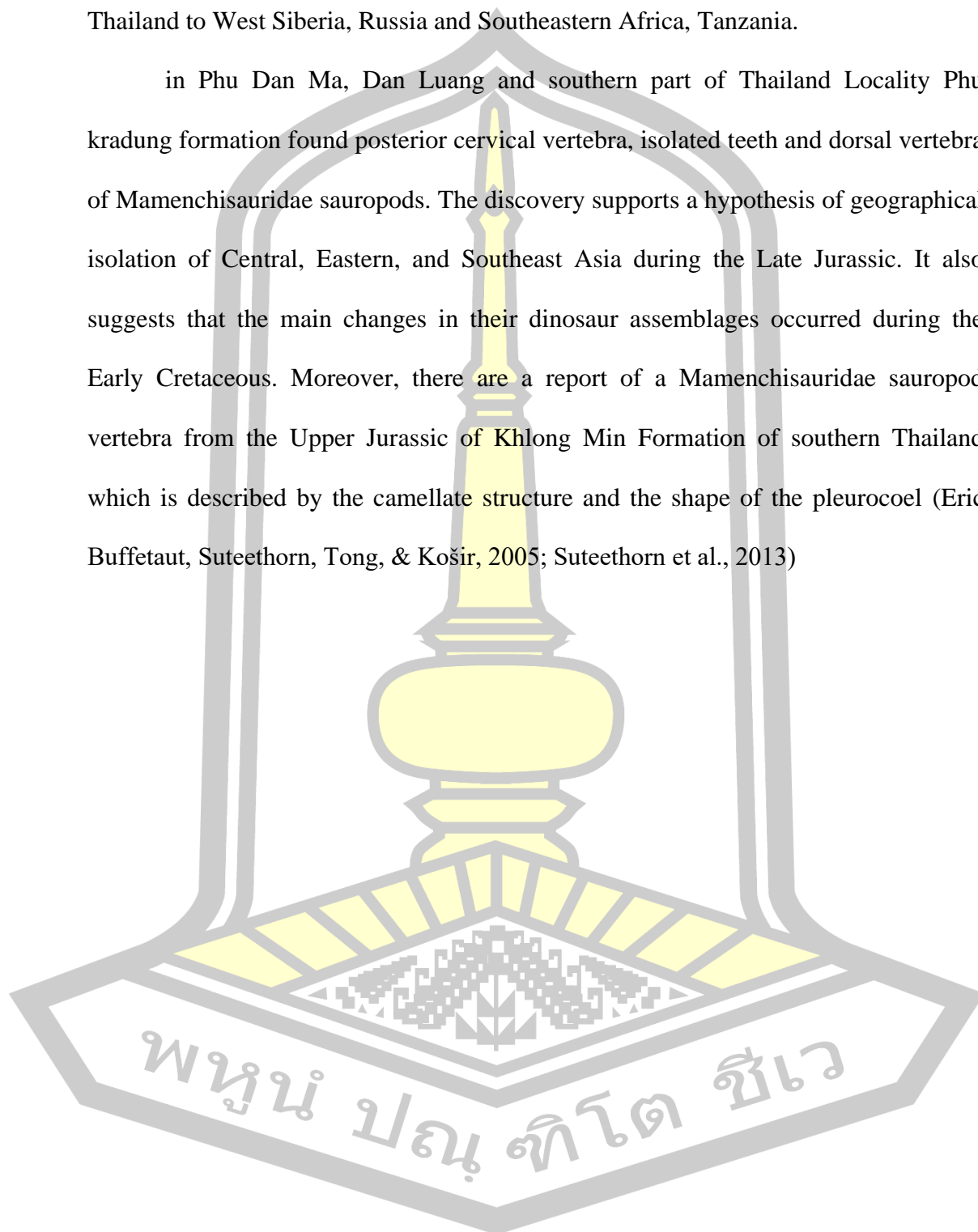
M. jingyaensis was discovered in localities of Meiwang and Sanjiang, Jingyan Co. and Dujia, Rongxian Co. recognized as the boundary between the Upper and Lower Shaximiao Formation. The principle characters include a typically spoon-shaped. dentition, elongated cervicals with low elongated neural spines, anterior dorsal neural spines are bifid, and anterior caudals are procoelous, assigning them unquestionably to the genus *Mamenchisaurus* Youngi, 1954. *M. sinocanadorum* is represented only by a left mandible and first through third cervicals. Its estimated body length is 26 m. However, specimens representing *M. sinocanadorum* are extremely restricted, the reliability of its diagnosis is questionable, and the type locality is 2,000 km from the other species. Thus, the probability of the current specimens belonging to this species is not very high. *M. hochuanensis* Young and Chao, 1972 compares closely in both size and morphology but there are relatively clear distinctions as the Jingyan and Rongxian cervicals have better developed pleurocoels and the tibia is thick and linear, whereas on the former the tibia is laterally compressed. *M. anyuensis* are not well developed but dorsal pleurocoels are relatively well developed in direct contrast to the new species which has well developed cervical pleurocoels but weak dorsal pleurocoels. Additionally, *M. anyuensis* has five sacral vertebrae in contrast to the four on *M. jingyanensis*. These comparisons justify the erection of the new species *Mamenchisaurus jingyanensis*.

2.5 The discovery of Mamenchisauridae Sauropods outside China

Mamenchisauridae sauropod was known as the endemic taxa of East Asia because all of specimens had been discovered only in China but the new studies

revealed the wider spread of this family of sauropods from China to Southeast Asia, Thailand to West Siberia, Russia and Southeastern Africa, Tanzania.

in Phu Dan Ma, Dan Luang and southern part of Thailand Locality Phu kradung formation found posterior cervical vertebra, isolated teeth and dorsal vertebra of Mamenchisauridae sauropods. The discovery supports a hypothesis of geographical isolation of Central, Eastern, and Southeast Asia during the Late Jurassic. It also suggests that the main changes in their dinosaur assemblages occurred during the Early Cretaceous. Moreover, there are a report of a Mamenchisauridae sauropod vertebra from the Upper Jurassic of Khlong Min Formation of southern Thailand which is described by the camellate structure and the shape of the pleurocoel (Eric Buffetaut, Suteethorn, Tong, & Kořir, 2005; Suteethorn et al., 2013)



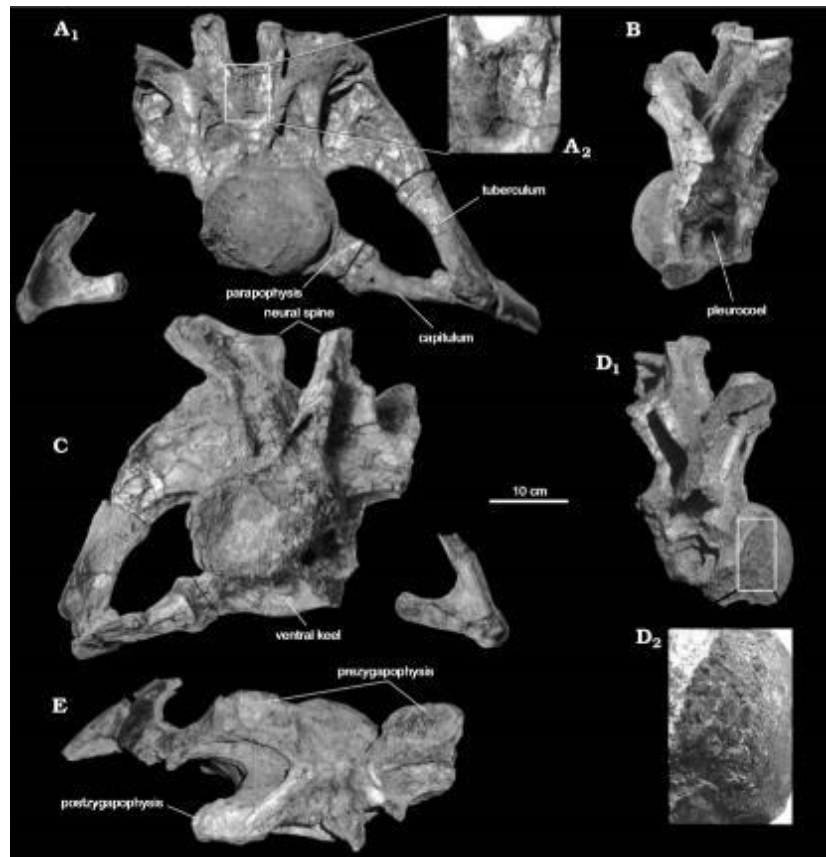


Fig 17 cervical vertebra of mamenchisauridae sauropod from Phu Dan Ma, Kalasin province. (Suteethorn et al., 2013)

In 2019, the paper of Isolated sauropod teeth and caudal vertebrae from the Middle Jurassic Itat Formation of the Berezovsk coal mine, Krasnoyarsk Territory, Russia was published. The characters of specimens are attributed to the endemic Asiatic eusauropod family Mamenchisauridae based mostly on phenetic similarity. The few large anterior teeth lack marginal denticles. In small, possible juvenile posterior teeth there are denticles on both mesial and distal crown margins. The anterior caudal vertebrae are deeply procoelous, while the posterior caudal vertebrae are amphicoelous, which is characteristic for the Mamenchisauridae. The Berezovsk sauropod remains represent the northernmost and westernmost record for the Mamenchisauridae and the first Middle Jurassic Asiatic eusauropod outside China.



Fig 18 first caudal vertebra and teeth of mamenchisauridae sauropod from Middle Jurassic Itat Formation of the Berezovsk coal mine, Krasnoyarsk (Averianov et al. 2019)

The study of taxonomic affinities of the putative titanosaurs from the Late Jurassic Tendaguru Formation of Tanzania in 2019 discovered the new taxa of mamenchisauridae sauropod name *Wamweracaudia keranjei* Described by a series of 30 articulated caudal vertebrae, two anterior caudal neural spines and two incomplete chevrons and the isolated anterior caudal vertebra that were originally referred to sauropod name *Janenschia robusta* by Janensch (1929a), although no basis was given for this attribution. The internal tissue structure is fine and spongy, lacking camellae. The centrum is procoelous, with a deeply concave anterior surface and strongly convex posterior ball ($CCI = 0.5$). Ventrally, the centrum is transversely flat and gently concave anteroposteriorly, whereas the lateral surface is dorsoventrally convex

and anteroposteriorly concave. Both surfaces lack ridges or excavations. There is some evidence for anterior chevron facets, and so it is likely that the absent posterior chevron facets have been eroded away. A simple caudal rib projects laterally and curves anteriorly, as in the anterior caudal vertebrae of *Wamweracaudia*, although it does not extend as far as the anterior margin of the centrum. This study revealed the fact that mamenchisauridae sauropod once lived in the Late Jurassic period of Southeastern Africa (Mannion et al. 2019).



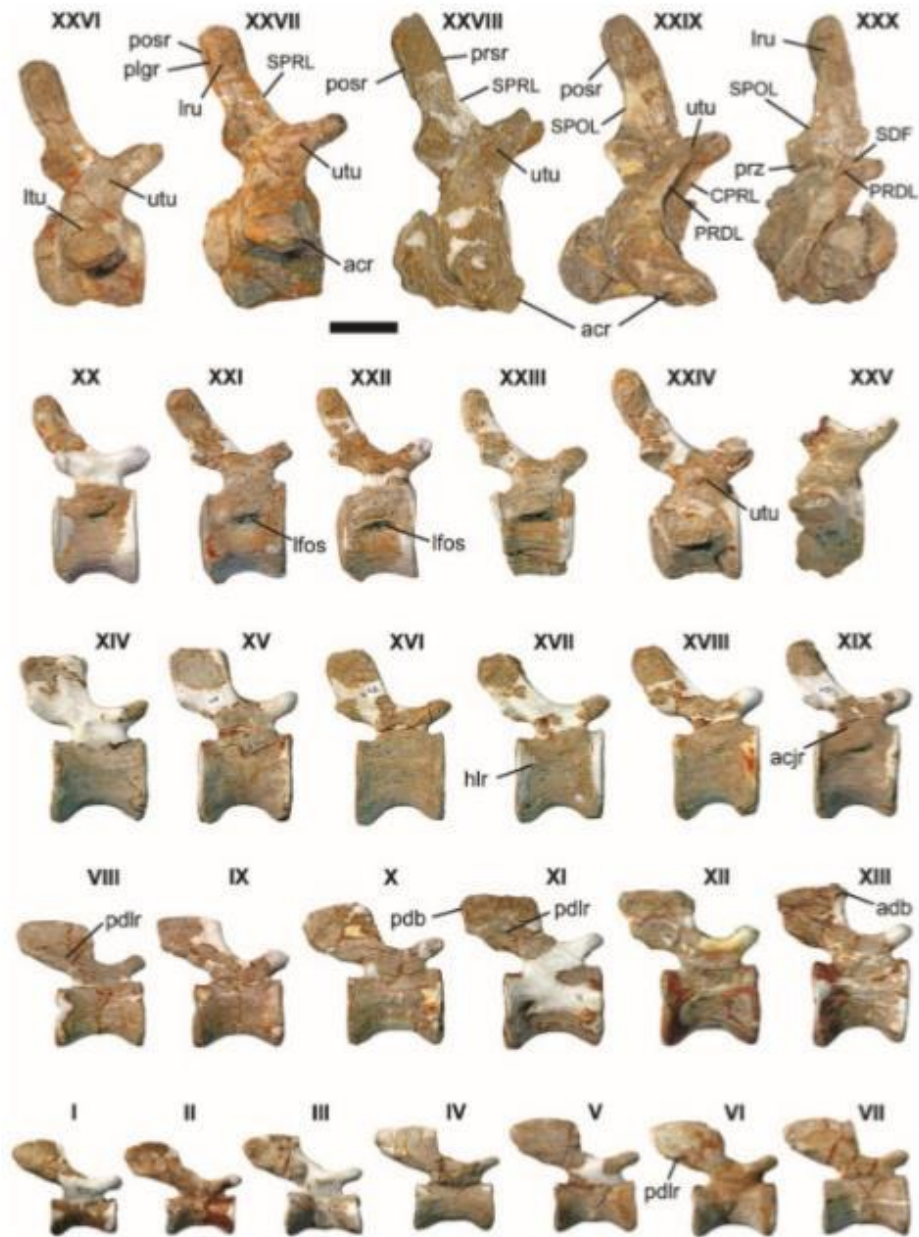


Fig 19 series of *Wamweracaudia keranjei* caudal vertebrae. (Mannion et al. 2019)

พหุ ม ประจักษ์ ชีวะ

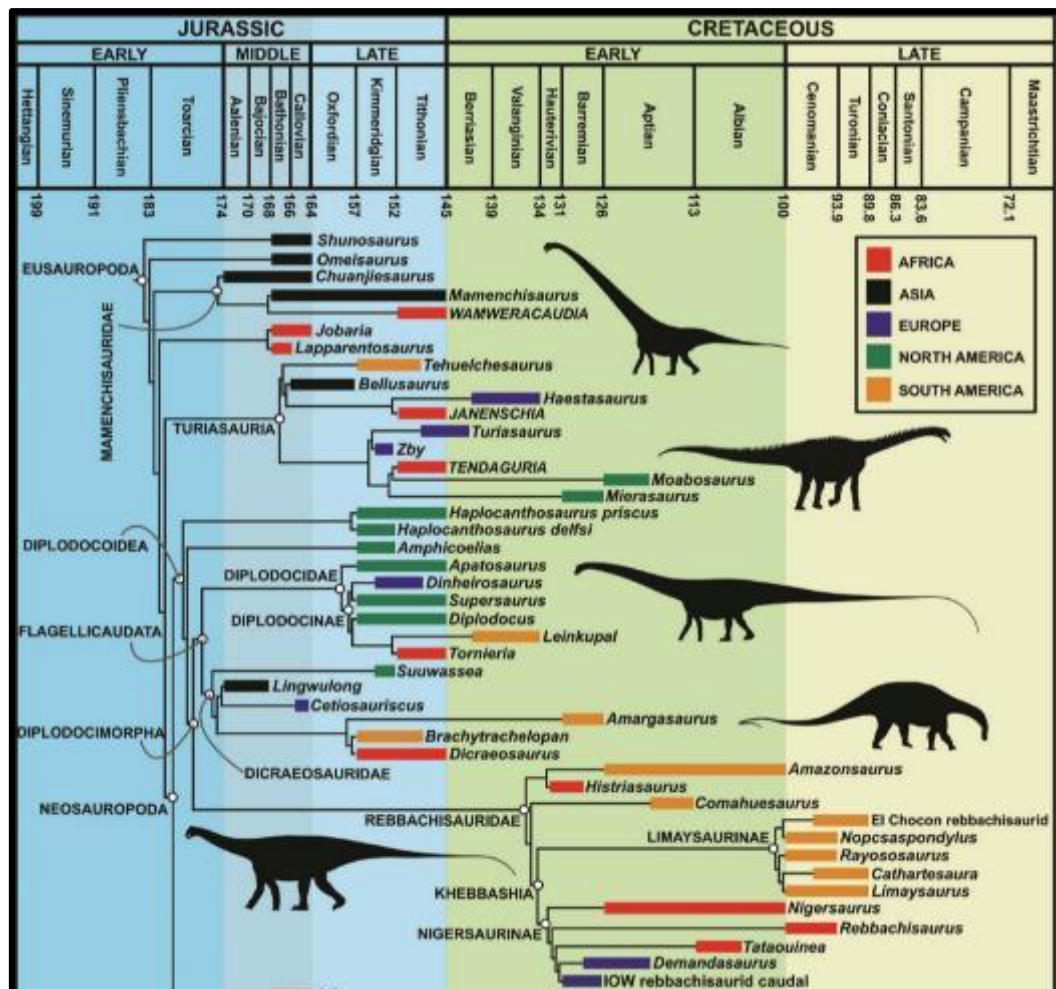
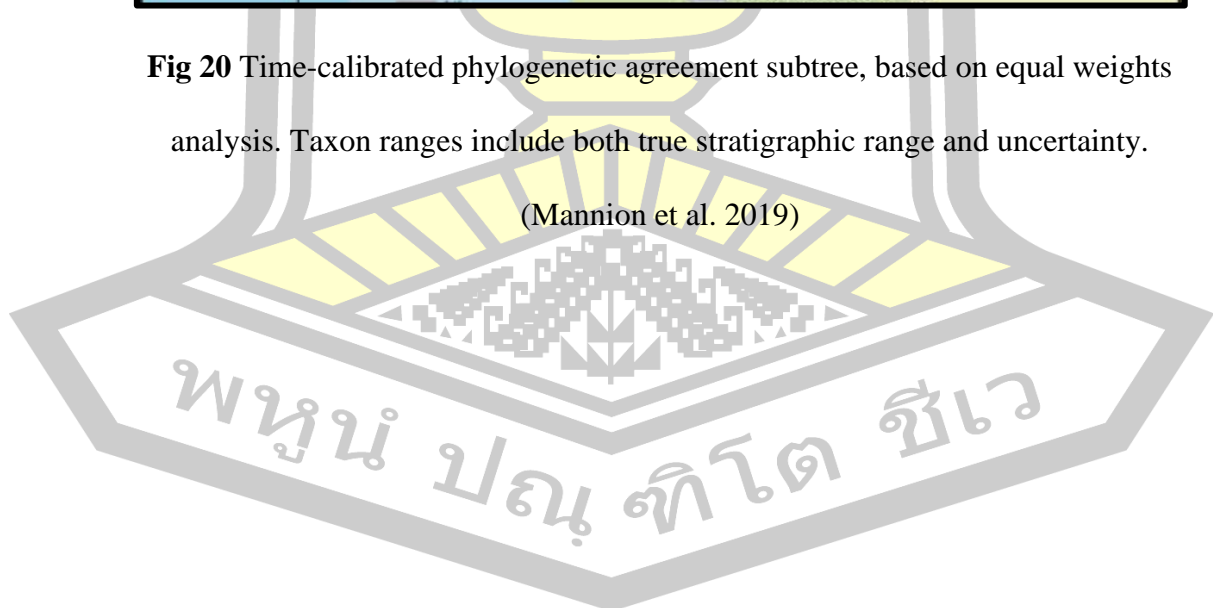


Fig 20 Time-calibrated phylogenetic agreement subtree, based on equal weights analysis. Taxon ranges include both true stratigraphic range and uncertainty.

(Mannion et al. 2019)



2.6 The discovery of Sauropod dinosaur in Thailand

In Thailand, all genera of dinosaurs including sauropods can be generally found in the red based on the facies of the continental sedimentary rocks called Khorat group, which is in the Mesozoic era (including Triassic, Jurassic and Cretaceous period), the rock name after Khorat plateau, which is divided by a range of hills called the Phu Phan Mountains into two basins: the northern Sakhon Nakhon Basin, and the southern Khorat Basin tilted towards the southeast, and drained by the Mun and Chi Rivers, tributaries to the Mekong River that forms the northeastern boundary of Thailand. Khorat group comprises nine formal formations: in ascending order of Huai Hin Lat, Nam Phong, Phu Kradung, Phra Wihan, Sao Khua, Phu Phan, Khok Kruat, Maha Sarakham, Phu Thok Formations. The rock-types include sandstone, pebbly sandstone, siltstone, mudstone, shale, rock salt, gypsum and anhydrite. These formations unconformably overlie Triassic and Permian rocks and underlie Tertiary and Quaternary deposits. The Khorat Group was dated as Upper Triassic to Cretaceous-Lower Tertiary as determined by fossil assemblage of vertebrates (Buffetaut et al., 1997), bivalves (Meesook et al., 1995) and palynomorphs (Racey et al., 1994, 1996). Rocks in the Khorat Group generally were exposed by folding structures as anticline and syncline on the Khorat plateau and its vicinity except in the southwestern part of the plateau (Department of Mineral Resources, 2014).

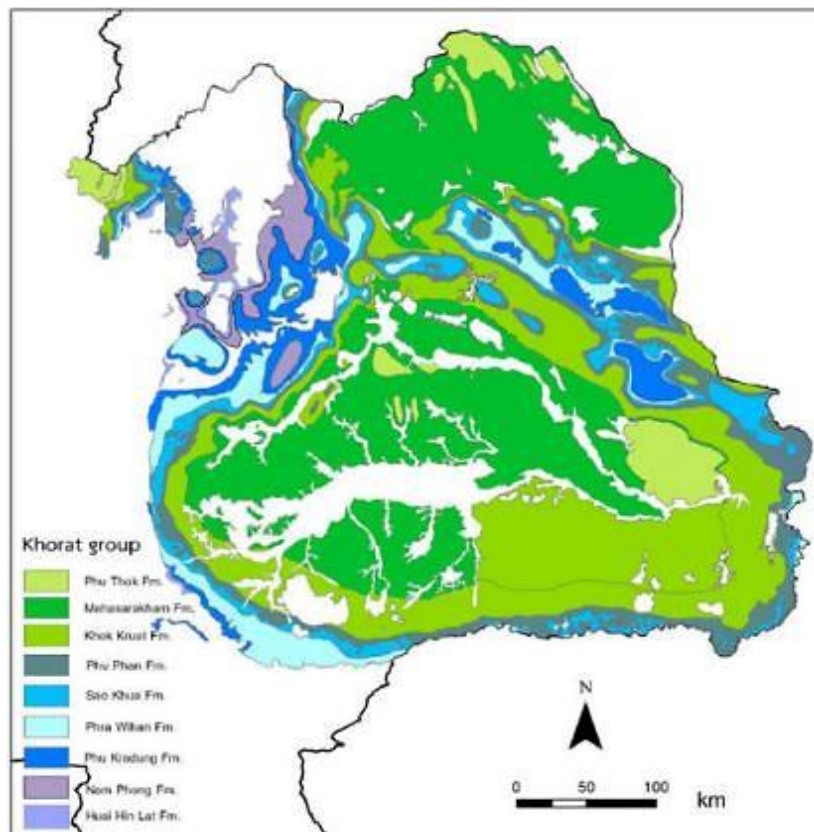


Fig 21 Map of northeast Thailand showing the distribution of Khorat group geological strata. (modified from Wongko et al. 2011)

After many times of revision, the latest revised age dating of Khorat group by palynological results can tell us that Huai Hin Lat was eliminated from the group, lower Nam Phong is in Rhaetian stage of late Triassic, Phu Kradung is in the joint between late Jurassic and early Cretaceous then the other formations are in the early Cretaceous from Berriasian to Aptian stage except Maha Sarakham and Phu Thok formation which are in the late Cretaceous. Moreover, we realized that the palaeoenvironment had changed from fluvial braided river to alluvial floodplain and end with the hypersaline lake with arid desert (Racey and Goodall, 2009).

The specimens of mamenchisauridae sauropods were found in the Phu Kradung Formation, this formation comprises fluvial channel sandstone, siltstone, and

mudstone with intermittent calcrete. Overall, mudstone and siltstone dominate the formation. The formation was deposited in a mainly lake-dominated floodplain cut by meandering and occasionally braided river channels. The formation is sandier in its upper part and shows a gradational conformable contact with the overlying Phra Wihan Formation. The thickness of the Phu Kradung Formation varies between 800-1,200 m, widely distributed along the western rim of the Khorat Plateau in parallel with the Huai Hin Lat Formation and the Nam Phong Formation.

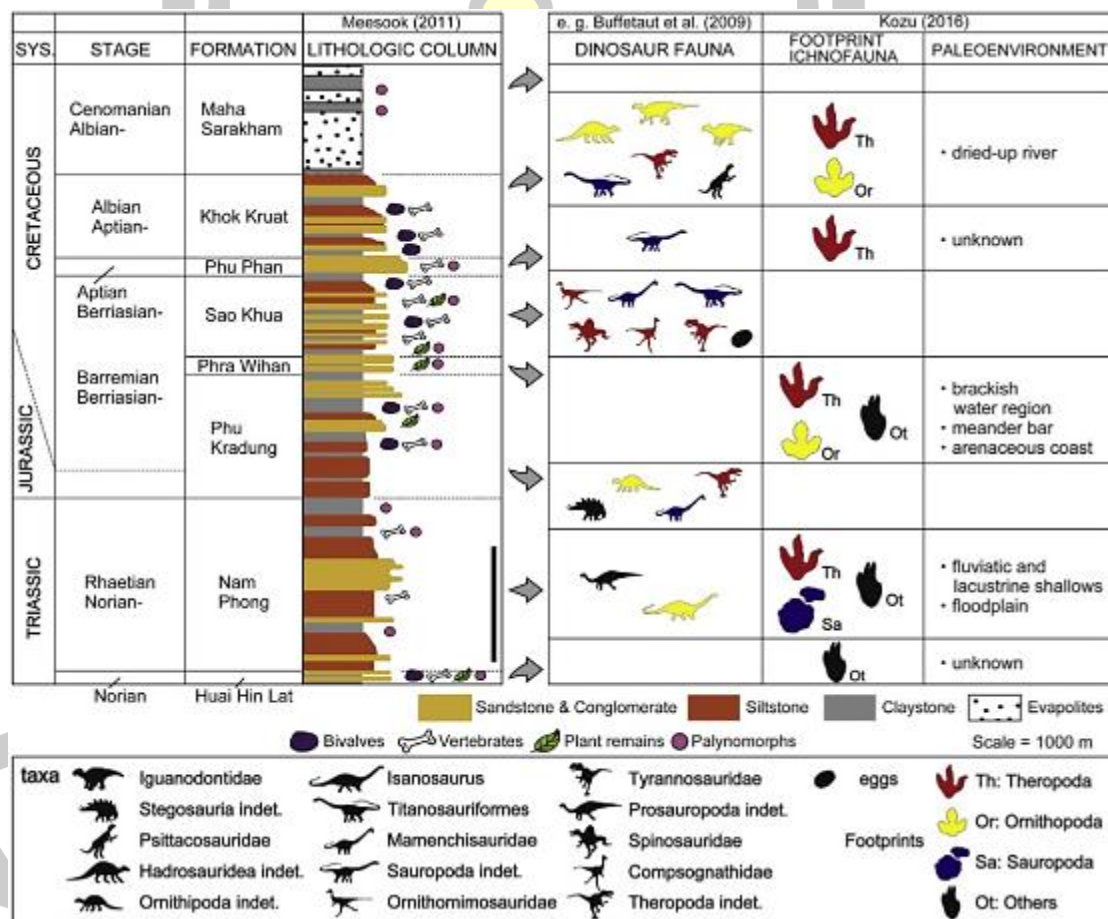


Fig 22 Lithostratigraphic column and dinosaur ichnofauna of the Khorat Group (modified from Buffetaut et al., 2009; Buffetaut and Suteethorn, 2011; Meesook, 2011; Shibata et al., 2011, 2015; Kozu et al. 2016.)

CHAPTER 3

MATERIAL AND METHOD

3.1 Geological setting

The Phu Noi locality is in Ban Din Chi village, Kham Muang District, Kalasin Province, Northeastern Thailand, which is one of the most abundant bonebed of non-marine vertebrate assemblage in Southeast Asia. The locality belongs to the lower part of the Phu Kradung Formation, the most basal formation of the Khorat Group (Racey, 2009; Racey & Goodall, 2009). It consists of fluvial sandstones, siltstones, and mudstones, which might be the Late Jurassic on the lower part by the vertebrate evidence and the Early Cretaceous by the palynology, detrital zircon thermochronology, and the fauna turnover of freshwater sharks, turtles, and crocodiles (Carter & Bristow, 2003; Chanthasit, Suteethorn, Manitkoon, Nonsrirach, & Suteethorn, 2019; Cuny et al., 2014; Liard et al., 2015; Manitkoon et al., 2023; Martin et al., 2018; Tong et al., 2019, 2015).

The locality has three fossiliferous layers of a complex paleochannel sequence: 1) the bottom layer of the palaeochannel which composed of the light grey conglomeratic sandstone (PNA), 2) A middle layer of siltstone and mudstone, approximately 10 meter above the bottom layer (PNB), and 3) A greyish siltstone inside the proximal floodplain deposit (PNC), approximately 400 meter West-South-West PNB (Cuny et al., 2014). The accommodation of sediments and sequence stratigraphy indicates that the bonebed was the lacustrine to fluvial environment such as the oxbow lake and low-energy floodplain (Cuny & Chanthasit, 2023; Cuny et al., 2014; Manitkoon et al., 2023).

It is considered to date from the Upper Jurassic due to the presence of hybodont shark, basal eucryptodiran turtles, Teleosauridae crocodiles, and neorithischia dinosaur. In addition, a large number of indeterminate taxa are currently being studied, such as brachyopid temnospondyl amphibians, ramphirinchid pterosaur, sinraptorid theropod and mamenchisaurid sauropod dinosaurs (this study). Almost all vertebrate taxon groups resemble the Middle to Late Jurassic vertebrates from the Junggar basin, Turpan basin, and Sichuan basin in Northwest and Southwest China, respectively (Li, Yang, & Hu, 2011; Tong et al., 2019).

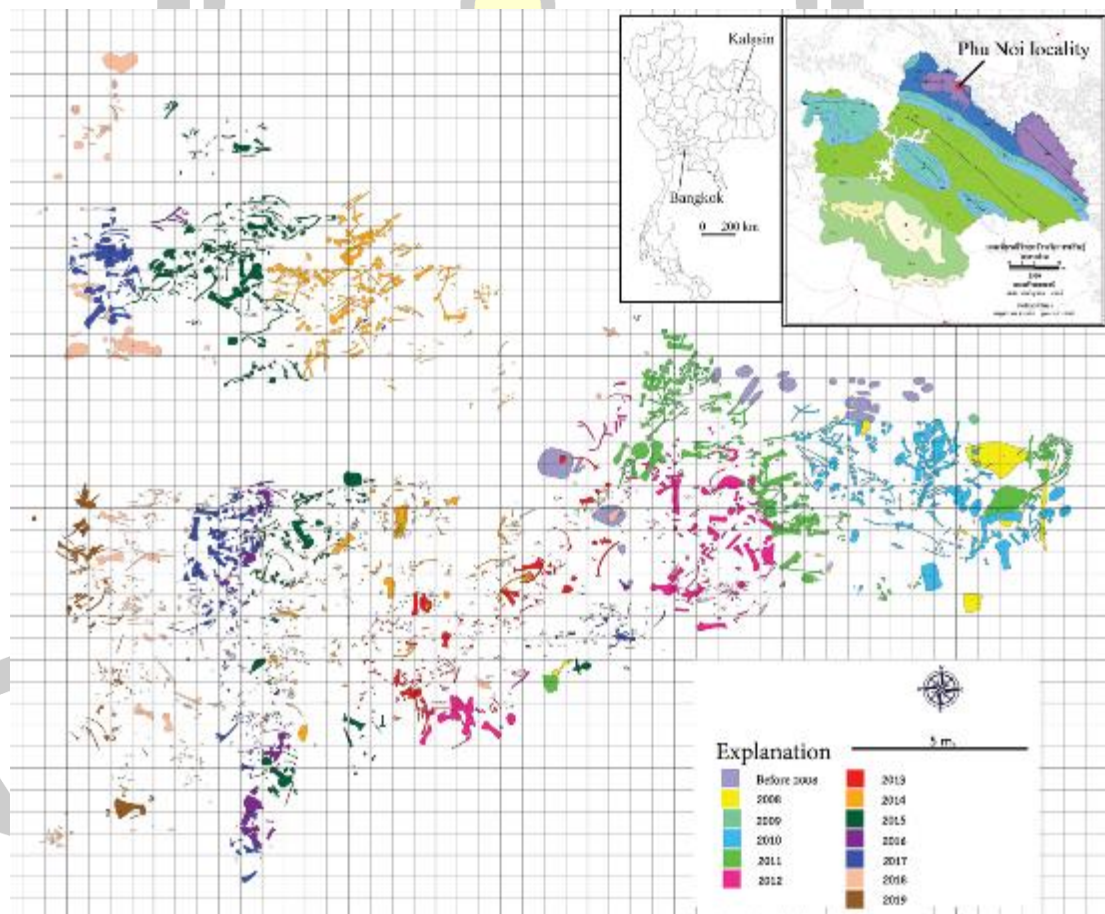


Fig 23 Bone map of Phu Noi locality, Kham Muang District, Kalasin Province, Thailand.

(Modified from Department of Mineral Resource, Palaeontological Research and Education Centre and Sirindhorn Museum (in prep.)).

3.2 Materials

The specimens in the study come from PNB and PNC as the fragments of skulls and isolated and partially articulated postcranial elements. Total number of specimens are 171, composed of 50 cranial elements, 44 isolated teeth, 64 elements of vertebrae, and 13 girdles and limb bones. A detailed list of bones is in table 2.

3.3 Methods

3.3.1 Descriptions and comparisons

All the descriptions were made directly from the specimens in this study. Comparisons were made from published descriptions, illustrations, and photographs with of other mamenchisaurids materials. Romerian orientational descriptors (e.g. anterior, posterior) has been using instead of standardised terms (e.g. cranial, caudal). The anatomical nomenclature of vertebral fossae and laminae are from Wilson, 1999, 2012 and Wilson, D’Emic, Ikejiri, Moacdieh, & Whitlock, 2011.

3.3.2 Preliminary phylogenetic analysis

To establish the phylogenetic position of Phu Noi mamenchisaurids, the data matrix of Moore et al., 2023 has been used. The matrix conducted both equal and implied weights parsimony analysis with the incorporates of 103 taxa and 449 characters (provided in the appendix).

Maximum parsimony analyses were carried out in TNT v1.5 (Goloboff & Catalano, 2016), with the memory buffer (“Maxtree”) set at 200,000 trees. The heuristic algorithm uses “New Technology Search” using 5 times “Stabilizing Consensus” with applying sectorial searches, drift, and tree fusing

(*xmult=replications 50 hits 10 css rss ratchet 5 fuse 5*). If the replications fill the memory buffer (“some replications overflowed”), a second round of Tree-Bisection-Reconnection branch swapping (TBR, using “Traditional search”) is applied to the resulting trees. The strict consensus and 50% majority rule were calculated from all trees. Under these parameters, two analyses were carried out, one using equal weighting (EQW hereafter) and one using extended implied weighting (EIW hereafter), with the k-value set at 12.000.

3.4 Institutional abbreviations

CV, Chongqing Museum of Natural History, Chongqing, China; DFMMh, Dinosaurier- Freilichtmuseum M'unchenhagen/Verein zur F'orderung der Nieders'achsischen Pal'aontologie (e.V.), Germany; FMNH, Field Museum of Natural History, Chicago, USA; GCP, Grupo Cultural Paleontol'gico de Elche, Museo Paleontol'gico de Elche, Elche, Spain; IVPP, Institute of Vertebrate Paleontology and Paleoanthropology, Beijing, China; PRC, Palaeontological Research and Education Centre, Mahasarakham, Thailand; QJGPM, Qijiang Petrified Wood and Dinosaur Footprint National Geological Park Museum, Chongqing, China; SM, Sirindhorn Museum, Kalasin, Thailand; ZDM, Zigong Dinosaur Museum, Sichuan, China; ZNM, Zhejiang Museum of Natural History, Hangzhou, China.

3.5 Anatomical abbreviation

3.5.1 Cranial element

al, alveolus; an, angular; aof, antorbital fenestra; ar, articular; asaf, anterior surangular foramen; aspm, ascending process of the premaxilla; boc, basioccipital; bpt, basipterygoid process; d, dentary; en, external naris; eoc, exoccipital; et, erupting tooth; f, frontal; itf, infratemporal fenestra; j, jugal; jp, jugal process; l, lacrimal; m,

maxilla; mb, main body; mg, Meckelian groove; n, nasal; nf, narial fossa; nvf, neurovascular foramen; orb, orbit; oc, occipital condyle; os, orbitosphenoid; p, parietal; paof, preantorbital fenestra; pf, parietal fenestra; pt, palatine; pm, premaxilla; po, postorbital; pop, paroccipital process; ppf, postparietal fenestra; prf, prefrontal; ppr, parasphenoid rostrum; psaf, posterior surangular foramen; pt, pterygoid; ptf, posttemporal fenestra; q, quadrate; qf, quadrate facet; qj, quadratojugal; r, root of tooth; rf, replacement foramen; rt, replacement tooth; sa, surangular; snf, subnarial foramen; soc, supraoccipital; sq, squamosal; stf, supratemporal fenestra; sys, symphysis.

3.5.2 Axial skeleton

acd1, anterior centrodiapophyseal lamina; acpl, anterior centroparapophyseal lamina; acsl, accessory lamina; adb, anterodistal blade; ant. p, anterior process; ar, anterior ridge; bb, bone bridge; cap, capitulum; c, centrum; ca, caudal vertebra; cdf, centrodiapophyseal fossa; cod, condyle; cot, cotyle; cpol, centropostzygapophyseal lamina; cpor, centropostzygapophyseal fossa; cppl, centroprezygapophyseal lamina; cporf, centroprezygapophyseal fossa; cr, caudal rib; cv, cervical vertebra; di, diapophysis; dv, dorsal vertebra; ep, epiphysis; eprl, epiphysal-prezygapophyseal lamina; hc, heamal canal; hyp, hypantrum; hypo, hyposphene; lvr, lateroventral ridge; nc, neural canal; ns, neural spine; os, oblique strut; pa, parapophysis; pacdf, parapophyseal centrodiapophyseal fossa; pacporf, parapophyseal centroprezygapophyseal fossa; pcpl, posterior centroparapophyseal lamina; pdb, posterodistal blade; pnf, pneumatic fossa; pnfo, pneumatic foramen; po, postzygapophysis; pocdf, postzygapophyseal centrodiapophyseal fossa; podl, postzygodiapophyseal lamina; posdf, postzygapophyseal spinodiapophyseal fossa; posf, postspinal fossa; posl, postspinal lamina; pos. p, posterior process; ppdl,

paradiapophyseal lamina; pr, prezygapophysis; prcdf, prezygapophyseal centrodiapophyseal fossa; prdl, prezygodiapophyseal lamina; prdf, prezygodiapophyseal fossa; prf, proximal facet; prpadf, prezygapophyseal paradiapophyseal fossa; prsdf, prezygapophyseal spinodiapophyseal fossa; prsf, prespinal fossa; prsl, prespinal lamina; r, ridge; sdf, spinodiapophyseal fossa; spdl, spinodiapophyseal lamina; spol, spinopostzygapophyseal lamina; spof, spinopostzygapophyseal fossa; sprl, spinoprezygapophyseal lamina; sys, synostosis; tpol, intrapostzygapophyseal lamina; tprl, intraprezygapophyseal lamina; tub, tuberculum; vk, ventral keel.

3.3.3 Appendicular skeleton

acf, acromial fossa; acr, acromial ridge; af, anconeal fossa; co, coracoid; dpc, deltopectoral crest; gl, glenoid; hh, humeral head; ltf, lateral triceps fossa; mtf, medial triceps fossa; rc, radial condyle; scb, scapular blade; uc, ulnar condyle.

3.3.4 Other abbreviation

CI, Consistency Index; EI, Elongation Index; EIW, extended implied weights; EWP, Equal weights parsimony; KS, Kalasin; MPT, most parsimonious tree; OTU, operational taxonomic unit; PN, Phu Noi; RI, Retention Index.

Table 2 specimens of Mamenchisauridae sauropods from Phu Noi locality

| Element | Specimen number | Side | Collection |
|--------------------------|------------------------|-------------|-------------------|
| Premaxilla (n = 4) | KS34-1706 | L | SM |
| | KS34-1766 | L | |
| | KS34-2199 | L | |
| | KS34-3279 | R | |
| Nasal (n = 1) | PN19-31A | R | PRC |
| Prefrontal (n = 2) | PN14-139 | L | |
| | PN15-218 | L | |
| Frontal (n = 4) | KS34-1691 | R | SM |
| | PN14-139 | LR | PRC |
| | PN15-218 | L | |
| | PN19-31 | R | |
| Parietal (n = 4) | KS34-1691 | R | SM |
| | PN14-139 | LR | PRC |
| | PN15-218 | L | |
| | PN19-31 | R | |
| Lacrimar (n = 1) | KS34-1226 | L | SM |
| Jugal (n = 4) | KS34-1387 | L | |
| | KS34-1508 | R | |
| | KS34-2607 | L | |
| | KS34-2955 | L | |
| Quadratojugal (n = 3) | KS34-1180 | L | PRC |
| | KS34-1718 | R | |
| | PN14-139E | L | |
| Postorbital (n = 5) | KS34-1492 | R | SM |
| | KS34-3136 | R | PRC |
| | KS34-3206 | R | |
| | PN14-139B | L | |
| | PN15-93 | R | |
| Squamosal (n = 6) | KS34-2208 | R | SM |
| | KS34-2609 | L | PRC |
| | KS34-3289 | L | |
| | PN14-139A | L | |
| | PN14-139F | R | |
| | PN944 | R | |
| Supraoccipital (n = 1) | PN14-139 | M | PRC |

Table 2 continued

| Element | Specimen number | Side | Collection |
|---|-----------------|------|------------|
| Exoccipital (n = 3) | KS34-1546 | L | SM |
| | KS34-1659 | L | |
| | PN14-139 | LR | PRC |
| Occipital condyle (n = 1) | | M | |
| Basioccipital process (n = 1) | | LR | |
| Besipterygoid process of basisphenoid (n = 1) | | LR | |
| Parasphenoid (n = 1) | | M | |
| Dentary (n = 8) | KS34-612 | R | SM |
| | KS34-978 | R | PRC |
| | KS34-1528 | R | SM |
| | KS34-1572 | L | |
| | KS34-2085 | L | |
| | PN14-322 | L | PRC |
| | PN18-17 | R | |
| | PN755 | L | |
| Anterior tooth (n = 16) | KS34-1556 | - | SM |
| | KS34-1571 | | |
| | KS34-1584 | | |
| | KS34-1698 | | |
| | KS34-2106 | | |
| | KS34-2180 | | |
| | KS34-2473 | | |
| | KS34-2526 | | |
| | KS34-2789 | | |
| | KS34-363 | | PRC |
| | KS34-364 | | |
| | PN14-265 | | |
| | PN14-334 | | |
| | PN16-111 | | |
| | PN16-114 | | |
| | PN16-116 | | |

Table 2 Continued

| Element | Specimen number | Collection |
|-----------------------------|-----------------|------------|
| Middle tooth (n = 16) | KS34-1621 | SM |
| | KS34-1779 | |
| | KS34-2028 | |
| | KS34-2252 | |
| | KS34-2434 | |
| | KS34-2481 | |
| | KS34-2567 | |
| | KS34-2602 | |
| | KS34-2655 | |
| | KS34-2733 | |
| | KS34-2879 | |
| | KS34-2985 | |
| | KS34-2996 | |
| | KS34-803 | |
| | PN16-103 | |
| | PN16-106 | |
| Posterior tooth (n = 12) | KS34-1408 | SM |
| | KS34-1579 | |
| | KS34-1641 | |
| | KS34-1668 | |
| | KS34-1697 | |
| | KS34-2181 | |
| | KS34-2250 | |
| | KS34-2841 | |
| | KS34-2869 | |
| | KS34-3106 | |
| | KS34-3276 | |
| | KS34-3340 | |

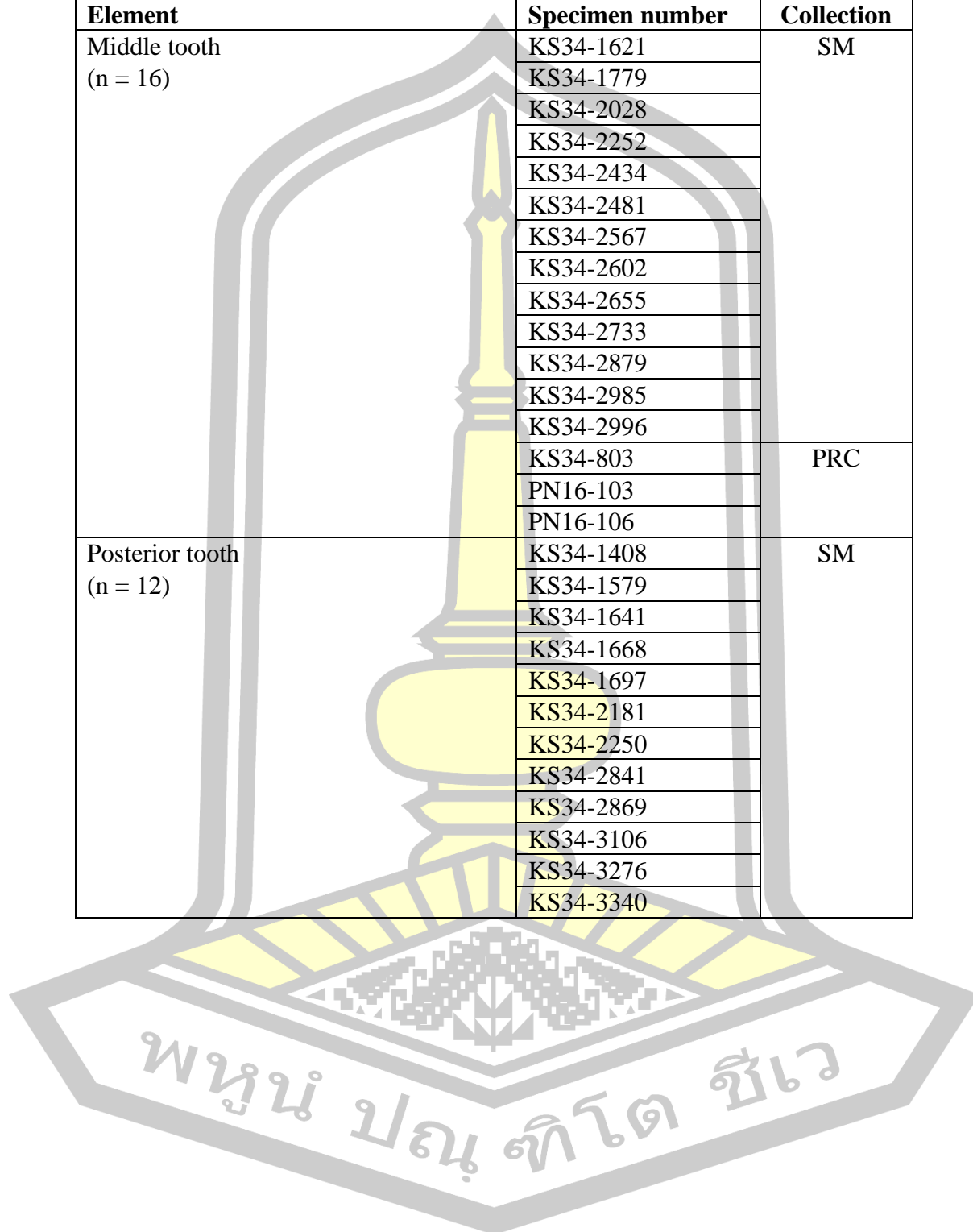


Table 2 Continued

| Element | Specimen number | Collection |
|---|--|------------|
| Anterior cervical centrum (n = 1) | PN17-47 | PRC |
| Middle cervical neural arch (n =1) | No number | |
| Middle cervical vertebra (n=1) | PN602 | |
| Posterior cervical neural arch (n = 2) | No number PN17-? | |
| Posterior cervical vertebra (n = 3) | PN 15-123 PN 138 PN 139 | |
| Anterior to middle cervical rib (n = 1) | PN9-49 | |
| Middle cervical rib (n = 5) | KS34-1970 KS34-2746 PN15-74 No number PN14-115 | |
| Anterior dorsal neural arch (n = 2) | PN15-16 PN582 | PRC |
| Anterior dorsal vertebra (n = 1) | PN581 | |
| Middle dorsal vertebra (n = 2) | PN15-49 PN692 | |
| Posterior dorsal neural arch (n = 1) | PN13-23 | |
| Posterior dorsal vertebra (n = 3) | PN17-147 No number (2 articulated) | |
| Anterior dorsal rib (n = 2) | KS34-3184 KS34-2466 | SM |
| Middle dorsal rib (n = 1) | No number | |
| Posterior dorsal rib (n = 3) | KS34-2787 KS34-1082 KS34-3014 | |

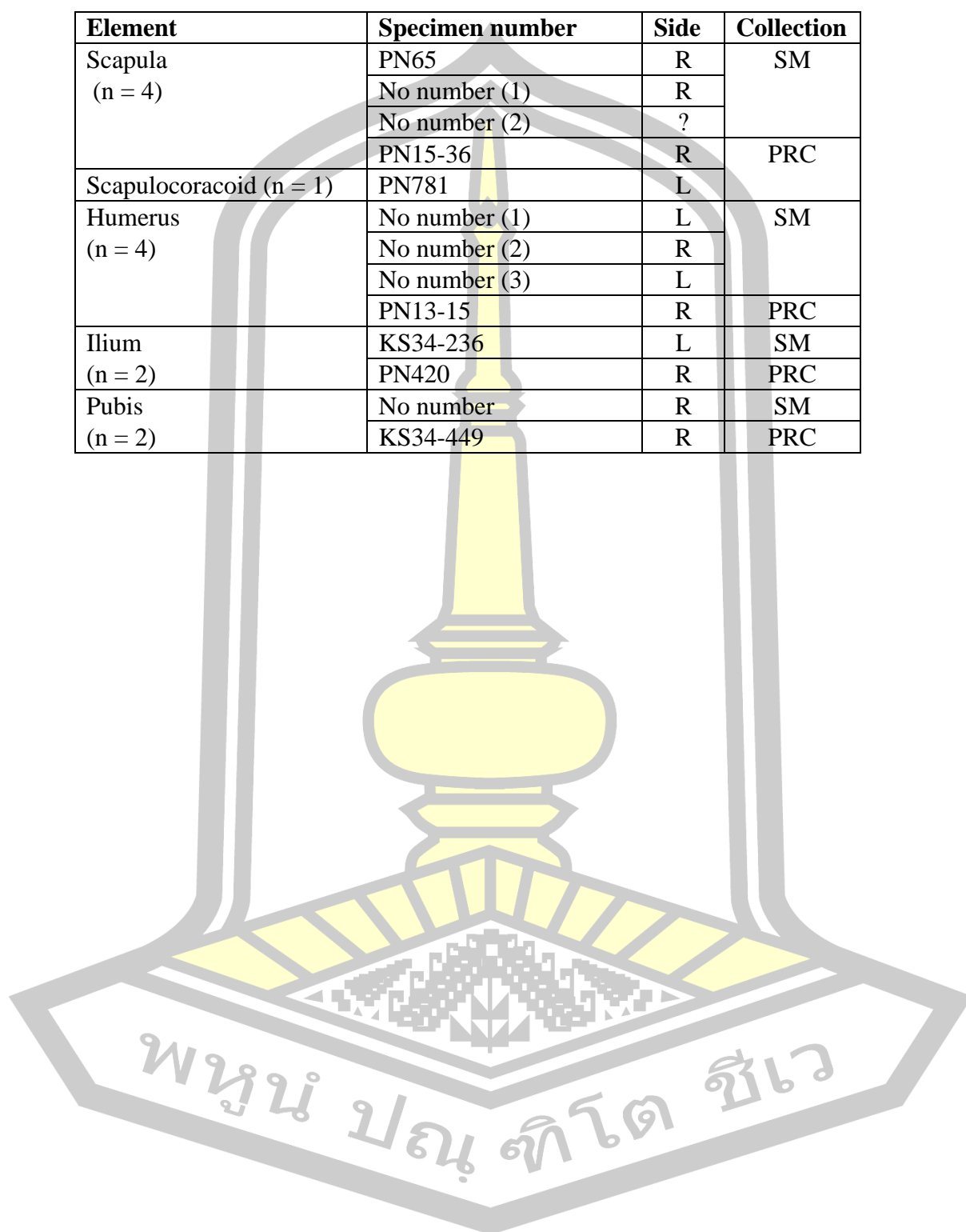
พหุ ประถมศึกษา

Table 2 Continued

| Element | Specimen number | Collection |
|--|-----------------|------------|
| Anterior caudal vertebra (n = 2) | No number | PRC |
| | PN14-146 | |
| Middle caudal vertebra (n = 9) | PN14-212A | |
| | PN14-212B | |
| | PN14-212C | |
| | PN14-212D | |
| | PN14-212E | |
| | PN14-212F | |
| | PN15-80 | |
| | PN15-81 | |
| | KS34-500 | |
| Middle to posterior caudal vertebra (n = 3) | PN645 | |
| | PN689 | |
| | PN13-14 | |
| Posterior caudal vertebra (n = 4) | PN16-04 | |
| | PN16-05 | |
| | PN16-06 | |
| | PN16-07 | |
| Distal caudal vertebra (n = 6) | PN14-34 | |
| | PN14-14 | |
| | PN14-17 | |
| | PN14-40 | |
| | PN14-31 | |
| | PN14-30 | |
| Anterior chevron (n = 6) | KS34-1004 | |
| | KS34-631 | |
| | PN13-11 | |
| | PN15-151 | |
| | PN15-186 | |
| | PN638 | |
| Middle chevron (n = 2) | KS34-2240 | SM |
| | KS34-2797 | |
| Posterior chevron (n = 3) | KS34-1166 | |
| | KS34-2244 | |
| | KS34-2311 | |

Table 2 Continued

| Element | Specimen number | Side | Collection |
|-------------------------|-----------------|------|------------|
| Scapula (n = 4) | PN65 | R | SM |
| | No number (1) | R | |
| | No number (2) | ? | |
| | PN15-36 | R | PRC |
| Scapulocoracoid (n = 1) | PN781 | L | |
| Humerus (n = 4) | No number (1) | L | SM |
| | No number (2) | R | |
| | No number (3) | L | |
| | PN13-15 | R | PRC |
| Ilium (n = 2) | KS34-236 | L | SM |
| | PN420 | R | PRC |
| Pubis (n = 2) | No number | R | SM |
| | KS34-449 | R | PRC |



CHAPTER 4

RESULTS

4.1 Descriptions and Comparison

4.1.1 Cranial materials

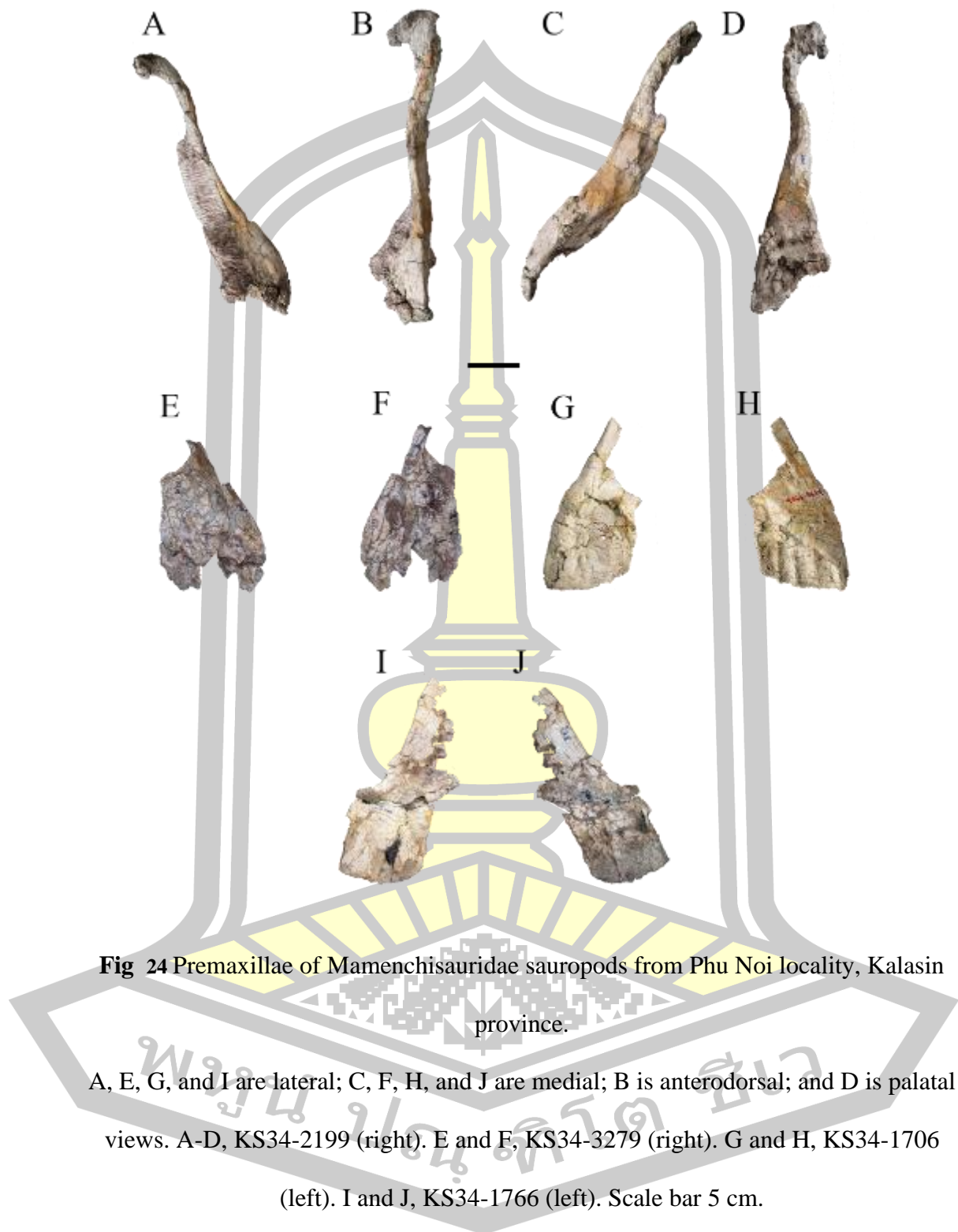
Premaxillae

All sauropods have four alveoli and four nutrient foramina in the premaxilla, possessed inside a thick sub-rectangular main body. The premaxillae represent the posterodorsally directed elongate and the medio-laterally narrow ascending process, which is initiated from the middle of the dorsal area of the main body. The shapes of bones are shared with all eusauropod and macronarians, as the ancestral state (Curry Rogers & Wilson, 2005; Wilson, 2002; Wilson & Sereno, 1998). On the other hand, they differ from diplodocoids and advanced titanosaurs, which are the derived state, anteroposterior directed of elongated sub-rectangular premaxillae (D’Emic, 2012; Tschoop, Mateus, & Benson, 2015; Whitlock, 2011; Wilson, 2002; Wilson & Sereno, 1998).

Four premaxillae from Sirindhorn Museum (Fig. 24) represented the anteroposteriorly short subrectangular main body with shallow narial fossa on the dorsal area and posterodorsal directed rod-like ascending process. Three left and one right premaxillae (KS34-1706, KS34-1766, and KS34-3279) with the additional preparing right premaxilla (KS34-2199) with four alveoli on the ventral dentigerous shelves resemble the non-mizzle premaxillae of the referred specimen of *Mamenchisaurus hochuanensis* (ZDM0126) and *Omeisaurus maoianus* (ZNM8510) (Ouyang & Ye, 2001; Tang, Jin, & Kang, 2001).

The elements are rather well preserved, which represent the main body with the dental area and the almost completed ascending process with the trace of the dorsomedial recess area of the narial fossa. Due to the completeness of KS34-1766 and the preparation of KS34-2199, these two specimens are representative of all.

The specimen KS34-1766 is the left premaxilla that preserves almost every part of the bone, which is transversely broken in half on the vertical level between the dorsal most lateral area of the main body and the proximal end of the ascending process with posteriorly lie narial fossa. The 110 degrees posteriorly lean of the sub-rectangular main body, which has an erupting tooth on the lower middle area of the lateral surface by the transverse compression. The overall distal edges are eroded but keep the main outline, including the blunt tip lateral dentigerous shelf. The medial surface shows compressed alveoli with four nutrient foramina, and three anteroposterior foramina possessed inside by the replacement teeth, the first foramen is broken and reveals the tooth inside. The lateral surface of the upper part of the bone, the ascending process with the adjacent anterior narial fossa, bends 110 degrees from the horizontal plain. Even with the cause of transverse compression, the narial fossa still show the trace of weakly recess cavity of narial fossa along the vertical area to the half of the height of ascending process, that distinguish the specimen from the non-posterior recess area of the dorsal process of maxilla.



The upper process area flattens on the medial surface without the posterior maxillary suture, that damaged and not preserved in all premaxillae. There is the

small, short step area on the anterior border between the main body and the ascending process, which not found in other three smooth anterior border premaxillae, might be the effect of compression.

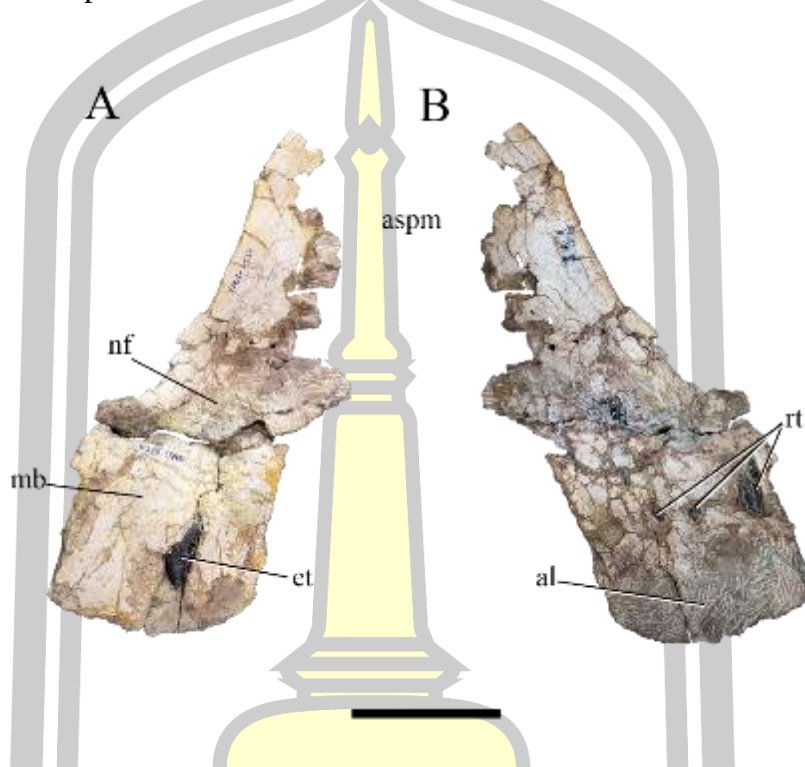


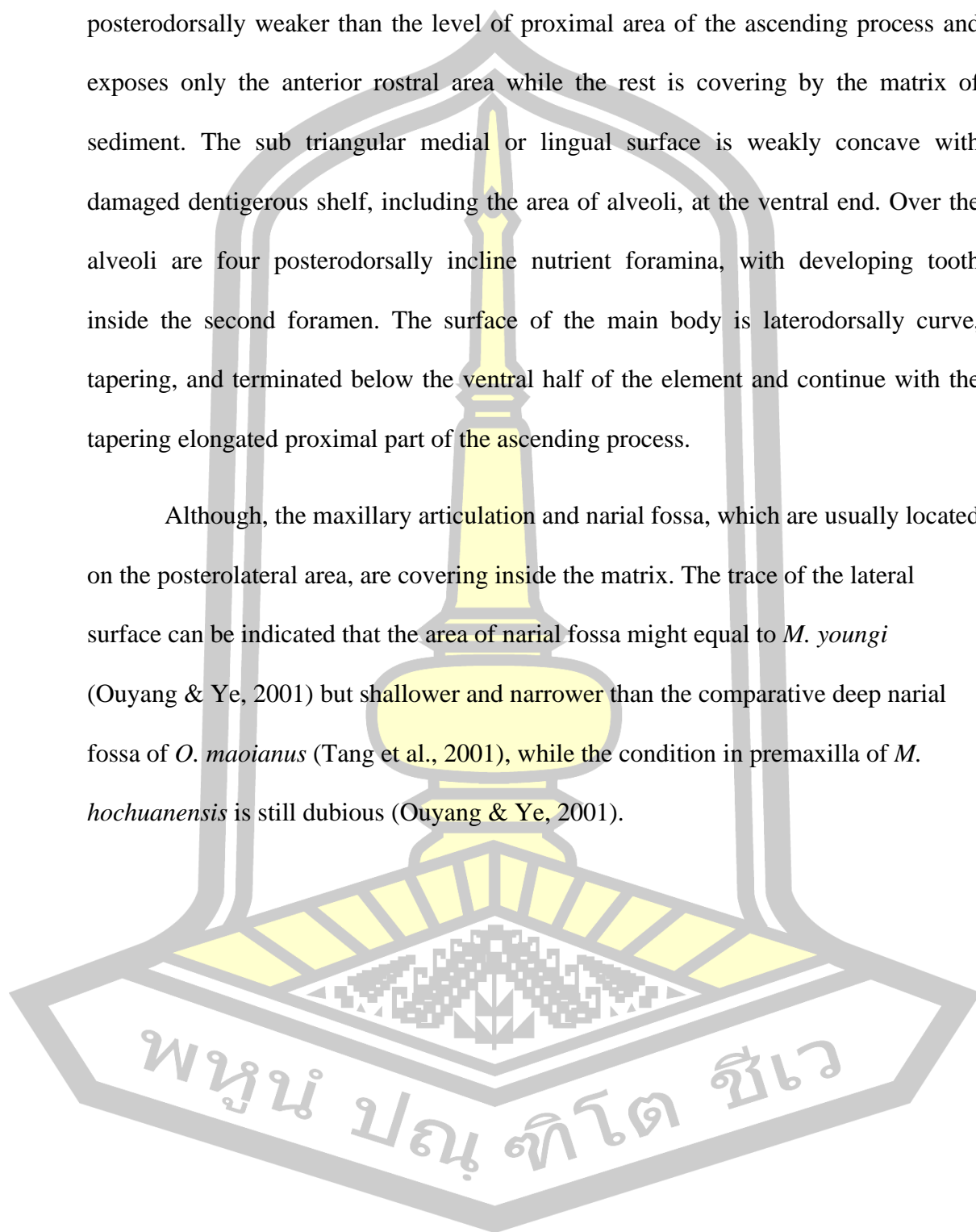
Fig 25 The left premaxilla KS34-1766.

A lateral; and B medial views. Scale bar represents 5 cm.

The right premaxilla KS34-2199 is almost perfectly preserved, completely preserve the parts of the element and the original dimensions. The medial surface is the smooth medially plain, which is the articulation area of the counterpart premaxilla, dorsoventrally line along the weakly sigmoid curve of the height of element. The transverse thickness of main body is increasing from the ventral portion to the middle height, where is the dorsal end of the palatal shelf. The thickest area is static dorsally then rapidly tapering at the initial area of the proximal half of ascending process.

The lateral surface is smooth and transversely convexing outward, which is posterodorsally weaker than the level of proximal area of the ascending process and exposes only the anterior rostral area while the rest is covering by the matrix of sediment. The sub triangular medial or lingual surface is weakly concave with damaged dentigerous shelf, including the area of alveoli, at the ventral end. Over the alveoli are four posterodorsally incline nutrient foramina, with developing tooth inside the second foramen. The surface of the main body is laterodorsally curve, tapering, and terminated below the ventral half of the element and continue with the tapering elongated proximal part of the ascending process.

Although, the maxillary articulation and narial fossa, which are usually located on the posterolateral area, are covering inside the matrix. The trace of the lateral surface can be indicated that the area of narial fossa might equal to *M. youngi* (Ouyang & Ye, 2001) but shallower and narrower than the comparative deep narial fossa of *O. maoianus* (Tang et al., 2001), while the condition in premaxilla of *M. hochuanensis* is still dubious (Ouyang & Ye, 2001).



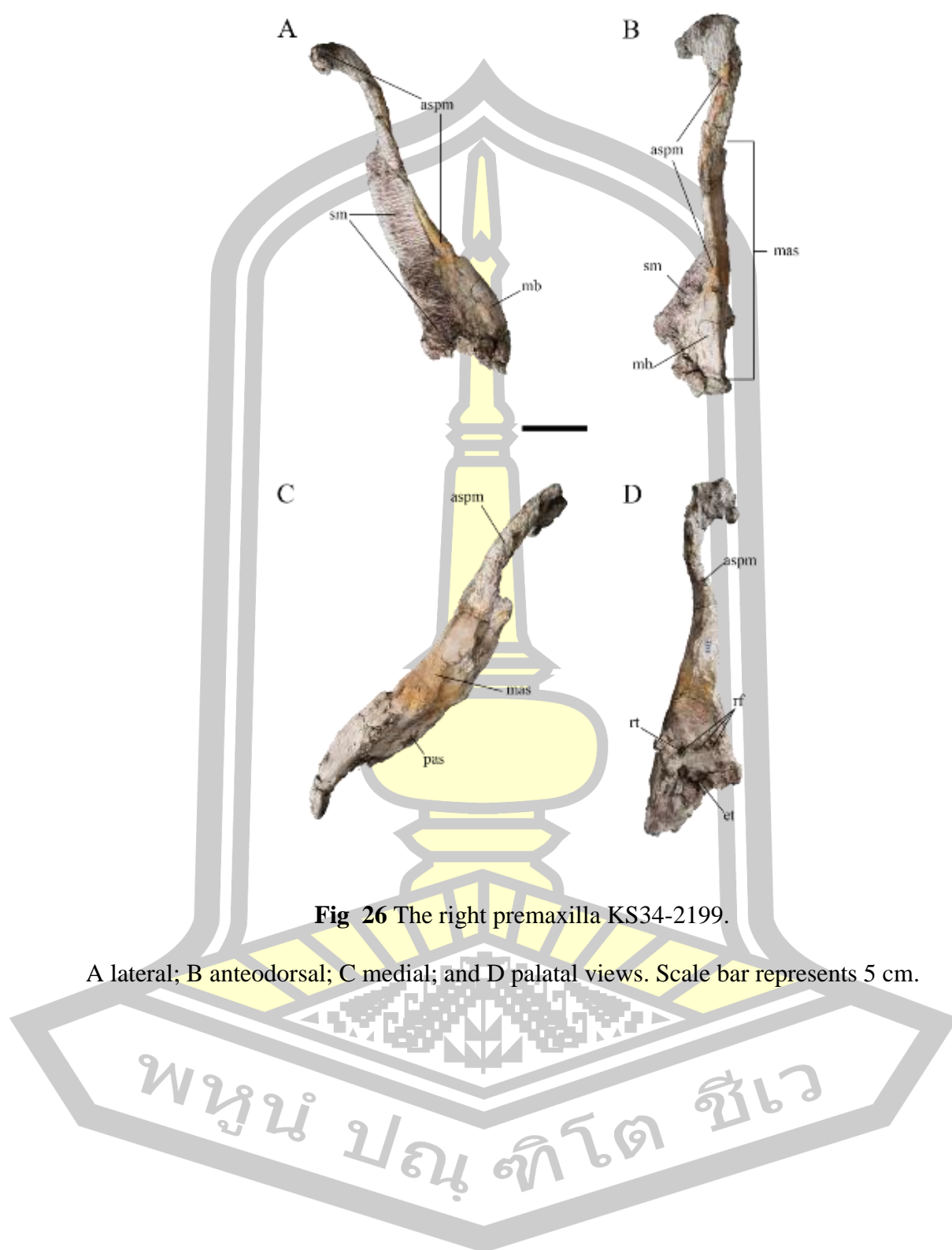


Fig 26 The right premaxilla KS34-2199.

A lateral; B anteodorsal; C medial; and D palatal views. Scale bar represents 5 cm.

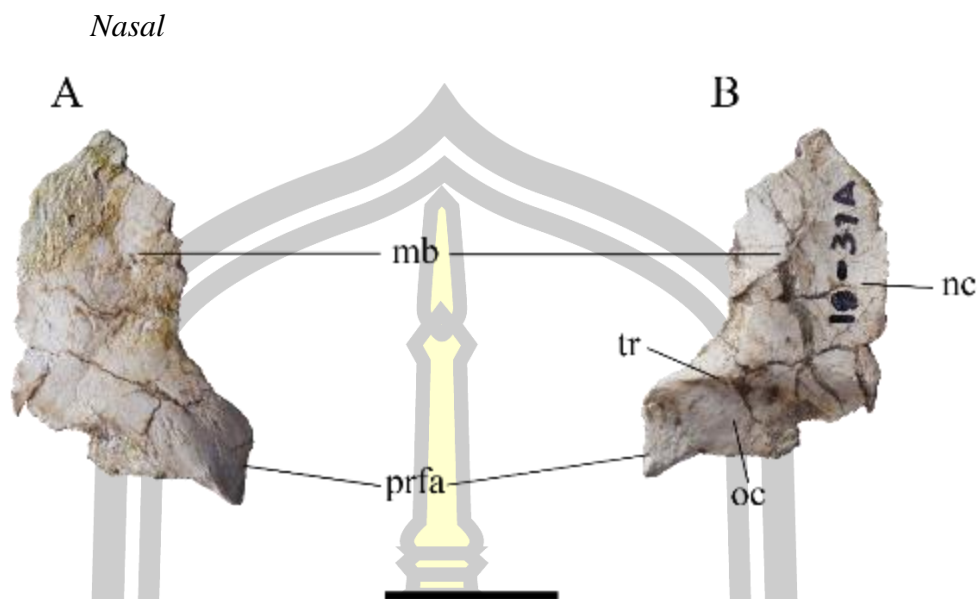


Fig 27 Nasals of Mamenchisauridae sauropod from Phu Noi locality, Kalasin province.
A is lateral; B is medial views. A and B, PN19-31A. Scale bar represents 5 cm.

The dorsoventrally compressed and extremely flattened laminate bone fragment from PRC collection (PN19-31A) is diagnosed to the main body of right nasal by the presence of prefrontal articular facet on the posteroventral edge. Moreover, it has two excavated area on the medial surface, the anteroposterior elongated nasal cavity, and the posterior mediolateral elongated orbital cavity, respectively. PN19-31A is the anterior half of nasal-frontal-parietal element, which will mention again in the frontal description.

Frontal-parietal

There are four specimens which have participated to other elements (Fig 28). PN15-218 is the articulated prefrontal-frontal-partial parietal and PN19-31 is frontal-parietal from the collection of PRC. The other two are KS34-1691 right frontal-parietals, and the partial fragmented left frontal KS34-2543, from the SM collection.

Due to the completeness of the preservation, PN19-31 is selected to be the representative of all specimens.

The right frontal-parietal PN19-31 (Fig. 29), which is the posterior half of the mentioned isolated right nasal PN19-31A, is 12.75 cm in anteroposterior length and 10.23 cm in mediolaterally width. The element occupies the two third of anteroposteriorly length of the dorsal roof to the posterior end of the skull. It preserves the subtriangular pointed lateroventral process, which is the posterodorsal margin of the anorbital fenestra, posteriorly and ventrally connected to prefrontal and lachrymal, respectively. The ventral surface has anteroposteriorly elongates middle weak depression and posterolaterally nasal cavity on the anterior end.

The main frontal-parietal portion is the strongly fused plate of right frontal and parietal, which preserves almost landmarks except the anteromedial region of the nasal articular surface. On the dorsal surface, the frontal bears numerous crack lines with middle impression area, which either the characteristic of the bone like the frontal of *Bellusaurus sui* IVPP V17768.5-7 (Moore et al., 2018) or cause by the taphonomic deformation (Fig 30). On the lateral area of the anterior surface represented two deep outwardly crescent cavities, which are the outer rim of the nasal articular facet and the deeper prefrontal facet, respect from the mediolateral direction. The orbital rim is located on the anterolateral border, subsequently outward curved to the widest elongated pointed postorbital process of the frontal at the middle of the specimen, or the posterolateral end of frontal.

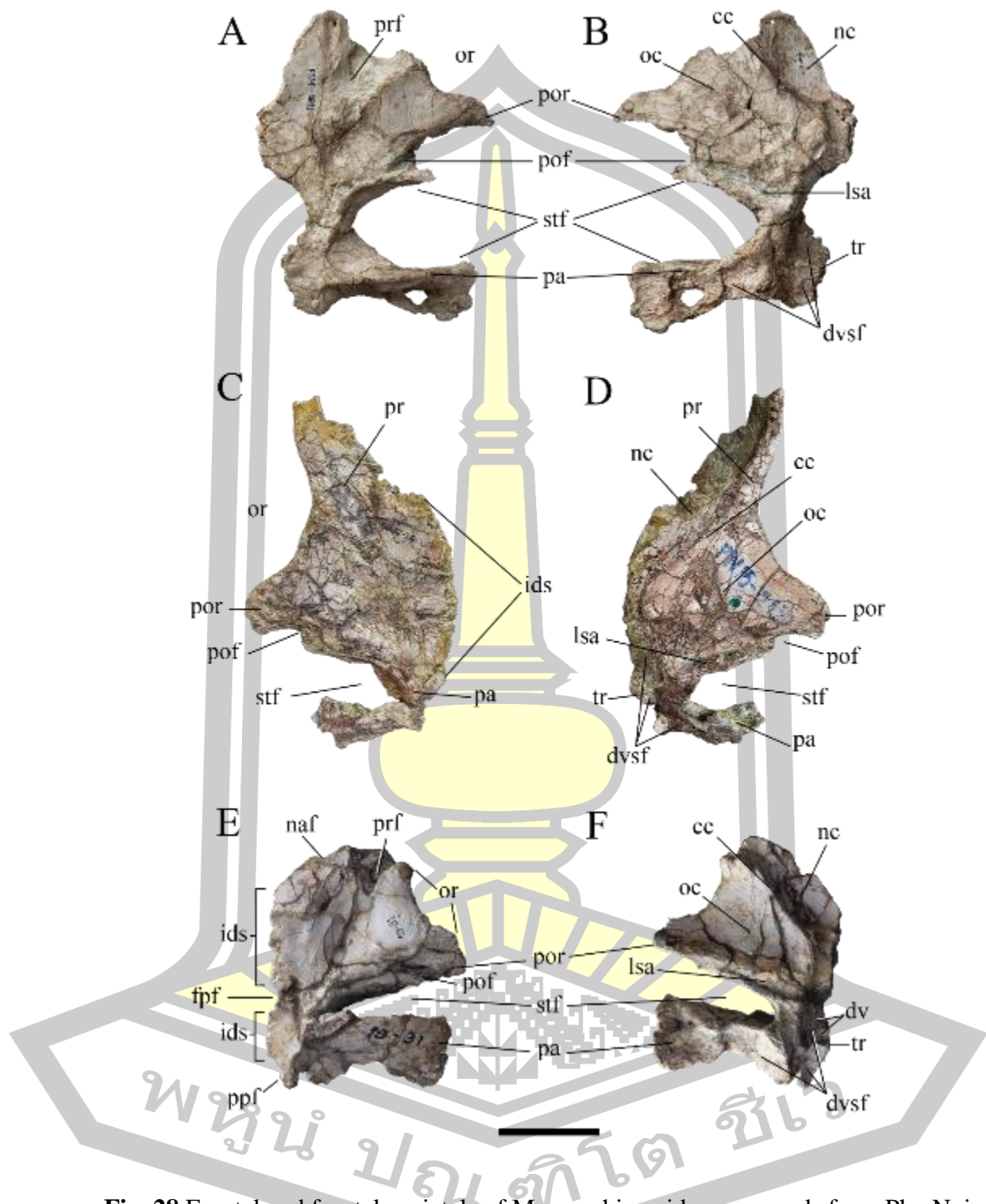
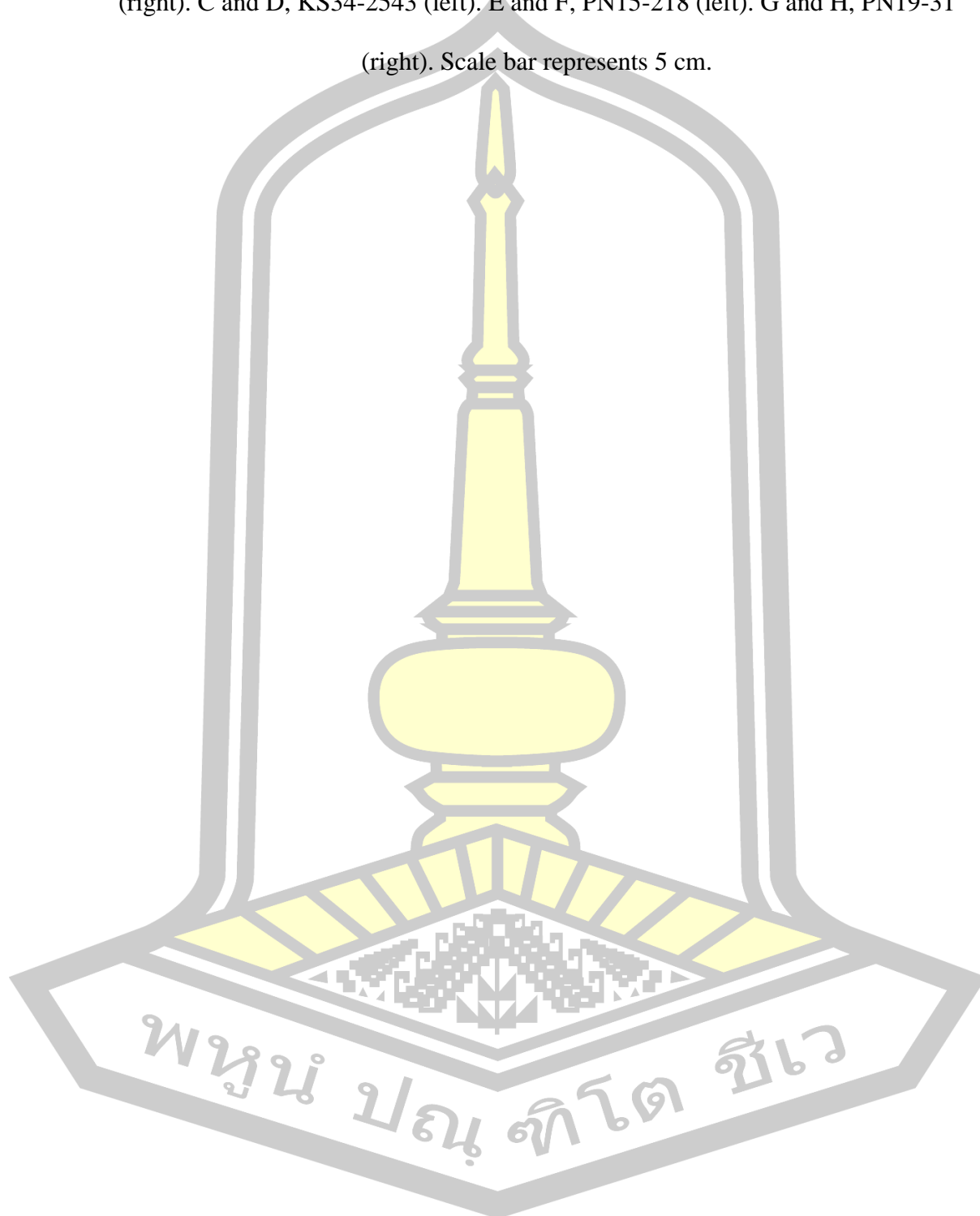


Fig 28 Frontal and frontal-parietals of Mamenchisauridae sauropods from Phu Noi locality, Kalasin province.

A, C, E, and G are lateral view; B, D, F, and H are medial view. A and B, KS34-1691 (right). C and D, KS34-2543 (left). E and F, PN15-218 (left). G and H, PN19-31 (right). Scale bar represents 5 cm.



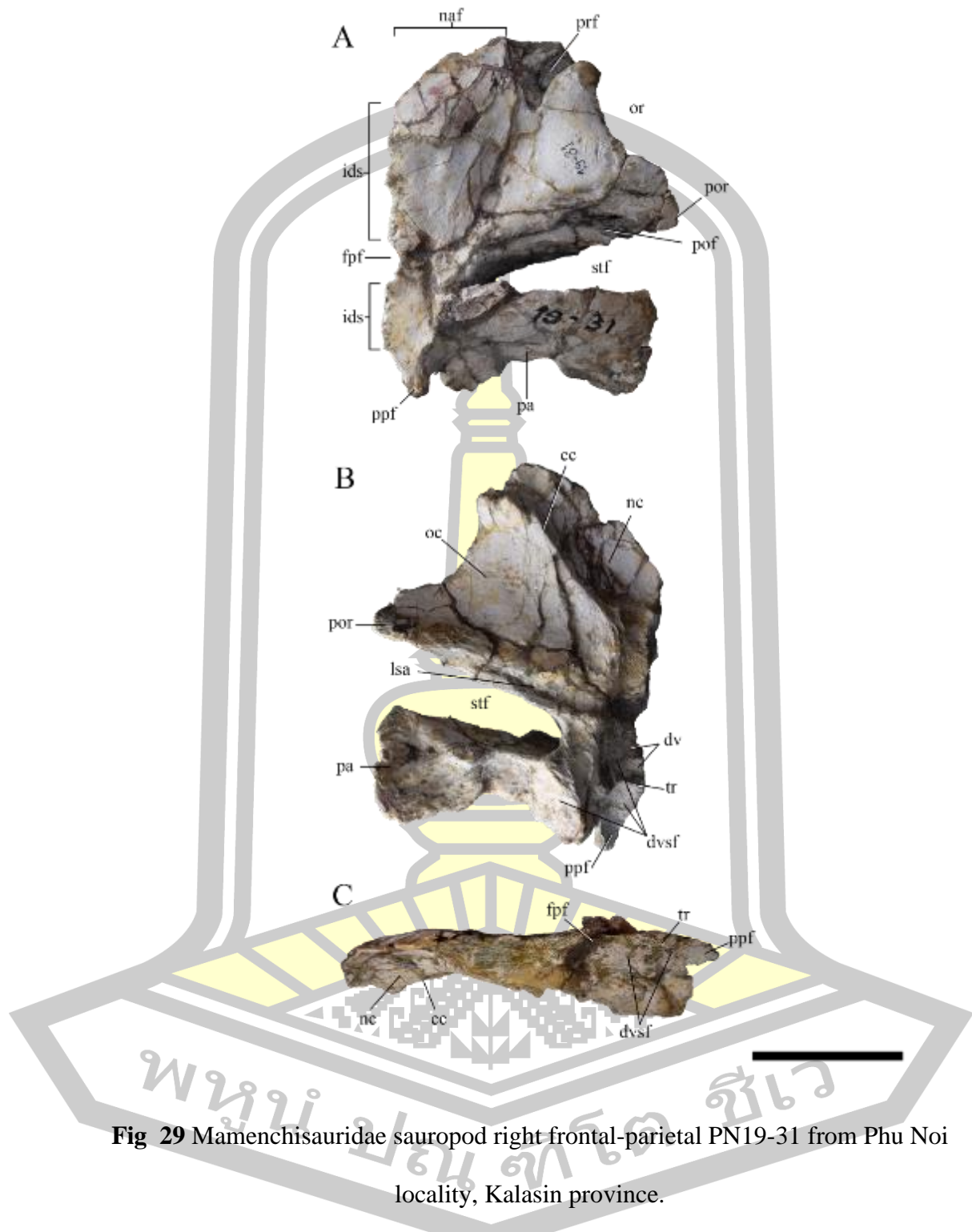


Fig 29 Mamenchisauridae sauropod right frontal-parietal PN19-31 from Phu Noi locality, Kalasin province.

A dorsal; B ventral; and C medial views. Scale bar represents 5 cm.

The orbital rim is thicker than the rest of the bone with small numerous tubercles on the smooth surface of the rim. The ventrolateral directed postorbital process, which occupies the posterolateral area of frontal and creates the anterolateral rim of the supratemporal fenestra, is lost but preserved in the fragment frontal KS34-2543 as elongated pointed process.

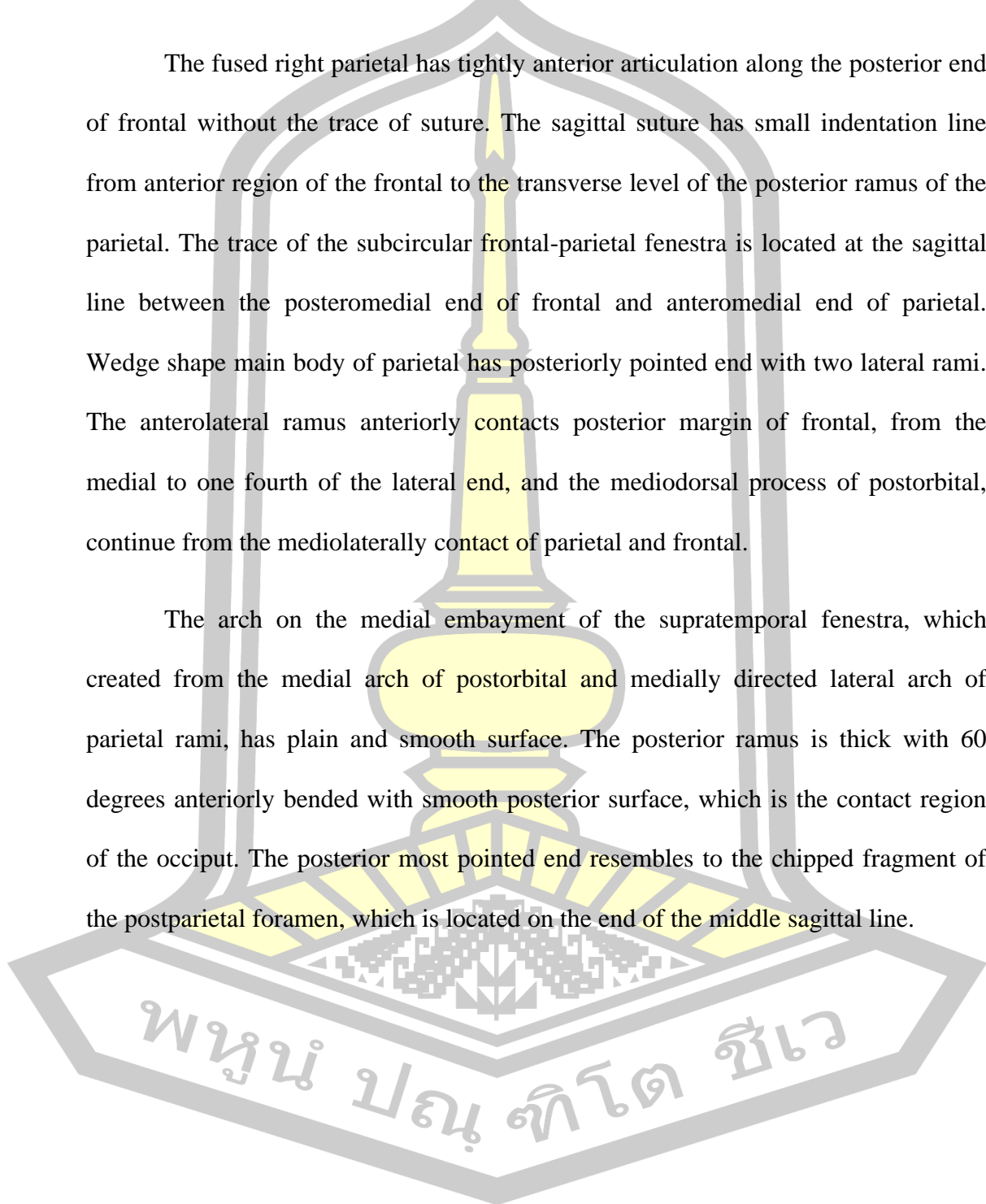
The main frontal-parietal portion is the strongly fused plate of right frontal and parietal, which preserves almost landmarks except the anteromedial region of the nasal articular surface. On the dorsal surface, the frontal bears numerous crack lines with middle impression area, which either the characteristic of the bone like the frontal of *Bellusaurus sui* IVPP V17768.5-7 (Moore et al., 2018) or cause by the taphonomic deformation (Fig 30). On the lateral area of the anterior surface represented two deep outwardly crescent cavities, which are the outer rim of the nasal articular facet and the deeper prefrontal facet, respect from the mediolateral direction. The orbital rim is located on the anterolateral border, subsequently outward curved to the widest elongated pointed postorbital process of the frontal at the middle of the specimen, or the posterolateral end of frontal. The orbital rim is thicker than the rest of the bone with small numerous tubercles on the smooth surface of the rim. The ventrolateral directed postorbital process, which occupies the posterolateral area of frontal and creates the anterolateral rim of the supratemporal fenestra, is lost but preserved in the fragment frontal KS34-2543 as elongated pointed process.

In Mamenchisaurids, the ventrolateral border of frontals has one third mediolateral transverse depth of the postorbital facet like in *M. youngi*, *O. maoianus*, and *Bellusaurus sui* (Moore, Mo, Clark, & Xu, 2018; Ouyang & Ye, 2001; Tang et

al., 2001), unless *Qijianglong guokr* (QJGPM 1001), which have highly elongated anterior parietal ramus (Xing et al., 2015) (Fig 30).

The fused right parietal has tightly anterior articulation along the posterior end of frontal without the trace of suture. The sagittal suture has small indentation line from anterior region of the frontal to the transverse level of the posterior ramus of the parietal. The trace of the subcircular frontal-parietal fenestra is located at the sagittal line between the posteromedial end of frontal and anteromedial end of parietal. Wedge shape main body of parietal has posteriorly pointed end with two lateral rami. The anterolateral ramus anteriorly contacts posterior margin of frontal, from the medial to one fourth of the lateral end, and the mediodorsal process of postorbital, continue from the mediolaterally contact of parietal and frontal.

The arch on the medial embayment of the supratemporal fenestra, which created from the medial arch of postorbital and medially directed lateral arch of parietal rami, has plain and smooth surface. The posterior ramus is thick with 60 degrees anteriorly bended with smooth posterior surface, which is the contact region of the occiput. The posterior most pointed end resembles to the chipped fragment of the postparietal foramen, which is located on the end of the middle sagittal line.



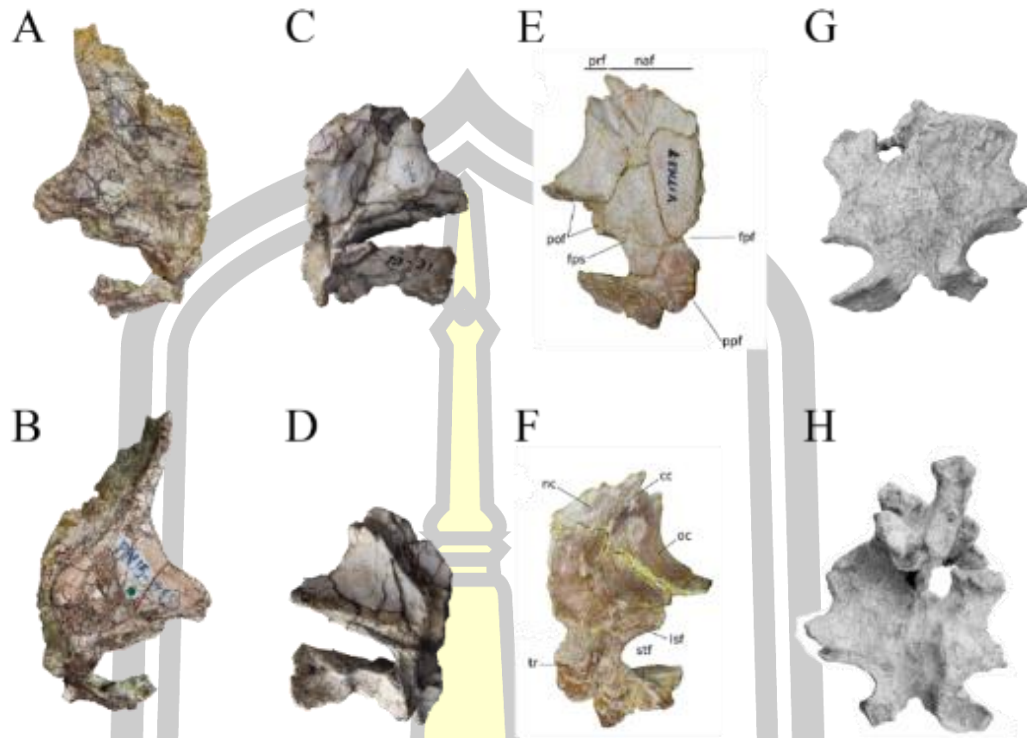


Fig 30 The comparison of frontal-parietals from Phu Noi locality, Kalasin province with *Bellusaurus sui* (V17768.7) and *Qijianglong guokr* (QJGPM 1001).

A, C, E, and G are dorsal view; B, D, F, and H are ventral view. A and E, PN15-218 (left). B and F, PN19-31 (right). C and H, IVPP V17768.7 (left). D and H, QJGPM 1001. Not to scale.

The ventral surface shows two main large cavities on the anterior half, the posterior portion of the nasal cavity at the anteroventral region on the bone, which posteriorly connected to the anteroposteriorly elongated channel of the anterior fenestra and the olfactory trough of cranial nerve I that reach to the endocranial cavity. The posterolateral larger cavity is the roof of orbital cavity, which housed the eyeball and separated from the nasal cavity by the single smooth edge anterolateral ridge of crista canaii. Posteriorly to the orbit, there are the pair of parallel mediolateral line of orbitosphenoid suture and frontal parietal suture. The lateral portion of the

orbit is the mentioned postorbital process, which have plain and smooth ventral surface.

The posterior area is the ventral surface of parietal, which has multiple recess areas and cavities on the sagittal region of the main body. The anteromedial most portion that connected to frontal, is the trace of the small sub elliptical frontoparietal fenestra, which had housed the pineal gland. Two cavities of diploic vein located in the shallow excavation area, posterior to the frontoparietal fenestra, which is anteroposteriorly arranged. Subsequently, there is the transverse ridge separates the dural venous sinuses into anterior and posterior compartment, which stacking on the area of diploic vein. The total number of diploic vein are three, two of them are mentioned on the posterior area of the recess sagittal region with additional one large elliptical vein on the middle of the ventral surface of parietal's posterior ramus.

Occipital

Because of the completeness, PN14-139 is the most important cranial from the locality, which is the assembled of articulated posterior region of the skull roof. The remain elements are left prefrontal, frontals, parietals, and supraoccipital on the dorsal portion, which have almost completely closed and fused sutures except the visible prefrontal sutures. On the posterior portion, there are exoccipitals with paraoccipital processes, occipital condyle, basioccipital processes, and basiptyergoid processes of the basisphenoid with anteriorly projected single parasphenoid on the medial portion. Unfortunately, the laterosphenoids, orbitosphenoids, and prootics are missing.

As the other pieces of the bone in the collections, the left prefrontal, one of three preserved elements, is articulated to the succeeding frontal. It is the elongate

element with tapering width on both proximal and distal ends, which the distal is taper than the proximal. In normal condition, the bones occupy the anterolateral area of the frontals and lines into the anterolateral arch to form the anterodorsal margin of the orbit. The middle and distal end are gently curve to the ventral direction and connect with the posterolateral area of the nasal and the posterior portion of the main body of lachrymal, respectively.

The dorsal surface of the frontals is filled with numerous crack lines, which are difficult to notice the midline suture, oppose to the less damaged ventral surface, which the midline suture is visible. It looks like the fused sub rectangular with weakly inward curve lateral edges, short offset on the posterolateral edges, and crescent prefrontal facet on the anterolateral area of the transverse plain anterior margin. The posterior margin is gently inward curve on the fused suture of the frontal-parietal area. As the dorsal cavity of the orbit, the ventral surface of frontal has large mediolateral weakly concave area of orbital cavity and the smaller elongated anteromedial concave posterior part of nasal cavity, that anterolateral separated by the lateromedially oblique line of crista cranii.

Parietals are completely fused to the counterpart, the preceding frontals, and the succeeding supraoccipital. By the anteroposterior compression, the bone and the supratemporal fenestra are anteroposterior narrower than the normal form. The anterolateral process, frontal wing of parietal, are transversely shorter than the posterolateral process, also known as occipital wing. The fronto-parietal fenestra and post parietal foramen are not detected, which might be absent, or the ossified bones are covering the foramina.

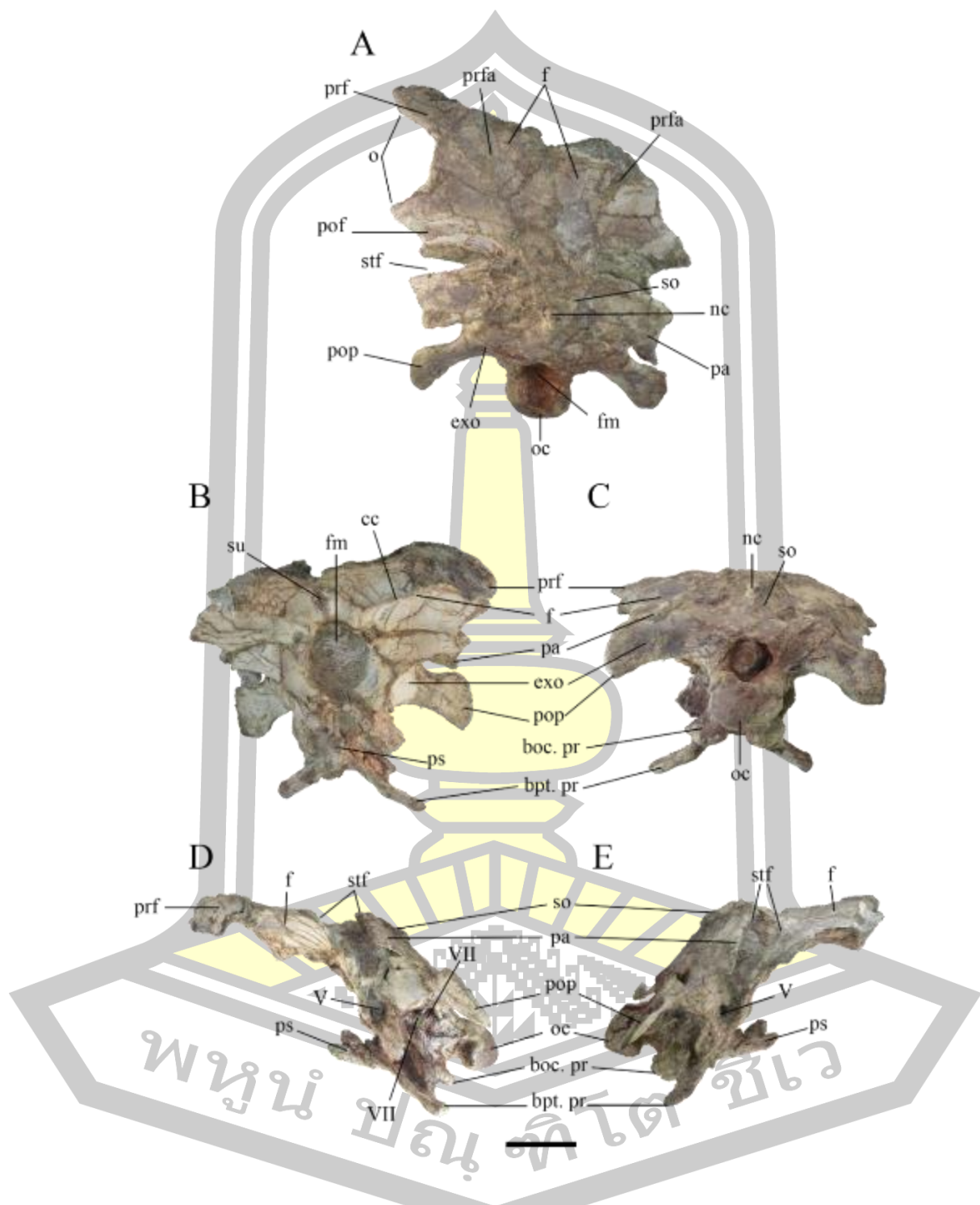


Fig 31 Mamenchisauridae occipital PN14-139 from Phu Noi locality, Kalasin province.

A posterodorsal; B anteroventral; C posterior; D left lateral; and E right lateral views.

Scale bar represents 5 cm.

Supraoccipital is equilateral sub triangular shape, which is located on the middle of posterodorsal portion. It anteriorly fused to the main body of the parietals, lateroventrally connected to exoccipital, and the ventral border forms the concave arch of the dorsal rim of foramen magnum. The apex of the bone is the middle vertical protrusion of the nuchal crest on the dorsal margin.

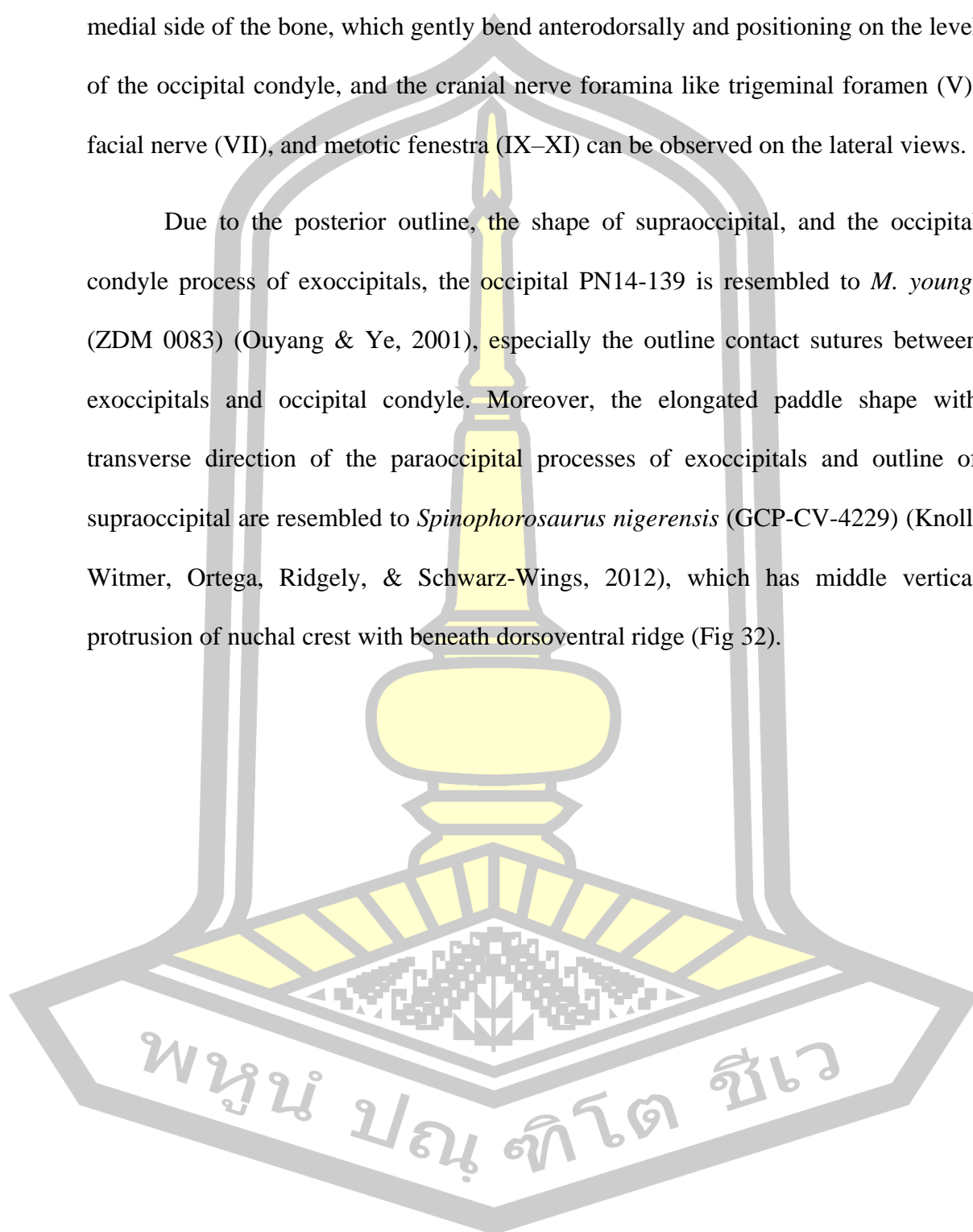
The winglike exoccipitals are almost completely dorsally and ventrally fused to the supraoccipital and basioccipital, respectively, which difficult to notice the sutures. The main body of the bone and its counterpart are the dorsolateral incline dorsal border with medial concave arches, which are the lateral margin of foramen magnum, and the ventral process that connect to the basioccipital and become the dorsolateral edges of the occipital condyle. The transversely directed winglike paraoccipital processes are elongated with expanded paddle like shape distal end, which have longer posteroventral edge than the posterodorsal.

Basioccipital is completely preserved with large, outstanding posterior directed of transversely wide ellipsoidal occipital condyle and the lateroventral direction pair of robust petal shape basioccipital processes. The dorsal surface of the occipital condyle represents wide but shallow anteroposterior directed trough to the foramen magnum, which might be the ventral support trough of the spinal cord and the beginning of the neural canal.

The ventral most part of the occiput beneath the basioccipital is the pair of ventrolateral directed in 45 degrees elongated slender shaft of basipterygoid process.

Moreover, there is the slender single straight middle parasphenoid on the internal or medial side of the bone, which gently bend anterodorsally and positioning on the level of the occipital condyle, and the cranial nerve foramina like trigeminal foramen (V), facial nerve (VII), and metotic fenestra (IX–XI) can be observed on the lateral views.

Due to the posterior outline, the shape of supraoccipital, and the occipital condyle process of exoccipitals, the occipital PN14-139 is resembled to *M. youngi* (ZDM 0083) (Ouyang & Ye, 2001), especially the outline contact sutures between exoccipitals and occipital condyle. Moreover, the elongated paddle shape with transverse direction of the paraoccipital processes of exoccipitals and outline of supraoccipital are resembled to *Spinophorosaurus nigerensis* (GCP-CV-4229) (Knoll, Witmer, Ortega, Ridgely, & Schwarz-Wings, 2012), which has middle vertical protrusion of nuchal crest with beneath dorsoventral ridge (Fig 32).



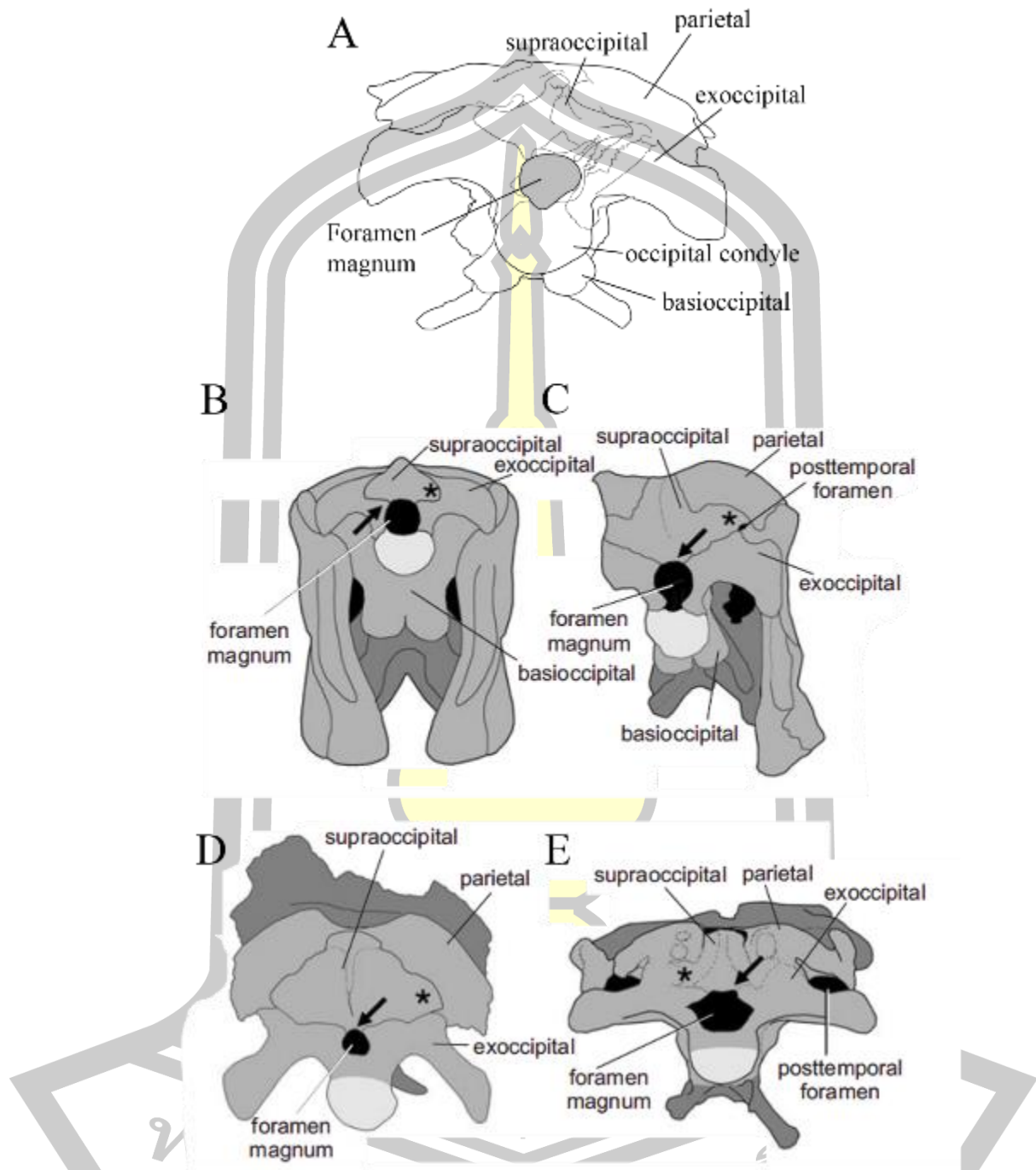


Fig 32 Comparison of Eusauropoda occipitals to Phu Noi specimens. All of illustrations are posterior view (not to scale).

A, PN14-139. B, *Shunosaurus lii* ZDM 65430 (Zhou and Zhang, 1983). C, *Mamenchisaurus youngi* ZDM 0083 (Ouyang and Ye, 2002). D, *Omeisaurus*

tianfuensis ZDM 5702 (He et al., 1988). E, *Spinophorosaurus nigerensis* GCP-CV-4229 (Remes et al., 2009). B to E, are from Xing et al., 2013 (fig.4).

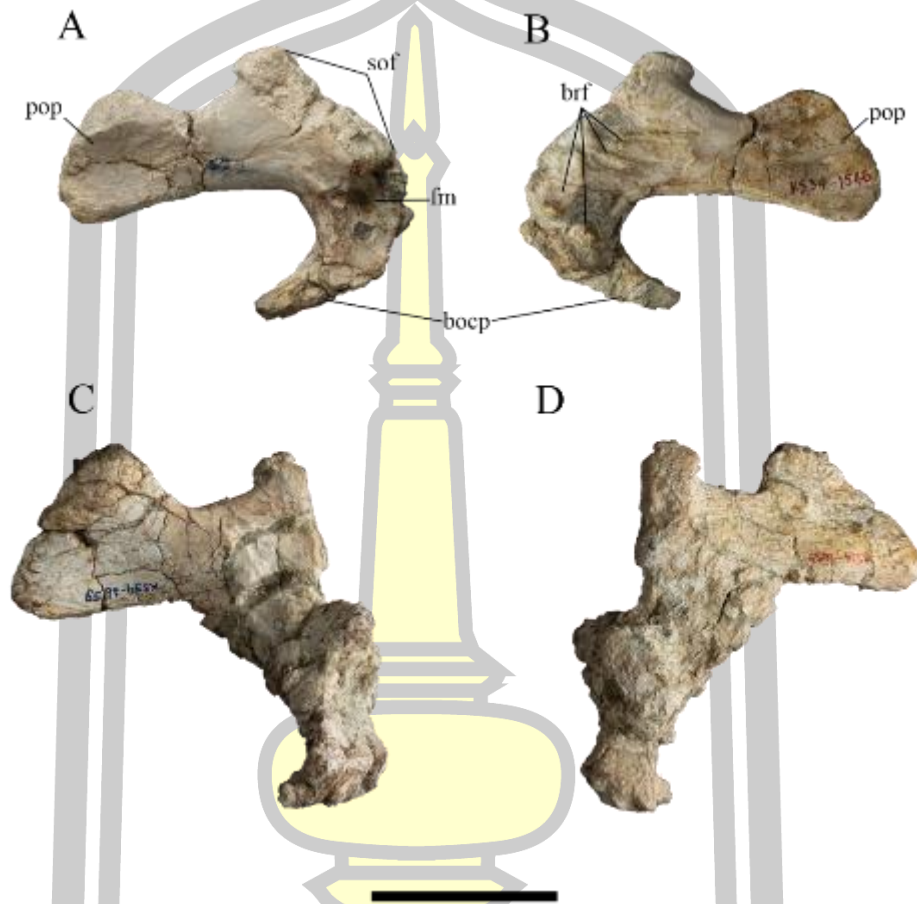


Fig 33 Exoccipitals of Mamenchisauridae sauropods from Phu Noi locality, Kalasin province.

A and C are posterior; B and D are internal views. A and B, KS34-1546 (left). C and D, KS34-1659 (left). Scale bar represents 5 cm.

Lachrymal

The lachrymal is the vertical pole like element, that separates the antorbital fenestra and the orbit. It is anterodorsally connecting with the dorsal process of maxilla, dorsally covered by nasal and prefrontal, anteroventrally attached to the

posterodorsal corner of the main body of maxilla, and ventroposteriorly covered by the lachrymal process of the jugal.

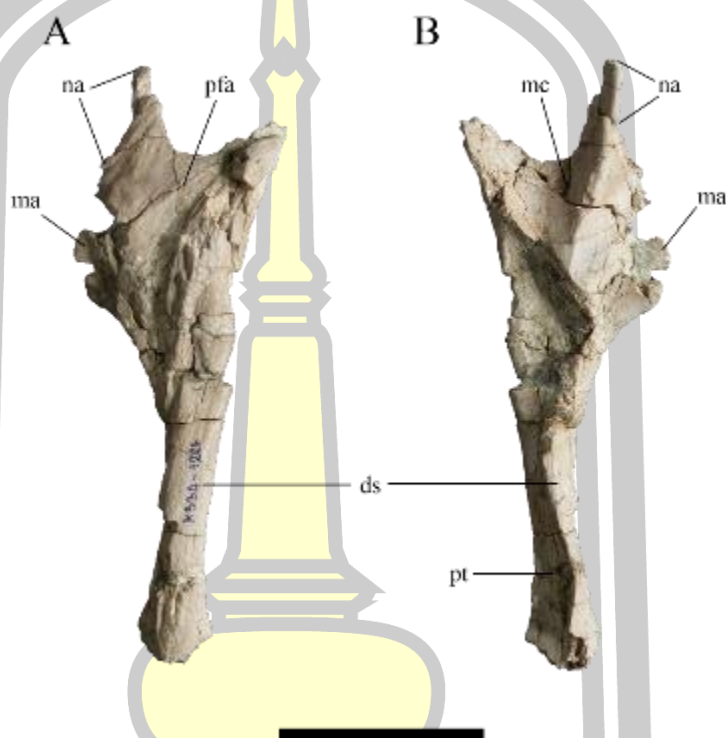


Fig 34 Left lachrymal KS34-1226.

A lateral; and B medial views. Scale bar represents 5 cm.

KS34-1226 is the Mamenchisauridae like lachrymal, which has vertically expanded laminate dorsal region with articular surfaces and processes and rod like vertical bar of bone. The lateral surface bears the large anterodorsal recess arch, for the placement of the distal portion of the ascending process of maxilla. The pair of small anterior processes are unknown while the small pointed dorsal process connects to the main body of nasal. Next from the process is the broken concave arch of the prefrontal articulation. The medial surface of lachrymal shaft has vertically deep

trough, continue from the subtriangular sharp edge excavation to the ventral end of the sigmoid curve trough. The anterior and dorsal portion of the medial surface are separated by the vertically oblique lamina of the dorsal process, which become the anterior mildly concave vertical arch and dorsal reverse subtriangular cavity.

Jugal

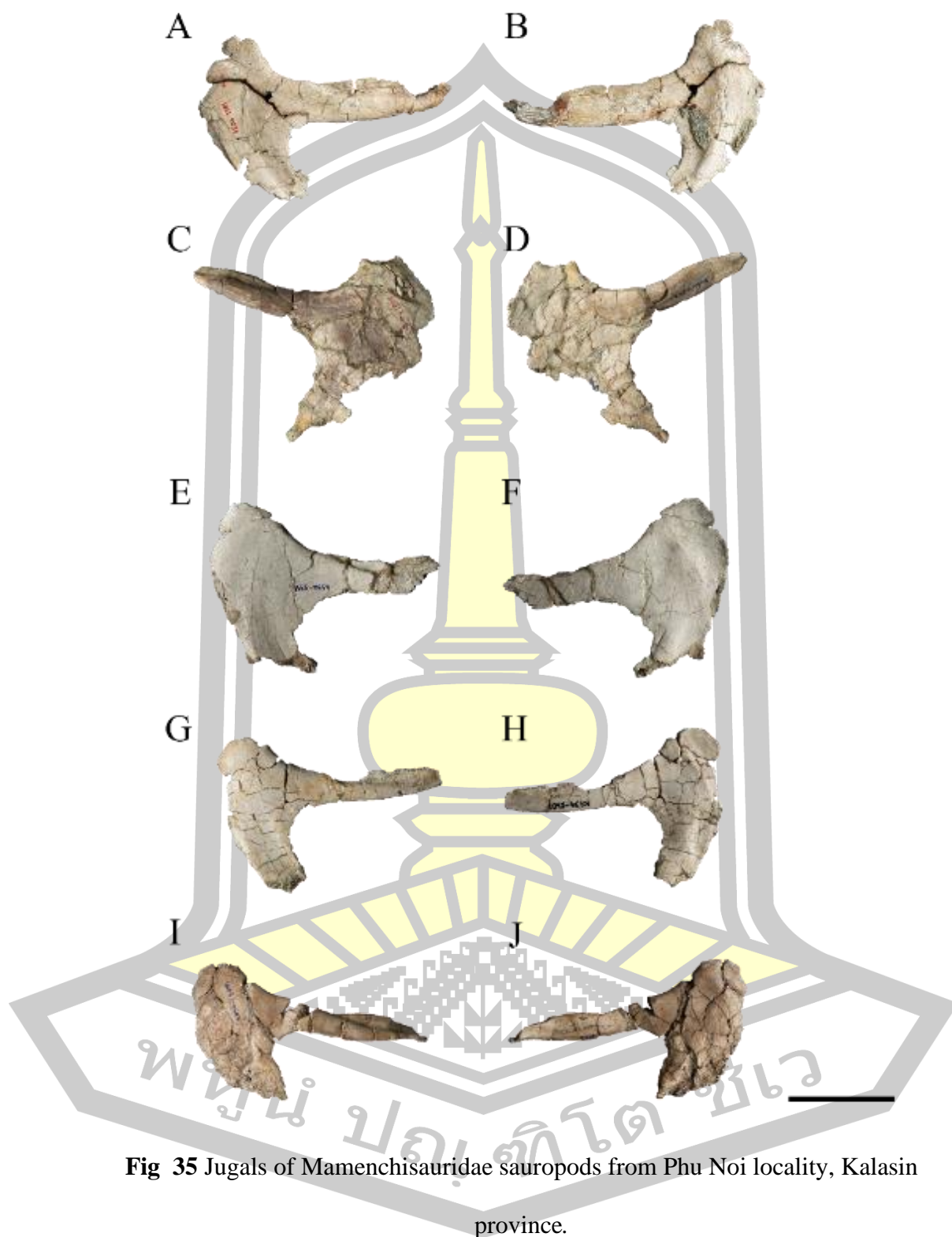
Jugal is the lower middle element of the skull, connecting between the posterior portion of the maxilla, articulated to the ventral process of the lachrymal, anteroventral process of the postorbital, and anteroventral process of quadratojugal. It has relatively small size, comparing to the cranial, with sub crescentic laminate main body and triradiate processes. The element composed of 1) the tiny lacrimal process at the dorsal area of the main body, 2) the posterior elongated and prominent postorbital process with dorsal recess area, from the middle to the distal end of the process, for the jugal process of the postorbital, and 3) the pointed posteroventral quadratojugal process.

There are five jugals from the collection of Sirindhorn Museum, which are separated to four left (KS34-1387, KS34-2511, KS34-2607, and KS34-2955) and one right side (KS34-1508). Due to the heavily compression on the bones, like every specimen in Phu Noi locality, it's hard to consider the details for diagnosing the elements. However, there might be at least two types of jugal among five specimens and the representative specimens are briefly described.

KS34-1387 (with KS34-2607, and KS34-2955) is the left jugal of *Mamenchisaurus* sp., considered from the broad crescent main body with long ventrodistal tip and the wide and elongated postorbital process (Ouyang & Ye, 2001).

The articular trough of the jugal process of postorbital is initial on the middle and terminated at distal end of the dorsal region of the postorbital process. While the medial surface of the main body bears the vertical smooth articular surface of maxilla, that dorsoventrally parallel along the anterior edge of jugal.





A, C, E, G, and I are lateral; B, D, F, H, and J are medial views. A and B, KS34-1387 (left). C and D, KS34-1508 (right). E and F, KS34-2511 (left). G and H, KS34-2607 (left). I and J, KS34-2955 (left). Scale bar represents 5 cm.

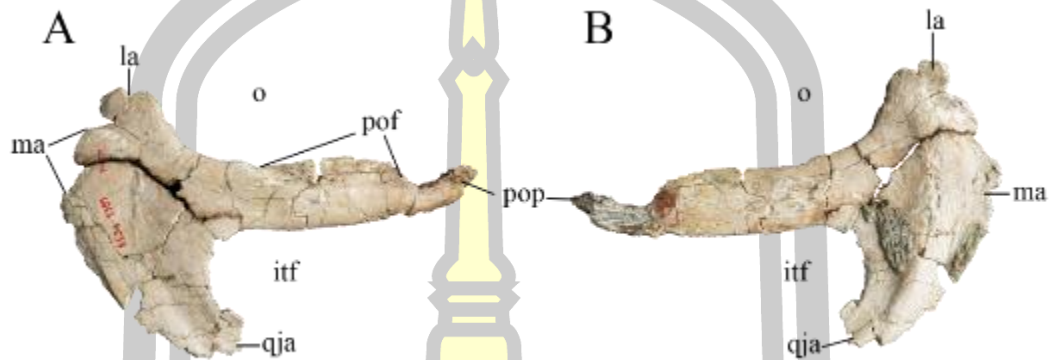


Fig 36 *Mamenchisaurus youngi* like left jugals KS34-1387.

A lateral; and B medial views. Scale bar represents 5 cm.

Postorbitals

There are one right postorbital from PRC (PN15-93) and five postorbitals from SM collection, which are two lefts (KS34-3212 and KS34-3311), and three rights elements (KS34-1492, KS34-3136, and KS34-3206). From the shape of the almost complete right postorbital KS34-1492 (Fig 37), the postorbital is the slender triradiate bone composed of large medially directed fan shape arch of dorsomedial process, small posteriorly pointed posterior process, and slender anteroventral process. Three mentioned processes are also called parietal process, squamosal process, and jugal process, respectively. Parietal process medially curves and contact with parietal medially, frontal anteriorly, and laterosphenoid ventrally, which form the anterolateral and lateral margin of the supratemporal fenestra. Squamosal process connects to the postorbital facet of the squamosal, that enclose the posterolateral area

of the supratemporal fenestra. The sub triangular cross section jugal process connects to the postorbital facet of the jugal, which seal the posterior margin of orbital cavity and anterior margin of infratemporal fenestra.

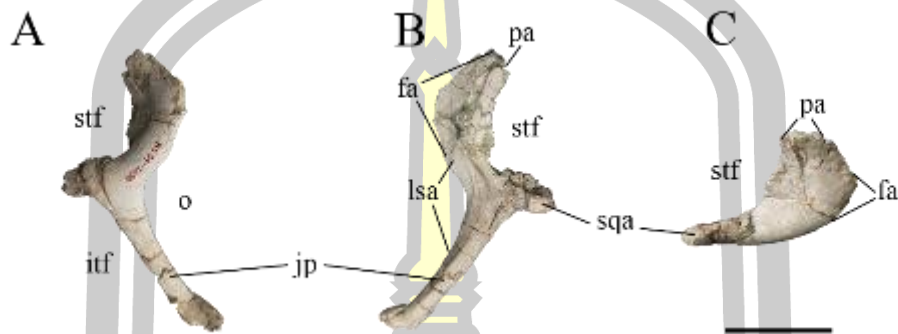


Fig 37 Right postorbital KS34-1492.

A lateral; and B medial views. Scale bar represents 5 cm.

The left KS34-3212 and KS34-3311, have more robustness outline, especially the dorsoposterior intersection region and jugal process. The continuous medial surface along the jugal process through the proximal portion of parietal process is smooth. Subsequently, the further fan shape area is abrupted becomes the shallow recess, which tapering to the distal end. The posteromedial arch of the inner fan shape border has longitudinal arch ridge, that create the narrow, obtuse angle posterior edge, which is the anterolateral border of supratemporal fenestra.

พหุ ประถมศึกษา

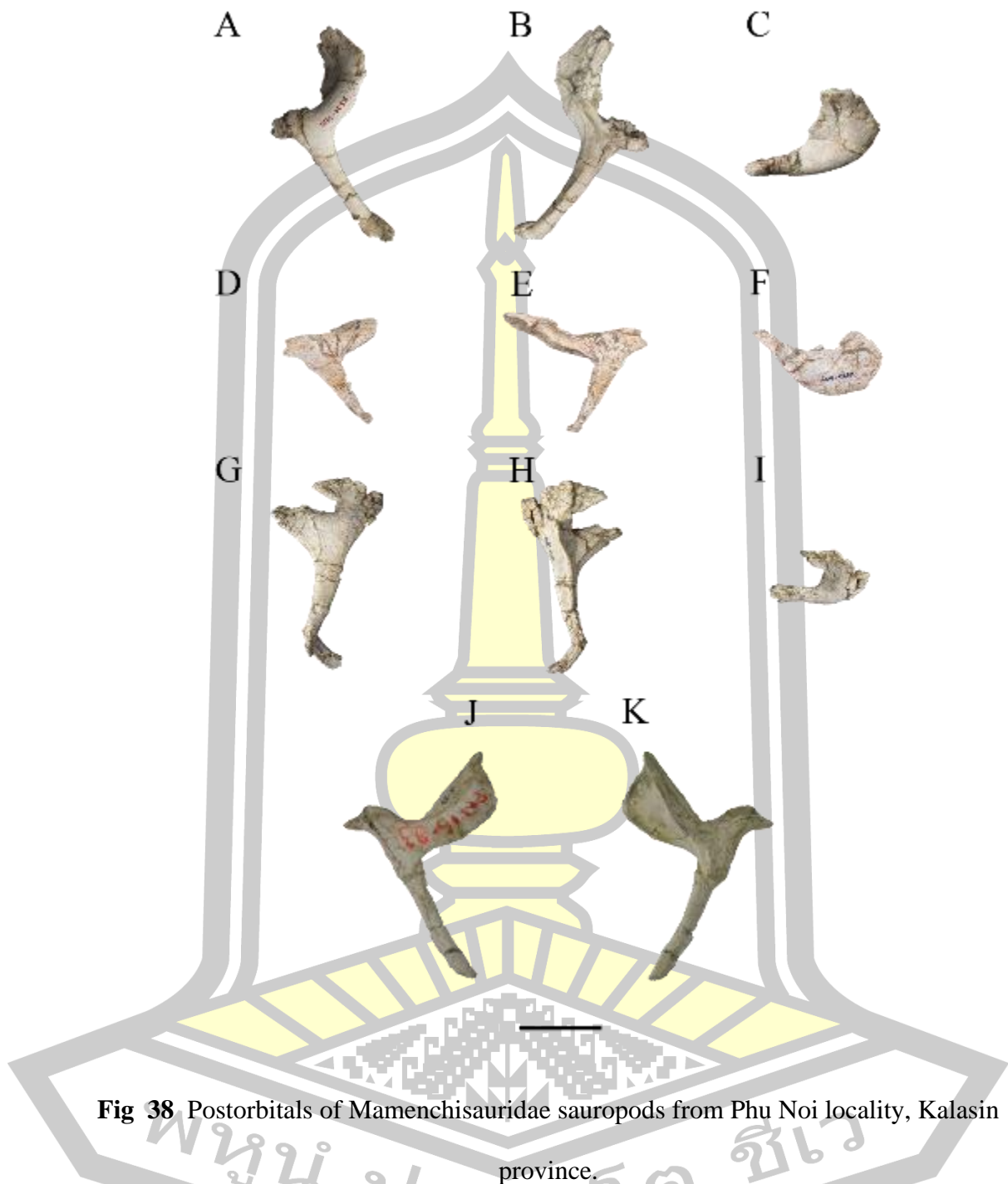


Fig 38 Postorbitals of Mamenchisauridae sauropods from Phu Noi locality, Kalasin province.

A, D, G, J, M, and P are lateral; B, E, H, K, N, and Q are medial; C, F, I, L, O are dorsal views. A, B, and C, KS34-1492 (right). D, E, and F, KS34-3136 (right). G, H, and I, KS34-3206 (left). J, K, and L, KS34-3212 (left). M, N, and O, KS34-3311 (left). P and Q, PN15-93 (right). Scale bar represents 5 cm.

Squamosal

There are four squamosals from SM collection, two left (KS34-2609 and KS34-3289) and two right (KS34-2208 and KS34-3221), and three from PRC, one left (PN139A) and two right (PN139F and PN944). All the specimens are incomplete with only medial or lateral portion preserved and the most complete specimens that might possess exclusive feature, KS34-3289 and PN139A, are selected to be the representative for all specimens.

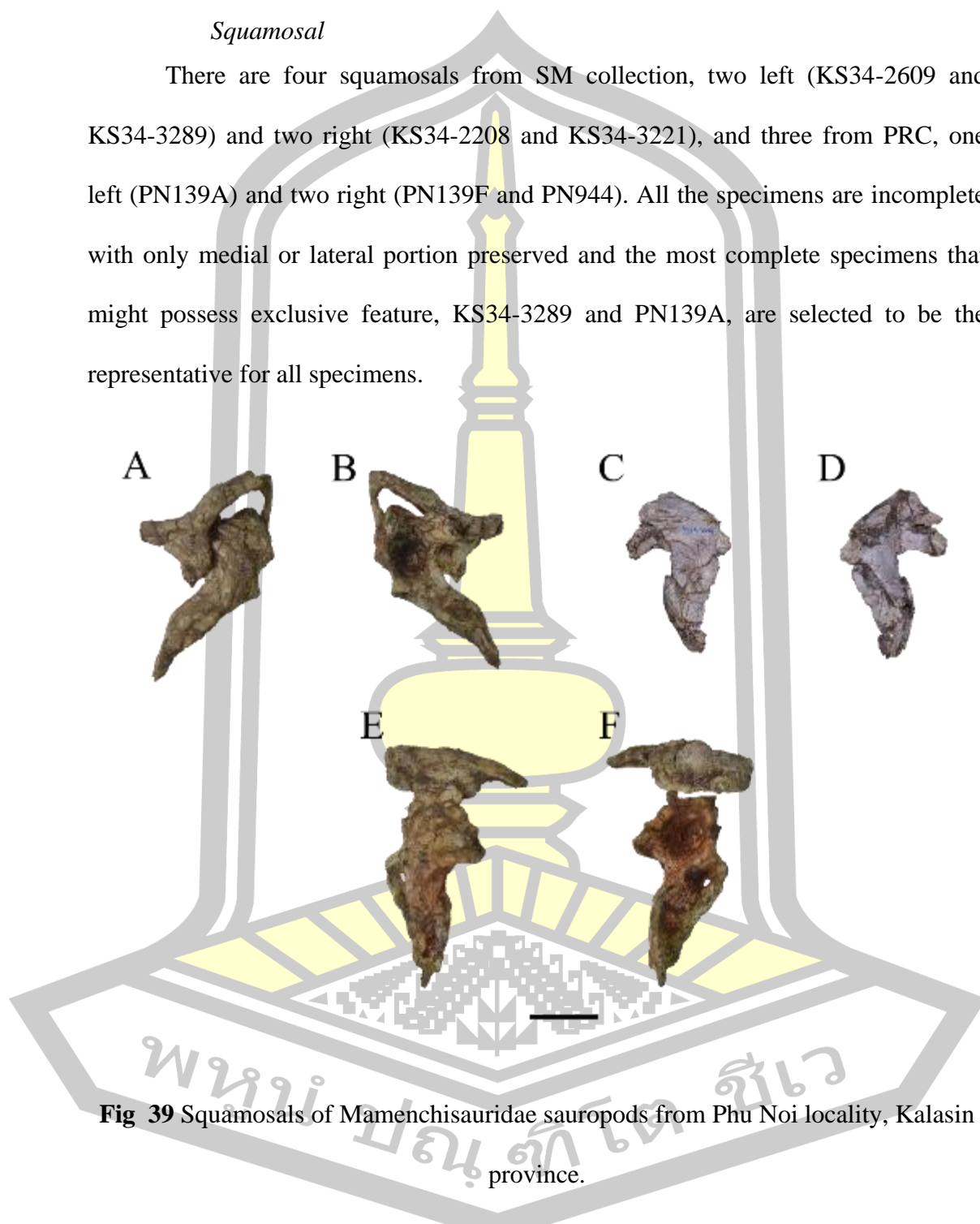


Fig 39 Squamosals of Mamenchisauridae sauropods from Phu Noi locality, Kalasin province.

A, C, E, are lateral; B, D, F, are medial views. A and B, PN139A (left). C and D, KS34-3289 (left). E and F, PN139F (right). Scale bar represents 5 cm.

The elements are triradiate bone with transversely narrow body and vertically directed sigmoid arch outline. It is formed by the stout medial process on the dorsal area, which is dorsomedially connects to parietal and medially and ventrally enveloped by opisthotic and paroccipital process, respectively. It anteriorly connects to postorbital to form the posterior and posterodorsal border of the infratemporal fenestra.

The small anterior surface has large concavity of the mandibular adductor muscle on the medial side, which occupies medial surface of both anterior process and dorsomedial intersection region. It bears short and narrow horizontal trough for the small posterior process (also called squamosal process) of the postorbital on the lateral side. The middle portion of the lateral surface bears weak upside-down sigmoid curve ridge, parallels to the anterior curve of the anterior process, is the outer posterodorsal rim of the lateral temporal fenestra. The deep posteromedial cotyle on the medial surface articulates with the lateral surface of quadrate's main body.

The lateral surface is smooth like the convex dorsal area, except the middle area behind the ridge of lateral temporal fossa, which bears numerous small aggregate porous of capillary blood vessels. There are the short and small anteroventrally arch of anterior process with blunt pointed distal end and thick ventral border, which continuous to the middle of the lateral surface as the ridge of lateral temporal fenestra.

On KS34-3221 and KS34-3289, the dorsal region of anterior process is damaged but still preserve the trace of anteroposteriorly directed subtriangular facet of postorbital. Surprisingly, there is the unique trace of narrower facet, located beyond

and parallel to the postorbital facet. The additional facet is not presented in squamosal of other sauropods, including other SM and PRC squamosals, which might be an autapomorphy of one Mamenchisaurid from Phu Noi. Moreover, the squamosal is the posterodorsal part of supratemporal fenestra that only connected to postorbital in the anterior and anterodorsal direction. The mentioned notch might be the ornamented ridge on the rim of the fenestra, or being a receptor for the postorbital, which has unique bifurcate squamosal process. Unfortunately, the postorbitals in the collection have only specimens that bears small single squamosal process and the incomplete one without the process.

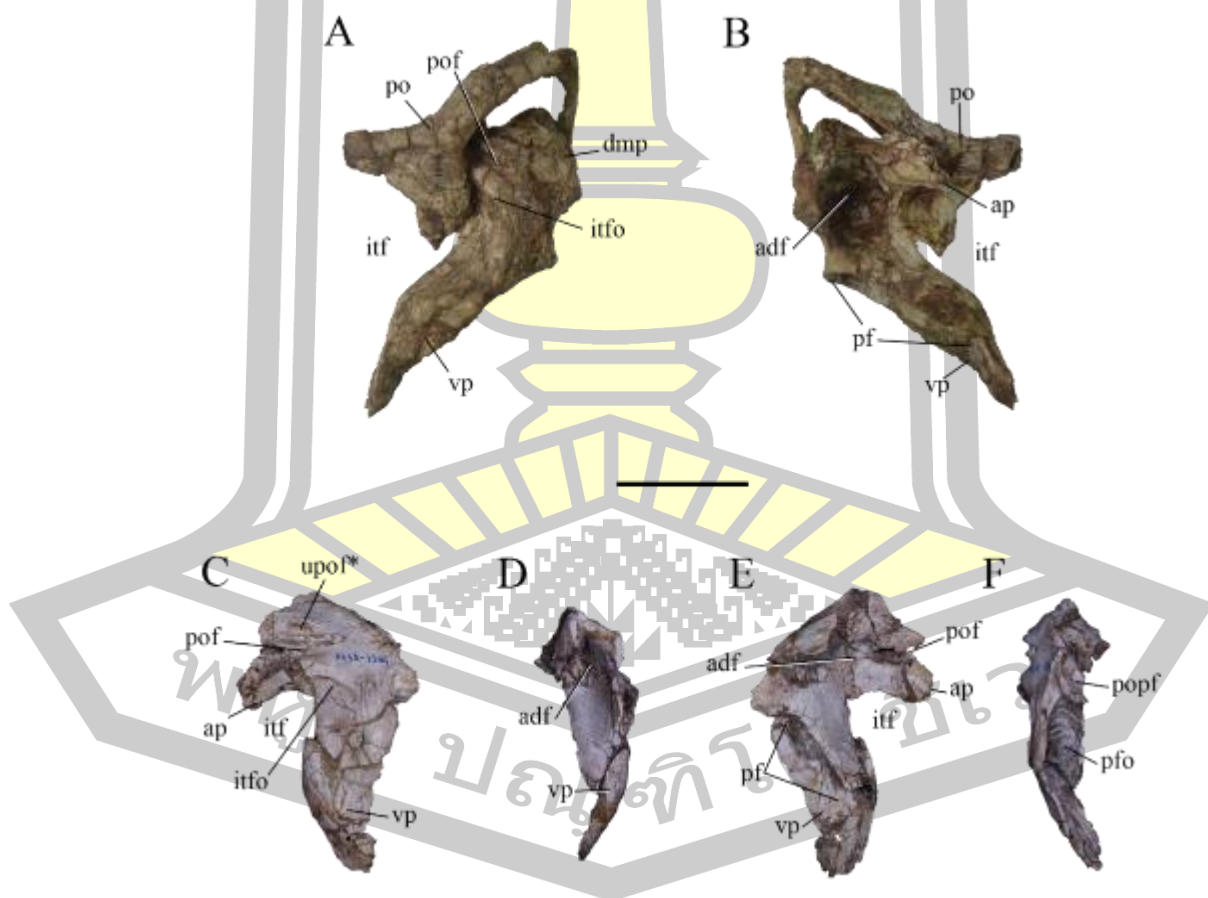
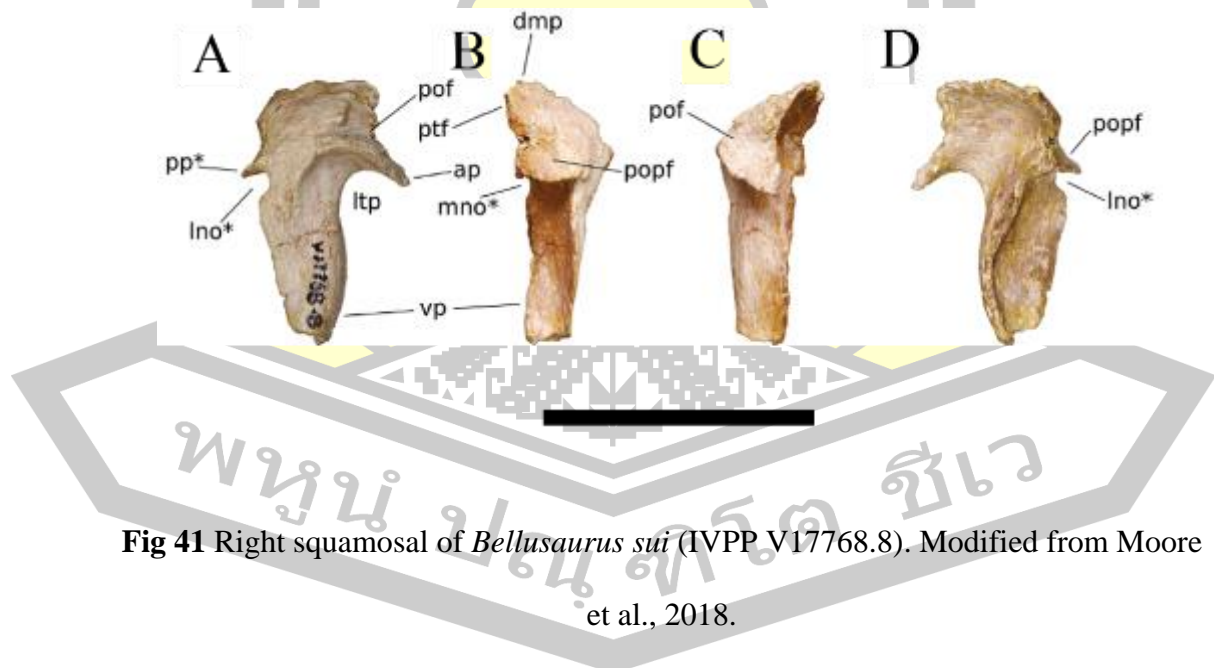


Fig 40 Two representatives of the squamosal of Mamenchisauridae sauropods from Phu Noi locality.

A and C are lateral; B and E are medial; D is anterior; F is posterior views. A and B, PN139A (left). C to F, KS34-3289. Scale bar represents 5 cm.

Only on the posterior surface of KS34-3289, there are the transversely compressed dorsal roof, which medially connects to the distal end of the occipital process of parietal, and lower wide angle, gently U shape concave paraoccipital shelf, that connect to the anteroventral region of the distal end of paraoccipital process. the shelf represents in non-sauropod sauropodomorphs but disappeared in early-branching eusauropods such as *Shunosaurus lii* and *M. youngi*. However, this process reappears again in *Bellusaurus* forming the shelf-like transversely broad process and becomes one of the autapomorphic character (Moore et al., 2018). the posterior process of KS34-3289 squamosal is different from *Bellusaurus* and can be assume as the autapomorphy.



A lateral; B posterior; C anterior; and D medial views. Scale bar represents 5 cm.

Beneath the shelf of paraoccipital process of the exoccipital, the ventral process of all specimens is continually line along the lateral edge as in other sauropods except *B. sui*, which have discrete notch at the posterodorsal margin of the process. Moreover, PN139A and the rest of element are *M. youngi* like squamosal with slender outline and possess more elongate ventral process than the *Bellusaurus* like squamosals, KS34-3221 and KS34-3289.

Quadratojugal

Quadratojugal is the L-shape elongated thin bone, which composes of thick and vertically directed articular surface of quadrate and the anteriorly directed, elongate jugal process. The dorsal arch of the bone is the ventroposterior border of the infratemporal fenestra. The quadrate articular surface is the posteriorly deep recess area on the medial side, which occupied the outer angular area from the dorsoposterior to proximoventral region. The area is dorsally demarcated then shallowing and terminated on the proximal region of jugal process. The transversely narrow laminate jugal process is approximately 2.5 times to the height of quadrate articulation with dorsoventrally expanded distal end. KS34-1180 and KS34-1718 are the *Mamenchisaurus* like quadratojugal, which have relatively high vertical area and the wide and deep sigmoid curve quadrate articular surface is almost standing 90 degrees against the jugal process.

PN14-139E is the part of articulated posterior skull roof (PN14-139), which has different shape to KS34-1180 and KS34-1718. It has pointed and tapering end of jugal process, with downward sigmoid curve. The posterior region of main body is subtriangular in outline with fragment of bone attaching on the medial surface. The quadrate articular process is 45 degrees anterodorsally directed, which made the

posteroventral border of the infra temporal fenestra has narrower angles than previous quadratojugals. All characteristic of bone should distinguish PN14-139 from other cranial elements of Mamenchisauridae sauropods.

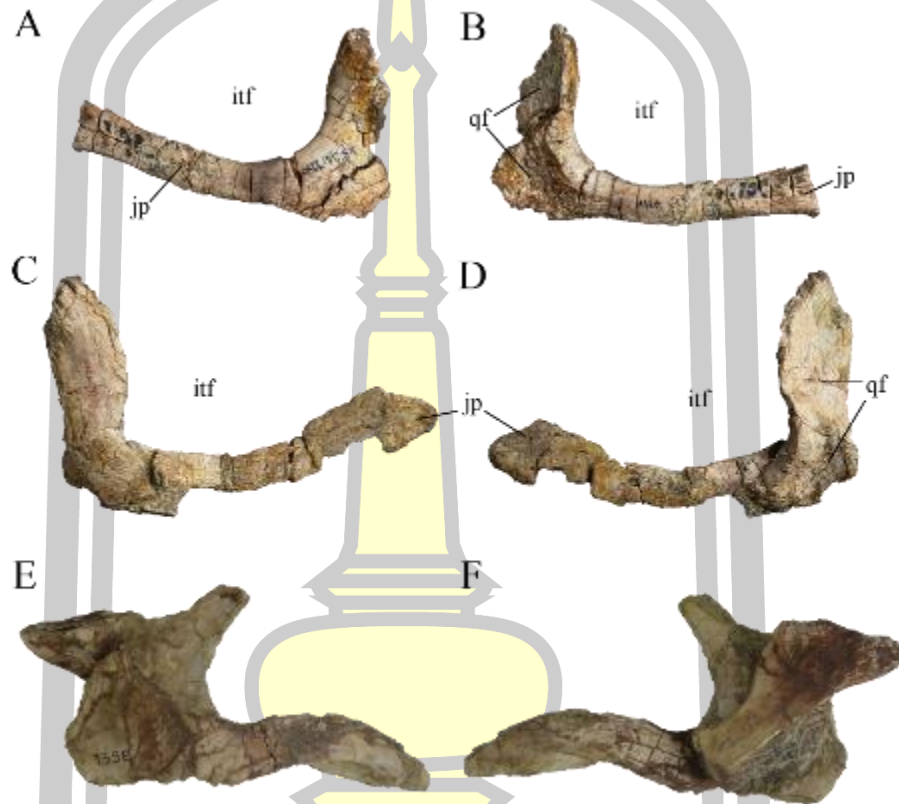


Fig 42 Quadratojugals of Mamenchisauridae sauropods from Phu Noi locality, Kalasin province.

A, C, and E are lateral; B, D, and F are medial views. A and B, KS34-1180 (left). C and D, KS34-1718 (right). E and F, PN14-139E. Scale bar represents 5 cm.

Dentary

There are 7 dentaries, 4 from SM collection (two right and two left) (Fig 43) with another four from PRC (one right and two left) (Fig 44). All of them are heavily

transversely compressed and labiolingually flatten with numerous fractures and ruptured area. Among the specimens, there are only three completely preserved dentaries with all descriptive landmarks.

The shape of dentaries is anteroposteriorly elongate subrectangular, which have the highest area at the anteroventral point of the symphysis then posteriorly recurve and tapering, and medially curves at the anterior portion. The dorsal and ventral rami are diverged at the posterior end, which are connected to the posterior elements of the mandible (e.g., surangular dorsolaterally, angular ventrolaterally, and splenial medially).

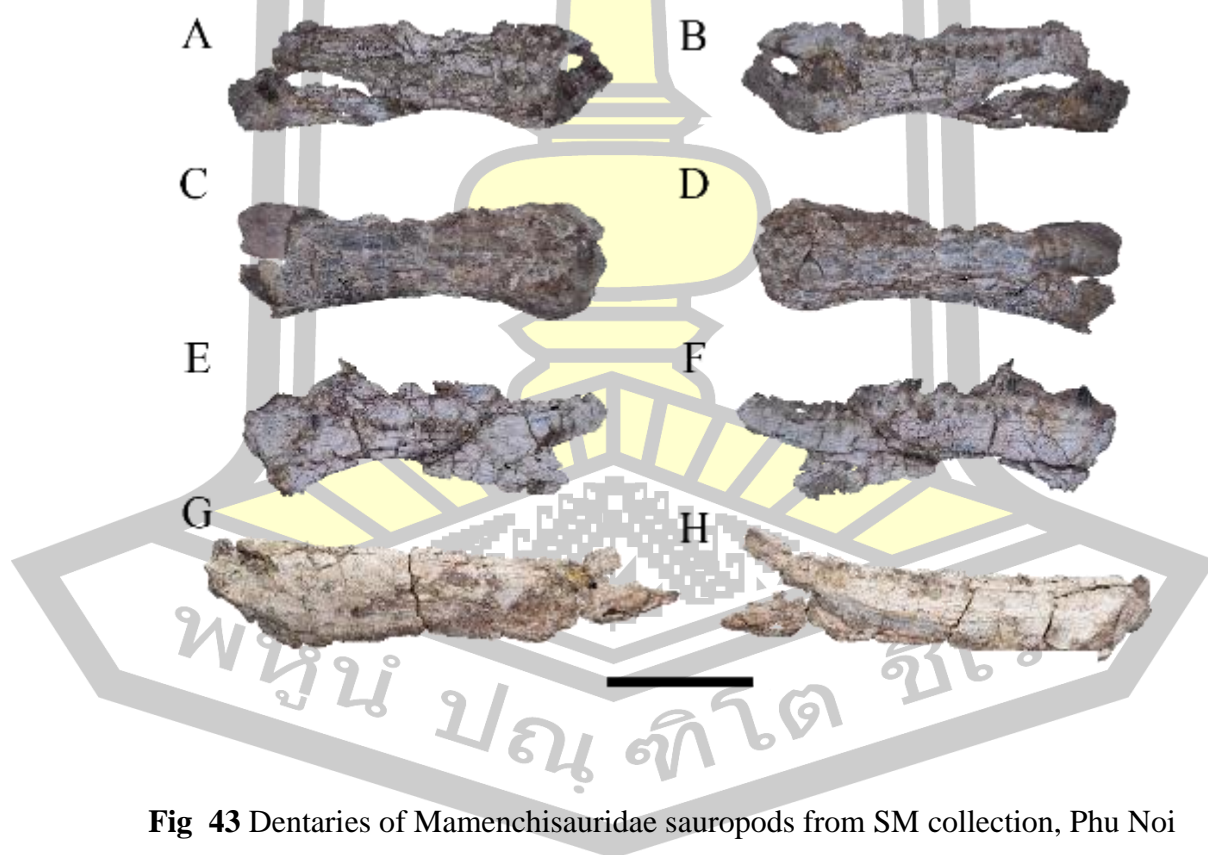


Fig 43 Dentaries of Mamenchisauridae sauropods from SM collection, Phu Noi locality, Kalasin province.

A, C, E, and G are lateral; B, D, F, and H are medial views. A and B, KS34-612. C and D, KS34-1528. E and F, KS34-1572. G and H, KS34-2085. Scale bar represents 5 cm.

The ventral border is transversely flat and weakly medially curve. The dorsal border has dentigerous shelf on the labial surface, which covers the labial surface of the roots and proximal portion of the tooth crowns, and the alveoli sockets, which are embed by the vertical elongated roots of the teeth. The lingual surface contains numerous features and characters of the element. It is the side that represents erupting teeth, which cover behind the labially dentigerous shelf. The nutrient foramina or replacement teeth foramina, which usually have the distal crown of the replacement teeth, mesiodistally lines below to the line of alveoli socket.

The anterior symphysis, which anteriorly bends 115 degrees of vertical subrectangular area, from the anterodorsally tip to anteroventrally chin like margin. And the subtriangular fossa called Meckelian groove, which is occupied for splenial and angular, presents at the distoventral area of dentary. The number of replacement tooth foramina and alveoli, from the observation of all dentaries, including the incomplete specimens, are approximately 23 to 24.

The number of alveolus counts are comparable to other reported Mamenchisauridae (*M. youngi* ZDM 0083: at least 20 (Ouyang & Ye, 2001; Pi et al., 1996); *M. hochuanensis* ZDM 0126 referred: at least 17 (Ouyang & Ye, 2001); *M. jingyanensis* CV 00734: 17 to 19 (Yihong Zhang, Li, & Zeng, 1998); *M. sinocanadorum* IVPP V10603: at least 19 (Moore et al., 2023)) and basal eusauropod *Shunosaurus* sp. (18–21) (Wilson & Sereno, 1998; Y Zhang, 1988).

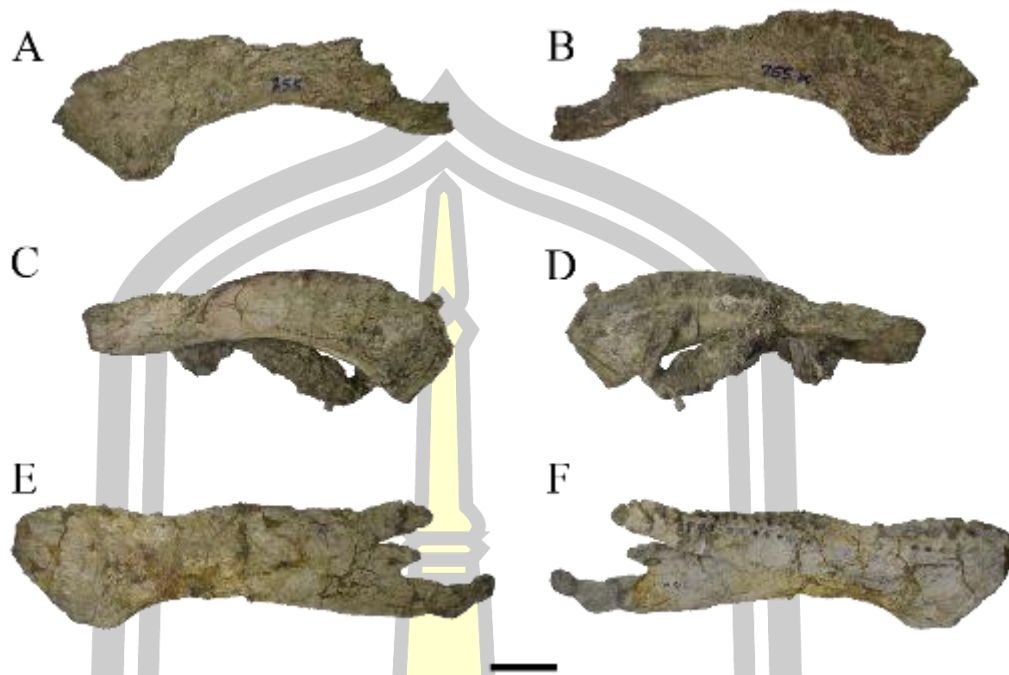


Fig 44 Dentaries of Mamenchisauridae sauropods from PRC collection, Phu Noi locality, Kalasin province.

A, C, E, and G are lateral; B, D, F, and H are medial views. A and B, PN 755. C and D, KS34-947. E and F, KS34-978. G and H, PN14-322. Scale bar represents 5 cm.

The left dentary KS34-2572 is the representative specimens to describe. It has high compression damaged on both lingual and labial surfaces, which affect the disappearance of labial neurovascular foramina and cause the erosion of all margins. The specimen is the most completed one except the distal end of dorsal and ventral rami and the most part of dentigerous shelf. There are the second, the eight, the root of ninth well-developed erupting teeth, one horizontal connected tooth at the middle of the dentary, and the probable 18th to 20th apical erupting present on the alveoli. Three apical crown of replacement teeth are possessed inside the 9th, 16th, and 20th nutrient foramina. Meckelian groove and the anteriorly mesioventral canal are

noticeable but the distal end of dorsal and ventral rami, which are divided at the dorsoventral position of 12th or 13th nutrient foramen, are loss. The labial surface shows weakly dorsal arch outline of the dentary, and one replacement tooth are revealed on the middle height on the anterior portion of the surface by the compression.

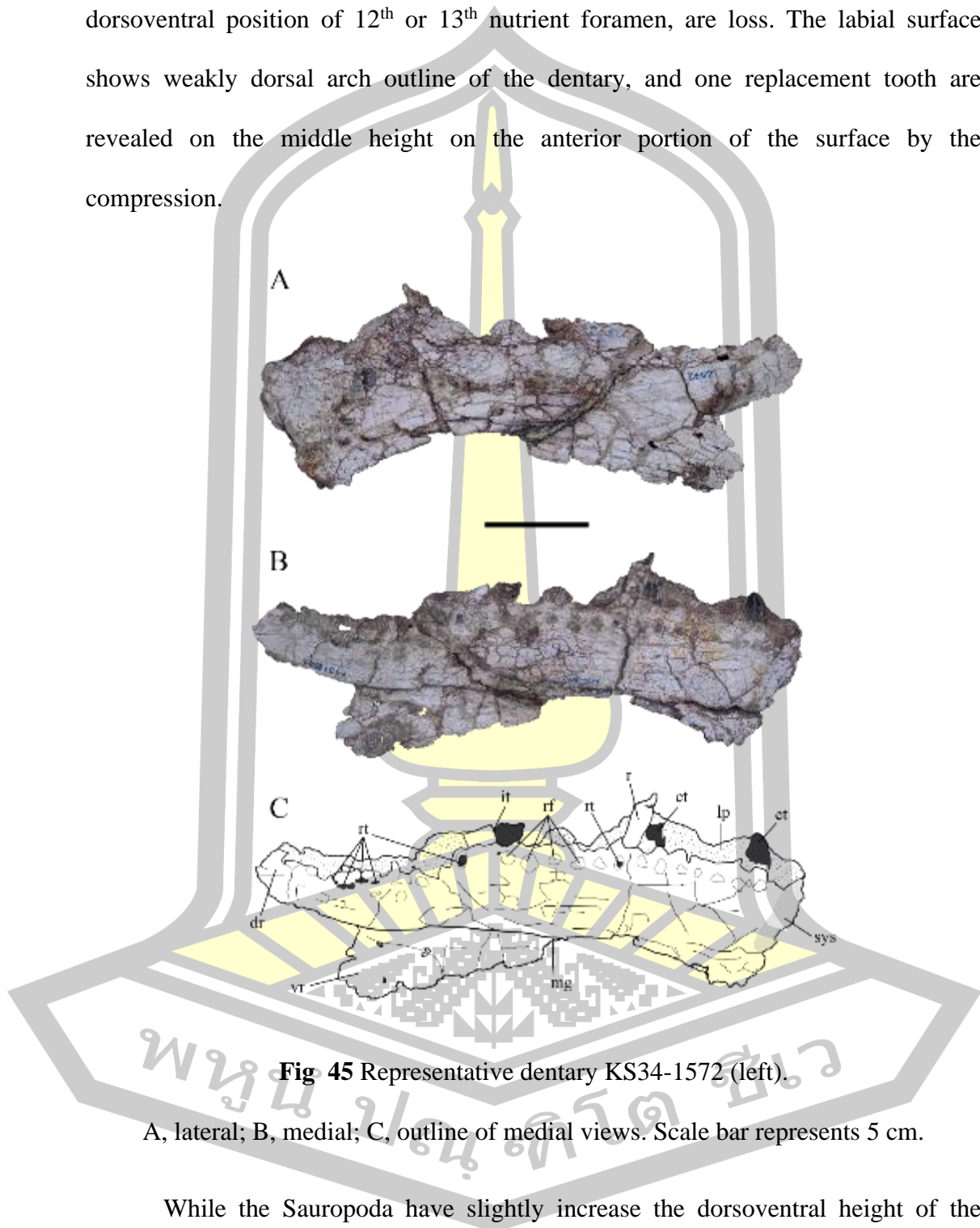


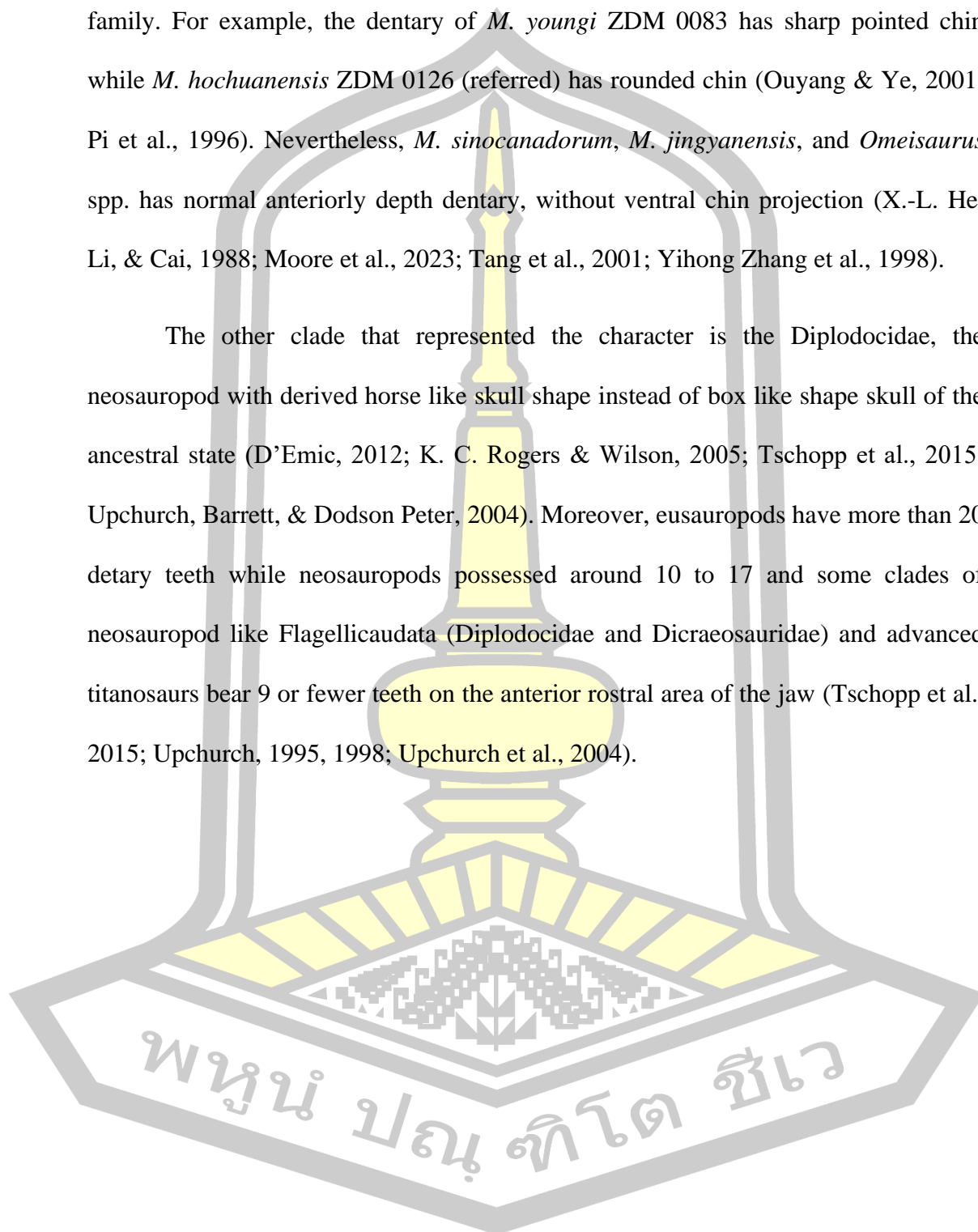
Fig 45 Representative dentary KS34-1572 (left).

A, lateral; B, medial; C, outline of medial views. Scale bar represents 5 cm.

While the Sauropoda have slightly increase the dorsoventral height of the dentary toward the symphysis, Mamenchisauridae is the only clade of eusauropod that represented the outstanding ventrally pointed, chin like projection under symphysis.

However, the level of the pointiness of the chin is intraspecific variation among the family. For example, the dentary of *M. youngi* ZDM 0083 has sharp pointed chin while *M. hochuanensis* ZDM 0126 (referred) has rounded chin (Ouyang & Ye, 2001; Pi et al., 1996). Nevertheless, *M. sinocanadorum*, *M. jingyanensis*, and *Omeisaurus* spp. has normal anteriorly depth dentary, without ventral chin projection (X.-L. He, Li, & Cai, 1988; Moore et al., 2023; Tang et al., 2001; Yihong Zhang et al., 1998).

The other clade that represented the character is the Diplodocidae, the neosauropod with derived horse like skull shape instead of box like shape skull of the ancestral state (D'Emic, 2012; K. C. Rogers & Wilson, 2005; Tschopp et al., 2015; Upchurch, Barrett, & Dodson Peter, 2004). Moreover, eusauropods have more than 20 dentary teeth while neosauropods possessed around 10 to 17 and some clades of neosauropod like Flagellicaudata (Diplodocidae and Dicraeosauridae) and advanced titanosaurs bear 9 or fewer teeth on the anterior rostral area of the jaw (Tschopp et al., 2015; Upchurch, 1995, 1998; Upchurch et al., 2004).



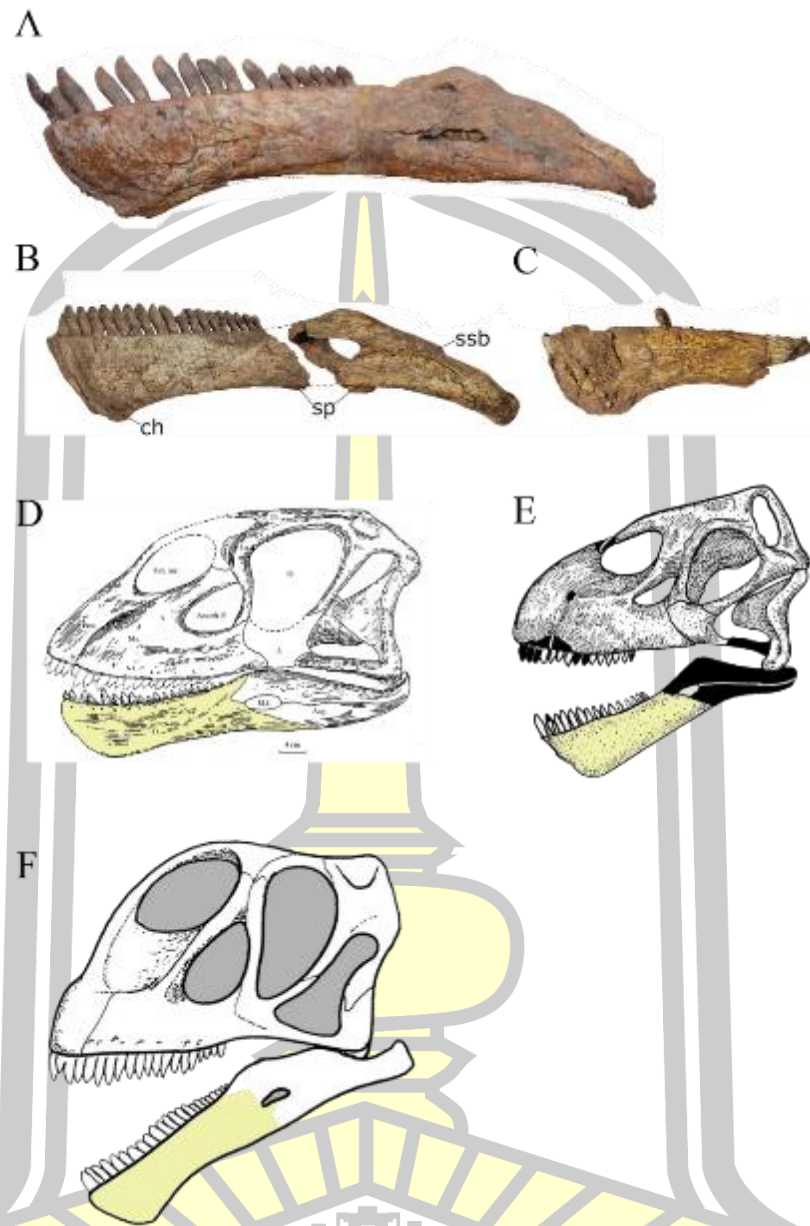


Fig 46 The dentary of Mamenchisauridae.

A) *Mamenchisaurus sinocanadorum* IVPP V10603. B) *Mamenchisaurus youngi* ZDM 0083. C) *Mamenchisaurus hochuanensis* (referred) ZDM 0126. D) *Mamenchisaurus jingyaensis* CV00734 (illustration). E) *Omeisaurus tienfuensis* (illustration). F) *Omeisaurus maoianus* (illustration). A to C, from Moore et al., 2023;

D from Zhang et al., 1998; E from He et al., 1988; F from Tang et al., 2001. Not to scale.

Teeth

From numerous isolated teeth of PRC and SM collections, the samples are selected to describe as the representative of all specimens. 14 and 38 teeth from PRC and SM, respectively have been selected. There are spatulate teeth, apically curve on the mesial edge and recurved distally on the distal edge, with diverse proportion and minor details, like the presents of distolingual boss, denticles, and wear facets of each specimen. Due to the posterior regression of tooth size and proportion along the jaw [Moore et al., 2018], the sampling teeth can be distinguished to the anterior, middle, and posterior teeth but cannot precisely determined whether from upper or lower part.

The anterior teeth have large and elongated crown with weak expansion and curvature on entire mesial and distal edge. The labial surface is flat plain on the crown base region, subsequently the convexity is increasing from the one third vertically to the apical end. Moreover, there are two shallow longitudinal grooves along the border of mesial and distal edges, which made the middle region become the large apicobasal prominence area.

The lingual surface is weakly concave with flat medial and distal edges but noticeably large weakly convex middle area on the apical half then gently shift to plain basal half. The basal half of lingual surface has thick plain surface with short, stepped margin between the main body of teeth and the edges. Both lingual and labial surfaces represent vertical irregular wrinkles, abundantly on basal to sparsely on

apical area. In unworn teeth, there are denticles on both mesial and distal edges, which are usually larger and prominent on the former than the latter edge.

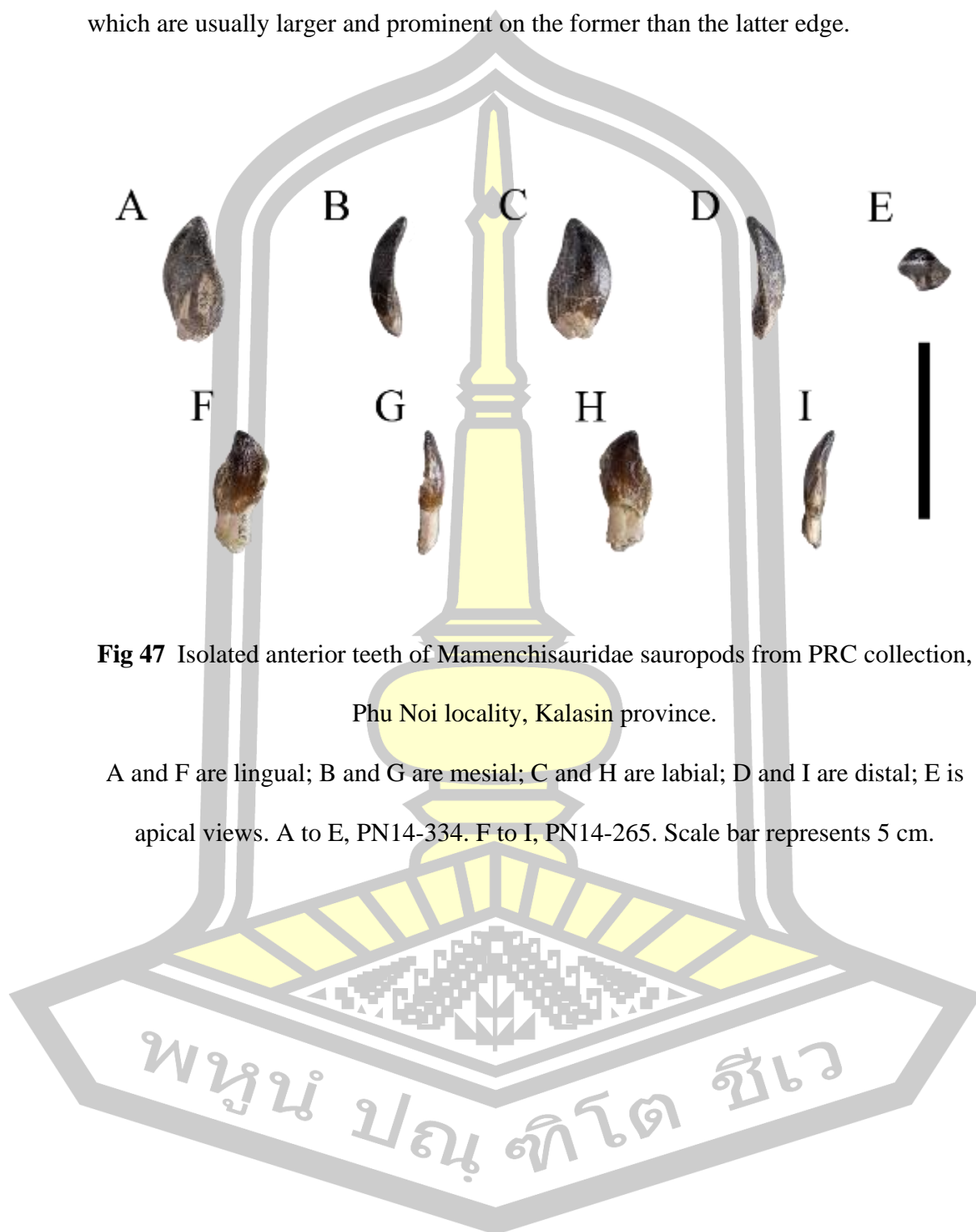


Fig 47 Isolated anterior teeth of Mamenchisauridae sauropods from PRC collection, Phu Noi locality, Kalasin province.

A and F are lingual; B and G are mesial; C and H are labial; D and I are distal; E is apical views. A to E, PN14-334. F to I, PN14-265. Scale bar represents 5 cm.

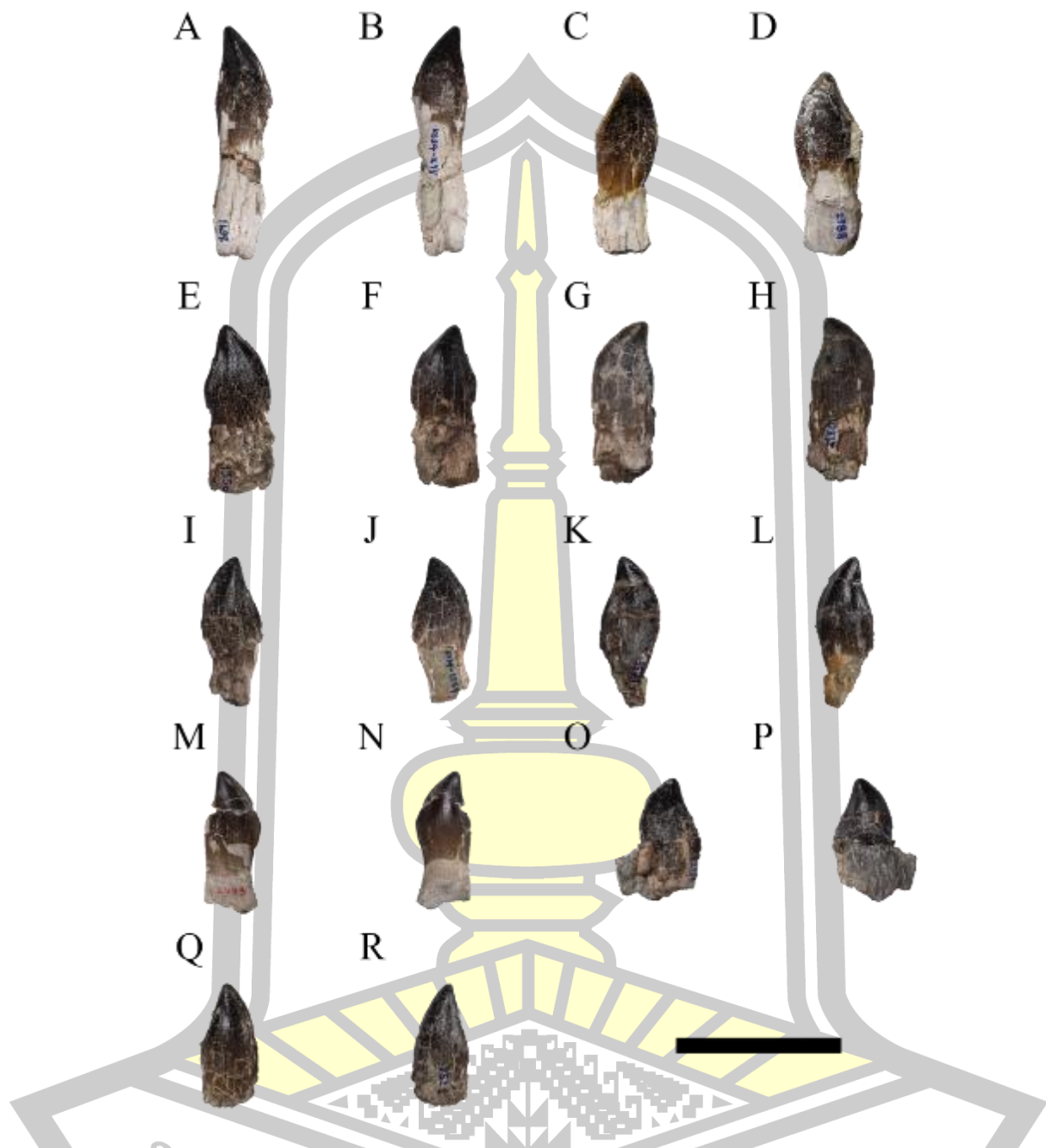


Fig 48 Isolated anterior teeth of Mamenchisauridae sauropods from SM collection, Phu Noi locality, Kalasin province.

A, C, E, G, I, K, M, O and Q are lingual; B, D, F, H, J, L, N, P, and R are mesial views. A and B, KS34-1698. C and D, KS34-2789. E and F, KS34-1556. G and H, KS34-2180. I and J, KS34-1584. K and L, KS34-1571. M and N, KS34-2473. O and P, KS34-2106. Q and R KS34-2526. Scale bar represents 5 cm.

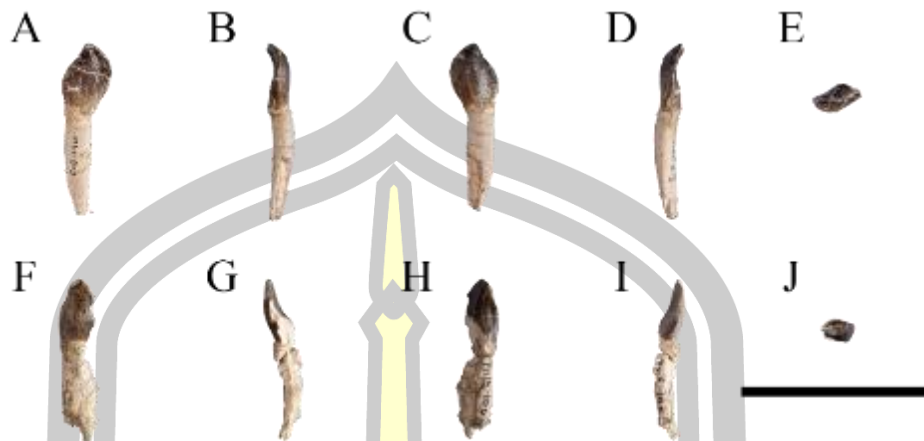


Fig 49 Isolated middle teeth of Mamenchisauridae sauropods from PRC collection, Phu Noi locality, Kalasin province.

A and F are lingual; B and G are mesial; C and H are labial; D and I are distal; E and J are apical views. A to E, KS34-803. F to J, PN16-106. Scale bar represents 5 cm.

The middle teeth have relatively shorter and broader crown with slender root, that transversely narrow than the width of crown. The maximum mesiodistal width of crown at the upper middle height are clearly distinct from the basal breadth and the curvature of crown is stronger than the anterior teeth, which the apical bends distolingual direction. The outline of posterior teeth is rounded teardrop to tubercle shape with pointed apical and gently curve mesial and distal edges with more convex and concave labial and lingual surfaces, compared to the anterior and middle teeth.

The present of denticles on both mesial and distal edges is the primitive form of tooth, which possesses among Eusauropoda. However, *Mamenchisaurus* spp. have denticles only on the mesial edge (Moore et al., 2023; Ouyang & Ye, 2001). The genera of mamenchisaurid that possesses both side denticles are *Omeisaurus* spp. (X.-L. He et al., 1988; Tang et al., 2001). This dental character might indicate the occurrence of *Omeisaurus* sp. in Phu Noi locality.

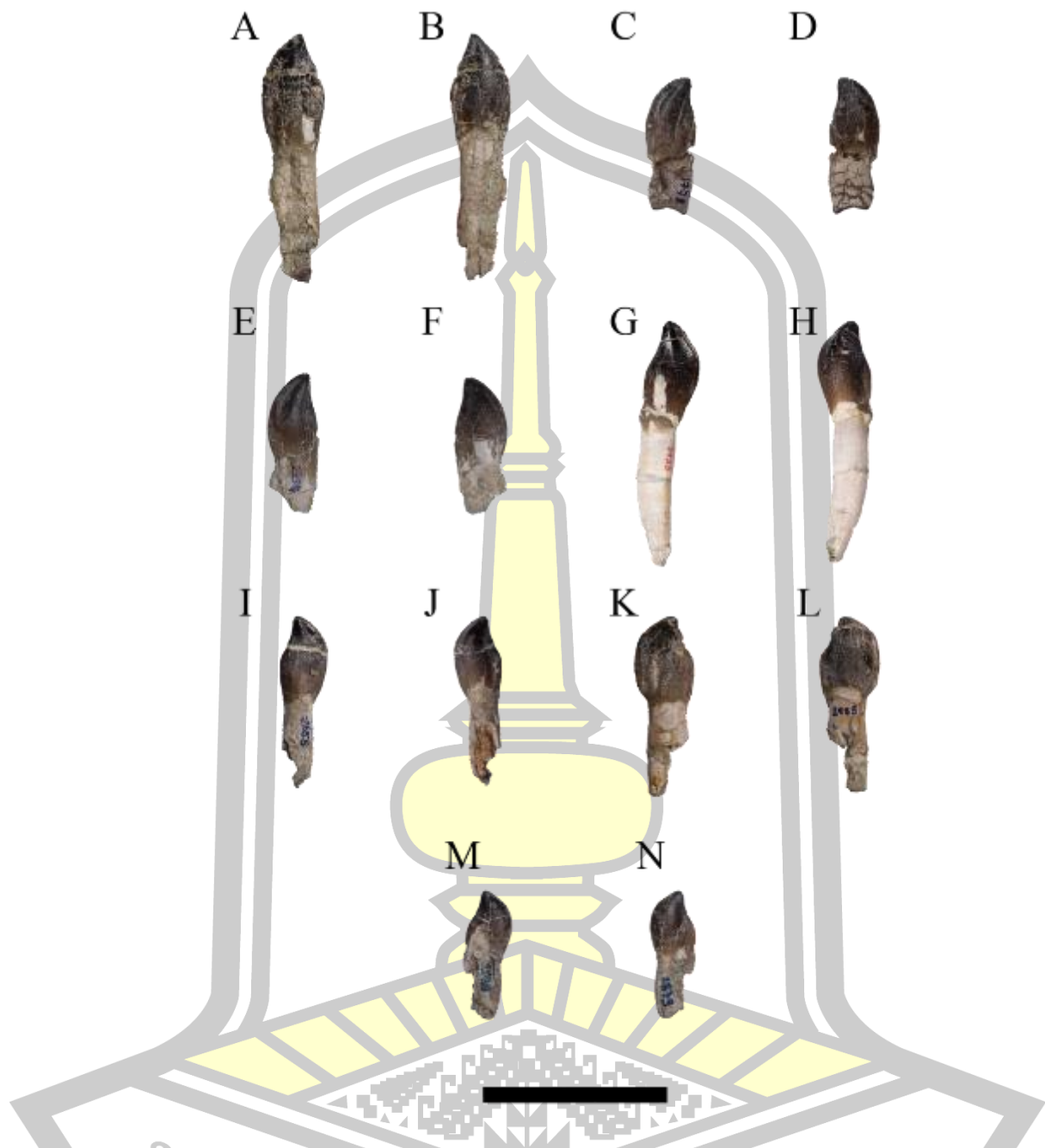
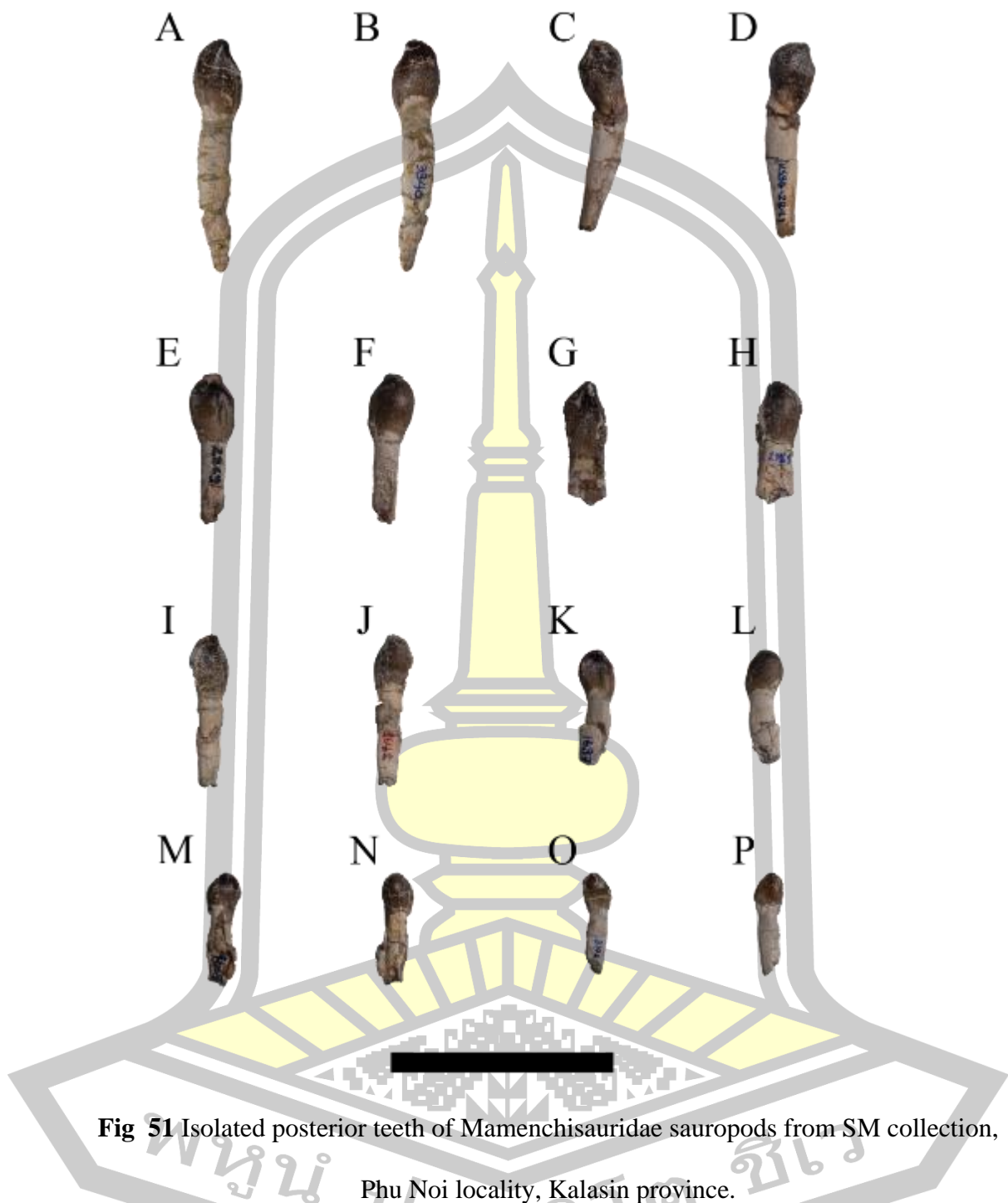


Fig 50 Isolated middle teeth of Mamenchisauridae sauropods from SM collection, Phu Noi locality, Kalasin province.

A, C, E, G, I, K, M, O, Q and S are lingual; B, D, F, H, J, L, N, P, R, and T are mesial views. A and B, KS34-2252. C and D, KS34-1779. E and F, KS34-2434. G and H, KS34-2733. I and J, KS34-2655. K and L, KS34-2707. M and N, KS34-2985. O and P, KS34-2879. Q and R KS34-2479. S and T, KS34-2110. Scale bar represents 5 cm.



A, C, E, G, I, K, M, O, Q and S are lingual; B, D, F, H, J, L, N, P, R, and T are mesial views. A and B, KS34-3340. C and D, KS34-1621. E and F, KS34-2841. G and H, KS34-2869. I and J, KS34-2181. K and L, KS34-1641. M and N, KS34-1688. O and P, KS34-1697. Q and R KS34-1668. S and T, KS34-3106. Scale bar represents 5 cm.

4.1.2 Postcranial Elements

Cervical vertebrae

Due to the incomplete and isolation of the majority specimens, the order of vertebra cannot be precisely designated, the separation between centrum and neural spine, either from diagenesis deformation or ontogenetic.

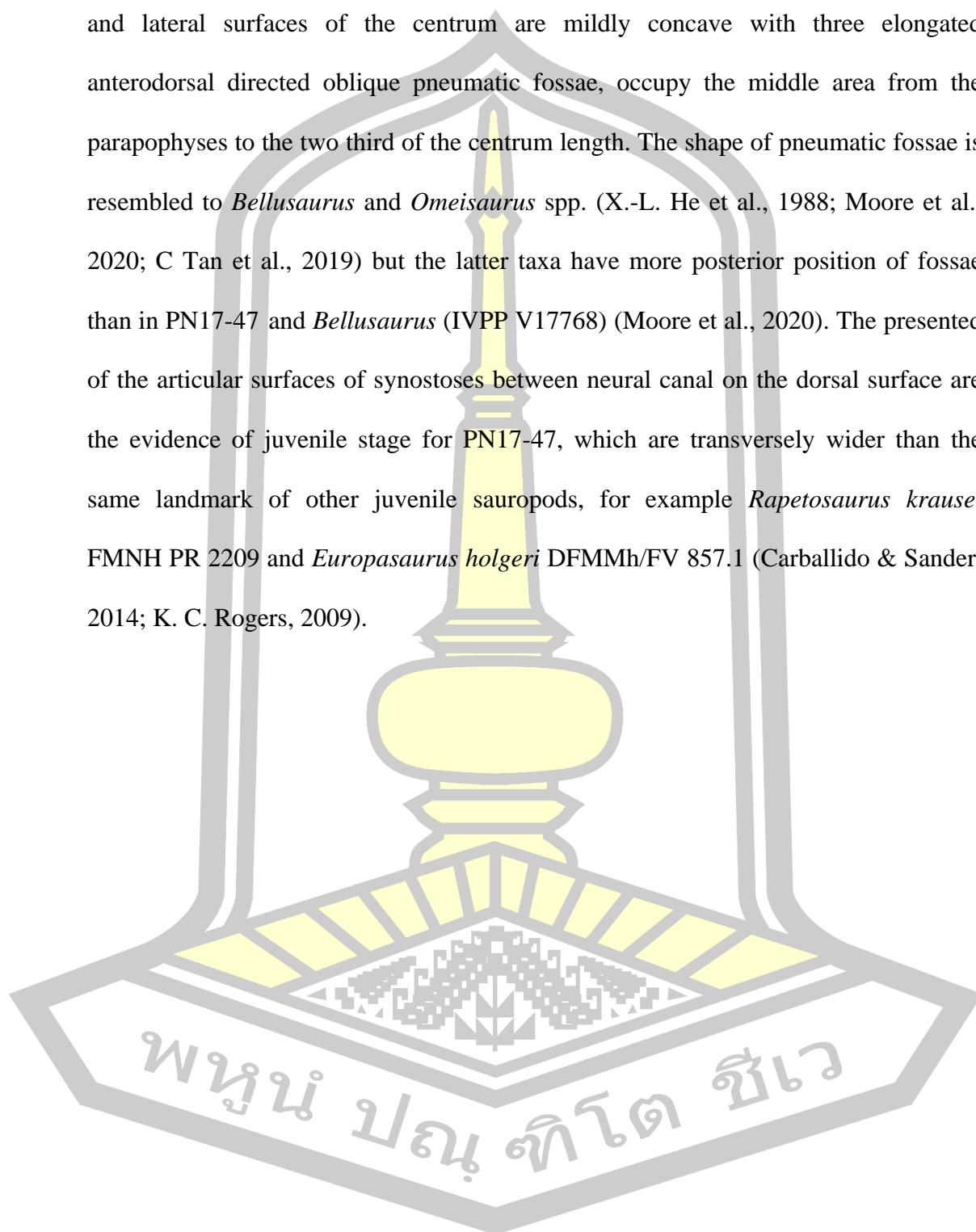
The cervical vertebrae are distinguished into the anterior to middle, middle, and posterior part, because there is no cervical centrum or neural arch that show distinctive proportions and characteristics of the anterior cervical vertebra.

Anterior to middle cervical vertebra

The cervical centra PN17-47 is the only one representative specimen for the part, by the proportion and elongation index value (2.52). The anterior condyle is strongly hemispherical shape while posterior cotyle is mildly concave. Both articular ends are elliptical outline, which have transversely wider than height, and the notch on the dorsal rim of the posterior cotyle is absent. The extension of anterior condyle is similar to *Omeisaurus* spp., which distinct by the higher height than width (X.-L. He et al., 1988; Tang et al., 2001). The ventral surface is transversely concave along the anteroposterior direction, without the single midline keel. The keel usually presents on the sagittal plain of the ventral surface of post axial cervical centra of the Eusauropoda like *Shunosaurus lii* (Y Zhang, 1988).

However, some mamenchisaurids are possessed the keel, for example *Omeisaurus* spp. (except *O. junghsiensis*), and *Xinjiangtitan shanshanensis* (X.-Q. Zhang, Li, Xie, Li, & You, 2020). The mamenchisaurids with the absent of keel are *Bellusaurus sui*, *Klamelisaurus gobiensis*, *Mamenchisaurus youngi*, *O. junghsiensis*, and *Qijianglong guokr* (Mo, 2013; Moore, Upchurch, Barrett, Clark, & Xing, 2020;

Ouyang & Ye, 2001; Xing et al., 2015; C. C. Young, 1939). The ventrolateral ridges and lateral surfaces of the centrum are mildly concave with three elongated anterodorsal directed oblique pneumatic fossae, occupy the middle area from the parapophyses to the two third of the centrum length. The shape of pneumatic fossae is resembled to *Bellusaurus* and *Omeisaurus* spp. (X.-L. He et al., 1988; Moore et al., 2020; C Tan et al., 2019) but the latter taxa have more posterior position of fossae than in PN17-47 and *Bellusaurus* (IVPP V17768) (Moore et al., 2020). The presented of the articular surfaces of synostoses between neural canal on the dorsal surface are the evidence of juvenile stage for PN17-47, which are transversely wider than the same landmark of other juvenile sauropods, for example *Rapetosaurus krausei* FMNH PR 2209 and *Europasaurus holgeri* DFMMh/FV 857.1 (Carballido & Sander, 2014; K. C. Rogers, 2009).



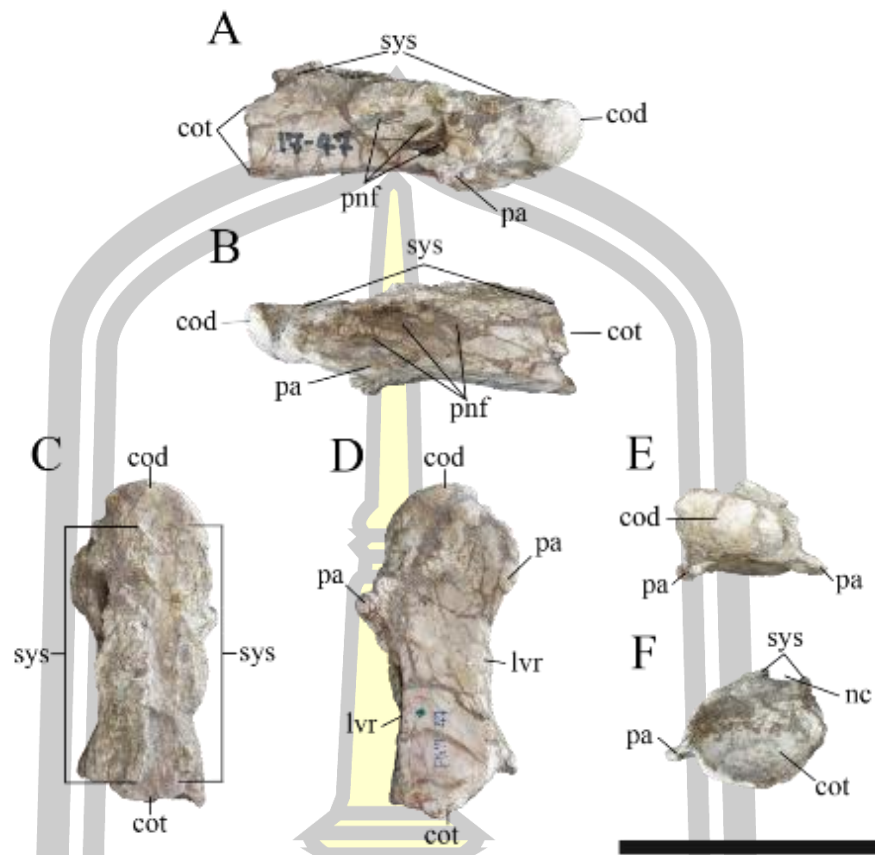


Fig 52 Anterior to middle cervical centrum of Mamenchisauridae sauropod from Phu Noi locality PN17-47.

A, right lateral; B, left lateral; C, dorsal; D, ventral; E, anterior; F, posterior views.

Scale bar represents 10 cm.

Middle cervical vertebrae

There are two specimens, which are the part of middle vertebrae, composed of the no number neural arch, and the dorsoventrally compressed vertebrae (PN-602). The no number neural arch (Fig 53 C & D) has relatively dorsoventral short and anteroposterior long neural spine with small anterior tip of spine, that resembled to dorsal tip of prespinal lamina (prsl), elongated horizontally curve sprl, and shortened spinopostzygapophyseal laminae (spol). The articular surfaces of diapophyses, prezygapophyses and postzygapophyses are broken.

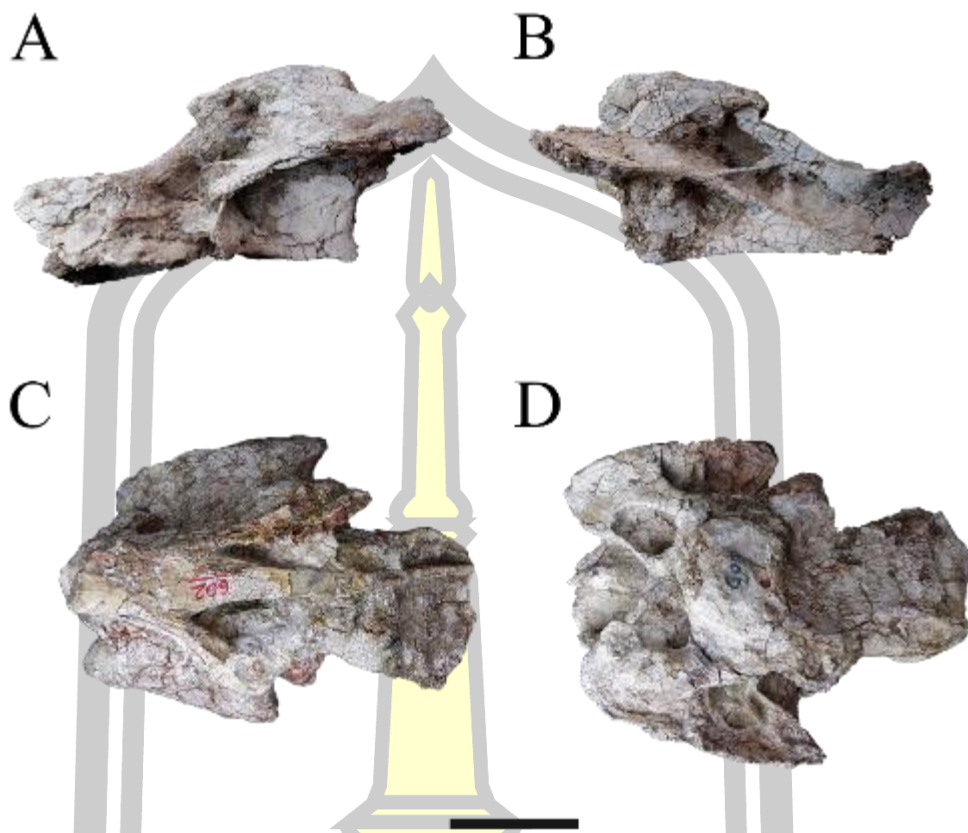


Fig 53 Middle cervical vertebrae of Mamenchisauridae sauropods from Phu Noi locality, Kalasin province.

A is left lateral; B is right lateral; C is dorsal; D is ventral views. A and B, no number middle cervical neural arch. C and D, PN602. Scale bar represents 10 cm.

On the anterior view, the remnants of pillar shape *cpri* are located vertically beneath the prezygapophyses, not separate to medial and lateral laminae. The large area of subtriangular fossa between the prezygapophyses and neural spine is the *sprf*, which has smooth ventral outer bone surface and rough vertical internal bone surface, with the dorsomedian tubercle of the anteriormost part of neural spine. The left and right lateral surfaces show the trace of *cpri*, *sprl*, *cpol*, *podl*, laterally flare flange of epipophyses, *spol*, and the small additional lamina horizontally connect the *sprl* to

podl, resemble to the epipophyseal prezygapophyseal laminae (eprl) in the cervical vertebrae of Rebbachisauridae. The posterior surface is composed of spinopostzygapophyseal fossa (spof), which is filled by the sediment, from the dorsal half portion. Postzygapophyses and epipophyses are laterally expanded, which ventromedially supported by the cpol. Lastly, the middle of the ventral most portion is the dorsal half of the arch of the neural canal.

The middle cervical vertebra PN 602 is anteroposteriorly elongated. Unfortunately, the vertebra is cruelly deformed in anteriorly oblique slope, thus the EI value cannot be calculated. The articular surfaces are subcircular opisthocoelous, which is mildly convex and moderately concave on the anterior and posterior, respectively. Parapophyses are anteroposteriorly flat subrectangular shape. Ventral surface is mildly transverse concave with posterior centroparapophyseal laminae (pcpl) on the lateral margins. By the heavily dorsoventrally compression, the lateral surfaces centrum cannot be observed to determine the present and details of pneumatopores (pleurocoel). The neural arch is approximately low, indicated by the height of the cpri, which shows the short stout structure. The articular surfaces of prezygapophyses are broader than cpri with laterally expanded arch. Intraprezygapophyseal laminae (tpri) medioventrally line between prezygapophyses, that enclosed the dorsal margin of neural canal. Between tpri, neural canal and cpri is the pair of prominent large oval shape fossae called centroprezygapophyseal fossae (cprf).

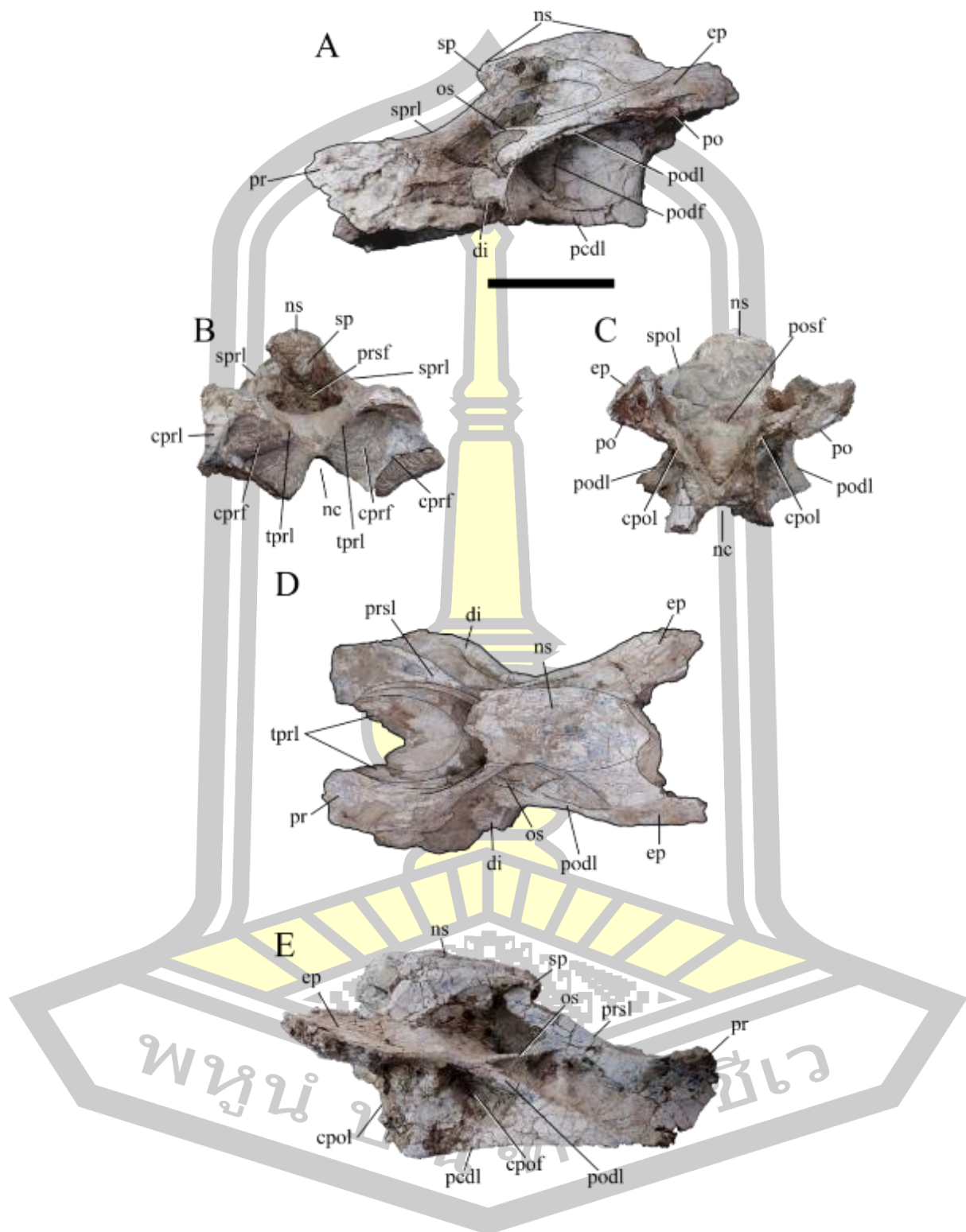


Fig 54 No number neural arch from Phu Noi locality.

A is left lateral; B is anterior; C is posterior; D is dorsal; and E is right lateral views.

Scale bar represents 10 cm.

Beyond the tpri is the vertical trough of prespinal fossa, laterally enclosed with the compressed area of spri and neural spine. The posteriorly directed of curve subtriangular transverse processes, forming by laterally expanded flange of prezygodiapophyseal laminae (prdi) and posterior centrodiapophyseal laminae (pcdi) represent numerous small fossae, bounded by the accessory laminae.

On the dorsal surface, the indetermining rib anteroposteriorly covers the area of neural spine through posterior concave articular surface of the centrum. The rib preventing the presence of postspinal lamina (posl) from the observation. The postzygapophyses got heavy damaged, the left one is totally disappeared while the right one remains but lack of outer surface. However, the prominent spinopostzygapophyseal laminae are presented, line from the neural spine to postzygapophyses and create the triangular spol under the mismatch fused rib. Lastly, the subtriangular transverse processes are ventrolaterally inclined smooth surfaces, that contrast to the mentioned ventral surfaces.

Posterior cervical vertebrae

There are five representative posterior cervical, composed of two neural arches, one unfused vertebra, and two continuous vertebrae of the same individual. Depend on the size, proportion, and EI value, the posterior cervicals have reducing in anteroposterior length, but higher neural spine with acute angle of spri and spol.

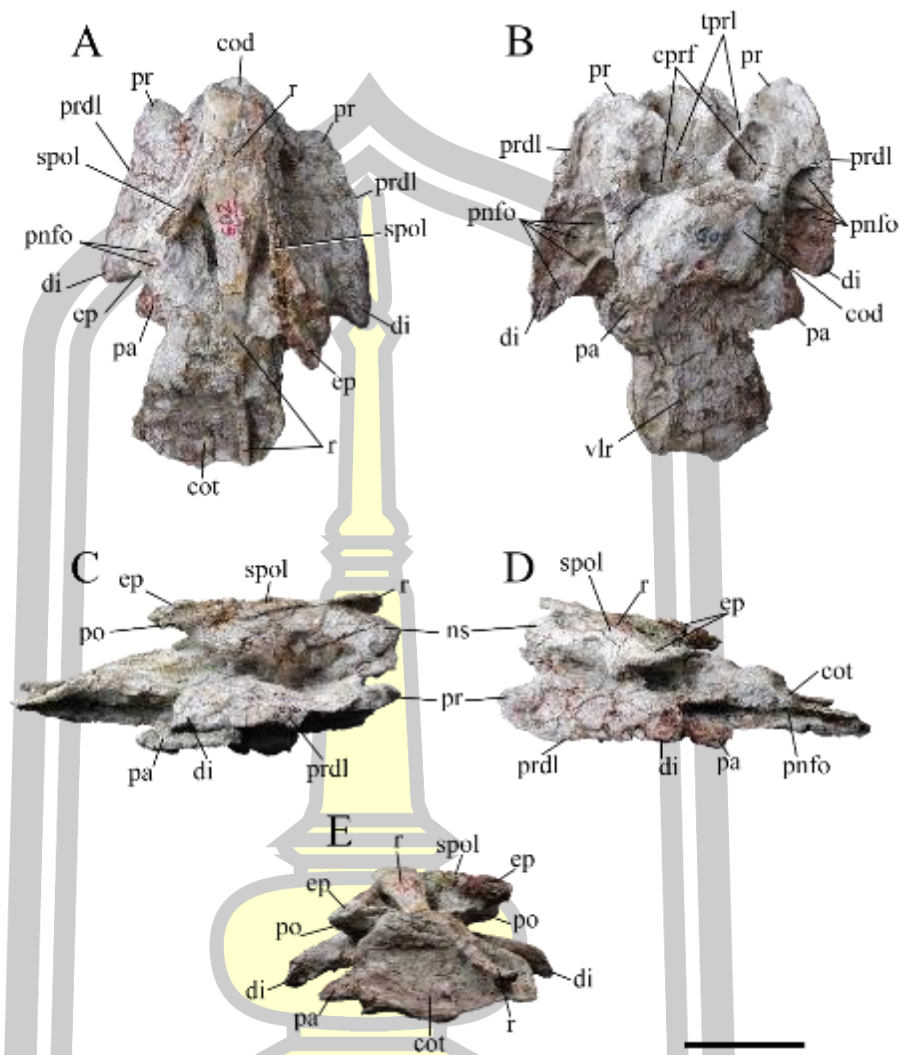


Fig 55 Middle cervical vertebra from Phu Noi locality PN 602.

A is dorsal; B is ventral; C is right lateral; D is left lateral; and E is posterior views.

Scale bar represents 10 cm.

PN 15-123 is from the juvenile individual, by the disarticulation of centrum and neural arch. The dorsal surface of the centrum has a pair of synostoses between the middle neural canal along the sagittal plane. The median keel and fossae of the ventral surface are absent while the lateral surfaces, which have concave outline of ventral border between parapophyses and cotyle rim, have small pneumatic cavities.

The oval shape pneumatic fossa only on the right lateral surface and triangular accessory laminae on the right lateral.

The left lateral surface of the neural arch has more well-preserved laminae than the counterpart. Anteriorly project of elongated pillar like cprls reach forward to the anterior most position of articular condyle of centrum. The diapophyses are crushed and compressed while the pcdl are preserved. The podl obliquely line from the center of the neural arch, which is posteriorly contacted with pcdl, to the ventral area of postzygapophyses. The neural spine has single summit on the middle line of lateral view, which has three accessory sub triangular fossae and laminae. Moreover, it has eprl like oblique strut on both lateral sides with a sub horizontal elongated triangular fossa, bounded by prdl, podl and eprl, on the left lateral surface.

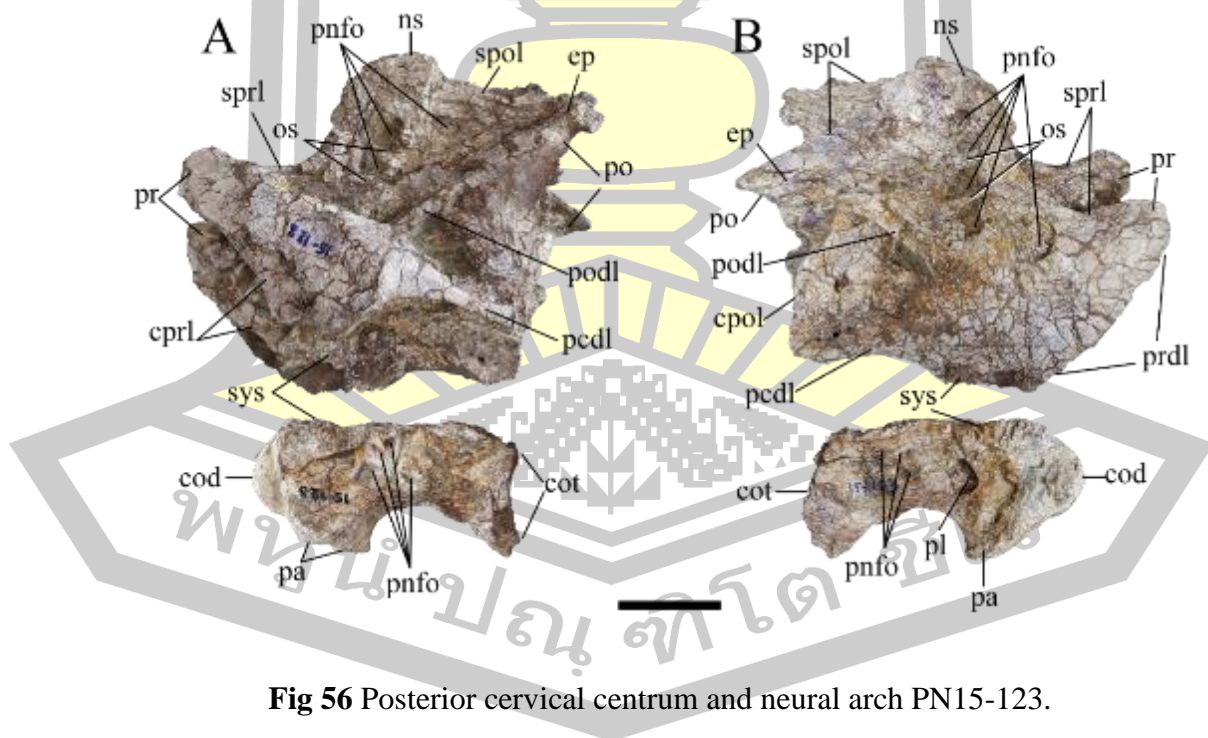


Fig 56 Posterior cervical centrum and neural arch PN15-123.

A is left lateral; B is right lateral views. Scale bar represents 10 cm.

There is a no number neural arch is from a juvenile individual like the PN15-123, confirm by the size and the pair of disarticulation synostoses on the ventral surface. The unique features of the neural arch are the numerous pneumatic fossae and accessory laminae, including the epri like lamina, on the lateral surfaces of neural spine, which called spinodiapophyseal fossa (spdf) and might be the effect of surface erosion. The overall shape from lateral views resemble to the posterior cervical neural arch, which is the same position of PN15-123.

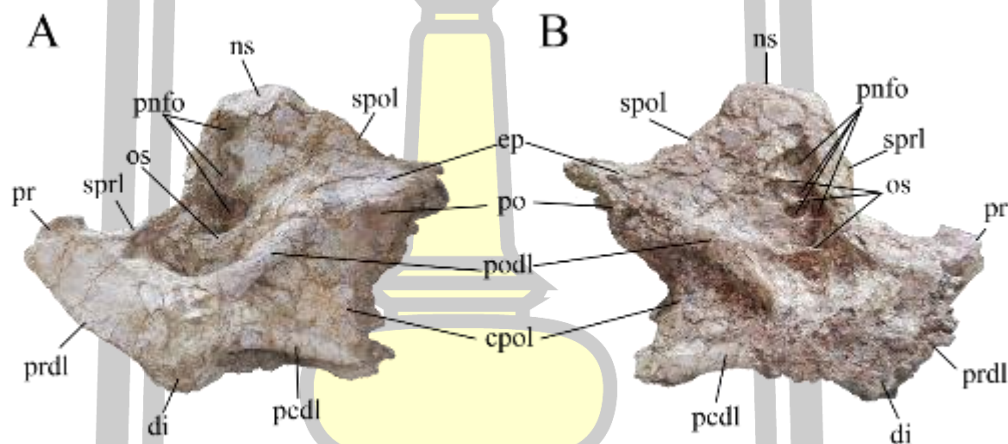


Fig 57 No number posterior cervical neural arch.

A is left lateral; B is right lateral views. Scale bar represents 10 cm.

The three last posterior cervical elements have interesting information. The single neural arch PN 17 - ? represents the similar laminae and pneumatic structures of the mentioned elements, while the two completely fused penultimate and ultimate like cervical vertebrae PN 138 to 139 have smaller size (both total length and height). Moreover, PN 138 to 139 are poorly preserved, its critically transverse compressed with eroded surfaces, especially the right lateral surface. The remaining structures on

the PN 138 and 139 are the oblique strut on the anterolateral area of the neural spine, which also determined as spinodiapophyseal fossa (sdf).

The sdf of Phu Noi cervical vertebrae occupy the entire anterior half of the lateral surfaces of the neural spines as in *Klamelisaurus*, *Omeisaurus* spp. and *Qijianglong* (Moore et al., 2020; C Tan et al., 2019; Chao Tan et al., 2021; Xing et al., 2015), differ from the vertically short neural spine with small subtriangular sdf in *Mamenchisaurus* spp., and *Xinjiangtitan* (Xinlu He et al., 1996; Ouyang & Ye, 2001; C.-C. Young & Zhao, 1972; X.-Q. Zhang et al., 2020). The strut is presented in every Phu Noi cervical vertebra, which have variation of angle, presence of laminae, and the size of juvenile and adult are not related. Interestingly, while the penultimate and ultimate cervical vertebrae of *M. youngi* (CV 17 and CV 18), the whole cervical series of *M. hochuanensis* (CV 2 to CV 19), the posterior cervical from Phu Noi have single spine like *Omeisaurus* spp. and *Qijianglong* or ambiguous bifid like *Mamenchisaurus* spp. but transverse compressed (X.-L. He et al., 1988; Xinlu He et al., 1996; Ouyang & Ye, 2001; C Tan et al., 2019; Xing et al., 2015).

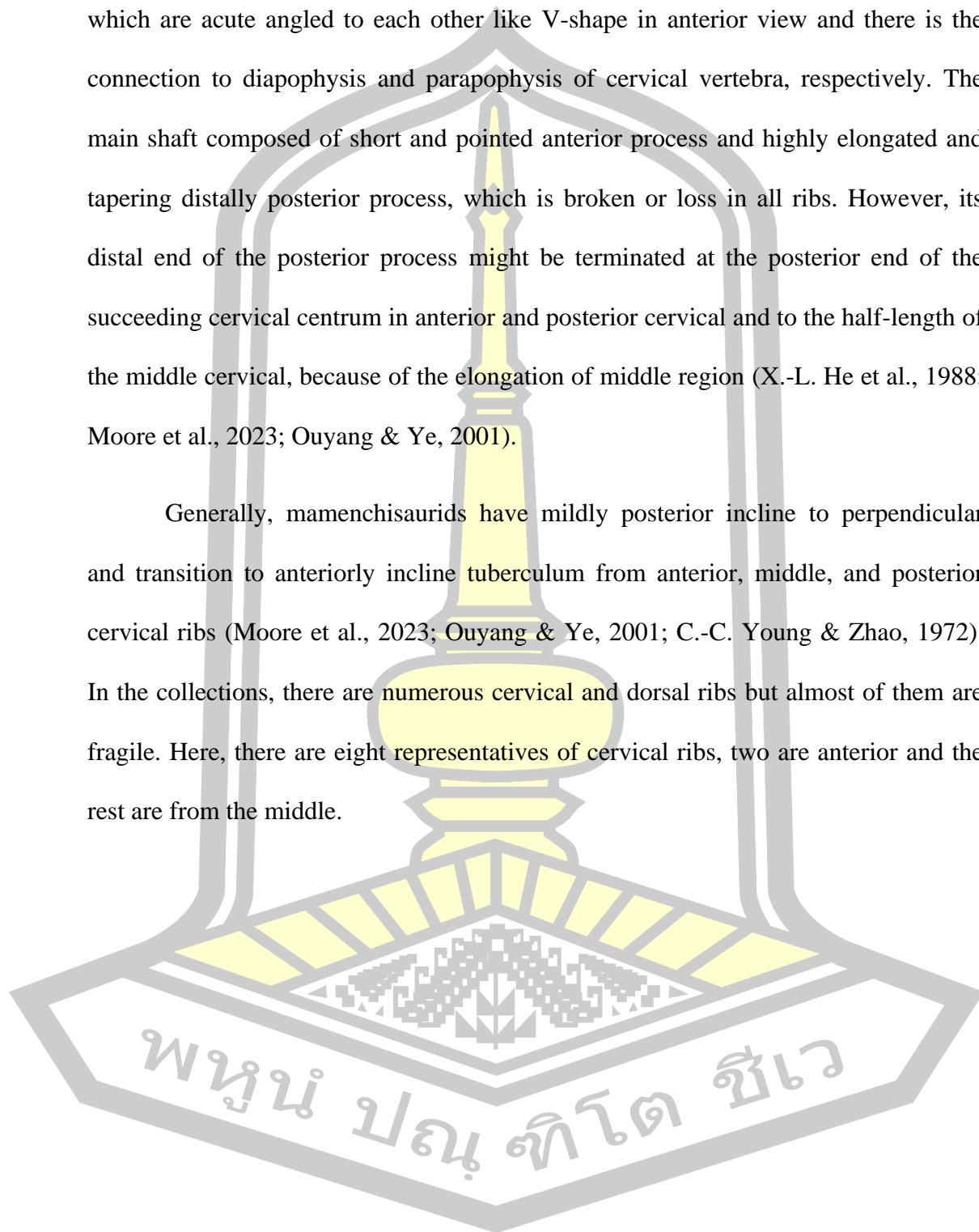
From the mentioned morphological features, all posterior cervical vertebrae are resembled to *Klamelisaurus*, *Omeisaurus* spp. and *Qijianglong*, which are distinct from *Mamenchisaurus* spp. by the absent of spine bifurcation. However, from the relative size of the larger neural arch and the smaller continuous and completely fused vertebrae, there might be from difference mamenchisauridae taxa.

Cervical ribs

The rib composed of main body at the one third of the total anteroposterior length of the bone, which is the intersection of the tetra radiate process. The main

articular facets are the vertically directed tuberculum and medially directed capitulum, which are acute angled to each other like V-shape in anterior view and there is the connection to diapophysis and parapophysis of cervical vertebra, respectively. The main shaft composed of short and pointed anterior process and highly elongated and tapering distally posterior process, which is broken or loss in all ribs. However, its distal end of the posterior process might be terminated at the posterior end of the succeeding cervical centrum in anterior and posterior cervical and to the half-length of the middle cervical, because of the elongation of middle region (X.-L. He et al., 1988; Moore et al., 2023; Ouyang & Ye, 2001).

Generally, mamenchisaurids have mildly posterior incline to perpendicular and transition to anteriorly incline tuberculum from anterior, middle, and posterior cervical ribs (Moore et al., 2023; Ouyang & Ye, 2001; C.-C. Young & Zhao, 1972). In the collections, there are numerous cervical and dorsal ribs but almost of them are fragile. Here, there are eight representatives of cervical ribs, two are anterior and the rest are from the middle.



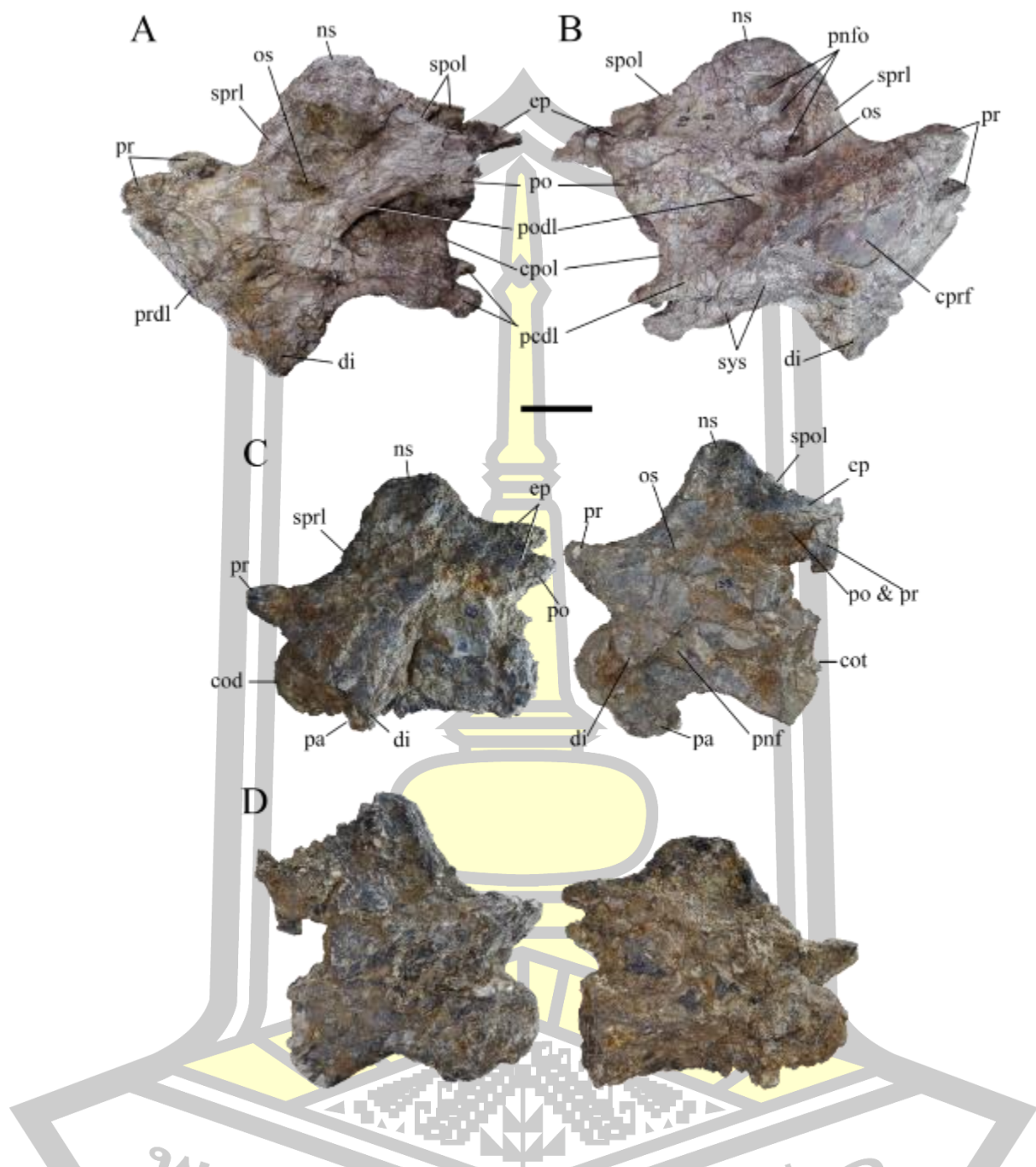
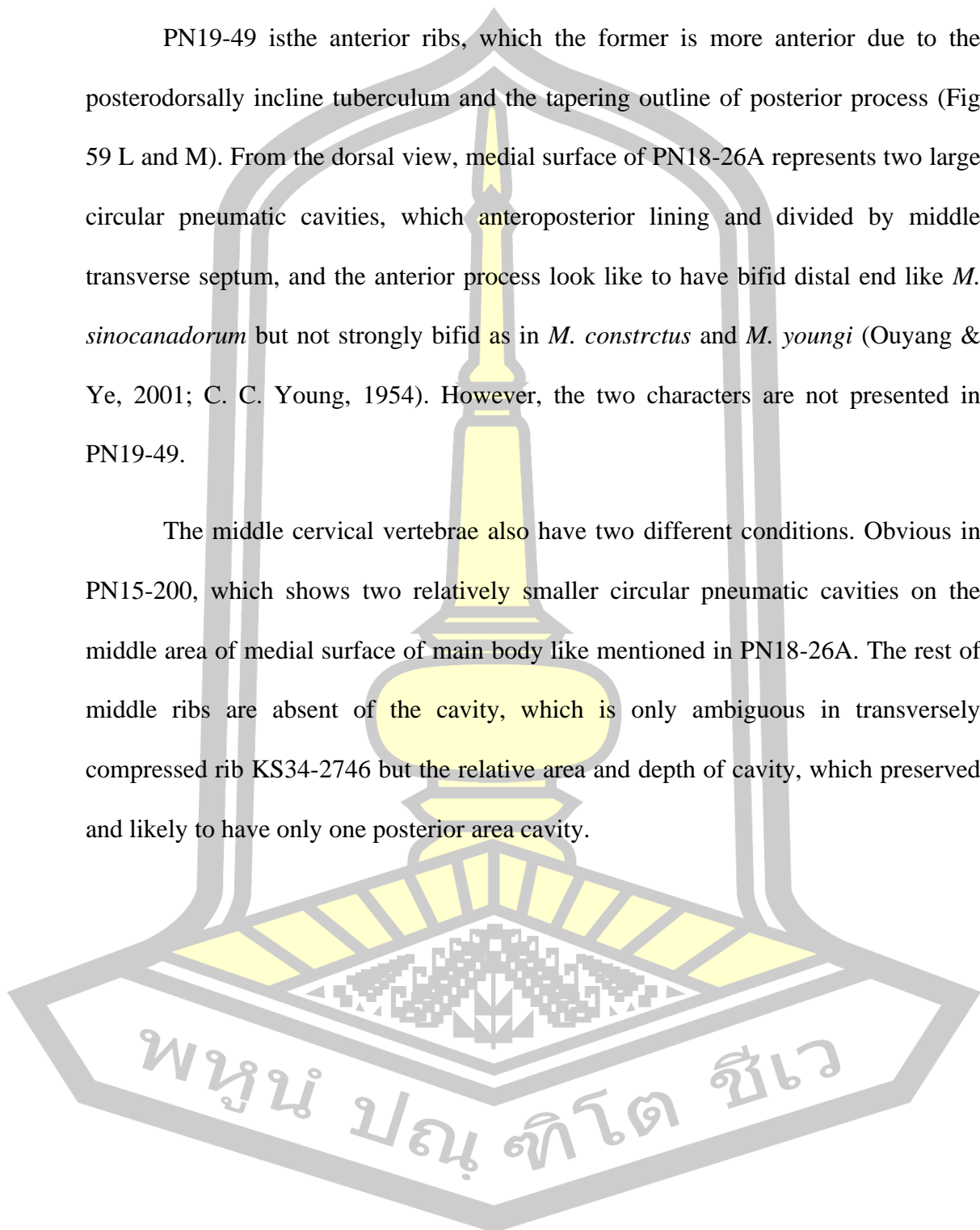


Fig 58 Three posterior most cervical elements of mamenchisaurid sauropods from Phu Noi locality.

A and C are left lateral; B and D are right lateral views. A and B, PN17-? C and D, PN 138 and PN 139 in articulate form. Scale bar represents 10 cm.

PN19-49 is the anterior ribs, which the former is more anterior due to the posterodorsally incline tuberculum and the tapering outline of posterior process (Fig 59 L and M). From the dorsal view, medial surface of PN18-26A represents two large circular pneumatic cavities, which anteroposterior lining and divided by middle transverse septum, and the anterior process look like to have bifid distal end like *M. sinocanadorum* but not strongly bifid as in *M. constrictus* and *M. youngi* (Ouyang & Ye, 2001; C. C. Young, 1954). However, the two characters are not presented in PN19-49.

The middle cervical vertebrae also have two different conditions. Obvious in PN15-200, which shows two relatively smaller circular pneumatic cavities on the middle area of medial surface of main body like mentioned in PN18-26A. The rest of middle ribs are absent of the cavity, which is only ambiguous in transversely compressed rib KS34-2746 but the relative area and depth of cavity, which preserved and likely to have only one posterior area cavity.



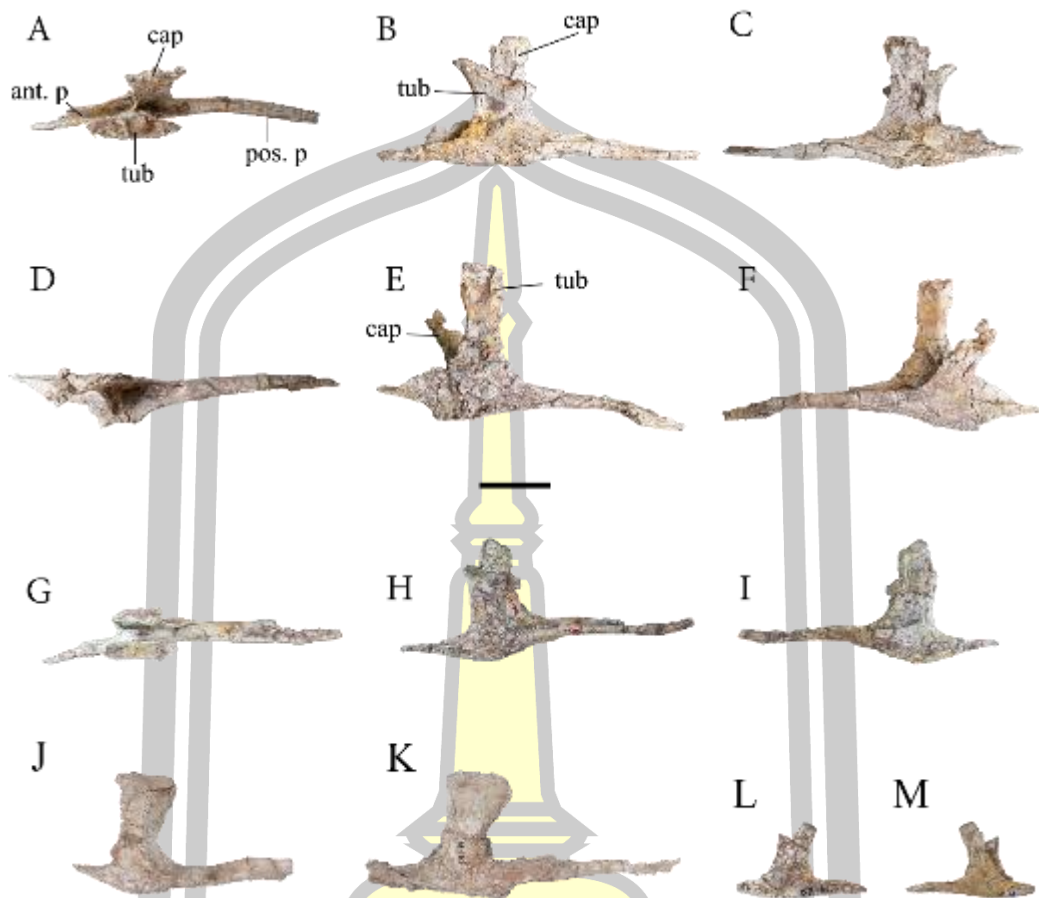


Fig 59 Cervical ribs of mamenchisaurid sauropods from Phu Noi locality.

A, D, G, M, and J are dorsal; B, E, H, J, K, N, and O are left lateral; C, F, I, and P are right lateral views. A to C, KS34-1970. D to F, KS34-2746. G to I, PN15-74. J, no number cervical rib. K, PN14-115. L, PN15-200. M and N, PN18-26A. O and P, PN19-49. Scale bar represents 10 cm.

Dorsal vertebrae

The dorsal vertebrae are anteroposteriorly short with opisthocelous articulation and laterally flare neural arches. The anterior dorsal elements have bifurcated neural spines, which are shorter than the height of neural arch, and vertically low level of parapophyses. While the middle and posterior dorsal have

single vertically directed and elongated neural spine, which have dorsoventrally directed prespinal and postspinal laminae (prsl and posl) along the middle area of middle and posterior dorsal vertebrae. The epipophyses and eprl are absent, while the transverse process flare laterally as the weakly downward curve arch in anterior dorsal to the dorsolateral directed of straight pointed processes in middle to posterior dorsal. The position of parapophyses, which are always located at the ventrolateral edge along the cervical series, is vertically migrated from the lateroventral rim of the centrum along the cervical to the middle height of centrum in the first dorsal. Subsequently, it gradually migrates to the upper level of neural arch, one fourth lower than the height of prezygapophyses.

The isolated anterior dorsal vertebrae from Phu Noi are resembled to *Mamenchisaurus* spp., by the presence of U-shape spine bifurcation (Ouyang & Ye, 2001; C.-C. Young & Zhao, 1972; Yihong Zhang et al., 1998). In *Klamelisaurus*, one of the distinct Mamenchisauridae from *Mamenchisaurus*, have V-shape bifurcation and small median boss on the middle notch of the spines (Moore et al., 2020).

Anterior dorsal vertebrae

Due to the heavily damaged of the specimens from Phu Noi locality, only three anterior dorsal elements are selected to describe (Fig 60). There are the neural arch PN15-16, complete but critically anteroposterior compressed vertebra PN581, and obligate anteroposterior compressed neural arch PN582. The description is mainly considered to PN581, which have the best preservation of lamina structures.

PN581 is the representative anterior dorsal vertebra specimen from three of the most well-preserved elements in the PRC collection (Fig 60 B and C) Based on

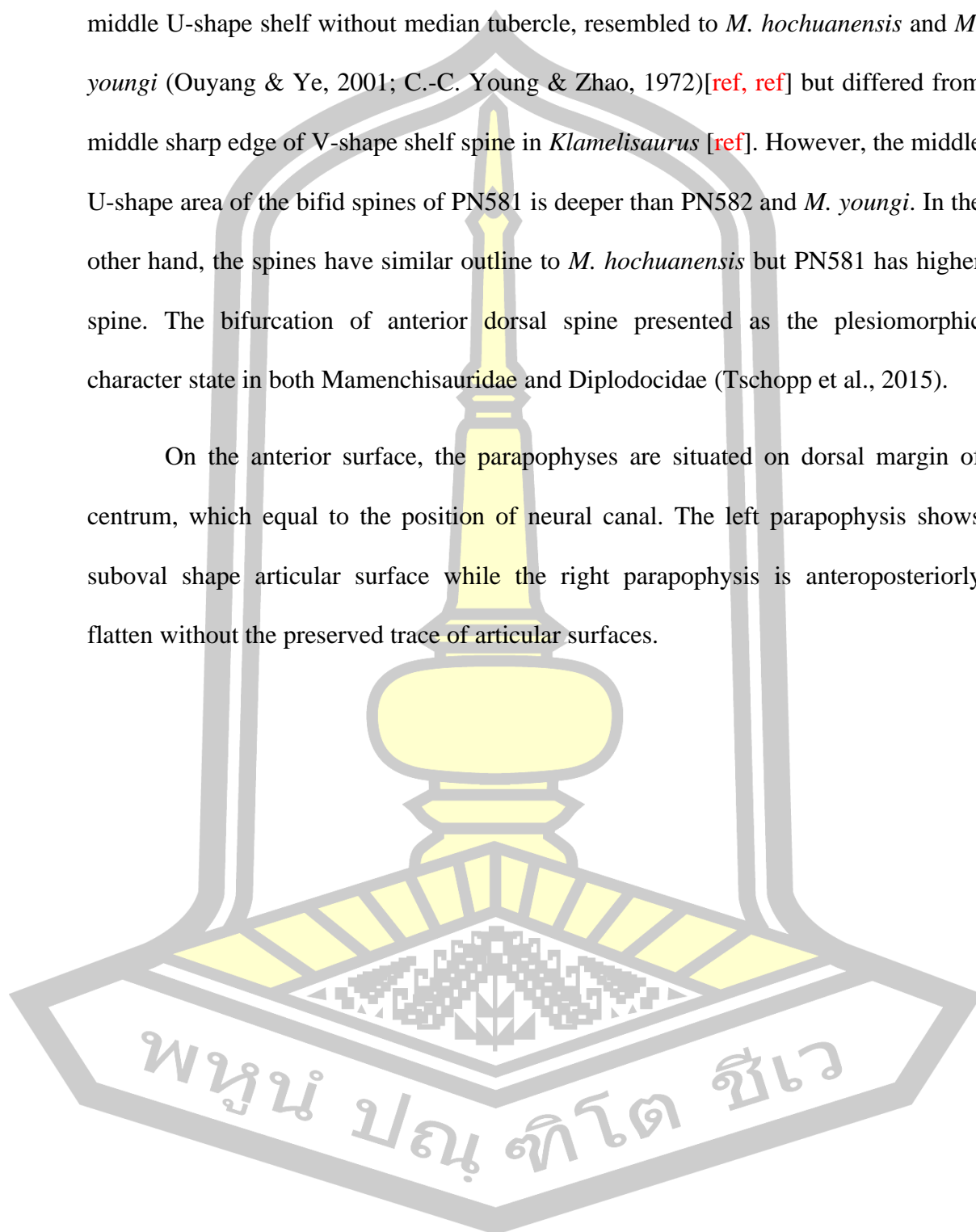
the position of the parapophysis, the shape of transverse process and neural spine, the vertebra is considered as the second dorsal. Even though it is completely preserved with all articulation and structures, the vertebra is critically compressed on anteroposterior plain. Especially, the lateral surfaces of neural arch, which is impossible to measure and describe. Because of the irregular compression, the mean height and width of the anterior and posterior surfaces are 54.89 cm and 69.87 cm, respectively. The centrum is horizontal axis ellipsoid with mildly convex articular surface, as in *Mamenchisaurus* spp. and *Omeisaurus* spp. (Chao et al., 2019; Ouyang & Ye, 2001; X. X. Ren, Sekiya, Wang, Yang, & You, 2021).

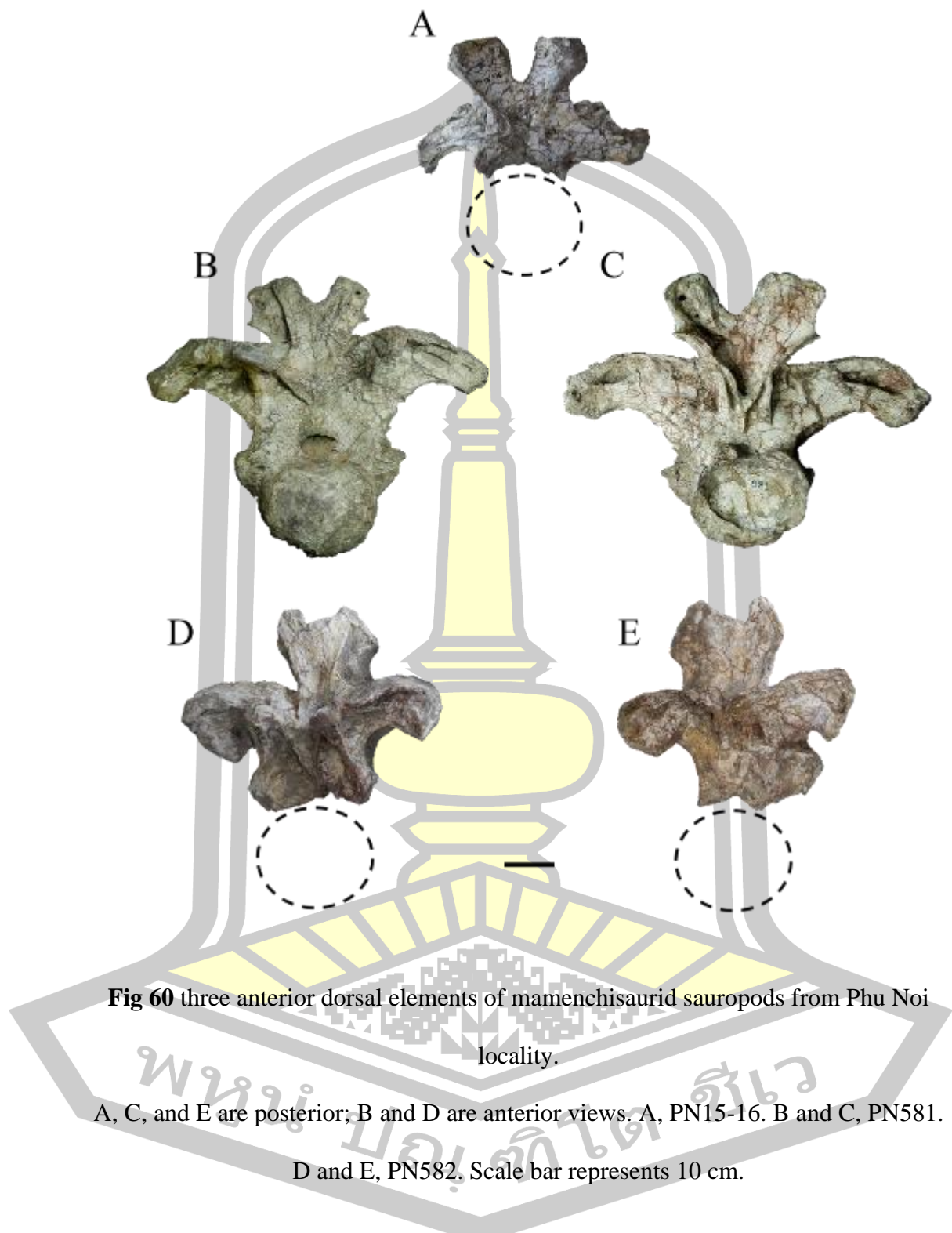
The posterior articular surface is concave, which means the centrum articulation of the specimen is opisthocoelous, which are strongly to weakly opisthocoelous from anterior to posterior position of the vertebrae as in mamenchisaurids (X.-L. He et al., 1988; Ouyang & Ye, 2001). The ventral surface is the conjoin arch of lateral surfaces without the median septum or ventral keel as in mamenchisaurids (X.-Q. Zhang et al., 2020). Moreover, ventral area is anteroposteriorly bounded by the edges of the anterior and posterior articular surfaces. There is one trace of shallow pleurocoel depression on the central area of right lateral surface with unclear margin like in *Mamenchisaurus youngi* (Ouyang & Ye, 2001). Contrasting to the anterior dorsal vertebrae of *M. hochuanensis*, and the first and second dorsal vertebrae of *Omeisaurus tienfuensis*, which are absent of pleurocoel (X.-L. He et al., 1988).

The neural arch is relatively wide, the height of the neural arch and spine is shorter than the width of transverse process, and the transverse process expand

horizontally, curving downward in distal end. The neural spine has bifurcation and middle U-shape shelf without median tubercle, resembled to *M. hochuanensis* and *M. youngi* (Ouyang & Ye, 2001; C.-C. Young & Zhao, 1972)[ref, ref] but differed from middle sharp edge of V-shape shelf spine in *Klamelisaurus* [ref]. However, the middle U-shape area of the bifid spines of PN581 is deeper than PN582 and *M. youngi*. In the other hand, the spines have similar outline to *M. hochuanensis* but PN581 has higher spine. The bifurcation of anterior dorsal spine presented as the plesiomorphic character state in both Mamenchisauridae and Diplodocidae (Tschopp et al., 2015).

On the anterior surface, the parapophyses are situated on dorsal margin of centrum, which equal to the position of neural canal. The left parapophysis shows suboval shape articular surface while the right parapophysis is anteroposteriorly flatten without the preserved trace of articular surfaces.





The two remain situate laminae of parapophysis are preserved: the anterior centroparapophyseal lamina (acpl) from the laterodorsal margin of the centrum to the

connect to the dorsal margin of neural canal and enclose two large symmetric oval shape centroprezygapophyseal fossae (cprf). This lamina gradually diminishing from the third dorsal vertebra in *M. youngi* (Jinyou & Buffetaut, 2011; Ouyang & Ye, 2001), while acutely disappeared by the fourth or fifth dorsal vertebra of other sauropods (Jinyou & Buffetaut, 2011).

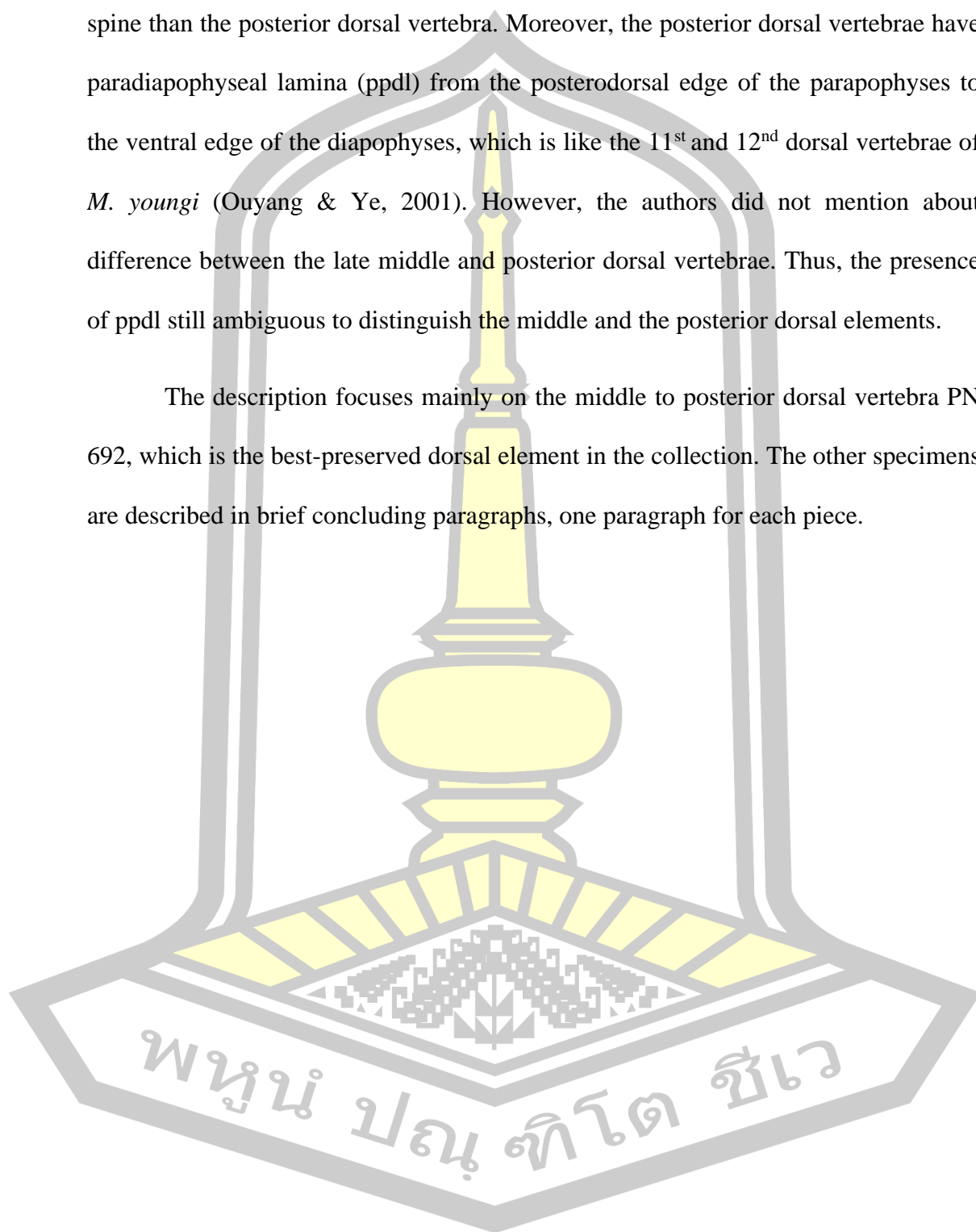
On the posterior surface, the postzygapophyses are represent as elongated ellipsoid facets, on the ventrolateral area of neural spine. The left and right spol line on the lateral border of neural spine. Cpol vertically supports the postzygapophyses from below. Between the postzygapophyses is the lamina called intrapostzygapophyseal lamina (tpol), which present in Y-shape bulge structure that fit to the space of tprl, shows the ventral end above the neural canal. Podl(s) are absent, either natural condition or the compression. The posterior surface area of neural spine is concave and present as the single large spine fossa, ventrally enclosed by the dorsal end of the tpol. The pair of elongate ellipsoid fossa present between tpol and cpol. The teardrop shape fossae are symmetrical presented on the upper and lower area of transverse processes are resembled to *M. hochuanensis* (C.-C. Young & Zhao, 1972). There are numerous pneumatic cavities on the left neural spine and both distal end of transverse processes. Other neural cavities on the lateral area of cpol(s) might be the cause of erosion damages.

Middle to posterior dorsal vertebrae

There are five specimens of the region to describe, which have four isolated and one large and tightly articulation of two vertebrae (Fig 62). The bifid spine gradually turning to shallow cleft and vertically elongated single spine posteriorly, like the pattern of spine alteration in mamenchisaurids and diplodocoids (Wilson,

2002). The middle dorsal vertebra has transversely broader but dorsoventrally shorter spine than the posterior dorsal vertebra. Moreover, the posterior dorsal vertebrae have paradiapophyseal lamina (ppdl) from the posterodorsal edge of the parapophyses to the ventral edge of the diapophyses, which is like the 11st and 12nd dorsal vertebrae of *M. youngi* (Ouyang & Ye, 2001). However, the authors did not mention about difference between the late middle and posterior dorsal vertebrae. Thus, the presence of ppdl still ambiguous to distinguish the middle and the posterior dorsal elements.

The description focuses mainly on the middle to posterior dorsal vertebra PN 692, which is the best-preserved dorsal element in the collection. The other specimens are described in brief concluding paragraphs, one paragraph for each piece.



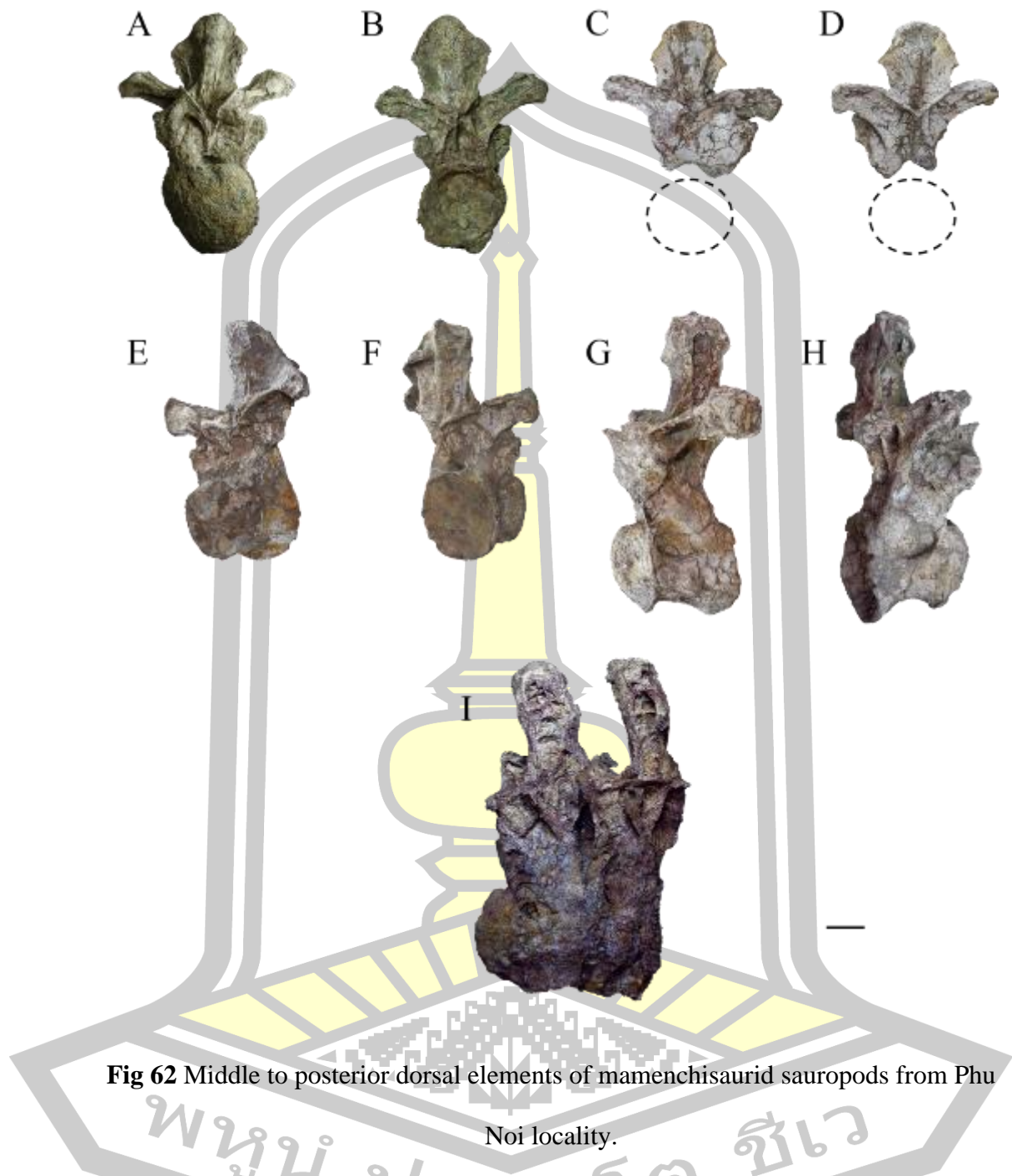
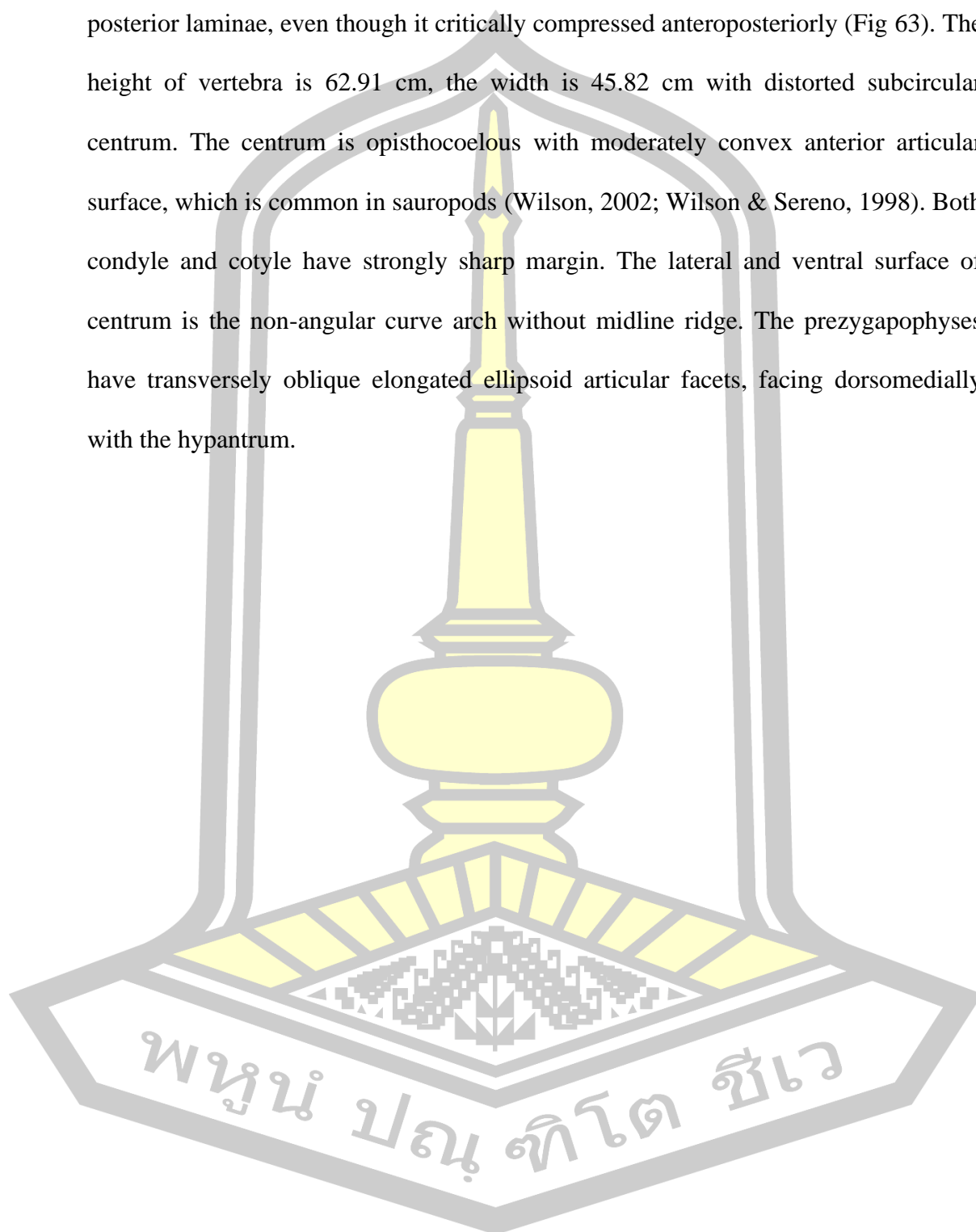
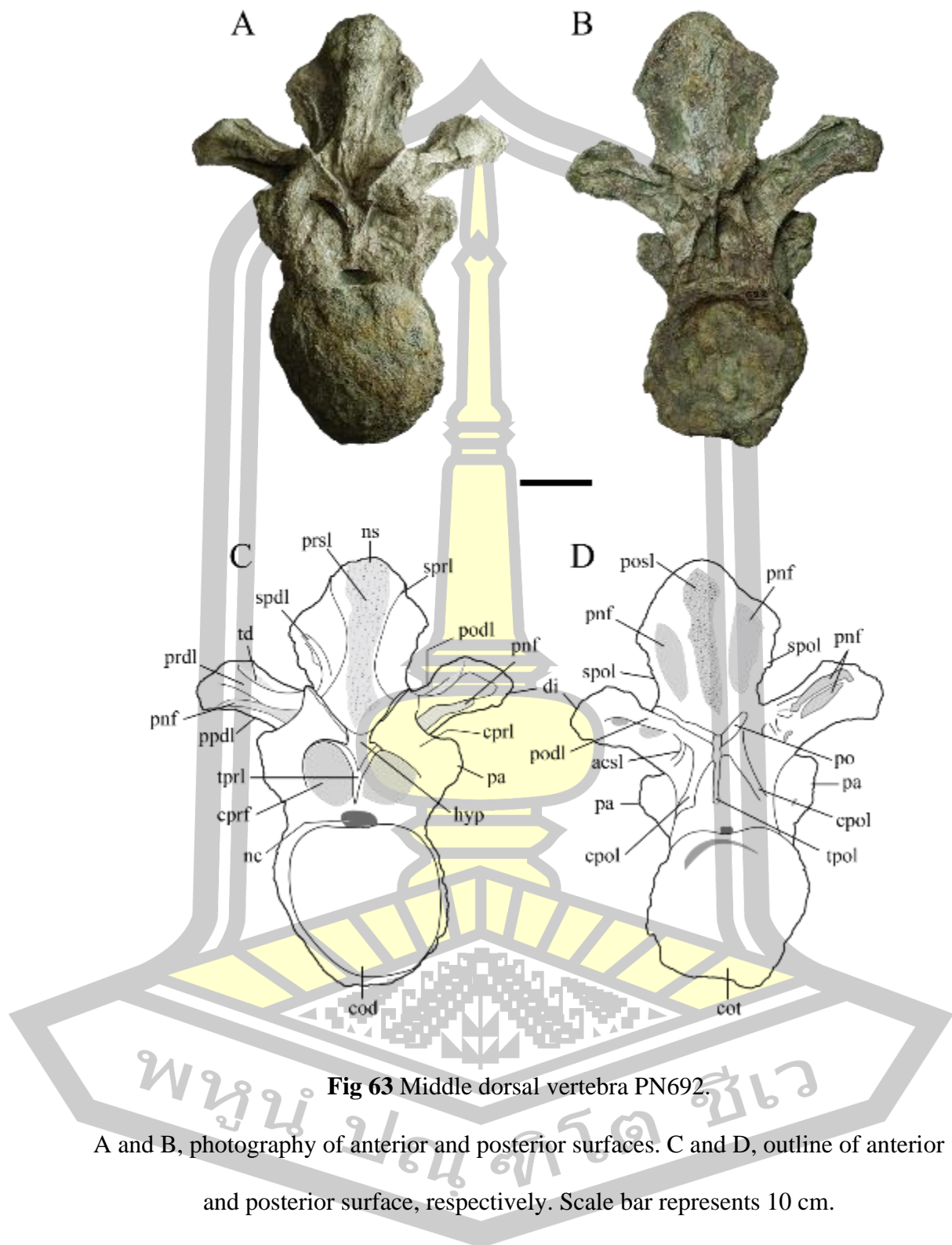


Fig 62 Middle to posterior dorsal elements of mamenchisaurid sauropods from Phu Noi locality.

A and C are anterior; B and D are posterior; E is anterolateral; F is posterolateral; G and I are left lateral; and H is right lateral views. A and B, PN 692. C and D, PN15-49. E and F, PN17-147. G and H, PN13-23. I, No number two articulated dorsal vertebrae. Scale bar represents 10 cm.

Like PN581, dorsal vertebra PN692 has completely preserved of anterior and posterior laminae, even though it critically compressed anteroposteriorly (Fig 63). The height of vertebra is 62.91 cm, the width is 45.82 cm with distorted subcircular centrum. The centrum is opisthocoelous with moderately convex anterior articular surface, which is common in sauropods (Wilson, 2002; Wilson & Sereno, 1998). Both condyle and cotyle have strongly sharp margin. The lateral and ventral surface of centrum is the non-angular curve arch without midline ridge. The prezygapophyses have transversely oblique elongated ellipsoid articular facets, facing dorsomedially with the hypantrum.





Robust cprls ventrolaterally support each prezygapophysis and connect with lower flatten trapezoid shape parapophysis by prezygoparapophyseal lamina (prpl).

Y-shape tpri presents on the central area, between the height of neural canal and prezygapophyses as in the second dorsal. The cprls and tpri bound the pair of subcircular cprf dorsolateral and dorsomedial, respectively. The transverse processes weakly flare dorsolateral with thick prdls, that dorsally bound elongated prezygapophyseal diapophyseal fossae (prdf) and connected to neural spine by curve arch of spinodiapophyseal lamina.

Like the posterior dorsal spines of Mamenchisauridae, there is broad robust petal shape single neural spine, which flare dorsolaterally through the semicircular distal end, bears thick rugose surface of ligament scar on the broad prsl. Sprl vertically brace along the lateral edges of prsl from the prezygapophyses to the distal end of the spine with outer texture of spine that bound by spdl and spol. On the posterior surface, the broad median posl, which occupy one third area of neural spine, vertically posture along the spine with a pair of dorsolateral oval shape fossae. There are the left and right lateral area of vertically elongated large spinopostzygapophyseal fossae (spof), laterally bounded by spinopostzygapophyseal laminae (spol) and medially bounded by posl.

Moreover, the posl ventrolaterally connects to postzygapophyses, which ventromedially facing and bear transversely flatten and elongate articular surfaces. The broken central area between postzygapophyses resemble to the remaining of hyposphene. Tpol vertically lines beneath the hyposphene and reaches to the height of parapophyses, which have broken trace of lamina to the dorsal margin of neural canal. The left and right cpol(s) dorsomedially line beside tpol from the laterodorsal margin of the centrum to the middle area under hyposphene and postzygapophyses.

The transverse processes are possessed by numerous fossae, which might be from the enclosing of structural lamination and from the damage that destroy the bone surface layer then expose the large elongated internal pneumatic chambers. The main laminae of transverse processes are pcdl(s) as the ventral arch from laterodorsal margin of centrum to ventral margin of diapophyses and podl(s) line on the dorsal margin of transverse processes. The accessory laminae are the small medially curved vertical laminae near cpol(s) and branch laminae of podl(s), that enclose left and right postzygodiapophyseal fossa (podf) while the right elongated fossa over the right podf is the exposed internal fossa.

Finally, ppdl, which connected between parapophyses and diapophyses and presents in the last three dorsal vertebrae of *Mamenchisaurus* spp., are absent. From the mentioned characteristics of the specimen, PN692 should be the middle dorsal vertebra.

PN13-23 (Fig 64) is considered to the posterior dorsal vertebra, which could be 9th to 12nd dorsal, by the presented of dorsoventrally high neural arch, the single robust and high neural spine, the reduction of hyposphene structure, the absence of tprl, and the presence of ppdl. Furthermore, PN17-147 and the articulated dorsal vertebrae (Fig 62 I) also should be the posterior dorsal vertebrae by the presence of ppdl.

The explicit posterior margin of the anterior condyle is only presented on the left lateral surface lines from the most ventral part of the centrum and ventrally connects to acpl, which might be the cause of compression. The pleurocoel are presented on both anterodorsal area of the lateral surfaces of centrum with clearly

curve ventral border and anterodorsally depressed curve border. The pleurocoel bear an inside elliptical pneumatic fossa. The dorsal area of pleurocoels and dorsally reach to the ventral area of the neural arch and. The neural arch is relatively slender, the dorsoventral high are equal to the neural spine and a bit higher but equally in the transverse width of centrum. The prezygapophyses, with half medially broken on the left one, are 45 degrees medially inward bend and have flat oval shape articular surfaces. The vertical lamina tp_{rl}, which presented on the anterior and middle dorsal vertebrae, is absent. The cp_{rls} and prezygoparapophyseal lamina (prpl) medioventrally and lateroventrally support the prezygapophyses, respectively. The subrectangular parapophyses located on the middle height of the neural arch and laterally flare by the outward bending of prpl on the upper part and acpl on the lower part.

The transverse processes are horizontal elongating on the posterolateral direction. The sub square shape diapophyses are located on the distal ends of the transverse processes, which have the small dorsal and ventral protrusions. The supported laminae of transverse processes and diapophyses are sp_{dl}, pr_{dl}, po_{dl}, pp_{dl}, pc_{dl} and accessory posterior lamina, that located near the cp_{ol}. The fossae of transverse processes are the horizontally elongated subtriangular parapophyseal prezygodiapophyseal fossa (papr_{df}) on the anterior surface, and the distally directed teardrop shape accessory pneumatic fossa near the distal end of the posterior surface. The articular surfaces of the postzygapophyses conjoin at the vertical midline of the vertebra.

The articular surfaces bend ventrolaterally to assemble with the prezygapophyses of the adjacent vertebra. postzygapophyses ventrally support by the ventrally broken median tpol, which connected to the dorsal margin of the neural canal, and the beside pair of cpol. The lozenge-shape postspinal fossa is on the mediodorsal area of the dorsal margin of postzygapophyses. The pillar like neural spine vertically stands on the middle to posterior area of the neural arch. It anteroposterior longer than the transverse width with sprls on the anterolateral borders, spdls on lateral, and spols with distally weak aliform process on posterolateral borders.

The prsl is not presented, which have smooth surface of median sprf instead. The posl is presented as the rough surface area, which could be the attachments of ligaments and tendons, between spols. Lastly, the lateral area of spdf exposed numerous pneumatic cavities with various polygon shape.

The dorsal vertebra PN13-23 is resembled to *Omeisaurus tienfuensis* but the postzygapophyses are the oblique straight line not upside-down parabola shape articular facets (X.-L. He et al., 1988).

The last-mentioned dorsal material is the fusion of two posterior dorsal vertebrae (Fig 62I), specified from the outline shape of the neural arch and spine with the location of articulation landmarks. Due to the large size and lateral compression, especially the neural spine, the observation is limited to the left lateral surface. The centrum is anteroposteriorly short and dorsoventral high with prominent subcircular anterior articular condyle of the first vertebra. The second vertebrae condyle is shorter and possess inside the posterior end of the first one. By the tightly centra articulation,

the specimen might be the 11th and 12th dorsal vertebrae, which have more strongly centra connection than other position in the dorsal series as many reports from specimens of mamenchisauridae.

The pleurocoel is large with subcircular shape border, located between the anterodorsal area of the lateral surface of centrum and the anteroventral area of neural arch, with a damaged teardrop shape internal pneumatic fossa. The neural arch and spine are relatively tall and anteroposteriorly short, as well as the centra. On the first vertebra, the neural arch shows entire preserved landmarks and laminae of the lateral surface.

By the distortion, right prezygapophysis bend dorsally above the left one, noticeable as the anterodorsal projection between left prezygapophysis and neural spine. The parapophysis have the remaining of posteriorly oblique ppdl as the connection remnant to the lost diapophysis.

The transverse process is broken, only remaining is the proximal portion, which has small accessory laminae and fossa with the traces of prdl, pcdl, spdl, and podl. The postzygapophyses show on both vertebrae, with clearly seen in the second, no evidence of hyposphene. The postzygapophyses is ventrally supported by a single middle tpol and a pair of ventrally expanded cpols beside tpol. There is a single neural spine, which have equal height as the neural arch but anteroposteriorly shorter.

The lateral surface of the spine is possessed by the numerous small crescents and subcircular cells of internal pneumatic cavities, which are unique among the specimens in the collection. The presented laminae of the spine are posl, prsl, sprl,

spdl. Even though the specimen is like the articulated 10th and 11th dorsal vertebrae of *M. anyuensis* (Xinlu He et al., 1996).

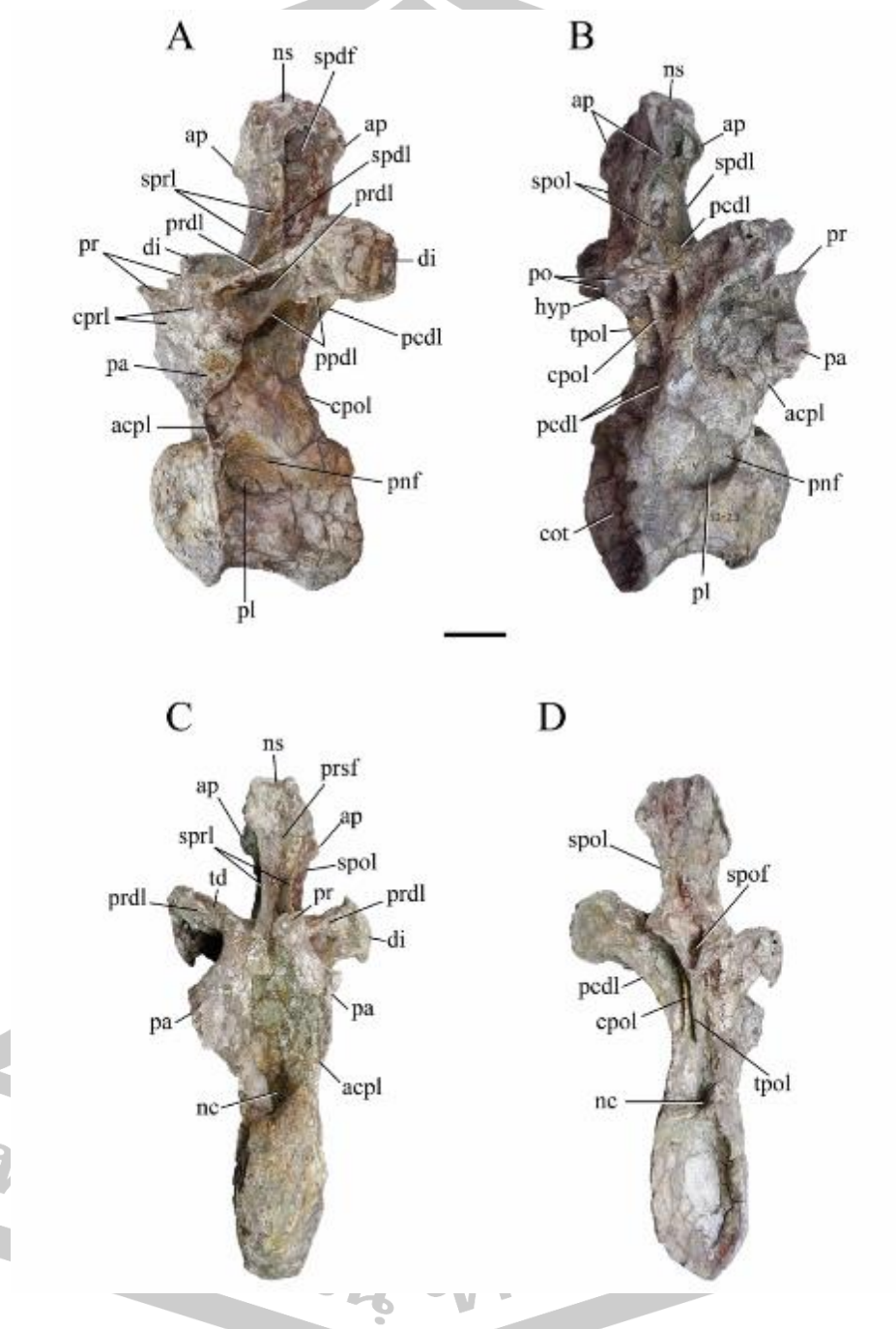


Fig 64 Posterior dorsal vertebra PN13-23.

A is left lateral; B is right lateral; C is anterior; D is posterior views. Scale bar represents 10 cm.

Anterior dorsal ribs

The ribs head has medially bended V-shape vertical bifurcation of two medial connecting structures, tuberculum on the upper and capitulum on the lower plain, which are like cervical ribs, but they are vertically bended according to the transitional position of diapophysis and parapophysis. The shaft is dorsoventrally directed arch, which is straight shaft in anterior dorsal rib but curving outward on the middle area of middle and posterior ribs, with anteroposterior parallel lateral ridge, that made the lateral surface of the rib have almost straight outline (Fig 65).



Fig 65 Anterior dorsal ribs of Mamenchisauridae sauropods from Phu Noi locality in anterior view.

A, KS34-3184 (right reverse). B, KS34-2466 (right reverse). Scale bar represents 10 cm.

Caudal vertebrae

In Mamenchisauridae, the caudal vertebrae differentiate into four sections, anterior, middle, posterior, and distal, which are determined from position, size, shape, and morphological features (Fig 66).



Fig 66 Caudal vertebrae of mamenchisaurids from Phu Noi locality.

A and C are posterior; B and F are anterior; D, E, G to K are left lateral views. A, no number anterior caudal. B, PN14-146 anterior to middle caudal. C, PN14-212A anterior to middle caudal. D, PN14-212B to F articulated middle caudal. E, PN15-80 middle caudal. G to I, KS34-689, KS34-645, and PN13-14 middle to posterior caudal.

J and K, distal caudal. Scale bar represents 10 cm.

Anterior caudal vertebrae

The large and robust no number anterior caudal vertebra is heavily anteroposterior compressed, preserving in the plaster with numerous damaged areas and critically fragile condition, which cannot overturn to observe the opposite side (Fig 67).

It has dorsoventrally short and transversely narrow subtriangular area of neural arch, with the relatively short horizontal protrusions of transverse processes on the middle to dorsal height of the centrum. Additionally with the wing like lamina from the top of the transverse process's protrusions to the middle area beneath the postzygapophyses. The neural spine is elongated rectangular shape, occupied one third of the total height, with transversely plane summit end and the postzygapophyses are presents, which can consider the posterior surface. The oval shape centrum, which has elongated height than width, is prominently convex. The large circular neural canal is possessed inside the middle area of the dorsoventral short but robust subtriangular neural arch. Above the neural arch are postzygapophyses with middle space between each other and the area of postspinal fossa, which is presented along the vertical area of the ventral half of the neural spine. The spine is vertically elongated rectangular shape with horizontal plain summit and being ventrolaterally bordered by the left and right spol(s).

PN14-146 is the anteroposteriorly compressed anterior caudal vertebra (Fig 68). The neural arch is narrower and shorter than the dorsal, which is transformed from the vertically elongated rectangular to trapezoid shape. The dorsoventrally broad and transversely elongate transverse process is reduced to small horizontal protrusion. Its ventrally migrate from the dorsolateral height above the neural canal to the three-

fourths height of the centrum. Moreover, the neural spine changed from vertically elongated straight pillar shape to slender petal shape, which is transversely broad in proximal and distal end with narrow middle shaft, in caudal region.

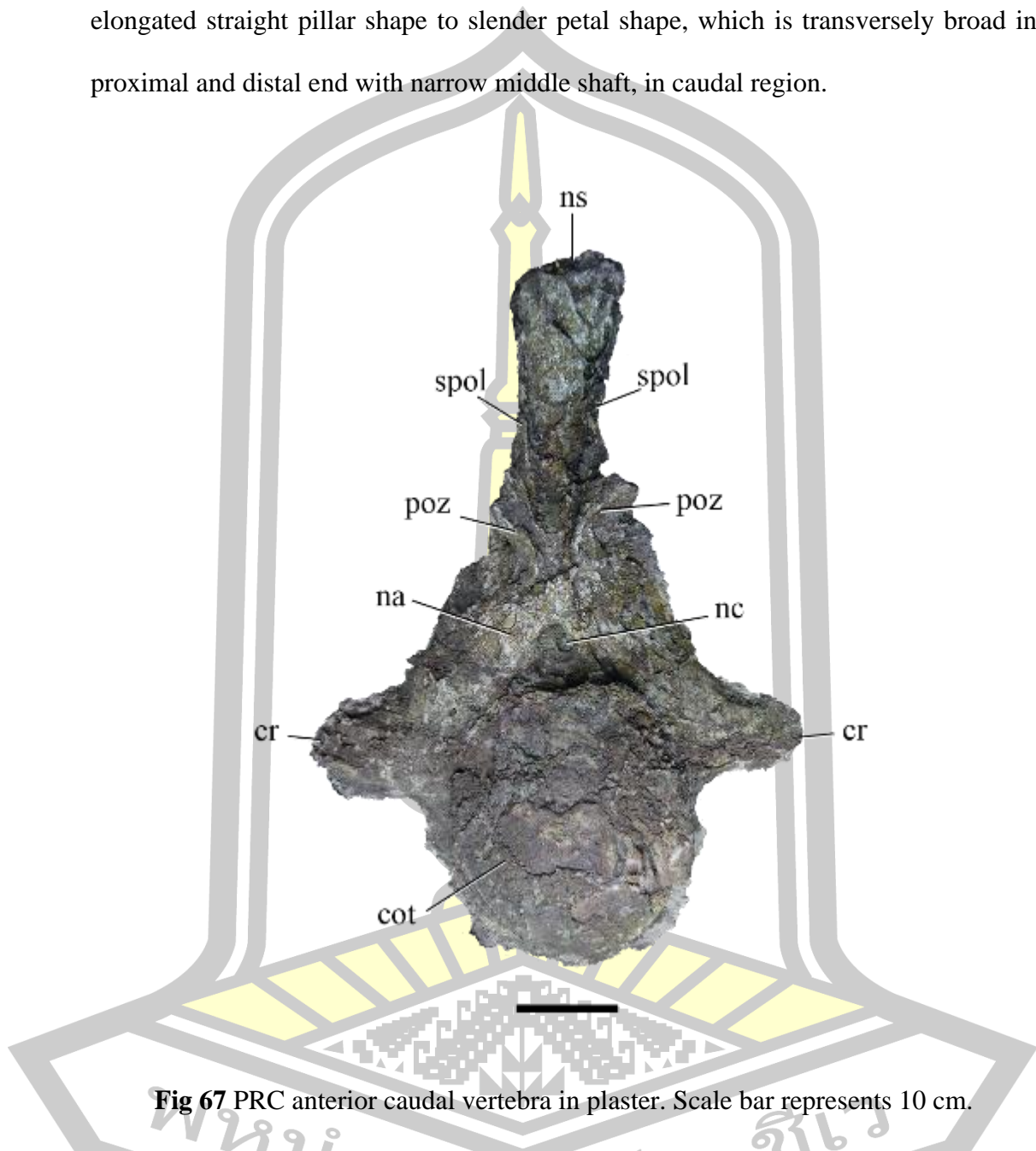


Fig 67 PRC anterior caudal vertebra in plaster. Scale bar represents 10 cm.

The prezygapophyses articular surfaces are 60 degrees dorsomedially bended, located shortly above neural canal, without the ventrally supported laminae like the dorsal neural arch. The remaining lamina and fossa are sprls that vertically line to the anterolateral margins of the neural spine and median subtriangular sprf between left and right prezygapophysis. The articular surfaces of postzygapophyses are

ventrolaterally bended with the ventrally supported from single median tpol. The spol(s) presented on the dorsolateral margin of the neural spine above the postzygapophyses. Furthermore, the dorsolateral edge of postzygapophyses is sharply pointed with acute angles. The shape and outline are resembled to *M. youngi*, *M. hochuanensis*.

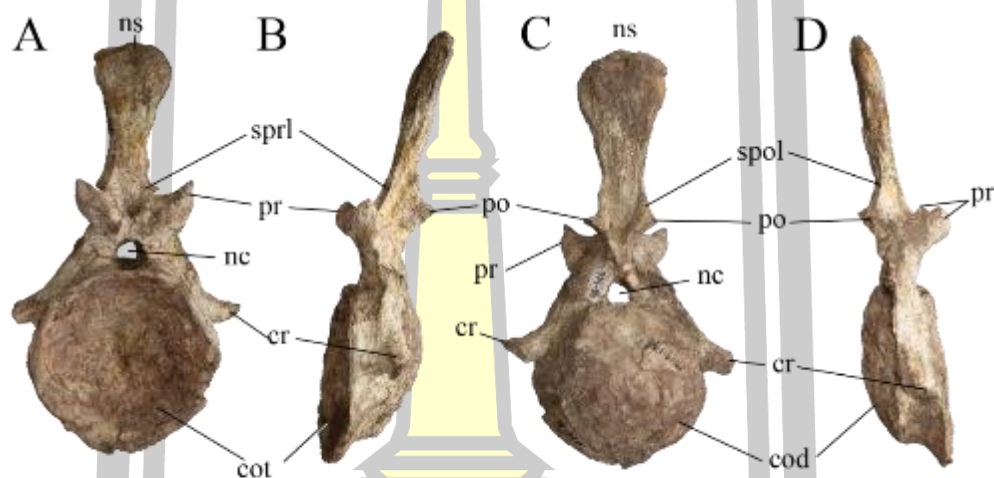


Fig 68 Anterior caudal vertebra PN14-146.

A, anterior; B, left lateral; C, posterior; D, right lateral views. Scale bar 10 cm.

From the specimens of *Mamenchisaurus* spp., *Omeisaurus* spp., *Chuanjiesaurus*, *Analong*, and *Wamweracaudia* (X.-L. He et al., 1988; Mannion, Upchurch, Schwarz, & Wings, 2019; Ouyang & Ye, 2001; X. X. Ren et al., 2021; Sekiya, 2011; C.-C. Young & Zhao, 1972), the anterior are strongly procoelous centra with vertically wing shape transverse process (also known as caudal rib). The vertical wings are posteriorly reduced width and gradually disappear to just transverse protrusion at the middle series of anterior caudal vertebrae as in KS34-500 (Fig 66 F). It initiates from the main body at the three quarters height of centra to the ventral

margin of the prezygapophyses, which is resembled to *prdl* in cervical and dorsal vertebrae. Both pre and postzygapophyses reduce to vertical narrow laminae and vertically bend to acute angle against the neural spine, which has straight, rod like shape bone with weakly incline posteriorly in the lateral view except weakly curve, petal shape spine in *Wamweracaudia*. From the comparison, PN14-146 has the most curve petal shape spine than *Wamweracaudia* opposite to the no number large caudal in plaster that has straight outline of spine like *Mamenchisaurus* and *Omeisaurus*.

Middle caudal vertebrae

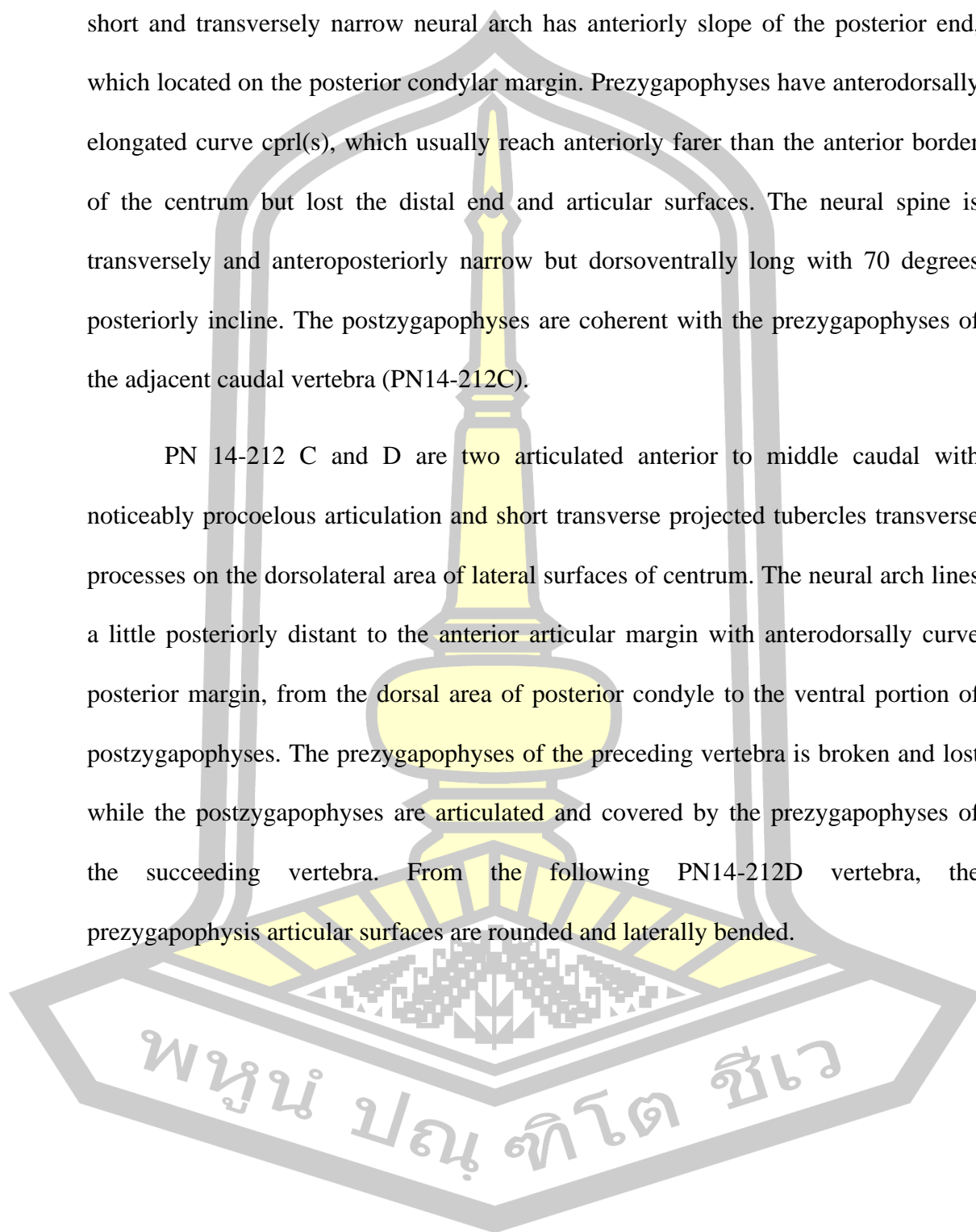
Middle caudal vertebrae are differed from anterior caudal by 1) the absent of mentioned vertical wing like lamina between transverse processes and the zygapophyses, 2) shorter neural spine, compare to centrum height, 3) transverse narrower but more lateral widen neural spine with posteriorly incline direction. The similarity of the anterior and the middle caudal vertebrae is the procoelous articulation of centrum, which slightly weaker than the anterior. Here, six articulated middle caudal series, PN14-212 A to F (Fig 66 C and D), are interpret as the representative of all middle caudal.

Middle caudal vertebra PN14-212A is heavily anteroposterior compressed and isolated from the subsequence vertebrae. Only well-preserved element is the vertically elongated neural spine with the remnants of the pre-postzygapophyses and slightly expansion of the distal end of petal shape spine.

Unlike the other vertebrae of the series, PN 14-212B is laterally compressed instead of anteroposteriorly. It has remarkable procoelous centrum with short and dorsoventrally compressed of rectangular shape left transverse process, located on the

ventral area of neural arch, beneath the ventral rim of the oval shape neural canal. The short and transversely narrow neural arch has anteriorly slope of the posterior end, which located on the posterior condylar margin. Prezygapophyses have anterodorsally elongated curve cprl(s), which usually reach anteriorly farer than the anterior border of the centrum but lost the distal end and articular surfaces. The neural spine is transversely and anteroposteriorly narrow but dorsoventrally long with 70 degrees posteriorly incline. The postzygapophyses are coherent with the prezygapophyses of the adjacent caudal vertebra (PN14-212C).

PN 14-212 C and D are two articulated anterior to middle caudal with noticeably procoelous articulation and short transverse projected tubercles transverse processes on the dorsolateral area of lateral surfaces of centrum. The neural arch lines a little posteriorly distant to the anterior articular margin with anterodorsally curve posterior margin, from the dorsal area of posterior condyle to the ventral portion of postzygapophyses. The prezygapophyses of the preceding vertebra is broken and lost while the postzygapophyses are articulated and covered by the prezygapophyses of the succeeding vertebra. From the following PN14-212D vertebra, the prezygapophysis articular surfaces are rounded and laterally bended.



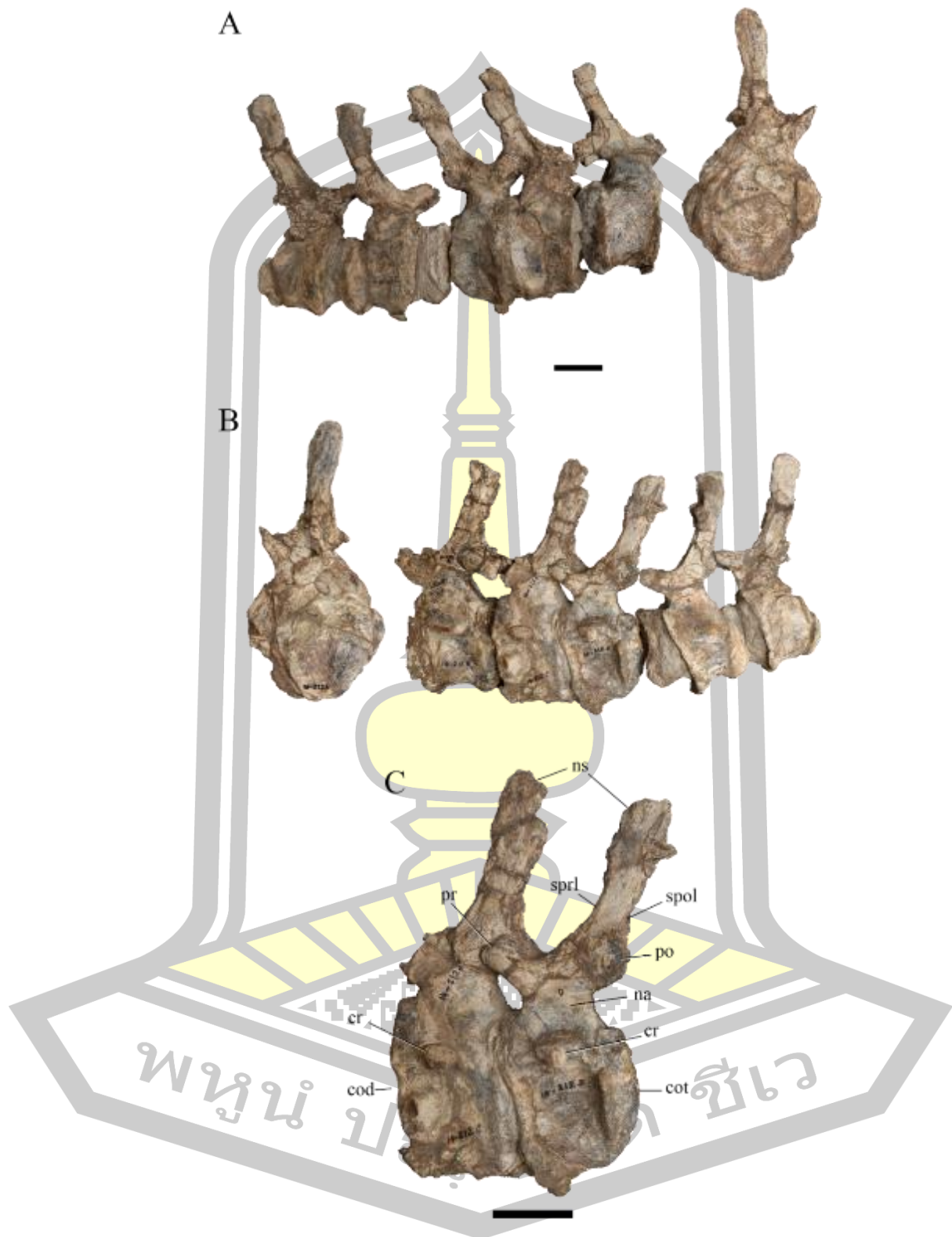


Fig 69 Middle caudal series PN14-212A to F.

A, right lateral; B, left lateral views; C, PN14-212C and D. Scale bar represents 10 cm.

The cprls are 45 degrees anterodorsally incline from the anterodorsal edge of neural arch to the anteriormost margin of anterior articular cotyle of the centrum. The sprls line from the dorsal margin of the articular surfaces of prezygapophyses then dorsally meeting and terminate at the one third vertical height of the neural spine. The oval shape postzygapophyses articular surfaces have equally dorsoventral height to the prezygapophyses. The 30 degrees posteriorly incline neural spine from the vertical plane has moderately height, which subequal to the centrum height, and the summit of spines are a bit posterior to the condyle of the centra.

PN 14-212 E and F are the last two articulated caudal vertebrae are from the anterior to middle caudal series of PN14-212. It is being compressed transversely, similar to the preceding elements. The blocklike centra, which have lessor length than height in lateral view, are procoelous. Vertically low neural arches rise little bit behind the anterior rim of the centrum in PN14-212E and equally in PN14-212F, while both posterior rims have continuous sigmoid curve outlines from posterior convex cotyle to the center of the arches. Elongated teardrop shape prezygapophyses reaching over the anterior rims of the centra with blunt and tapers distal end. The dorsoventrally high neural spines, which have 1.2 and 1.3 times of centra height, are weakly posterodorsal directed with weakly anterior curvature. The transverse processes are still presented as the small protrusions, located above the center of the lateral surfaces of the centra not on the neural arches.

Other middle vertebrae from the collection of PRC are PN15-80 and 81, which have 180 degrees turning opposite to each other. The bones are transversely compressed, that create the pleurocoel like fossa on the right lateral surface of PN15-80. The ventral surface of the centra is transversely concave with clear straight anteroposterior line of ventral margin. The second vertebra PN15-80 shows the noticeable pair of articular surfaces of the chevron, on the anterior portion of the ventral surface of the centrum.

Posterior caudal vertebrae

The posterior caudal have four major transitions from the middle. 1) the centra articulation change from procoelous to weakly amphicoelous, 2) the centrum is more anteroposteriorly elongate and dorsoventrally shorter, 3) the neural arch and spine are transversely narrower and dorsoventrally shorter, and 4) prezygapophyses line horizontally, which connect to anteroposteriorly broad spine from lateral views.

KS34-645 (Fig 66 G to I) has weakly biconcave centrum with flatten border and the anteroposterior length is greater than the dorsoventral height, making it looks anteroposteriorly elongated. The dorsoventrally short neural arch is located on the anterior to three forth of the centrum. the absent of transverse processes, also known as caudal ribs, is the indicator to represent the middle to distal position of the caudal series. Prezygapophyses are located on the anterodorsal most areas of the neural arch, which almost anteriorly reach to the anterior articular surface of the centrum. Moreover, the prezygapophyses are connected to the horizontal line of the proximal area of the neural spine, which is transversely compressed and represented the broad outline shape in lateral views. The spine is relatively dorsoventrally short, which has weakly dorsoposterior direction, compared to the preceded caudal vertebrae. At the

posteroproximal end of the spine, there are the protrusion of compressed postzygapophyses, which have inwardly curved outline to the weakly curved posterior border of the neural arch.

Distal caudal vertebrae

The distal caudals are increased the relative anteroposterior length but shorten the height, more than the posterior caudal. The neural arch is minimized in height and length, which rises from the one to three quarter of centrum length. Pre and post zygapophyses are diminished and the single neural spine change from short and robust, weakly posterior incline process of rectangular shape bone lamination to elongated obtuse angle paddle shape spine, which have expanded and round distal end.

PN16-4 to PN16-7 (Fig 66 J) is the articulation of distal caudal vertebrae, which are designated as the proximal region of distal caudals by the anteroposteriorly elongated and dorsoventrally shorten centra. Furthermore, the prezygapophyses are reduced and shorten as in the neural arches, which setting on the central area of the dorsal surfaces of centra. Moreover, the neural spines are abbreviated to the 45 degrees posterodorsally inclined of paddle shape laminated bone, which lost the thickness and became the transversely narrowed laminated sheet of bones.

PN14-34, PN14-14, PN14-17, PN14-40, PN14-51, and PN14-30 (Fig 66 K) are isolated distal caudal elements, which could be rearticulated to six continuous distal caudal vertebrae. Due to the size and proportion, they are the more distal elements than the mentioned PN16-4 to PN16-7 caudal vertebrae. The

prezygapophyses are lost by the poor preserved and the remaining neural spines are more posterodorsally elongated than the mentioned proximodistal caudals.

Chevron (haemal arch)

There are three major types of chevrons in the collections, the Y-shape chevron from anterior region, sledge shape chevron from the middle region, and the anteroposterior horizontal shaft like posterior chevron from the posterior region of the caudal vertebra columns. In usually, the transition of chevron morphology only occurred in Mamenchisauridae, Diplodocoidea, and some clades of advanced titanosaurs, which are the plesiomorphic states among the mentioned clades (Moore et al., 2023, 2020). Other clade of eusauropods and macronarians have gradually reduced the relative size and the length of distal blade of the chevrons along their tail, from Y-shape to V-shape chevron like *Camarasaurus* (Otero, Gallina, Canale, & Haluza, 2012).

For the Y-shape chevrons, there are eight well-preserved specimens from PRC (Fig 70). All of them have proximal half with the closure of transversal bone bridge between the rami of proximal articular facets. The difference is from PN14-24, the No number chevron, and PN639, which have short distant between proximal facets and the facets might be connected by its expansion of the edge of facets like crus-bridge in the chevrons of Diplodocoidea (Otero et al., 2012; Tschopp et al., 2015). Moreover, the two latter mentioned chevrons have narrow width and vertically short area of haemal canal, might be indicated that there are at least two genera of sauropods in the locality.

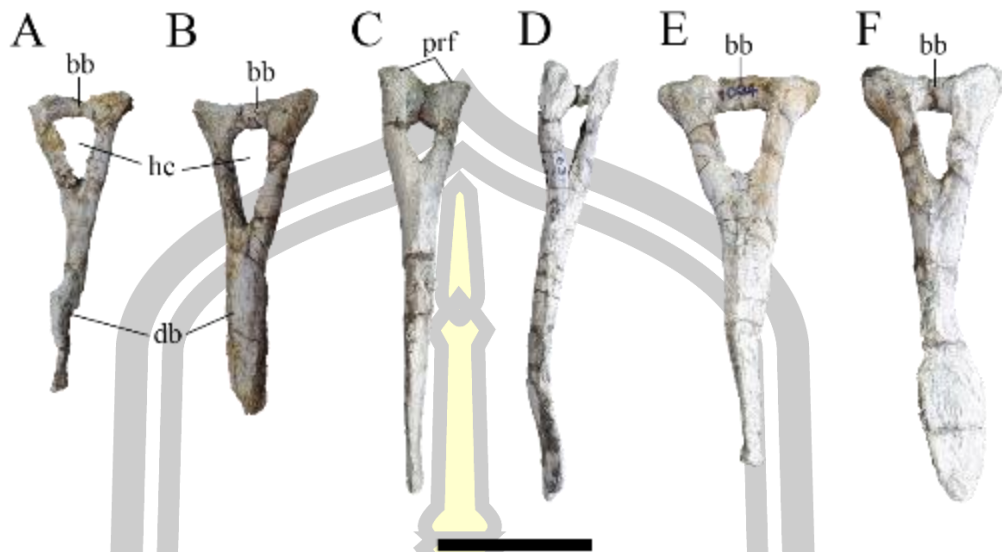


Fig 70 Y-shape anterior chevrons of sauropods from PRC collection in anterior view.

A, PN15-186. B, PN15-151. C, PN13-11. D, KS34-631. E, KS34-1004. F, PN638.

Scale bar represents 10 cm.

The sledge shape middle chevron developed the anteroventral directed of laminate anterior distal process, which resembled to another distal blade, while the primary blade turns to the thicker posteroventral blade (Otero et al., 2012). The angle between the anterior and posterior blades are wider and shorter posteriorly while the proximal rami gradually lost its height and moving to the middle area of the bone through the caudal column.

Lastly, the posterior chevron is the pair of horizontal bars of bone, which have short proximal articular facets in the middle length, transversely narrow and anteroposterior elongated ellipsoidal cavity in between the counterpart, narrow diamond outline from dorsoventral view, and sagittal suture on the dorsal surface of the posterior surface. The anterior and posterior processes are relatively elongate, which are the character of eusauropods like *Shunosaurus* and *Mamenchisaurus* spp.

while *Omeisaurus* spp. have asymmetric posterior chevrons and Diplodocoidea have both symmetric and asymmetric (Hatcher, 1901; Tschopp et al., 2015).

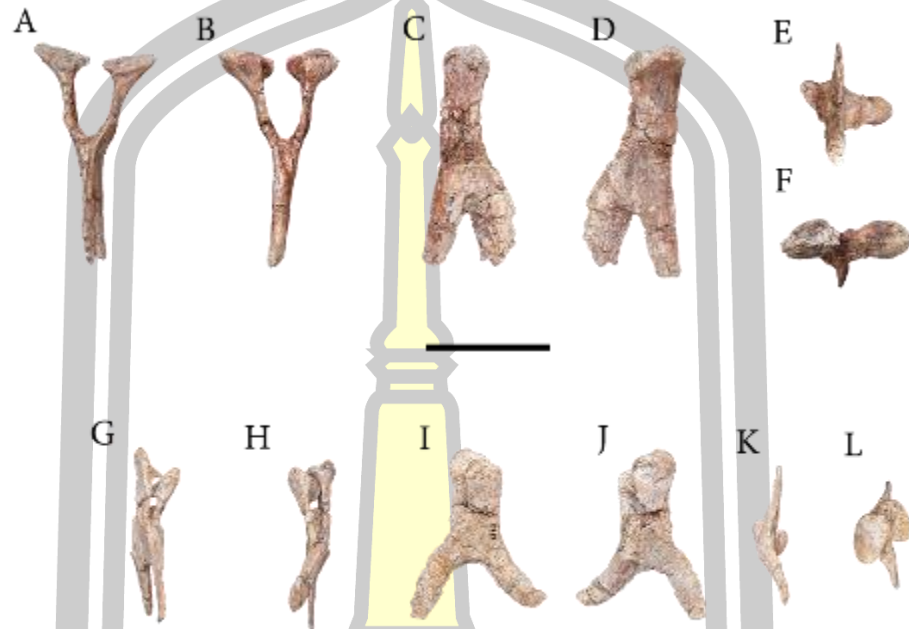


Fig 71 Middle chevron of Mamenchisauridae sauropods from Phu Noi locality, Kalasin province.

A and G are anterior; B and H are posterior; C and I are left lateral; D and J are right lateral; E and K are ventral; F and L are dorsal views. A to F, KS34-2240. G to L, KS34-2797. Scale bar represents 10 cm.

พหุบัน ปณ จิต ชีเว

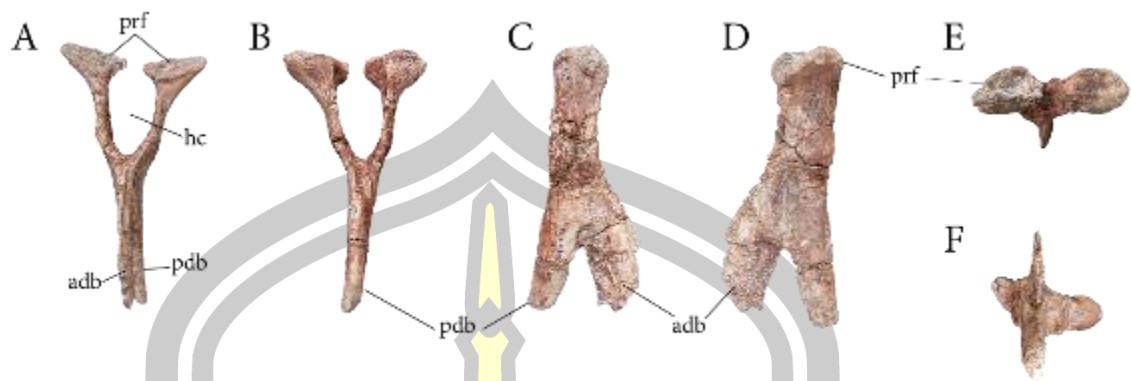


Fig 72 Middle chevron of mamenchisaurid sauropods KS34-2240 from Phu Noi locality, Kalasin province.

A is anterolateral; B is posterolateral; C is right lateral; D is left lateral; E is ventral; F is dorsal views. Scale bar represents 10 cm.

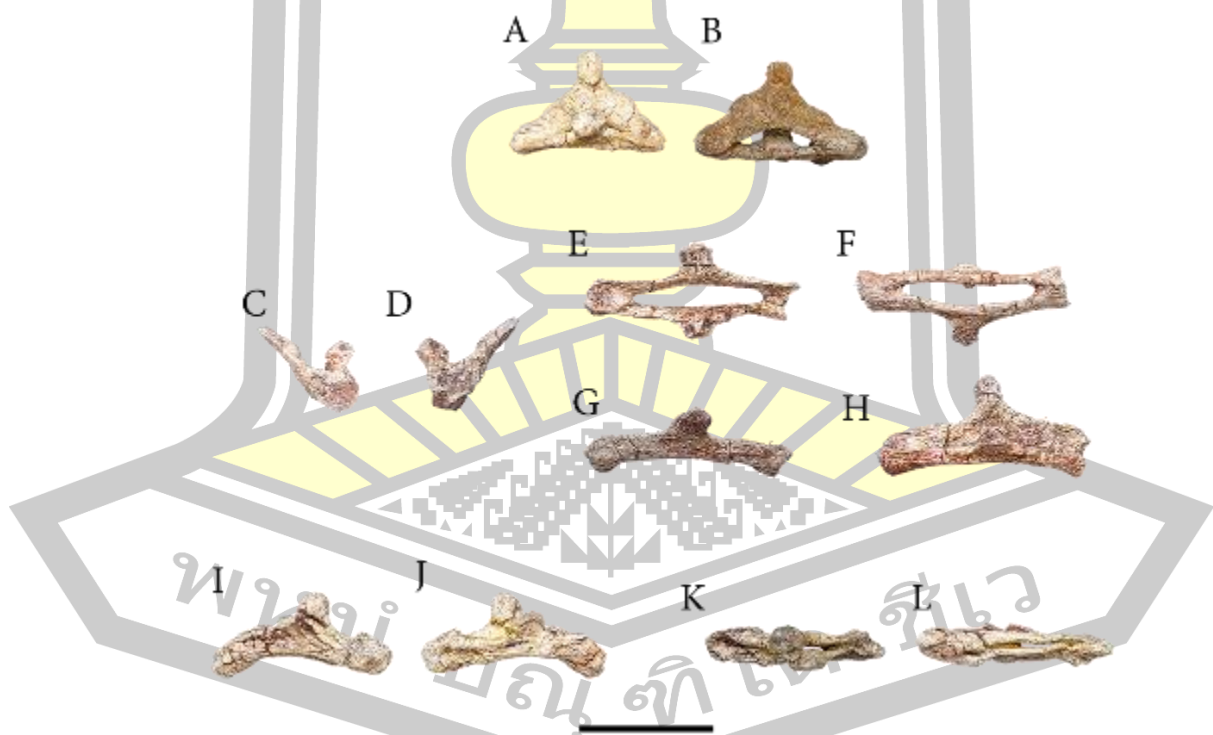


Fig 73 Posterior Chevron of Mamenchisauridae sauropods from Phu Noi locality, Kalasin province.

A, E, and K are dorsal; B, F, and L are ventral; C is anterior; D is posterior; G and I are left lateral; H and J are right lateral; A and B, KS34-1166. C to H, KS34-2244. I to L, KS34-2311. Scale bar represents 10 cm.

Pectoral girdle

The pectoral girdle covers the anterior region of the torso, embracing the external area of the thorax from the dorsolateral to ventral area. It comprises four main elements: clavicle, sternal plates, coracoid, and scapula. In adult individuals, coracoid and scapula are fused and called scapulocoracoid, which have the remaining synostosis line in subadult but completely fused in mature adult and the elderly individual (Holtz et al., 2004; Ikejiri, Tidwell, Trexler, Tidwell, & Carpenter, 2005). The Phu Noi specimens have only two major elements, five isolated scapulae and one scapulocoracoid, from the collections.

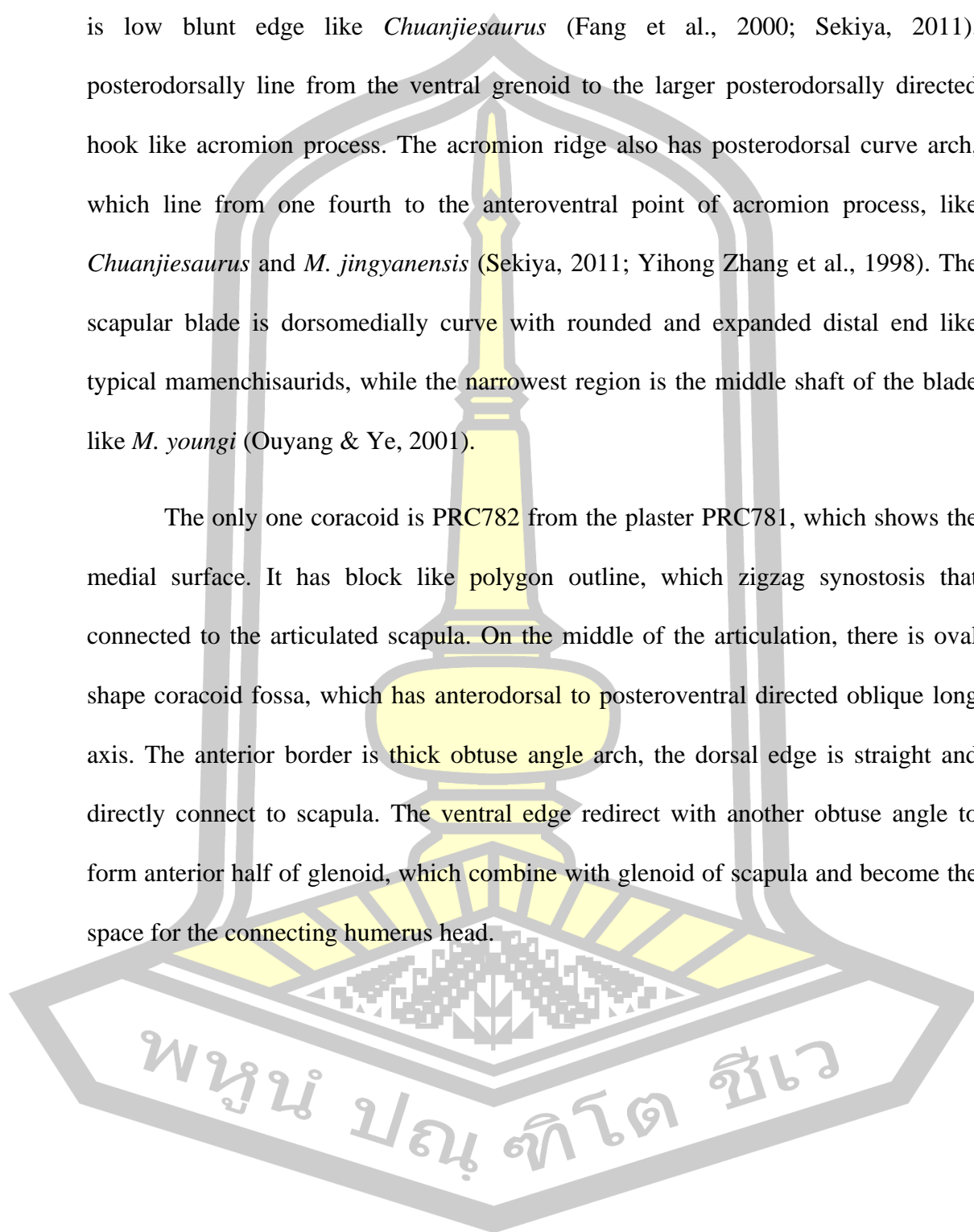
Scapula and scapulocoracoid

Two of seven specimens are from PRC collection, PN15-36 and PRC781, while the rest from SM collection have no specimens number except PN65. All of them preserved in plaster due to the heavily transverse compression, that made them extremely fragile and cannot move out the plaster to observe the opposite side (except PN15-36).

PN15-36 and PRC781 are the most completed and well-preserved pectoral girdle elements in the collections, which have similar outline of scapula. The former is right scapula with anteroposteriorly narrow of irregular fan shape acromion plate (proximal plate like area), which dorsally increasing in width. the anterior edge is sub vertically straight with weakly posterior incline. The dorsal edge composed of obtuse angle of subtriangular outline, which divided at the middle length. The ventral end is

the relatively small posterior projected hook like glenoid. The acromion ridge, which is low blunt edge like *Chuanjiesaurus* (Fang et al., 2000; Sekiya, 2011), posterodorsally line from the ventral glenoid to the larger posterodorsally directed hook like acromion process. The acromion ridge also has posterodorsal curve arch, which line from one fourth to the anteroventral point of acromion process, like *Chuanjiesaurus* and *M. jingyanensis* (Sekiya, 2011; Yihong Zhang et al., 1998). The scapular blade is dorsomedially curve with rounded and expanded distal end like typical mamenchisaurids, while the narrowest region is the middle shaft of the blade like *M. youngi* (Ouyang & Ye, 2001).

The only one coracoid is PRC782 from the plaster PRC781, which shows the medial surface. It has block like polygon outline, which zigzag synostosis that connected to the articulated scapula. On the middle of the articulation, there is oval shape coracoid fossa, which has anterodorsal to posteroventral directed oblique long axis. The anterior border is thick obtuse angle arch, the dorsal edge is straight and directly connect to scapula. The ventral edge redirect with another obtuse angle to form anterior half of glenoid, which combine with glenoid of scapula and become the space for the connecting humerus head.



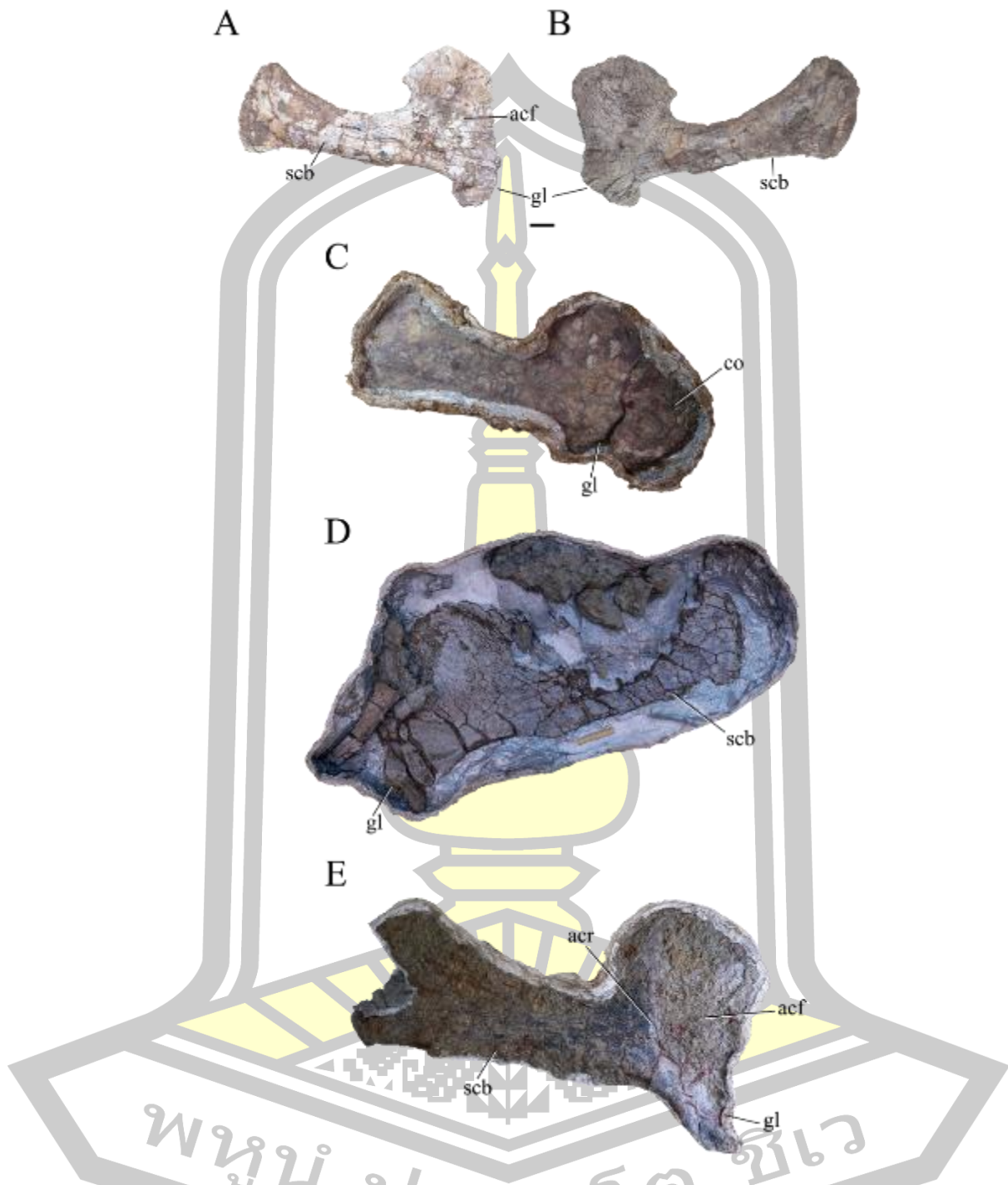


Fig 74 Scapula of mamenchisaurid from Phu Noi locality, Kalasin province. A and E are lateral; B, C, and D are medial views.

A and B, PN15-36 right scapula. C, left PN781 scapulocoracoid. D, SM no number left scapula. E, SM no number right scapula. Scale bar represent 10 cm.

Forelimb

Humerus

Initiate with humeri from PRC, the three specimens, PN13-15, PN17-104 and PN17-142, have different outline shape and robustness. Moreover, these long bones are fragile with incomplete important landmarks like deltopectoral crest by erosion, compression or the damage via the transportation and preparation. All of specimens, except PN17-142, are available to describe only on one side.

PN13-15 is a large and robust right humerus in anterior view with almost equal width of gradually expand transverse expanded toward proximal and distal ends. The outline is resembled to asymmetric elongated hourglass shape. The proximal end has curve dorsomedially toward the medial direction while the distal end has weakly incline straight edge toward the ventromedial direction. Medial edge is strongly concave from the proximomedial border then recurve at the half dorsoventral height of the shaft to the distomedial border. Lateral edge has straight outline from the proximolateral edge to the two third of total dorsoventral height, which is the ventral end of middle shaft, then recurve to expanding distal end. The deltopectoral crest is gradually risen from the ventral half of the proximal area then gradually peak in both height and thickness at the half of the bone. The crest is terminated and acutely disappear at the top of the ventral half of the shaft, above the narrowest point of bone. The proximal half area has large middle depression fossa for muscle attachment. Unfortunately, the distal end is anteroposteriorly compressed, that deformed and reduced the shape and size of medial and lateral anterodistal processes.

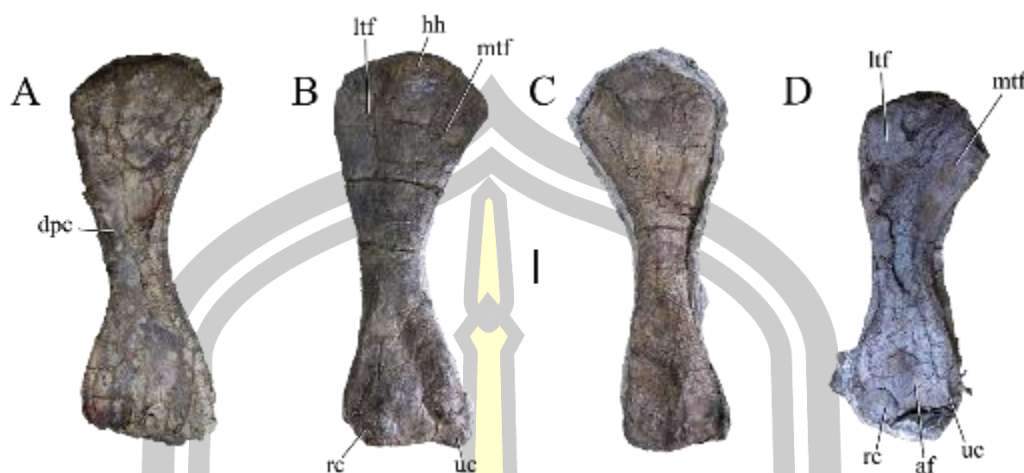


Fig 75 Humeri of Mamenchisauridae sauropods from Phu Noi locality, Kalasin province. A is anterior; B to D are posterior views.

A, PN13-15. B, C and D are SM no number. Scale bar represents 10 cm.

Due to the descriptions, the humerus PN13-15 is resembled to *Mamenchisaurus* spp. via the medially curve of proximal end and robust outline. The deltopectoral crest is transversely narrower but ventrally longer than *M. constructus* but more prominent crest and transversely wider than *M. youngi*. Humerus shaft is more robust than *M. youngi*, relatively shorter but transversely wider, even it has similar incline straight distal end.

PN17-104 is slender and elongate left humerus than PN13-15 with slightly larger distal end than the proximal end. The outstanding transversely thick deltopectoral crest, continuing from the lateral edge of proximal end to the height of midshaft might cause by the plastic deformation, which means the proximal end is anteriorly bended to made proximal width narrower than normal condition.

Another three humeri from SM collection are preserved in plaster, which are exposed the posterior surfaces. The largest and most robust left humerus is resembled

to PN13-15, which might be the same taxon and could be pairing as the counterpart (left and right elements). The longest and slenderest right humerus is resembled to the left humerus of *M. youngi* while the last moderately robust left humerus, which loss the humeral head and obviously smaller than the latter, is resembled to the left humerus of *M. youngi*.

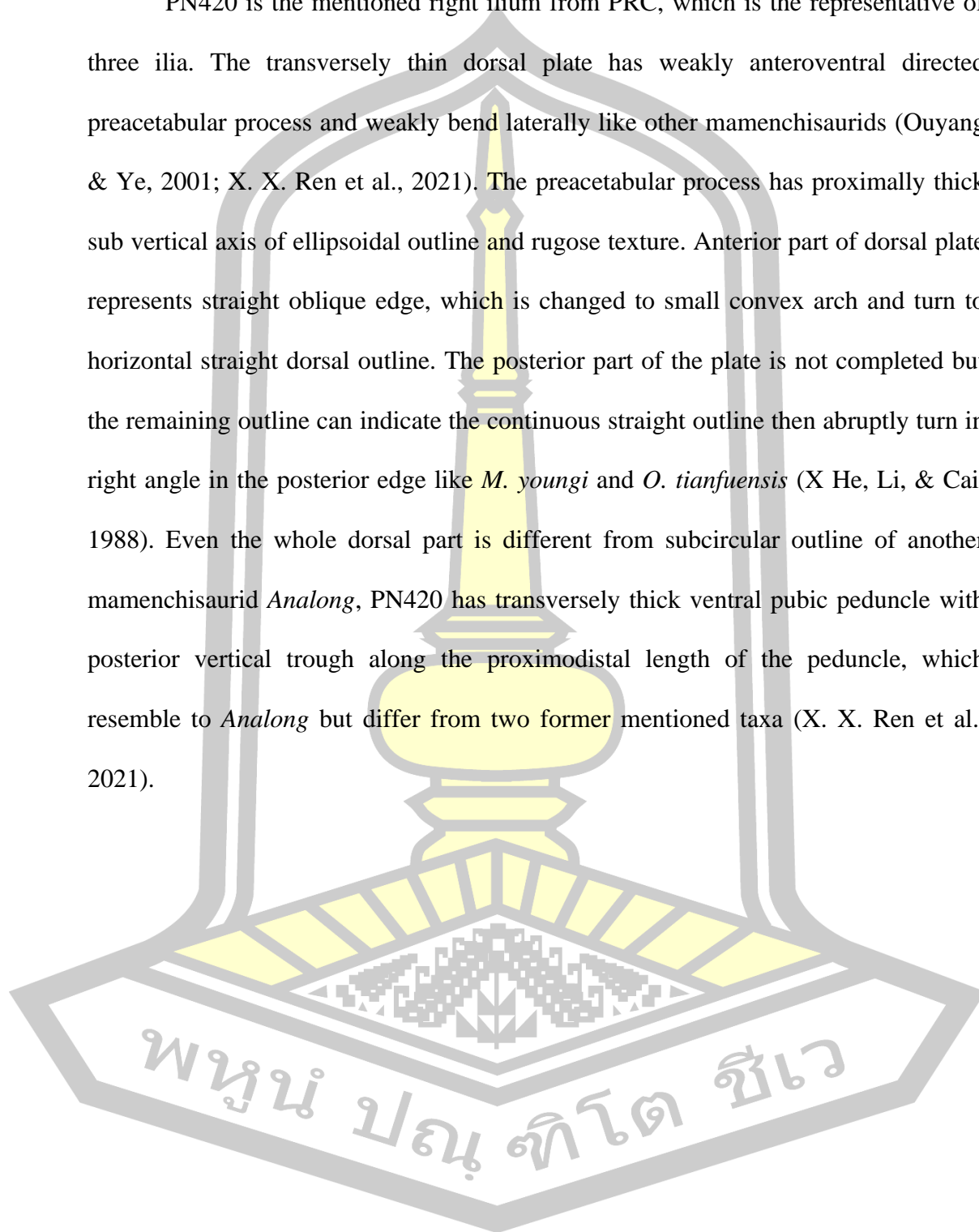
Pubic girdle

The pubic girdle located between the medial portion of femur and laterally cover and connected to sacral vertebrae by the sacricostal yoke of sacral ribs, respectively. The girdle composes of three elements, the sub thin semicircular plate of Ilium on dorsal region with ventrally vertical shaft of pubic peduncle, anteroventral directed sub rectangular plate of transversely narrow pubis on anteroventral region and posteroventral directed ischium on posteroventral region. The three elements assemble their proximal concave arches together and represents the large subcircular acetabulum, which is the fenestra for the proximomedial head of femur. In other archosaur, the acetabulum is narrower and represents depression fossa of bone, extends from inner border to the fenestra area (Ouyang & Ye, 2001; X. X. Ren et al., 2021; Sekiya, 2011).

Due to the completeness and clearly characters, the specimens of ilium and pubis have been selected to study. There are three ilia, two from SM are preserved in plasters, which exposed only the medial surface, and one completely preserve both medial and lateral surfaces ilium from PRC. Furthermore, there are two pubes, one from PRC and one from SM collection.

Ilium

PN420 is the mentioned right ilium from PRC, which is the representative of three ilia. The transversely thin dorsal plate has weakly anteroventral directed preacetabular process and weakly bend laterally like other mamenchisaurids (Ouyang & Ye, 2001; X. X. Ren et al., 2021). The preacetabular process has proximally thick sub vertical axis of ellipsoidal outline and rugose texture. Anterior part of dorsal plate represents straight oblique edge, which is changed to small convex arch and turn to horizontal straight dorsal outline. The posterior part of the plate is not completed but the remaining outline can indicate the continuous straight outline then abruptly turn in right angle in the posterior edge like *M. youngi* and *O. tianfuensis* (X He, Li, & Cai, 1988). Even the whole dorsal part is different from subcircular outline of another mamenchisaurid *Analong*, PN420 has transversely thick ventral pubic peduncle with posterior vertical trough along the proximodistal length of the peduncle, which resemble to *Analong* but differ from two former mentioned taxa (X. X. Ren et al., 2021).



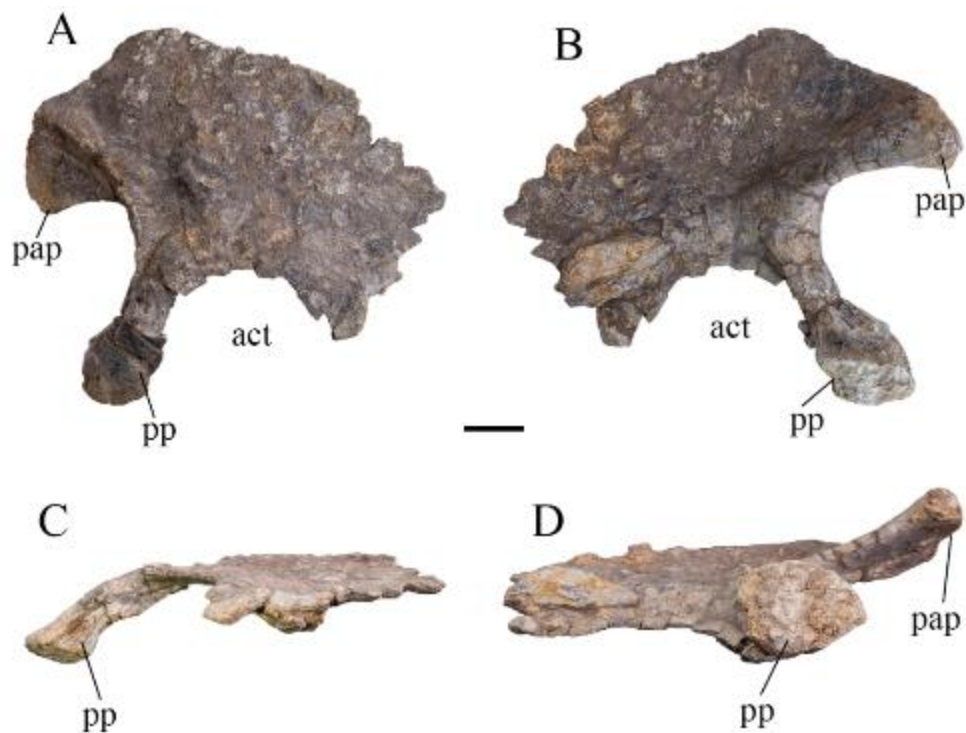


Fig 76 Right ilium PN420 of mamenchisaurid sauropod from Phu Noi locality, Kalasin province.

A, medial; B, lateral; C, posterior; D, ventral views. Scale bar represents 10 cm.

pubis

There are two transversely compressed pubes in the collections, KS34-449 left pubis from PRC and the no number right pubis from SM, respectively. The former and latter show lateral and medial surfaces in the plasters, respectively, which identify by the ridge of ilial articular surface along the proximal end of KS34-449 and the rugose articular surface for the counterpart along the distal end and the flat plain of the proximal area of SM pubis. The pubes represent the closed obturator foramen, which can identify the adult stage of two individuals (Ikejiri et al., 2005). KS34-449 lost the posterior border along the anteroventral process while SM pubis has complete distal end, which can predict the eroded outline as elongated anteroventral process.

Both are resembled to the pubes of *Omeisaurus tianfuensis*, which have similar outline and details. Moreover, the other reported pubes of mamenchisaurids are distinct from PRC and SM specimens. For example, *Analong* pubes have robust outline shape with broad and relatively shorter distal end while *M. youngi* has narrow subtriangular shape pubis (Ouyang & Ye, 2001; X. X. Ren et al., 2021).

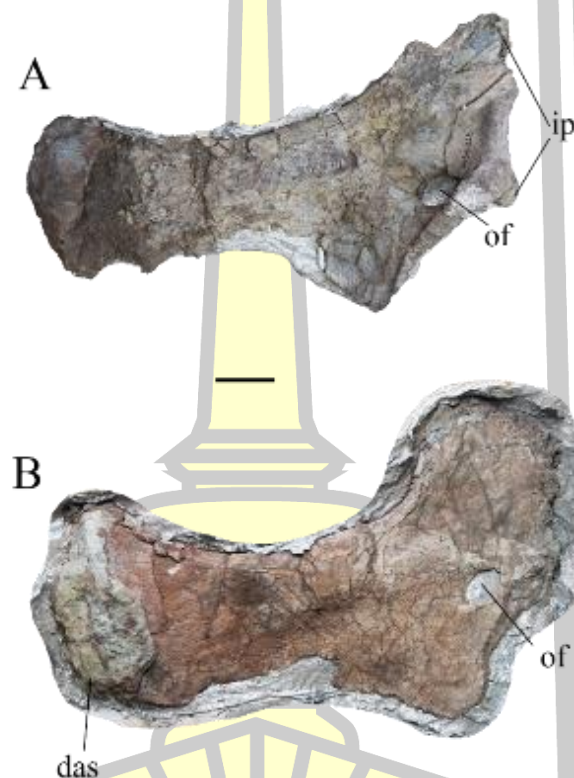


Fig 77 Pubes of mamenchisaurid sauropods from Phu Noi locality, Kalasin province.

A, right pubis KS34-449 in lateral view. B, no number right pubis in medial view.

Scale bar represents 10 cm.

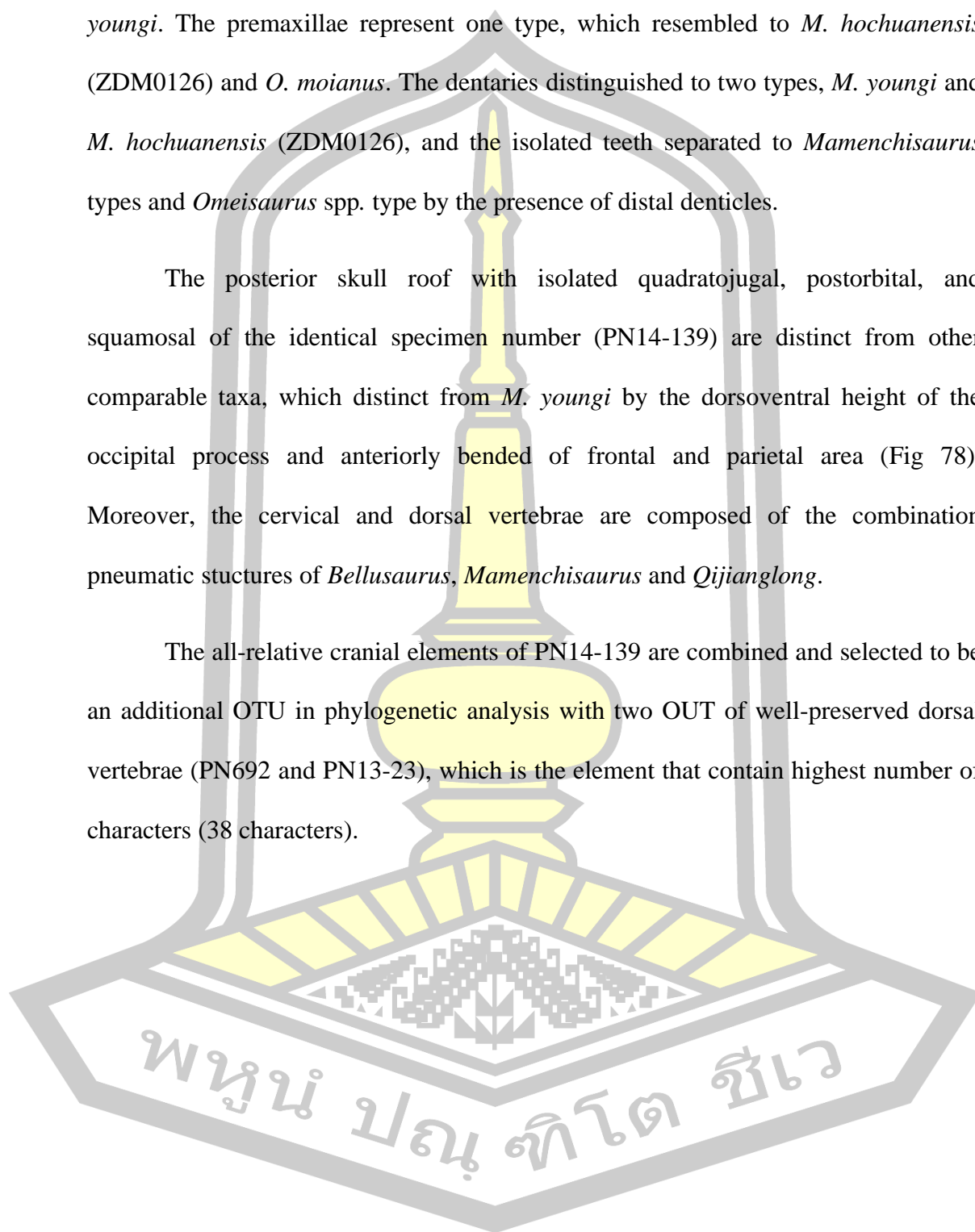
4.2 Summary of comparison

From the descriptions and comparisons of 171 specimens, we can elucidate that Phu Noi locality has yielded at least five types of Mamenchisauridae sauropods (Table 3). There are numerous elements of *M. youngi* from cranials and postcranials. The humeri, pectoral, and pubic girdles are resembled to the genus *Mamenchisaurus*.

Frontal-parietal and squamosal are resembled to *Bellusaurus sui* and *M. youngi*. The premaxillae represent one type, which resembled to *M. hochuanensis* (ZDM0126) and *O. moianus*. The dentaries distinguished to two types, *M. youngi* and *M. hochuanensis* (ZDM0126), and the isolated teeth separated to *Mamenchisaurus* types and *Omeisaurus* spp. type by the presence of distal denticles.

The posterior skull roof with isolated quadratojugal, postorbital, and squamosal of the identical specimen number (PN14-139) are distinct from other comparable taxa, which distinct from *M. youngi* by the dorsoventral height of the occipital process and anteriorly bended of frontal and parietal area (Fig 78). Moreover, the cervical and dorsal vertebrae are composed of the combination pneumatic structures of *Bellusaurus*, *Mamenchisaurus* and *Qijianglong*.

The all-relative cranial elements of PN14-139 are combined and selected to be an additional OTU in phylogenetic analysis with two OUT of well-preserved dorsal vertebrae (PN692 and PN13-23), which is the element that contain highest number of characters (38 characters).



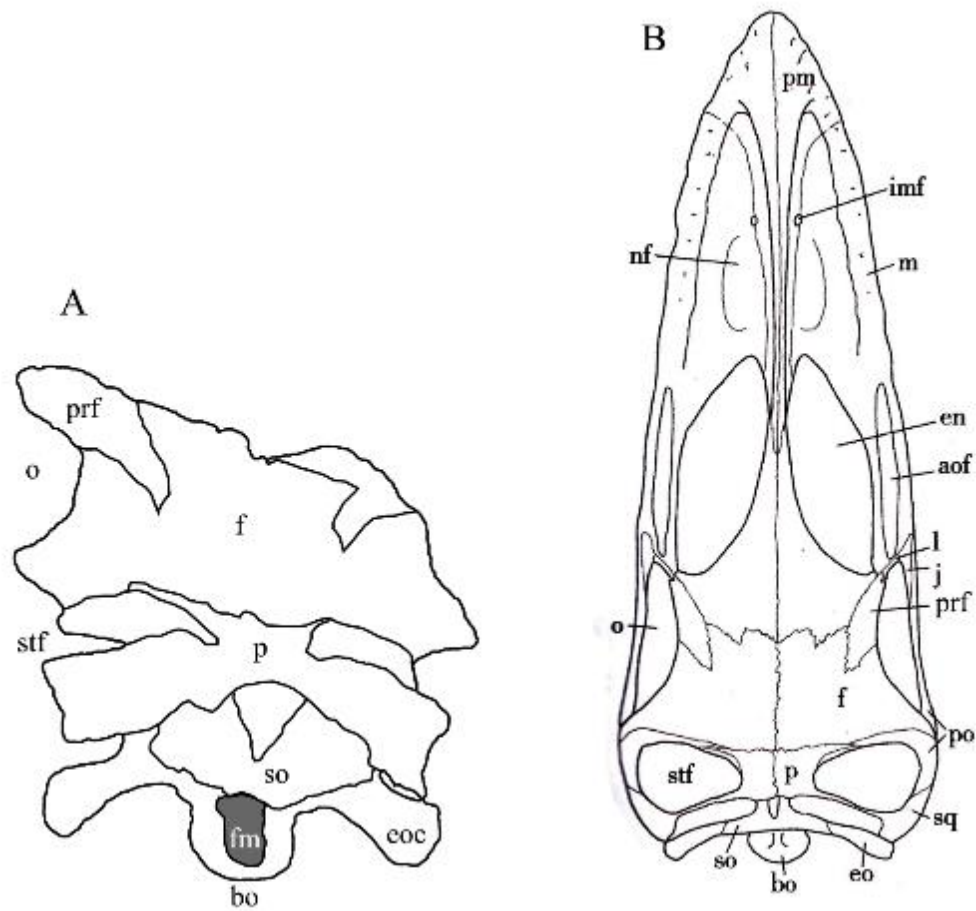


Fig 78 Comparison between the dorsal surfaces of the skull outline.

A, PN14-139. B, *M. youngi* ZDM0083 (modified from (Ouyang & Ye, 2001)). Not to scale.

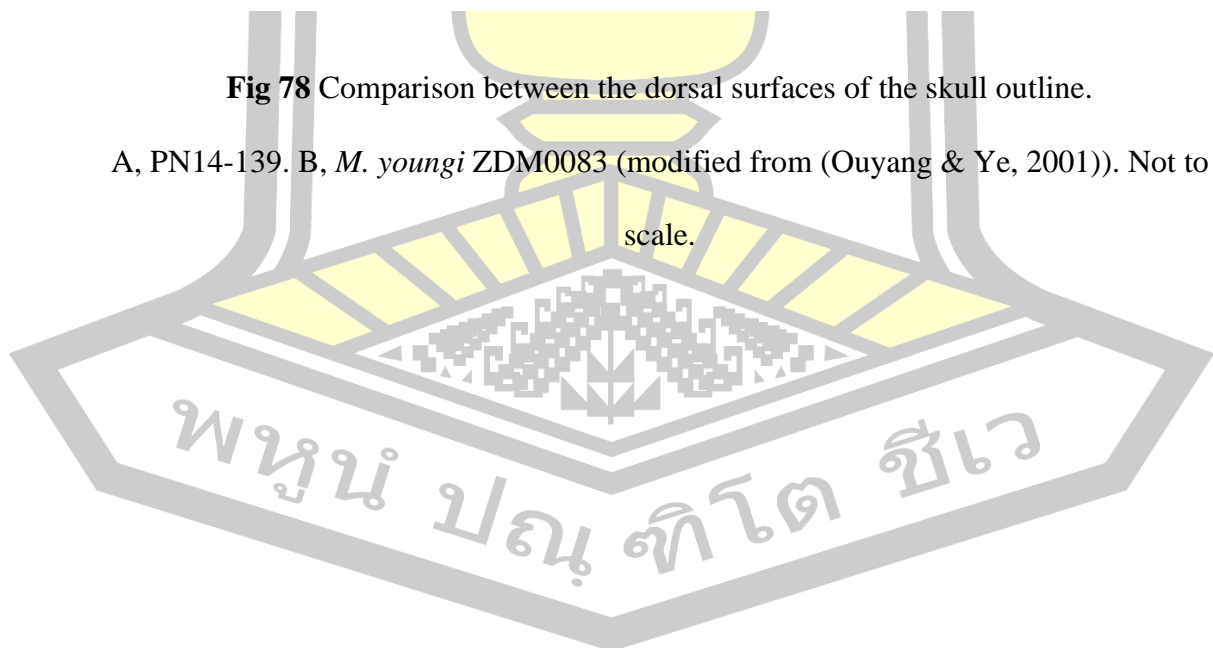


Table 3 types of Mamenchisauridae elements of Phu Noi locality from PRC and SM collections. Type 1, *M. youngi*; type 2, *M. hochuanensis* and *O. moianus*; type 3, *Bellusaurus sui*; type 4, *O. tianfuensis*; type 5, Phu Noi form (more than 1 taxa).

| Element | Types | | | | | Annotations |
|--|----------|----------|----------|----------|----------|--|
| | 1 (n) | 2 (n) | 3 (n) | 4 (n) | 5 (n) | |
| Premaxilla | | 4 | | | | |
| Lacrima | 1 | | | | | |
| Jugal | 4 | | | | | |
| Quadratojugal | 2 | | | | | |
| Postorbital | 3 | | | | 1 | part of skull roof |
| Squamosal | 2 | | 1 | | | |
| Nasal | | | 1 | | | part of <i>Bellusaurus</i> like frontal-parietal |
| Prefrontal-Frontal-parietal | 1 | | 1 | | | |
| Exoccipital | 1 | | | | 1 | part of skull roof |
| posterior skull roof (+ squamosal + quadratojugal) | | | | | 1 | Phu Noi new taxon in systematic palaeontology |
| Dentary | 2 | 4 | | | | |
| Isolated teeth | 22 | | | 12 | | |
| Anterior cervical centrum | | | | | 1 | Phu Noi form resemble to <i>Omeisaurus</i> and <i>Bellusaurus</i> |
| Middle cervical vertebra | 1 | | | | 1 | Phu Noi form resemble to <i>Qijianglong</i> but distinct in pneumatic structure |
| Posterior cervical vertebra | 2 | | | | 3 | Phu Noi form resemble to <i>Qijianglong</i> but distinct in pneumatic structure |
| Cervical rib | | | | | 6 | Phu Noi form resemble to <i>M. youngi</i> |
| Anterior dorsal vertebra | 3 | | | | | <i>M. youngi</i> or <i>M. hochuanensis</i> |
| Middle dorsal vertebra | | | | | 2 | Phu Noi form shows oval shape depression on the transverse processes like <i>Bellusaurus</i> |
| Posterior dorsal vertebra | 2 | | | | 2 | Phu Noi form shows horizontal streaks of pneumatic cavities along lateral surfaces of neural spine |
| Dorsal rib | 2 | | | | | <i>Mamenchisaurus</i> |
| Anterior caudal vertebra | 2 | | | | | <i>Mamenchisaurus</i> |
| Anterior to middle caudal vertebra | 9 | | | | | <i>Mamenchisaurus</i> |

Table 3 Continued

| Element | Types | | | | | Annotations |
|-------------------------------------|----------|----------|----------|----------|----------|---|
| | 1 (n) | 2 (n) | 3 (n) | 4 (n) | 5 (n) | |
| Middle to posterior caudal vertebra | 10 | | | 3 | | <i>Mamenchisaurus</i> and <i>O. tianfuensis</i> |
| Anterior chevron | 6 | | | | | <i>Mamenchisaurus</i> |
| Middle chevron | | 3 | | | | |
| Posterior chevron | | 2 | | | | |
| Scapula | 5 | | | | | |
| Humerus | 4 | | | | | |
| Ilium | 2 | | | | | |
| Pubis | 2 | | | | | |

4.3 Preliminary phylogenetic analysis and implications

To establish the phylogenetic position of Mamenchisaurid sauropods from Phu Noi locality, the data matrix of Moore et al., 2023 (Moore et al., 2023) has been used. This is the up-to-date version of the wide array sauropodomorphs and eusauropods dataset from Moore et al., 2020 (Moore et al., 2020), which developed from Carballido et al., 2015 (Carballido et al., 2015) and Gonzalez Riga et al., 2018 (Gonzalez Riga, Mannion, Poropat, Ortiz David, & Coria, 2018) composed of 103 sauropod OTU taxa and 449 characters.

Maximum parsimony analyses were carried out in TNT v1.5 (Goloboff & Catalano, 2016), using extended implied weighting (EIW hereafter), with a K-value set at 12.000. The memory buffer (“Maxtree”) set at 200,000 trees. Analytical approach following Moore et al., 2023 by treat characters 11, 14, 15, 27, 40, 51, 104, 122, 147, 148, 195, 205, 259, 297, 430, 432, 438 and 449 as order and five characters: 14, 20, 122, 130 and 258 were made inactive prior to analysis.

The heuristic algorithm uses “New Technology Search” using 5 times “Stabilizing Consensus” with applying sectorial searches, drift, and tree fusing, which is the command code: *'xmult-replications 50 hits 10 css rss ratchet 5 fuse 5'*. If the replications fill the memory buffer (“some replications overflowed”), a second round of Tree-Bisection-Reconnection branch swapping (TBR, using “Traditional search”) is applied to the resulting trees. Suboptimal trees were setting up to five steps longer to calculate the Bremer support of the nodes. The 50% majority consensus was calculated from all trees. Three representative specimens of mamenchisaurids from Phu Noi are selected, due to the completeness and high number of the representation characters.

- 1) the articulated skull roof PN14-139
- 2) the middle dorsal vertebra PN692
- 3) the posterior dorsal vertebra PN13-23

Both EQW and EIW analysis resulted in 200,000 MPTs of 2087 steps, including the 50% majority consensus of all MPTs as tree 200,001. It recovers 23 Eusauropod taxa into the node of Mamenchisauridae, which have 8 synapomorphies (15:?, 19:1, 115:2, 140:1, 150:0, 216:1, 380:1, 430:5). Phu Noi dorsal vertebrae (PN692 and PN13-23) are the sister group in the polytomy node of *Xinjiangtitan*, *Hudiesaurus* with 2 synapomorphies (338:0, 341:1). The skull roof PN14-139 is in the polytomy node of paraphyly *Mamenchisaurus* spp. (including *M. constructus*), *Qijianglong*, *O. junghsiensis* with 8 synapomorphies (16:1, 120:1, 121:0, 147:2, 159:1, 163:1, 406:1, 447:1) and PN14-139 has one distinct character (8:1). The last internal node contains *M. youngi*, Shishugou cervicodorsals and the sister group of

Klamelisaurus and Phu Kradung taxon (Phu Dan Ma cervicodorsal SM KS26-4) with 5 synapomorphies (31:0, 148:1, 174:1, 404:1, 449:0).

From the 50% majority consensus MPT, Mamenchisauridae is the clade of sauropods, which have 1) ambiguous value between the highest average elongation index value divided by the mean average value of the posterior articular surface mediolateral width and dorsoventral height; 2) dorsoventral height divided by posterior centrum height of the posterior-most cervical and anterior-most dorsal neural spines are less than 1.0; 3) internal tissue structure of cervical and anterior-most dorsal vertebrae are camellate; 4) Cervical ribs, longest shafts extend beneath three vertebrae or more; 5) Middle-posterior dorsal neural arches, hyposphene shape is narrow, ventral end subequal to or only slightly wider than dorsal tip; 6) subtriangular process at anteroventral corner of scapular blade; 7) ratio of dorsoventral height of iliac blade above pubic peduncle to anteroposterior length of ilium is equal or greater than 0.35; 8) cervical vertebrae number is 18.

The characters of the Phu Noi dorsal vertebrae (PN692 and PN13-23) are 1) neural canal surrounded by the neural arch, not enclosed in a deep fossa in the dorsal surface of the centrum; 2) zygapophyseal articulation angle of the posterior dorsal neural arches steeply oriented, 30° or greater relative to horizontal line.

The node of polytomy *Mamenchisaurus* spp. with Phu Noi skull roof (PN14-139) composed of 8 synapomorphies 1) posterior articular face dorsoventral height to mediolateral width ratio of the anterior cervical centra are less than 1.0; 2) absent of ventral midline keel on the postaxial cervical centra; 3) parapophyses of the postaxial cervical centra lack of dorsally excavated; 4) anterior articular face shape of the

middle-posterior dorsal centra are strongly convex, with degree of convexity approximately consistent along the dorsal sequence; 5) anteroposterior width of the dorsal neural spines are narrows dorsally to form a triangular shape in lateral view, with the base approximately twice the width of the dorsal tip; 6) middle-posterior dorsal neural spines are strongly developed triangular aliform processes so that the lateral tips of these processes extend further laterally than the postzygapophyses; 7) middle and posterior cervical neural spines, lateral surface between prdl, podl, and spol has 3 or more coels separated from each other by low ridges; 8) bifurcated anterior process of the cervical ribs. However, PN14-139 lacks the part of specimens, which represented the mentioned synapomorphies. The only one exist character of the specimen that separate it from other taxa is character 9:1 (ratio of basiptyergoid processes length to basal diameter is 3.0 or greater).

For the overview summary, the clade Mamenchisauridae composed of the sauropod members from the node of *Cetiosauriscus stewarti* and *Omeisaurus tianfuensis* to the node of *Klamelisaurus gobiensis* and Phu Kradung taxon (Phu Dan Ma cervicodorsal). The dorsal vertebrae (PN692 and PN13-23) might be the same taxon, which is primitive than the skull roof (PN14-139) from the more derive node of *Mamenchisaurus* spp. Lastly, Phu Dan Ma cervicodorsal (SM KS26-4) is in the distinct derive node of *Klamelisaurus gobiensis*.

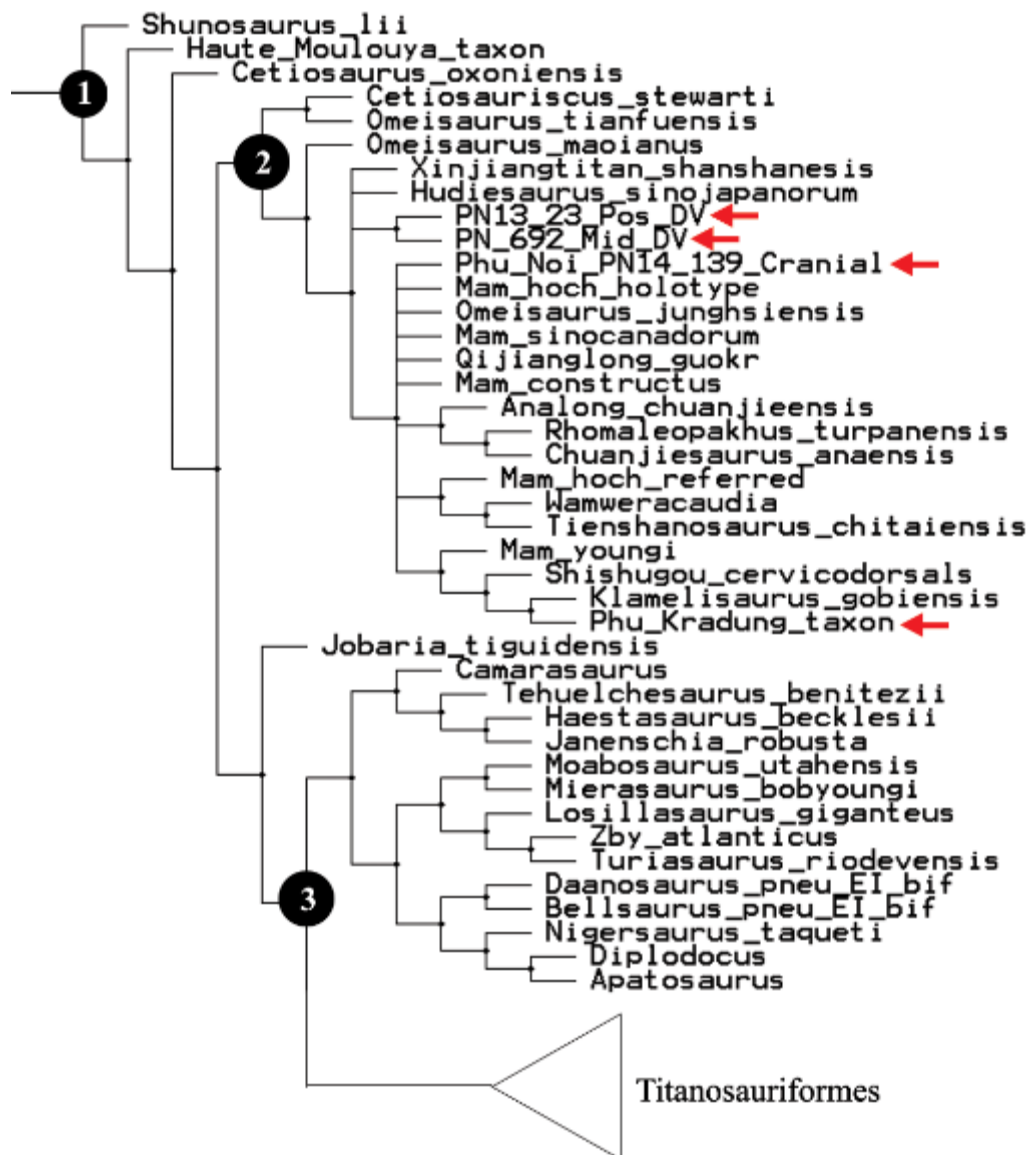


Fig 79 50% majority consensus of 200,000 MPTs from the EQW analysis (2087 steps).

Based on the wide array sauropodomorphs and eusauropods dataset of Moore et al., 2023, produced in TNT 1.5. Node number shows the major clade of Sauropoda. 1 is Eusauropoda; 2 is Mamenchisauridae; 3 is Neosauropoda. Red arrows show the position of Thai mamenchisaurids.

CHAPTER 5

DISCUSSION AND CONCLUSION

5.1 Diversity of Mamenchisauridae sauropods from the Phu Noi locality

From the description and comparison, Phu Noi locality has yields at least four types of Mamenchisauridae sauropods, which correlated to the Southwestern and Northwestern China taxa. Three types of specimens, which resemble to *M. youngi*, *M. hochuanensis* (ZDM0126) and *O. moianus*, and *Bellusaurus sui*, have identical morphological features to distinguish. The *O. tianfuensis* type specimens are still ambiguous because of the disarticulated middle to posterior caudal vertebrae are lack of morphological features of the specific genera. Although the isolated teeth are identical in the genus *Omeisaurus*, these teeth still have possibility to be Phu Noi form, which presents combination of morphological features and phylogenetic characters of various Mamenchisauridae. For now, the presence of *O. tianfuensis* is insufficient to confirm and must be waiting for more complete specimens.

The fifth and the final form is Phu Noi form that represent by the unique posterior skull roof with squamosal postorbital and quadratojugal (PN14-139), which has combination of morphological features of Mamenchisauridae sauropods. The outline of the dorsal surface resembles to *M. youngi* with more anteriorly bend and transverse elongated occipital wings of the parietals and less angular on the suture between supraoccipital and parietals.

PN692 resemble to middle dorsal vertebra of *Mamenchisaurus* spp. by the lamina structures with additional depression on the transverse process, which

resemble to the dorsal vertebra of *Bellusaurus sui*. PN13-23, the posterior dorsal vertebra by the presence of ppdl, represents the overall outline and pneumatic structure of *Mamenchisaurus* spp. with additional pneumatic cavities on the neural spine and transverse process.

Following to the phylogenetic analysis, the two different position dorsal vertebrae are the sister taxa in the 50% majority rule consensus tree. This result might be interpreted that two dorsal vertebrae, middle (D5 to D8) and posterior position (D9 to D12), are from the similar taxon. Moreover, the posterior skull roof (PN14-139) is in the very close node, only one step further than the vertebrae, which might be the identical or the close related taxa. In summary, the Phu Noi type is currently considered a new taxon of Mamenchisauridae sauropods.

5.2 Systematic palaeontology

Dinosauria Owen, 1842

Saurischia Seeley, 1887

Sauropodomorpha von Huene, 1932

Sauropoda Marsh, 1878

Eusauropoda Upchurch, 1995

Mamenchisauridae Young and Chao, 1972

Mamenchisauridae indet. C

The reasons to purpose the Phu Noi taxon to Mamenchisauridae indet. C because the topology of dorsal vertebrae is located outside the polytomy node of

Mamenchisaurus spp. Although the posterior skull is in the *Mamenchisaurus* node, but the genuine position of Phu Noi taxon could be the outgroup of the genus. Another reason is the reports of Mamenchisauridae indet. A and B are already reported from the isolated teeth of Dan Luang locality, Upper Phu Kradung Formation, Mukdahan province, Northeastern of Thailand and from the isolated dorsal vertebra of Khlong Thorn District, Khlong Min Formation, Krabi province, Southern of Thailand, respectively (E Buffetaut & Suteethorn, 1998, 2004; Eric Buffetaut et al., 2005). However, the status of Mamenchisauridae indet. A is ambiguous due to the morphological features of teeth are resembled to both *Mamenchisaurus* spp. and the Euhelopodidae titanosauriformes (Suteethorn et al., 2013).

5.3 Palaeobiogeography of Mamenchisauridae sauropods

The occurrence of Mamenchisauridae is from the Middle Jurassic to Early Cretaceous of the East Asia, mainly on the South China terranes in China. The oldest reports are from the Middle Jurassic bone bearing horizons of Chuanjie Formation, Lufeng country, Yunnan province, Southwest China and Hongqin Formation, Anhui province, Eastern China (Fang et al., 2000; X.-X. Ren, Huang, & You, 2018; X. X. Ren et al., 2021; Sekiya, 2011). Around the Late Bathonian (late Middle Jurassic) to Early Oxfordian (early Late Jurassic) the diversity of Mamenchisauridae is at the highest peak by the fossil record of numerous species of *Mamenchisaurus* spp. and *Omeisaurus* spp. from the Lower and Upper Shaximiao Formation, Sichuan basin, Southwest China (Li et al., 2011). Moreover, the clade also dispersal to the Northwest China, which represent by numerous taxa (e.g. *Bellusaurus*, *Klamelisaurus*, *M. sinocanadorum*, and *Xinjiangtitan*) from Shishugou Formation and Qigu Formation,

Junggar basin, Xinjiang Uygur Autonomous Region, Northwest China, in the slight younger age but mainly contemporaneous to Shaximiao Formation (Callovian to Late Oxfordian) (Moore et al., 2023, 2018; Russell & Zheng, 1993). In this interval of time, the mamenchisaurid also disperse to Sibumasu terrane, which have a record of one dorsal vertebra from Khlong Min Formation, Southern Thailand (Eric Buffetaut et al., 2005).

From the Middle to Late Jurassic, the domination of mamenchisaurids and only few neosauropods of the East Asia is opposite to other landmasses, which have diversified of neosauropods and only one report of the mamenchisaurid *Wamweracaudia* from Tendaguru Formation, Tanzania, Southeast Africa (Mannion et al., 2019). The East Asia Isolation Hypothesis (EAIH) is the famous hypothesis to interpret the exclusive diversity of the East Asia (Xu et al., 2018). In Late Jurassic, the proto-East Asia region, including China and Indochina terranes, were completely separated from the Laurasia by the north-south direction epicontinental seaway of the west Urals cause the endemism that made the domination of mamenchisaurids (Xing et al., 2015). However, the Middle Jurassic mamenchisaurids roamed to the Southeast Africa before the isolation and left the fossil record of their descendant in the Late Jurassic of Southeast Africa (Eric Buffetaut et al., 2005; Mannion et al., 2019).

In the Late Jurassic Kimmeridgian to Tithonian, there are two records of China's mamenchisaurids, *Hudiesaurus* and *Rhomaleopakhus*, from Kalazha Formation, Turpan Basin, Northwest China and the mentioned African mamenchisaurid *Wamweracaudia* from Tanzania. In Thailand, both Lower and Upper Phu Kradung Formation are controversially indicated in the interval time.

Our Phu Noi mamenchisaurids (indet. C) from this study are the recently additional taxa of the Late Jurassic Kimmeridgian to Tithonian mamenchisaurids, which increase the record taxa of the Late Jurassic. However, from the combination of diagnostic characters, Phu Noi mamenchisaurids is resembled to the Lower and Upper Shaximiao Formation (Callovian to Oxfordian) (Li et al., 2011). This circumstance can be interpreted in two opposite point of view: 1) The Lower Phu Kradung Formation is the Callovian to Oxfordian in spatiotemporal age instead of Tithonian to Berriasian, which previously dating by the key Early Cretaceous palynomorph *Dicheiropollis etruscus* (Racey & Goodall, 2009). 2) The Shaximiao mamenchisaurids dispersed to Indochina terrane and surviving through the temporal time scale to the entire present age of Phu Kradung Formation, which related to the record of cf. *Mamenchisaurus* sp. from Phu Dan Ma, Kalasin province (Suteethorn et al., 2013).

Lastly, the last two Mamenchisaurids are from Early Cretaceous Aptian Age of China, *M. anyuensis* and *Qijianglong*. The taxa are from Upper Suining Formation to Penglazhen Formation, which was indicated as the end of the Late Jurassic. However, from the update radiometric dating of zircon detrital, the interval time are indicated to the Aptian of Early Cretaceous (Wang, Norell, Pei, Ye, & Chang, 2019). This study has changed the overview of the spatiotemporal distribution of mamenchisaurid, which was limited at the end Jurassic, and support the occurrence of the clade in both Upper and Lower Phu Kradung Formation.

5.4 Conclusion

1. Phu Noi locality has yield at least four types of Mamenchisauridae sauropods, three resemble to the Late Jurassic Chinese taxa and the one new taxon.

2. The materials of Mamenchisauridae indet. C has distinct morphological features and phylogenetic affinity from other taxa in the clade.
3. Mamenchisauridae sauropod in Thailand had been distributed from the Middle Jurassic of the Sibumasu terrane to the Late Jurassic-Early Cretaceous of the Indochina terrane.
4. The Upper and Lower Phu Kradung Formation have different taxa of mamenchisaurids as in other vertebrates.

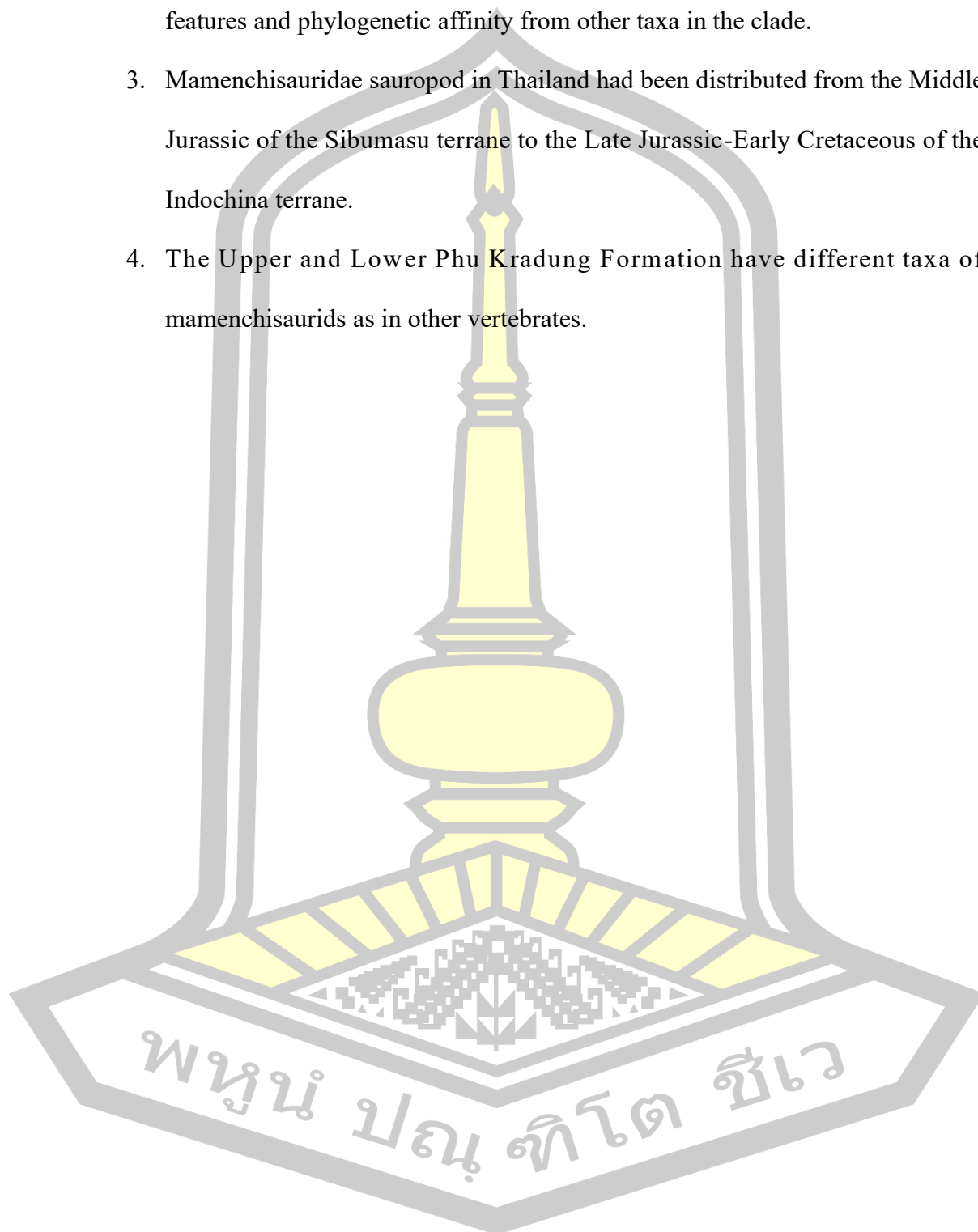


Table 4 Summary list of Mamenchisauridae and the geological formation occurrence

| Taxon | Formation / Age / Basin | Localities | Ref. |
|---|--|---|---|
| <i>Mamenchisaurus anyuensis</i> | Upper Suining / Early-Mid K (Aptian) / Sichuan | Sichuan, SW China | He et al., 1996 |
| <i>Qijianglong guokr</i> | Upper Suining to Penglazhen / Early-Mid K (Aptian) / Sichuan | Qijiang, Chongqing, SW China | Xing et al., 2015 |
| Phu Kradung taxon cf. <i>Mamenchisaurus</i> sp. | Upper Phu Kradung / Late J to Early K / | Phu Dan Ma, Kalasin, NE Thailand | Suteethorn et al., 2013 |
| <i>Hudiesaurus sinojapanorum</i> | Kalazha / Kimmerigian - Tithonian / Turpan Basin | Shanshan, Xinjiang, NW China | Dong, 1997; Upchurch et al., 2021 |
| <i>Rhomaleopakhus turpanensis</i> | | | |
| <i>Wamweracaudia keranjei</i> | Tendaguru / Late Jurassic | Quarry P, Tendaguru hill, Tanzania, SE Africa | Mannion et al., 2019 |
| Phu Noi Mamenchisauridae indet. C | Lower Phu Kradung / Late J / | Phu Noi, Kalasin, Thailand | This study |
| <i>Tianshanosaurus chitaiensis</i> | Shishugou / Oxfordian / Junggar | Qitai, Xinjiang, China | Young, 1937 |
| <i>Mamenchisaurus sinocanadorum</i> | Upper Shishugou / Late J / Junggar | Xinjiang, NW China | Russell & Zheng, 1993; Moore et al., 2023 |
| <i>Xinjiangtitan shanshanensis</i> | Qigu/ early Late J | | Wu et al., 2013; Zhang et al., 2018 |
| <i>Bellusaurus sui</i> | Mid Shishugou / Early Oxfordian / Junggar 161.5 | | Dong, 1990; Moore et al., 2018; 2020 |
| <i>Mamenchisaurus hochuanensis</i> | Upper Shaximiao / Mid-Late J / Sichuan | Chongqing, SW China | Young & Zhao, 1972 |
| <i>Mamenchisaurus constructus</i> | | Sichuan, SW China | Young, 1954; 1958 |

Table 4 Continued

| Taxon | Formation / Age / Basin | Localities | Ref. |
|---|---|---------------------------------|--|
| <i>Mamenchisaurus youngi</i> | Upper Shaximiao / Mid-Late J / Sichuan | Sichuan, SW China | Pi et al., 1996; Ouyang, & Ye. 2002 |
| <i>Omeisaurus maoianus</i> | | | Tang et al., 2001 |
| <i>Mamenchisaurus hochuanensis</i> (referred specimen) | | | Ouyang & Ye, 2002 |
| <i>Omeisaurus junghsiensis</i> | Lower Shaximiao / Mid-J / Sichuan maximum burial age: Bajocian 166.0 | Sichuan, SW China | Young, 1939; Dong, 1983 |
| <i>Omeisaurus tianfuensis</i> | | | He et al., 1984; He et al., 1988 |
| <i>Omeisaurus puxiani</i> | | | Tan et al., 2021 |
| <i>Chuanjiesaurus anaensis</i> | Chuanjie / Mid-J / Lufeng Basin | Lufeng, Yunnan, SW China | Fang et al., 2000; Sekiya, 2011 |
| <i>Analong chuanjieensis</i> | | | Fang et al., 2000; Sekiya, 2011; Ren et al., 2020 |
| <i>Huangshanlong anhuiensis</i> | Hongqin / Mid-J / Tunxi Beginning stage: Aalenian 174.70 Ending stage: Callovian 161.5 | Huangshan, Anhui, E China | Huang et al., 2014 |
| <i>Anhuilong diboensis</i> | | | Ren et al., 2018 |
| Klongthom cf. Mamenchisaurid | Khlong Min / Mid-J / | Khlong Thom, Krabi, Thailand | Buffetaut et al., 2005 |

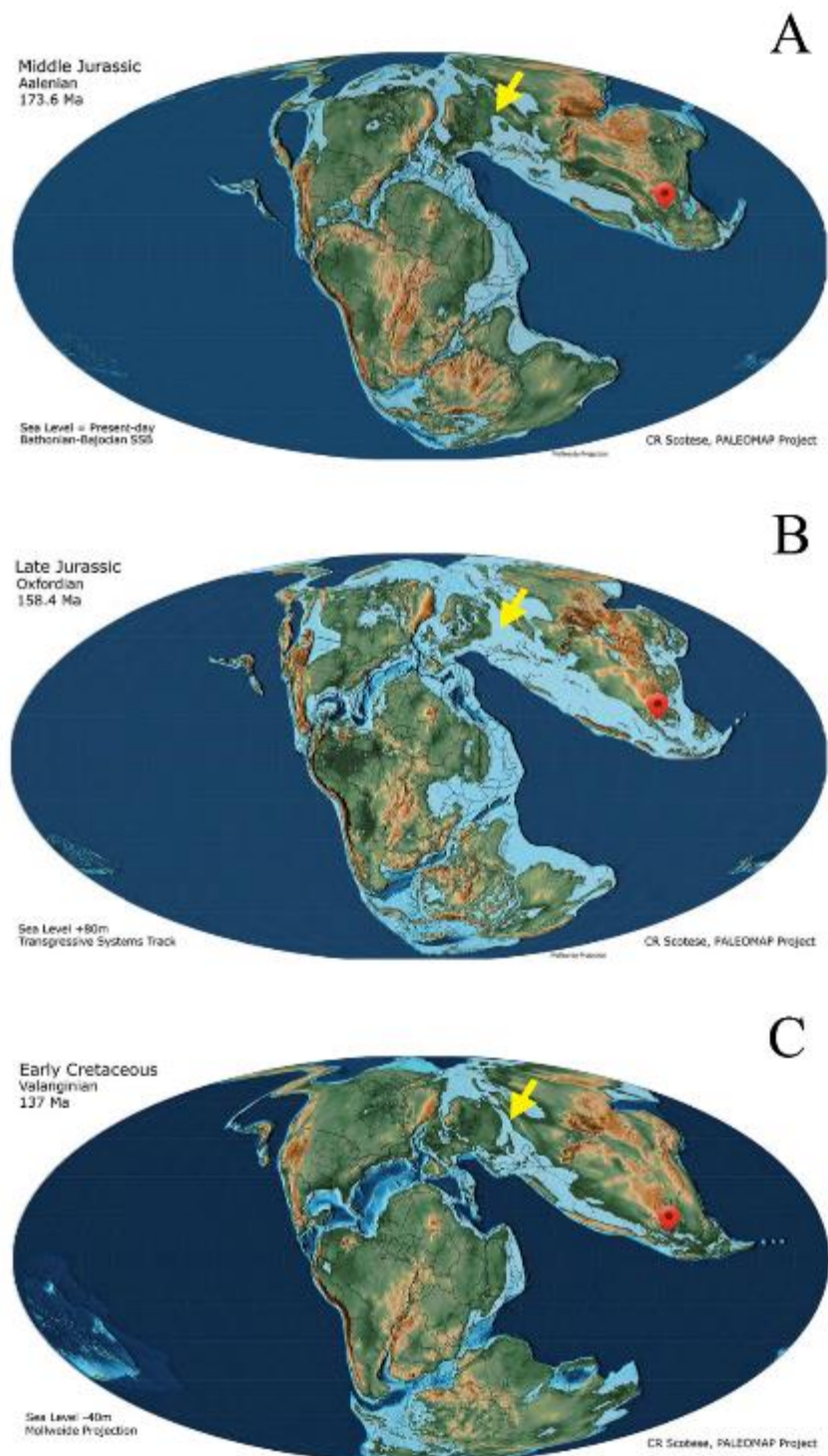


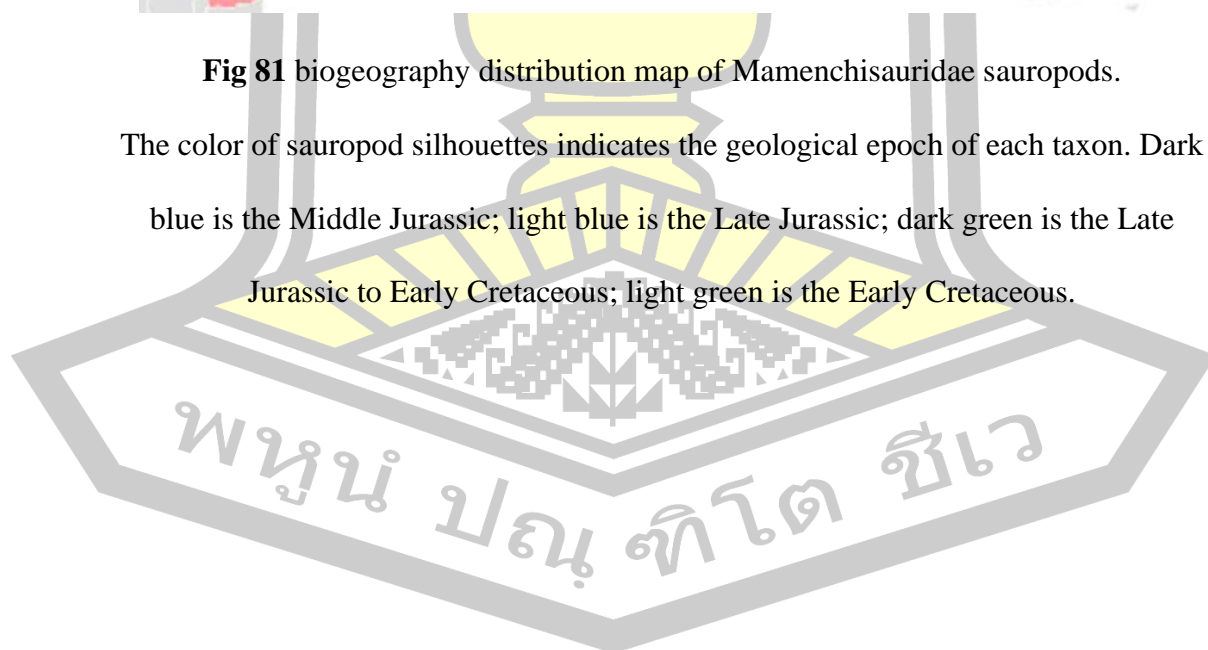
Fig 80 Palaeogeographic maps represents the appearance of the epicontinental seaway
Turgai strait in yellow arrow.

A. The world map of Middle Jurassic; B. The world map of Late Jurassic; C. The world map of Early Cretaceous. The location of Thailand is the red pin (modified from Scotese, 2014b, 2014a)



Fig 81 biogeography distribution map of Mamenchisauridae sauropods.

The color of sauropod silhouettes indicates the geological epoch of each taxon. Dark blue is the Middle Jurassic; light blue is the Late Jurassic; dark green is the Late Jurassic to Early Cretaceous; light green is the Early Cretaceous.



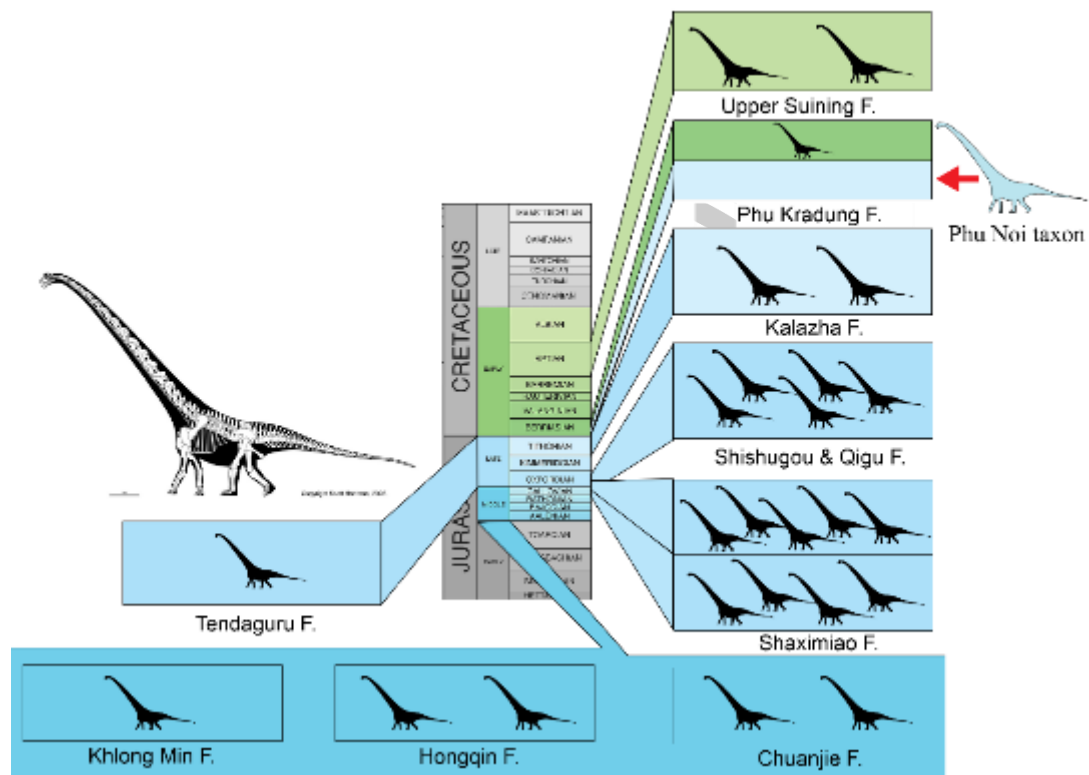
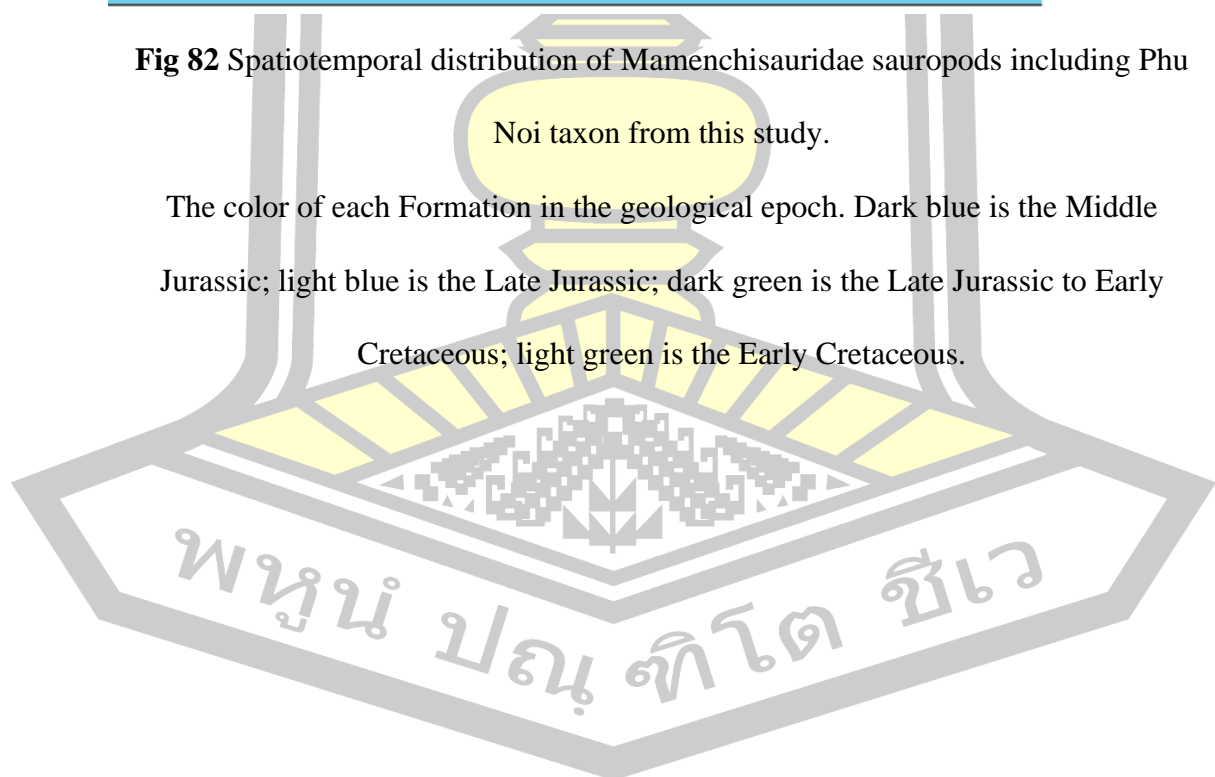


Fig 82 Spatiotemporal distribution of Mamenchisauridae sauropods including Phu Noi taxon from this study.

The color of each Formation in the geological epoch. Dark blue is the Middle Jurassic; light blue is the Late Jurassic; dark green is the Late Jurassic to Early Cretaceous; light green is the Early Cretaceous.



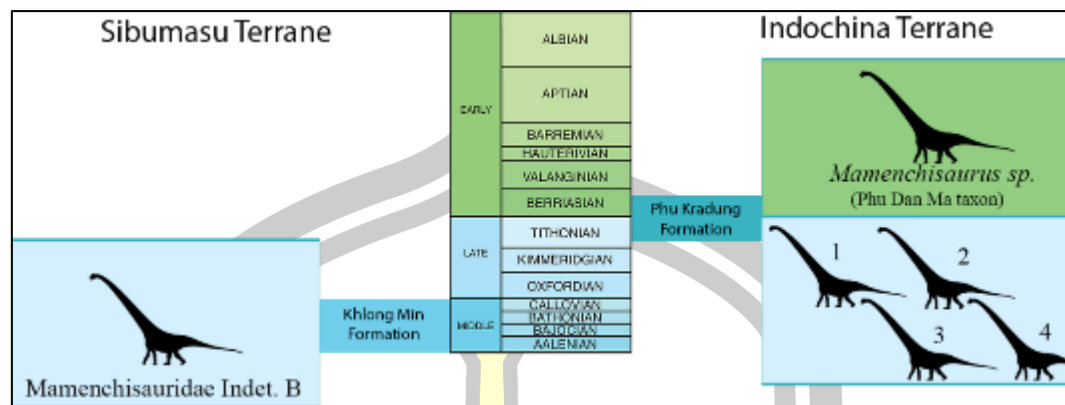


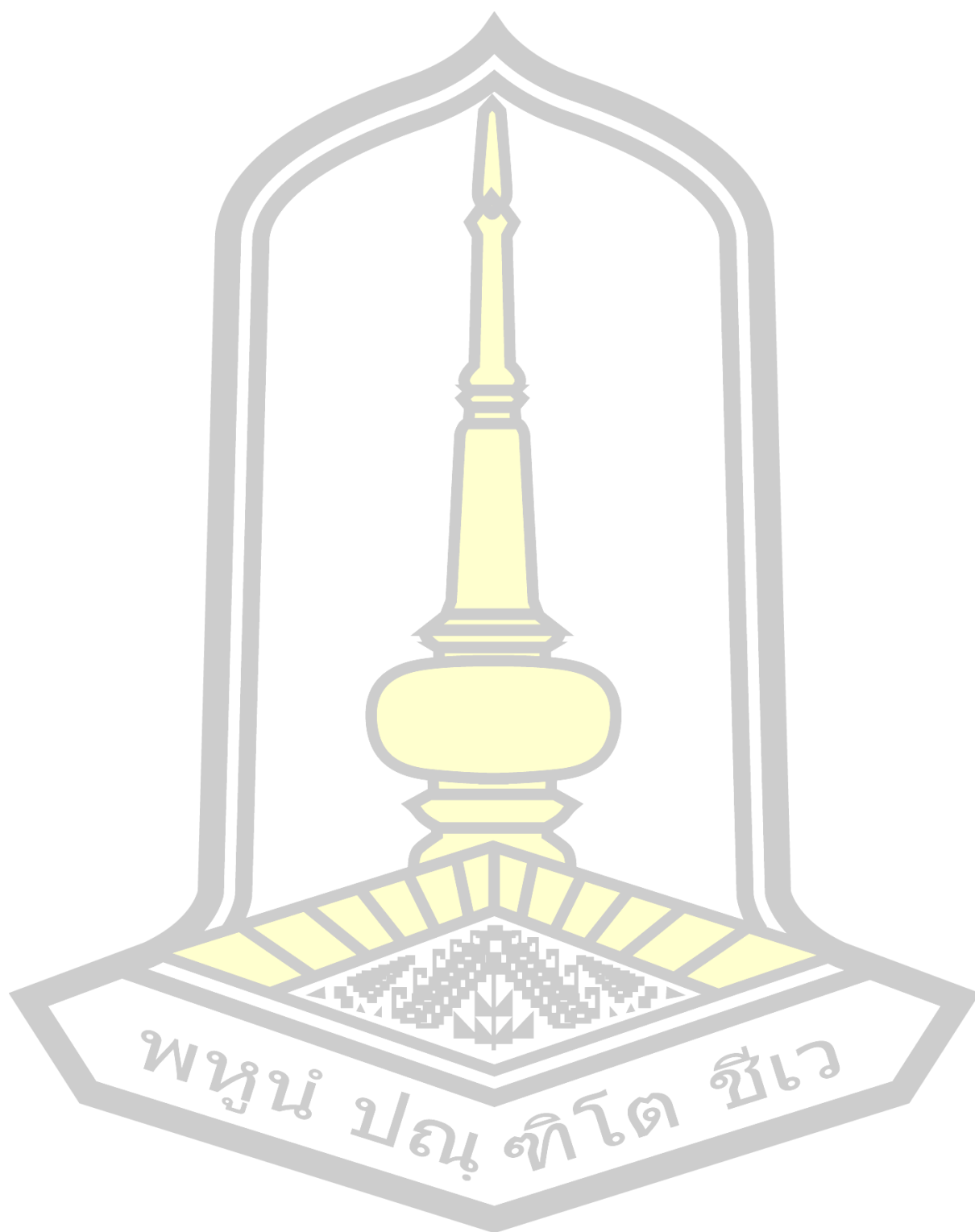
Fig 83 The diversity of Mamenchisauridae sauropods in Thailand.

1, *M. youngi* type; 2, *M. hochuanensis* and *O. maoianus* type; 3, *Bellusaurus sui* type;

4, Phu Noi type including Mamenchisauridae Indet. C.



REFERENCES



- Baron, M. G., Norman, D. B., & Barrett, P. M. (2017). A new hypothesis of dinosaur relationships and early dinosaur evolution. *Nature*, 543(7646), 501–506. <https://doi.org/10.1038/nature21700>
- Buffetaut, E., & Suteethorn, V. (1998). Early Cretaceous dinosaurs from Thailand and their bearing on the early evolution and biogeographical history of some groups of Cretaceous dinosaurs. *New Mexico Museum of Natural History and Science Bulletin*, 14, 205–210.
- Buffetaut, E., & Suteethorn, V. (2004). Comparative odontology of sauropod dinosaurs from Thailand. *Revue de Paléobiologie*, 151–159.
- Buffetaut, Eric, Suteethorn, V., Tong, H., & Košir, A. (2005). First dinosaur from the Shan-Thai Block of SE Asia: A Jurassic sauropod from the southern peninsula of Thailand. *Journal of the Geological Society*, 162(3), 481–484. <https://doi.org/10.1144/0016-764904-053>
- Carballido, J. L., Pol, D., Parra Ruge, M. L., Padilla Bernal, S., Páramo-Fonseca, M. E., & Etayo-Serna, F. (2015). A new early cretaceous brachiosaurid (Dinosauria, Neosauropoda) from northwestern Gondwana (Villa de Leiva, Colombia). *Journal of Vertebrate Paleontology*, 35(5), e980505.
- Carballido, J. L., & Sander, P. M. (2014). Postcranial axial skeleton of *Europasaurus holgeri* (Dinosauria, Sauropoda) from the Upper Jurassic of Germany: Implications for sauropod ontogeny and phylogenetic relationships of basal Macronaria. *Journal of Systematic Palaeontology*, 12(3), 335–387. <https://doi.org/10.1080/14772019.2013.764935>
- Carter, A., & Bristow, C. S. (2003). Linking hinterland evolution and continental basin sedimentation by using detrital zircon thermochronology: a study of the Khorat Plateau Basin, eastern Thailand. *Basin Research*, 15(2), 271–285.
- Chanthasit, P., Suteethorn, S., Manitkoon, S., Nonsrirach, T., & Suteethorn, V. (2019). Biodiversity of the Late Jurassic/Early Cretaceous Phu Noi, Phu Kradung Formation, Kalasin, Thailand. *Advancing Paleontological Research and Specimen Conservation in Southeast Asia, The International Symposium and Workshop*, 14–16. Bangkok.
- Chao, T. A. N., Hui, D. A. I., Jian-Jun, H. E., Feng, Z., Xu-Feng, H. U., Hai-Dong, Y. U., ... others. (2019). Discovery of Omeisaurus (Dinosauria: Sauropoda) in the Middle Jurassic Shaximiao Formation of Yunyang, Chongqing, China. *Vertebrata Palasiatica*, 57(2), 105.
- Cuny, G., & Chanthasit, P. (2023). First record of hybodont egg capsules from the Jurassic of Thailand. *Annales de Paléontologie*, 109(4), 102652.
- Cuny, G., Liard, R., Deesri, U., Liard, T., Khamha, S., & Suteethorn, V. (2014). Shark faunas from the Late Jurassic—Early Cretaceous of northeastern Thailand. *Paläontologische Zeitschrift*, 88, 309–328.

- Curry Rogers, K. A., & Wilson, J. A. (2005). *The Sauropods: Evolution and Paleobiology* (1st ed.; K. A. C. Rogers & J. A. Wilson, Eds.). Retrieved from <http://www.jstor.org/stable/10.1525/j.ctt1pnp34>
- D'Emic, M. D. (2012). The early evolution of titanosauriform sauropod dinosaurs. *Zoological Journal of the Linnean Society*, 166(3), 624–671. <https://doi.org/10.1111/j.1096-3642.2012.00853.x>
- Fang, X. S., Pang, Q. J., Lu, L. W., Zhang, Z. X., Pan, S. G., Wang, Y. M., ... Cheng, Z. W. (2000). Lower, middle, and upper jurassic subdivision in the Lufeng region, Yunnan Province. *Proceedings of the Third National Stratigraphical Congress of China*, 208–214.
- Goloboff, P. A., & Catalano, S. A. (2016). TNT version 1.5, including a full implementation of phylogenetic morphometrics. *Cladistics*, 32(3), 221–238.
- Gonzalez Riga, B. J., Mannion, P. D., Poropat, S. F., Ortiz David, L. D., & Coria, J. P. (2018). Osteology of the Late Cretaceous Argentinean sauropod dinosaur *Mendozasaurus neguyelap*: implications for basal titanosaur relationships. *Zoological Journal of the Linnean Society*, 184(1), 136–181.
- Hatcher, J. B. (1901). *Diplodocus* (Marsh): its osteology, taxonomy, and probable habits, with a restoration of the skeleton. *Memoirs of the Carnegie Museum*, 1(1), 1–63. <https://doi.org/10.5962/p.234818>
- He, X.-L., Li, K., & Cai, K. (1988). The Middle Jurassic dinosaur fauna from Dashanpu, Zigong, Sichuan. Vol. IV. Sauropod Dinosaurs (2) *Omeisaurus tianfuensis*. Chengdu: Sichuan Publishing House of Science and Technology.
- He, X, Li, K., & Cai, K. (1988). *Sauropod dinosaurs* (2) *Omeisaurus tianfuensis* (null, Ed.).
- He, Xinlu, Yang, S., Cai, K., Li, K., Liu, Z., By, T., & Downs, W. (1996). A new species of sauropod, *Mamenchisaurus anyuensis* sp. nov. *Geosciences*, 83–86.
- Holtz, T. R., Molnar, R. E., Currie, P. J., Weishampel, D. B., Dodson, P., & Osmólska, H. (2004). The Dinosauria. *Mesozoic Biogeography of Dinosauria*, pp. 627–642. University of California Press Berkeley, CA.
- Ikejiri, T., Tidwell, V., Trexler, D. L., Tidwell, V., & Carpenter, K. (2005). *Thunder-lizards: The sauropodomorph dinosaurs* (null, Ed.).
- Jinyou, M., & Buffetaut, E. (2011). A Sauropod Dorsal Vertebra from the Middle Jurassic of Guangxi, China. *วารสารวิทยาศาสตร์และเทคโนโลยี*, 1(30).
- Knoll, F., Witmer, L. M., Ortega, F., Ridgely, R. C., & Schwarz-Wings, D. (2012). The braincase of the basal sauropod dinosaur *Spinophorosaurus* and 3D reconstructions of the cranial endocast and inner ear. *PLoS One*, 7(1), e30060.
- Li, K., Yang, C., & Hu, F. (2011). Dinosaur assemblages from the Middle Jurassic Shaximiao Formation and Chuanjie Formation in the Sichuan-Yunnan Basin, China. *Volumina*

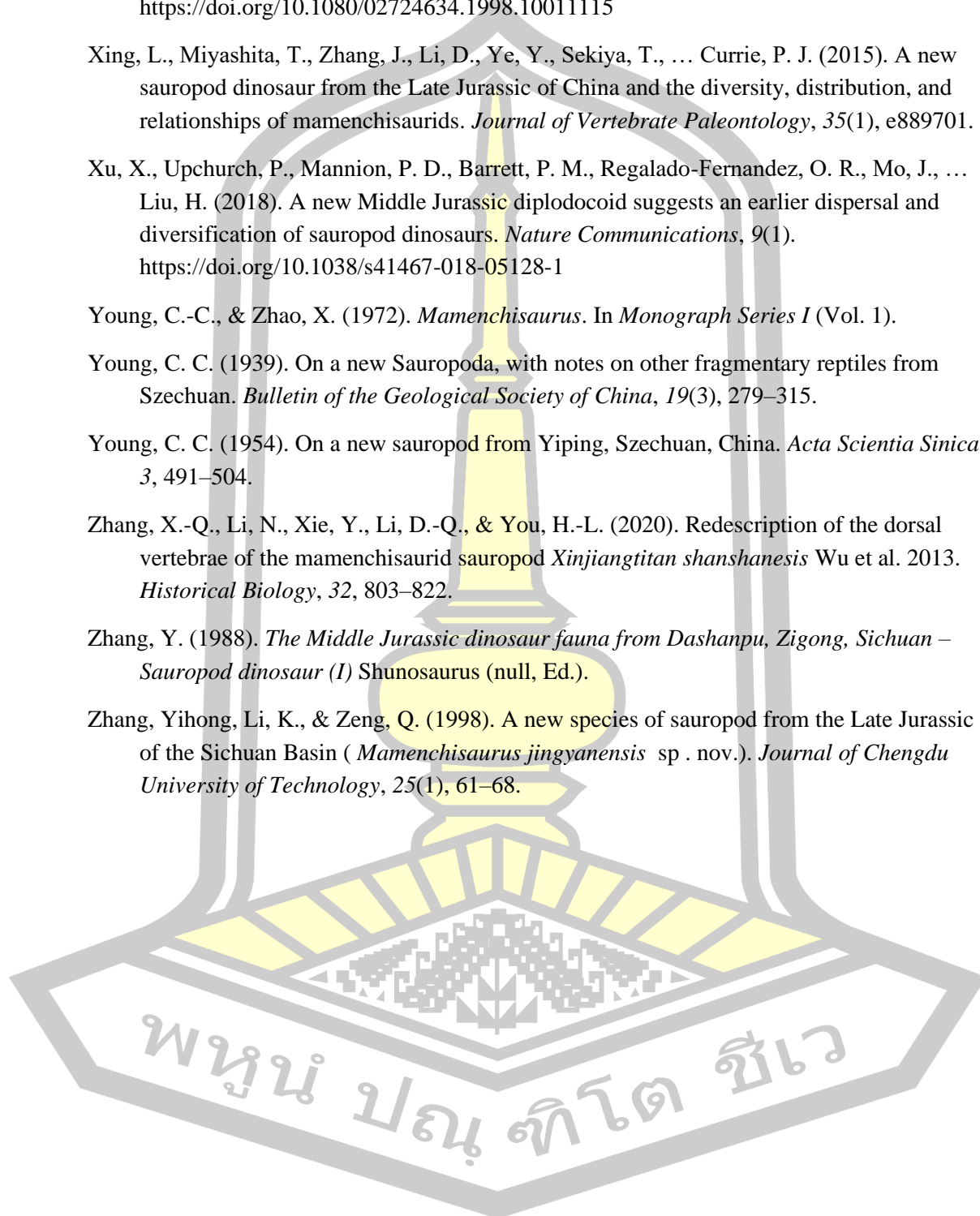
Jurassica, 9(9), 21–42.

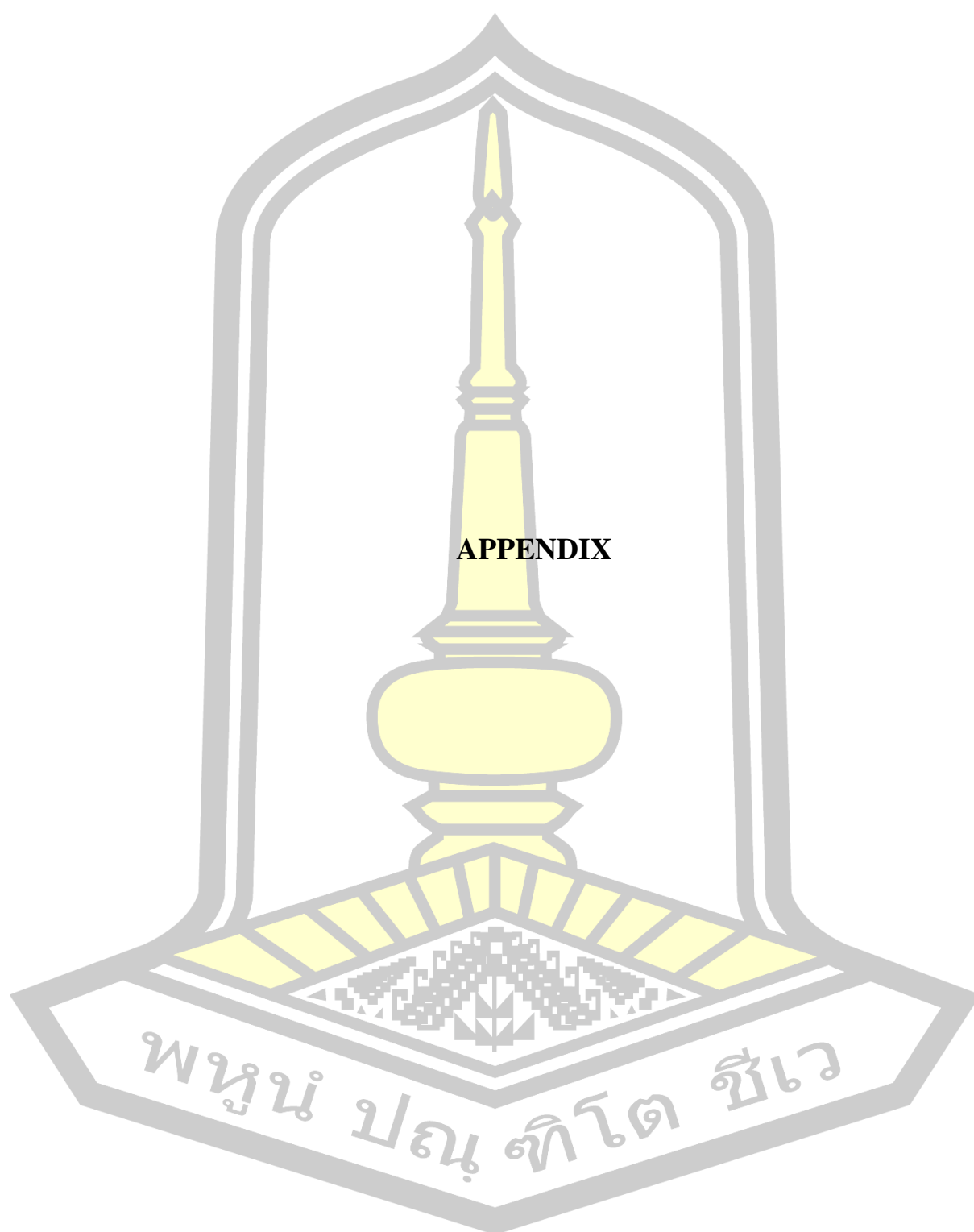
- Liard, R., Cuny, G., Martin, J., Liard, T., Deesri, U., & Suteethorn, S. (2015). Phu Noi, a mesozoic vertebrate locality from the Jurassic of Thailand. *5th GEOINDO, International Conference on Geology, Geotechnology, and Mineral Resources of Indochina*, 23–24.
- Manitkoon, S., Deesri, U., Khalloufi, B., Nonsrirach, T., Suteethorn, V., Chanthasit, P., ... Buffetaut, E. (2023). A New Basal Neornithischian Dinosaur from the Phu Kradung Formation (Upper Jurassic) of Northeastern Thailand. *Diversity*, 15(7). <https://doi.org/10.3390/d15070851>
- Mannion, P. D., Upchurch, P., Schwarz, D., & Wings, O. (2019). Taxonomic affinities of the putative titanosaurs from the Late Jurassic Tendaguru Formation of Tanzania: Phylogenetic and biogeographic implications for eusauropod dinosaur evolution. *Zoological Journal of the Linnean Society*, 185(3), 784–909. <https://doi.org/10.1093/zoolinnea/zly068>
- Martin, J. E., Suteethorn, S., Lauprasert, K., Tong, H., Buffetaut, E., Liard, R., ... Claude, J. (2018). A new freshwater teleosaurid from the Jurassic of northeastern Thailand. *Journal of Vertebrate Paleontology*, 38(6), e1549059.
- Mo, J. (2013). *Topics in Chinese dinosaur paleontology: Bellusaurus sui* (null, Ed.).
- Moore, A. J., Barrett, P. M., Upchurch, P., Liao, C.-C., Ye, Y., Hao, B., & Xu, X. (2023). Re-assessment of the Late Jurassic eusauropod *Mamenchisaurus sinocanadorum* Russell and Zheng, 1993, and the evolution of exceptionally long necks in mamenchisaurids. *Journal of Systematic Palaeontology*, 21(1), 2171818. <https://doi.org/10.1080/14772019.2023.2171818>
- Moore, A. J., Mo, J., Clark, J. M., & Xu, X. (2018). Cranial anatomy of *Bellusaurus sui* (Dinosauria: Eusauropoda) from the Middle-Late Jurassic Shishugou Formation of northwest China and a review of sauropod cranial ontogeny. *PeerJ*, 6, e4881.
- Moore, A. J., Upchurch, P., Barrett, P. M., Clark, J. M., & Xing, X. (2020). Osteology of *Klamelisaurus gobiensis* (Dinosauria, Eusauropoda) and the evolutionary history of Middle-Late Jurassic Chinese sauropods. *Journal of Systematic Palaeontology*, 18(16), 1299–1393. <https://doi.org/10.1080/14772019.2020.1759706>
- Otero, A., Gallina, P. A., Canale, J. I., & Haluza, A. (2012). Sauropod haemal arches: Morphotypes, new classification and phylogenetic aspects. *Historical Biology*, 24(3), 243–256. <https://doi.org/10.1080/08912963.2011.618269>
- Ouyang, H., & Ye, Y. (2001). *The first Mamenchisaurian skeleton with complete skull: Mamenchisaurus youngi: Di yi ju bao cun wan zheng tou gu de Mamexi long*. Sichuan ke xue ji shu chu ban she.
- Pi, L., Ou, Y., Ye, Y., Museum, Z. D., By, T., & Downs, W. (1996). A new species of sauropod from Zigong, Sichuan, *Mamenchisaurus youngi*. *Geosciences*, 87–91.
- Racey, A. (2009). Mesozoic red bed sequences from SE Asia and the significance of the

- Khorat Group of NE Thailand. *Geological Society, London, Special Publications*, 315(1), 41–67.
- Racey, A., & Goodall, J. G. S. (2009). Palynology and stratigraphy of the Mesozoic Khorat Group red bed sequences from Thailand. *Geological Society Special Publication*, 315, 69–83. <https://doi.org/10.1144/SP315.6>
- Ren, X.-X., Huang, J.-D., & You, H.-L. (2018). The second mamenchisaurid dinosaur from the Middle Jurassic of Eastern China. *Historical Biology*.
- Ren, X. X., Sekiya, T., Wang, T., Yang, Z. W., & You, H. L. (2021). A revision of the referred specimen of *Chuanjiesaurus anaensis* Fang et al., 2000: a new early branching mamenchisaurid sauropod from the Middle Jurassic of China. *Historical Biology*, 33(9), 1872–1887. <https://doi.org/10.1080/08912963.2020.1747450>
- Rogers, K. C. (2009). The Postcranial Osteology of *Rapetosaurus krausei* (Sauropoda: Titanosauria) from the Late Cretaceous of Madagascar. *Journal of Vertebrate Paleontology*, 29(4), 1046–1086. Retrieved from <http://www.jstor.org/stable/20627121>
- Rogers, K. C., & Wilson, J. (2005). *The sauropods: evolution and paleobiology*. Univ of California Press.
- Russell, D. A., & Zheng, Z. (1993). A large mamenchisaurid from the Junggar Basin, Xinjiang, People's Republic of China. *Canadian Journal of Earth Sciences*, 30(10), 2082–2095.
- Scotese, C. R. (2014a). Atlas of Early Cretaceous Paleogeographic Maps, PALEOMAP Atlas for ArcGIS, The Cretaceous, Maps 23-31 . *Mollweide Projection*, Vol. 2. Evanston, IL: PALEOMAP Project.
- Scotese, C. R. (2014b). Atlas of Jurassic Paleogeographic Maps, PALEOMAP Atlas for ArcGIS. *The Jurassic and Triassic, Maps 32-42, Mollweide Projection*, Vol. 4. Evanston, IL: PALEOMAP Project.
- Sekiya, T. (2011). Re-examination of *Chuanjiesaurus anaensis* (Dinosauria: Sauropoda) from the Middle Jurassic Chuanjie Formation, Lufeng County, Yunnan Province, Southwest China. In null (Ed.), *Memoir of the Fukui Prefectural Dinosaur Museum*.
- Suteethorn, S., Loeuff, J. Le, Buffetaut, E., Suteethorn, V., & Wongko, K. (2013). First evidence of a mamenchisaurid dinosaur from the Upper Jurassic-Lower Cretaceous Phu Kradung Formation of Thailand. *Acta Palaeontologica Polonica*, 58(3), 459–469. <https://doi.org/10.4202/app.2009.0155>
- Tan, C, Dai, H., He, J.-J., Zhang, F., Hu, X.-F., Yu, H.-D., ... You, H.-L. (2019). *Discovery of Omeisaurus (Dinosauria: Sauropoda) in the Middle Jurassic Shaximiao Formation of Yunyang* (null, Ed.).
- Tan, Chao, Xiao, M., Dai, H., Hu, X.-F., Li, N., Ma, Q.-Y., ... others. (2021). A new species of Omeisaurus (Dinosauria: sauropoda) from the Middle Jurassic of Yunyang, Chongqing, China. *Historical Biology*, 33(9), 1817–1829.

- Tang, F., Jin, X., & Kang, X. (2001). *Omeisaurus maoianus: a complete Sauropoda from Jingyan, Sichuan*. China Ocean Press.
- Tong, H., Naksri, W., Buffetaut, E., Suteethorn, S., Suteethorn, V., Chantasit, P., & Claude, J. (2019). *Kalasinemys*, a new xinjiangchelyid turtle from the Late Jurassic of NE Thailand. *Geological Magazine*, 156(10), 1645–1656.
- Tong, H., Naksri, W., Buffetaut, E., Suteethorn, V., Suteethorn, S., Deesri, U., ... Claude, J. (2015). A new primitive eucryptodiran turtle from the Upper Jurassic Phu Kradung Formation of the Khorat Plateau, NE Thailand. *Geological Magazine*, 152(1), 166–175.
- Tschopp, E., Mateus, O., & Benson, R. B. J. (2015). A specimen-level phylogenetic analysis and taxonomic revision of Diplodocidae (Dinosauria, Sauropoda). *PeerJ*, 2015(4). <https://doi.org/10.7717/peerj.857>
- Upchurch, P. (1995). *The evolutionary history of sauropod dinosaurs*. Retrieved from <https://royalsocietypublishing.org/>
- Upchurch, P. (1998). The phylogenetic relationships of sauropod dinosaurs. *Zoological Journal of the Linnean Society*, 124(1), 43–103.
- Upchurch, P., Barrett, P. M., & Dodson Peter. (2004). Sauropoda. In D. B. Weishampel, P. Dodson, & H. Osmólska (Eds.), *The Dinosauria* (2nd ed., pp. 259–322). <https://doi.org/https://doi.org/10.1525/california/9780520242098.003.0015>
- Wang, J., Norell, M. A., Pei, R., Ye, Y., & Chang, S.-C. (2019). Surprisingly young age for the mamenchisaurid sauropods in South China. *Cretaceous Research*, 104, 104176. <https://doi.org/https://doi.org/10.1016/j.cretres.2019.07.006>
- Whitlock, J. A. (2011). A phylogenetic analysis of Diplodocoidea (Saurischia: Sauropoda). *Zoological Journal of the Linnean Society*, 161(4), 872–915. <https://doi.org/10.1111/j.1096-3642.2010.00665.x>
- Wilson, J. A. (1999). A nomenclature for vertebral laminae in sauropods and other saurischian dinosaurs. *Journal of Vertebrate Paleontology*, Vol. 19, pp. 639–653. <https://doi.org/10.1080/02724634.1999.10011178>
- Wilson, J. A. (2002). Sauropod dinosaur phylogeny: critique and cladistic analysis. In *Zoological Journal of the Linnean Society* (Vol. 136).
- Wilson, J. A. (2012). *New Vertebral Laminae and Patterns of Serial Variation in Vertebral Laminae of Sauropod Dinosaurs* *Vertebrate Paleontology of the Arabian Peninsula* *View project Fossil marine biodiversity in time and space* *View project New vertebral lamiNae aNd PatterNs of serial variationN iN vertebral lamiNae of sauroPod diNosauRs* (Vol. 32). Retrieved from <https://www.researchgate.net/publication/261698589>
- Wilson, J. A., D’Emic, M. D., Ikejiri, T., Moacdieh, E. M., & Whitlock, J. A. (2011). A nomenclature for vertebral fossae in sauropods and other saurischian dinosaurs. *PLoS ONE*, 6(2). <https://doi.org/10.1371/journal.pone.0017114>

- Wilson, J. A., & Sereno, P. C. (1998). Early Evolution and Higher-Level Phylogeny of Sauropod Dinosaurs. *Journal of Vertebrate Paleontology*, 18, 1–79.
<https://doi.org/10.1080/02724634.1998.10011115>
- Xing, L., Miyashita, T., Zhang, J., Li, D., Ye, Y., Sekiya, T., ... Currie, P. J. (2015). A new sauropod dinosaur from the Late Jurassic of China and the diversity, distribution, and relationships of mamenchisaurids. *Journal of Vertebrate Paleontology*, 35(1), e889701.
- Xu, X., Upchurch, P., Mannion, P. D., Barrett, P. M., Regalado-Fernandez, O. R., Mo, J., ... Liu, H. (2018). A new Middle Jurassic diplodocoid suggests an earlier dispersal and diversification of sauropod dinosaurs. *Nature Communications*, 9(1).
<https://doi.org/10.1038/s41467-018-05128-1>
- Young, C.-C., & Zhao, X. (1972). *Mamenchisaurus*. In *Monograph Series I* (Vol. 1).
- Young, C. C. (1939). On a new Sauropoda, with notes on other fragmentary reptiles from Szechuan. *Bulletin of the Geological Society of China*, 19(3), 279–315.
- Young, C. C. (1954). On a new sauropod from Yiping, Szechuan, China. *Acta Scientia Sinica*, 3, 491–504.
- Zhang, X.-Q., Li, N., Xie, Y., Li, D.-Q., & You, H.-L. (2020). Redescription of the dorsal vertebrae of the mamenchisaurid sauropod *Xinjiangtitan shanshanensis* Wu et al. 2013. *Historical Biology*, 32, 803–822.
- Zhang, Y. (1988). *The Middle Jurassic dinosaur fauna from Dashanpu, Zigong, Sichuan – Sauropod dinosaur (I) Shunosaurus* (null, Ed.).
- Zhang, Yihong, Li, K., & Zeng, Q. (1998). A new species of sauropod from the Late Jurassic of the Sichuan Basin (*Mamenchisaurus jingyanensis* sp . nov.). *Journal of Chengdu University of Technology*, 25(1), 61–68.





Appendix 1. The Phylogenetic analysis in this study was based on Moore et al., 2023 modified from Carballido et al., 2015; Gonzalez Riga et al., 2018; and Moore et al., 2020.

1. Premaxillary anterior margin, shape

0) without step or with anteroposteriorly short muzzle, less than 0.25 of skull length (measured up to the anterior point of the ascending process of premaxilla)

1) elongate, boot-shaped snout, equal to or greater than 0.25 of skull length

2. External naris, greatest diameter to greatest diameter of orbit ratio

0) greater than 1.0

1) 1.0 or less

3. Parietal occipital process, dorsoventral height to greatest diameter of foramen magnum ratio

0) greater than 1.0

1) 1.0 or less

4. Parietal, distance separating supratemporal fenestrae to long axis of supratemporal fenestra ratio

0) 1.0 or greater

1) less than 1.0

5. Quadratojugal, anterior process to dorsal process length ratio

0) 1.3 or less

1) greater than 1.3

6. Supraoccipital, dorsoventral height to foramen magnum dorsoventral height ratio

0) 1.0 or greater

1) less than 1.0

7. Occipital condyle, dorsoventral height to combined occipital condyle + basal tubera dorsoventral height ratio

0) less than 0.6

1) 0.6 or greater

8. Basal tubera, mediolateral width to occipital condyle mediolateral width

0) less than 1.5

1) 1.5 or greater

9. Basipterygoid processes, length to basal diameter ratio

- 0) less than 3.0
- 1) 3.0 or greater

10. Surangular, dorsoventral height to maximum dorsoventral height of angular ratio

- 0) 2.0 or greater
- 1) less than 2.0

11. Tooth crowns, slenderness index values (apicobasal length of the tooth crown divided by its maximum mesiodistal width)

- 0) less than 2.0
- 1) 2.0 to <4.0
- 2) 4.0 or greater

12. Maxillary teeth, number

- 0) 17 or more
- 1) fewer than 17

13. Dentary teeth, number

- 0) greater than 15
- 1) 15 or fewer

14. Cervical vertebrae, number

- 0) 13 or fewer
- 1) 14-15
- 2) more than 15

15. Cervical centra, highest average elongation index value [aEI; centrum anteroposterior length (excluding articular ball) divided by the mean average value of the posterior articular surface mediolateral width and dorsoventral height] of

- 0) less than 3.0
- 1) between 3.0 and <4.0
- 2) greater than 4.0

16. Anterior cervical centra, posterior articular face dorsoventral height to mediolateral width ratio

- 0) greater than 1.0
- 1) less than 1.0

17. Middle-posterior cervical centra, posterior articular face dorsoventral height to mediolateral width ratio

- 0) 1.0 or less
- 1) greater than 1.0

18. Posterior cervical neural arch to centrum dorsoventral height ratio, measured on anterior face of vertebra (arch height measured from dorsal surface of centrum to base of prezygapophyses)

- 0) 0.5 or greater
- 1) less than 0.5

19. Posterior-most cervical and anterior-most dorsal neural spines, dorsoventral height divided by posterior centrum height

- 0) 1.0 or greater
- 1) less than 1.0

20. Dorsal vertebrae

- 0) 13 or more
- 1) 12 or fewer

21. Anterior dorsal centra, posterior articular face mediolateral width to dorsoventral height ratio

- 0) less than 1.3
- 1) 1.3 or greater

22. Middle-posterior dorsal centra, posterior articular face mediolateral width to dorsoventral height ratio

- 0) less than 1.0
- 1) 1.0 or greater

23. Posterior dorsal neural spines, dorsoventral height divided by posterior centrum dorsoventral height

- 0) 1.0 or greater
- 1) less than 1.0

24. Sacral vertebrae, number

- 0) five or fewer
- 1) six or more

25. Anterior caudal centra, mediolateral width to dorsoventral height (excluding chevron facets) of anterior surface ratio

0) less than 1.0

1) 1.0 or greater

26. Anterior caudal centra, lowest aEI [centrum anteroposterior length (excluding articular ball) divided by the mean average value of the anterior surface mediolateral width and dorsoventral height] value of

0) less than 0.6

1) 0.6 or greater

27. Anterior caudal centra, anteroposterior length of posterior condylar ball to mean average radius [(mediolateral width + dorsoventral height) divided by 4] of anterior articular surface of centrum ratio

0) zero (posterior articular surface of centrum is flat or concave)

1) less than or equal to 0.3 (posterior articular surface of centrum is mildly convex)

2) greater than 0.3 (posterior articular surface of centrum is strongly convex)

28. Middle caudal centra, mediolateral width to dorsoventral height (excluding chevron facets) of anterior surface ratio

0) less than 1.0

1) 1.0 or greater

29. Middle caudal centra, aEI [centrum anteroposterior length (excluding articular ball) divided by the mean average value of the anterior surface mediolateral width and dorsoventral height (excluding chevron facets)] value

0) less than 1.4

1) 1.4 or greater

30. Posterior caudal centra, mediolateral width to dorsoventral height (excluding chevron facets) of anterior surface ratio

0) less than 1.2

1) 1.2 or greater

31. Posterior caudal centra, aEI [centrum anteroposterior length (excluding articular ball) divided by the mean average value of the anterior surface mediolateral width and dorsoventral height (excluding chevron facets)] value

0) less than 1.7

1) 1.7 or higher

32. Anterior-most caudal neural spines, dorsoventral height divided by centrum height

0) 1.2 or greater

1) less than 1.2

33. Anterior caudal neural spines, maximum mediolateral width to anteroposterior length ratio

- 0) less than 1.0
- 1) 1.0 or greater

34. Anterior caudal neural spines, maximum mediolateral width to minimum mediolateral width ratio

- 0) less than 2.0
- 1) 2.0 or greater (spines expand dorsally, forming club or mace shaped spinous processes)

35. Anterior chevrons (excluding first chevron), dorsoventral height of haemal canal divided by total chevron height

- 0) less than 0.40
- 1) 0.40 or greater

36. Scapular acromion process, dorsoventral height to minimum dorsoventral height of scapular blade ratio

- 0) less than 3.0
- 1) 3.0 or greater

37. Scapular blade, maximum (measured at or close to distal end) to minimum dorsoventral height ratio

- 0) 2.0 or greater
- 1) less than 2.0

38. Coracoid, anteroposterior length to dorsoventral height of scapular articulation ratio

- 0) 1.0 or greater
- 1) less than 1.0

39. Sternal plate, maximum length divided by humerus proximodistal length

- 0) less than 0.65
- 1) 0.65 or greater

40. Humerus to femur proximodistal length ratio

- 0) 0.8 or less
- 1) <0.8 to 0.9
- 2) greater than 0.9

41. Humerus, maximum mediolateral width of proximal end divided by proximodistal length

- 0) 0.4 or greater

- 1) less than 0.4
42. Humerus, minimum mediolateral width divided by proximodistal length
- 0) 0.15 or greater
- 1) less than 0.15
43. Humerus shaft eccentricity, mediolateral to anteroposterior width ratio at midshaft
- 0) greater than 1.5 (usually close to 1.8)
- 1) 1.5 or lower (usually close to 1.3)
44. Radius to humerus proximodistal length ratio
- 0) 0.65 or greater
- 1) less than 0.65
45. Radius, maximum diameter of the proximal end divided by proximodistal length
- 0) less than 0.3
- 1) 0.3 or greater
46. Radius, mediolateral width of proximal to distal end ratio
- 0) 1.0 or greater
- 1) less than 1.0
47. Radius, distal end mediolateral width to mid- shaft mediolateral width ratio
- 0) less than 2.0
- 1) 2.0 or greater
48. Radius, distal end mediolateral to anteroposterior width ratio
- 0) 1.5 or greater
- 1) less than 1.5
49. Radius, distal condyle orientation
- 0) perpendicular or bevelled less than 20° to long axis of shaft
- 1) bevelled at least 20° to long axis of shaft
50. Ulna, ratio of maximum mediolateral width of proximal end to ulna length
- 0) gracile, ratio is less than 0.4
- 1) stout, ratio is 0.4 or greater
51. Ulna, ratio of mediolateral width of proximal end (equivalent to anteromedial arm) to anteroposterior width of proximal end (equivalent to anterolateral arm)
- 0) less than 1.4

1) 1.4 to <2.0

2) 2.0 or greater

52. Metacarpals, longest metacarpal to radius proximodistal length ratio

0) less than 0.40

1) 0.40 or greater

53. Metacarpals, metacarpal I proximal end dorsoventral height to mediolateral width ratio

0) less than 1.8

1) 1.8 or greater

54. Metacarpals, metacarpal I to metacarpal II or III proximodistal length ratio

0) less than 1.0

1) 1.0 or greater

55. Metacarpals, metacarpal I to metacarpal IV proximodistal length ratio

0) less than 1.0

1) 1.0 or greater

56. Manual ungual on digit I to metacarpal I proximodistal length ratio

0) 0.5 or greater

1) less than 0.5

57. Ilium, pubic peduncle (measured at the articular surface), anteroposterior to mediolateral width ratio

0) greater than 0.5

1) 0.5 or less

58. Pubis, iliac articular surface, anteroposterior to mediolateral width ratio

0) less than 2.0

1) 2.0 or greater

59. Pubis, dorsoventral height of ischial articulation of the pubis divided by pubis proximodistal length is

0) 0.4 or greater

1) less than 0.4

60. Ischium to pubis proximodistal length ratio

0) greater than 0.8

1) 0.80 or less

61. Ischium, ratio of anteroposterior length of proximal plate to ischium proximodistal length

- 0) greater than 0.25
- 1) 0.25 or less

62. Ischium, ratio of anteroposterior length of iliac peduncle to anteroposterior length of proximal plate

- 0) less than 0.7 (large ischial contribution to acetabulum)
- 1) 0.7 or greater (small ischial contribution to acetabulum)

63. Ischium, ratio of dorsoventral width across the distal shaft (mediolateral in taxa with fully coplanar shafts) to ischium proximodistal length

- 0) 0.2 or greater
- 1) less than 0.2

64. Ischium, ratio of dorsoventral width of distal end of shaft to minimum shaft dorsoventral width (both dimensions are mediolateral in taxa with fully coplanar shafts)

- 0) 1.5 or greater
- 1) less than 1.5

65. Femur shaft eccentricity, mediolateral width to anteroposterior width ratio at midshaft

- 0) less than 1.85
- 1) 1.85 or greater

66. Femoral distal condyles, tibial to fibular condylar anteroposterior length ratio

- 0) less than 1.2
- 1) 1.2 or greater

67. Tibia, distal end mediolateral width to long axis of a cross-section horizontally through the mid-shaft ratio

- 0) 2.0 or greater
- 1) less than 2.0

68. Tibia, distal end, mediolateral to anteroposterior width ratio

- 0) 1.5 or greater
- 1) less than 1.5

69. Fibula, mediolateral width of distal end to mediolateral width at midshaft ratio

- 0) 2.0 or greater
- 1) less than 2.0

70. Astragalus, mediolateral width to maximum proximodistal height ratio

- 0) 1.8 or greater
1) less than 1.8
71. Astragalus, mediolateral width to maximum anteroposterior length ratio
0) 1.5 or greater
1) less than 1.5
72. Metatarsals, metatarsal I to metatarsal V proximodistal length ratio
0) less than 1.0
1) 1.0 or greater
73. Metatarsals, metatarsal III to tibia proximodistal length ratio
0) less than 0.25
1) 0.25 or greater
74. Metatarsals, metatarsal V proximal end to distal end maximum mediolateral width ratio
0) 1.6 or greater
1) less than 1.6
75. Premaxilla, posterolateral processes and lateral processes of maxilla
0) without midline contact
1) with midline contact forming marked narial depression, subnarial foramen not visible laterally
76. Premaxillary anterior margin, shape
0) with step
1) without step
77. Premaxilla maxilla sutural contact, shape in lateral view
0) straight
1) sinuous
78. Maxillary ascending process, medial plate-like projections
0) do not contact each other on the midline
1) contact each other on the midline
79. Maxilla, preantorbital fenestra
0) absent
1) present
80. Lacrimal, anterior process

- 0) absent
 - 1) present
81. Jugal quadratojugal contact
- 0) articulation point includes the posterior margin of jugal
 - 1) posterior margin of jugal excluded from articulation and only the ventral margin of the jugal contributes to articulation
82. Prefrontal, shape of posterior end in dorsal view
- 0) acute, with a subtriangular outline
 - 1) broadly rounded or "square"
83. Frontal, medial convexity in dorsal view
- 0) absent
 - 1) present
84. Parietal, elongate posterolateral process
- 0) present
 - 1) absent
85. Parietal, contribution to post-temporal fenestra
- 0) present
 - 1) absent
86. Supratemporal fenestra, lateral exposure
- 0) visible laterally, temporal bar shifted ventrally
 - 1) not visible laterally, obscured by temporal bar
87. Postorbital, ventral process
- 0) anteroposterior and mediolateral diameters equal, or mediolaterally compressed
 - 1) anteroposteriorly compressed
88. Infratemporal (or laterotemporal) fenestra, anterior extension
- 0) reaching midpoint of orbit
 - 1) reaching or surpassing anterior margin of orbit
89. Squamosal quadratojugal contact
- 0) present
 - 1) absent
90. Quadratojugal, anterior ramus, ventral triangular projection (close to the anterior tip)

- 0) absent
1) present
91. Quadrate, excavation in the posterior surface
0) absent or shallow
1) deep
92. Quadrate fossa, orientation
0) posterior
1) posterolateral
93. Palatobasal contact for basiptyergoid articulation has a dorsomedially orientated hook or finger like projection, which curves round to clasp the end of the basiptyergoid process
0) present
1) absent
94. Palatine, dorsomedial blade (that articulates with maxilla), lateral margin
0) curved
1) straight
95. Vomer, anterior articulation with
0) maxilla
1) premaxilla
96. Paroccipital process, ventral non-articular process
0) absent
1) present
97. Basal tubera, degree of divergence
0) no divergence, or restricted to ventral half of basal tubera
1) extends into dorsal half of basal tubera, usually fully divergent
98. Basioccipital, fossa/fossae on the posterior surface of the basal tubera
0) absent
1) present
99. Basioccipital, foramen/foramina between basal tubera and basiptyergoid processes
0) present
1) absent
100. Basisphenoid quadrate contact

0) absent

1) present (posterior surface of basal tubera bordered laterally and ventrally by a raised lip)

101. Basipterygoid processes, shape in cross-section

0) elliptical or subtriangular

1) subcircular

102. External mandibular fenestra

0) present

1) absent

103. Dentary, posteroventral process, shape

0) single

1) forked

104. Tooth rows

0) restricted anterior to orbit

1) restricted anterior to antorbital fenestra

2) restricted anterior to external naris

3) restricted anterior to subnarial foramen

105. Teeth, occlusal (wear) pattern

0) interlocking, V-shaped facets

1) high-angled planar facets

2) low-angled planar facets

106. Tooth crowns, orientation

0) aligned anterolingually, tooth crowns overlap

1) aligned along jaw axis, crowns do not overlap

107. Tooth crowns in upper and lower tooth rows, relative diameters

0) subequal

1) lower crowns smaller than upper crowns

108. Tooth crowns, shape in labial view

0) spatulate or spoon like (i.e. constricted at the base relative to midheight of the crown)

1) parallel-sided (i.e. little expansion above the root)

109. Tooth crowns, cross-sectional shape at mid- crown

- 0) D-shaped
- 1) cylindrical

110. Tooth crowns, lingual surface

- 0) concave or flat
- 1) convex

111. Tooth crowns, apicobasally orientated lingual ridge

- 0) present
- 1) absent

112. Tooth crowns, distinct mesial and distal carinae (labiolingually thinner than the rest of the tooth crown) along the full crown length

- 0) absent
- 1) present

113. Tooth serrations/denticles

- 0) present
- 1) absent

114. Maxillary teeth, shape

- 0) straight along axis
- 1) twisted axially through an arc of 30-45°

115. Cervical and anterior-most dorsal vertebrae, internal tissue structure

- 0) solid
- 1) camerate
- 2) camellate

116. Atlantal intercentrum, occipital facet shape

- 0) rectangular in lateral view, length of dorsal aspect subequal to that of ventral aspect
- 1) expanded anteroventrally in lateral view, anteroposterior length of dorsal aspect shorter than that of ventral aspect, producing an anteroventral lip

117. Cervical axis, midline ventral keel

- 0) absent
- 1) present

118. Postaxial cervical centra, anterior half of ventral surfaces are

- 0) flat or mildly convex mediolaterally
1) concave mediolaterally
119. Postaxial cervical centra, posterior half of ventral surfaces are
0) flat or mildly convex mediolaterally
1) concave mediolaterally
120. Postaxial cervical centra, ventral midline keel
0) present
1) absent
121. Postaxial cervical centra, parapophyses dorsally excavated
0) absent
1) present
122. Postaxial cervical centra, lateral surfaces
0) lack an excavation or have a shallow fossa
1) possess a deep foramen that is not divided into portions by accessory laminae
2) have a deep foramen that is divided into separate portions by one prominent and occasionally several smaller accessory laminae
123. Middle cervical centra, lateral pneumatic fossa/ foramen extends almost to the posterior end of the centrum, leaving only a thin strip of bone
0) absent
1) present
124. Middle-posterior cervical centra, parapophyses, dorsal surfaces
0) face dorsally or slightly dorsolaterally
1) deflected to face strongly dorsolaterally, such that the cervical ribs are displaced ventrally at least the same height as the centrum
125. Middle-posterior cervical centra, parapophyses
0) restricted to anterior half of centrum (excluding condylar ball)
1) elongate, extending more than half of the centrum length (excluding condylar ball)
126. Cervical neural arches, preepipophyses present on prezygapophyses
0) absent
1) present
127. Cervical neural arches, epipophyses present on postzygapophyses
0) absent

1) present

128. Cervical neural arches (post-Cv3), epipophyses

0) extend beyond the posterior margin of the postzygapophyses (usually as prongs)

1) do not extend beyond the posterior margin of the postzygapophyses

129. Cervical vertebrae with an accessory lamina, which runs from the postzygodiapophyseal lamina (PODL) up to the spinoprezygapophyseal lamina (SPRL)

0) absent

1) present

130. Middle-posterior cervical neural arches, centroprezygapophyseal lamina

0) single

1) bifurcates into medial and lateral branches that both contact the prezygapophysis

131. Middle-posterior cervical neural arches, intrap- ostzygapophyseal lamina projects beyond the posterior margin of the neural arch [including the centropostzygapophyseal laminae (CPOL)], forming a prominent subrectangular projection in lateral view

0) absent

1) present

132. Postaxial cervical and anterior dorsal neural spines

0) unbifurcated

1) bifurcated

133. Cervical bifurcated neural spines (excluding the posterior-most cervical vertebrae), median process at base of notch

0) absent

1) present

134. Middle cervical neural spines, abrupt increase in height (height approximately doubled), following low anterior cervical neural spines (occurs around Cv6?8)

0) absent

1) present

135. Middle cervical neural spines, dorsal surface with mediolaterally orientated midline ridge flanked by small fossae at its anterior and posterior ends

0) absent

1) present

136. Posterior-most cervical and anterior dorsal neural arches, spinodiapophyseal lamina (SPDL)

- 0) single structure
 - 1) divided into anterior and posterior spinodiapophyseal laminae
137. Posterior-most cervical and anterior dorsal unbifurcated neural spines, prespinal lamina
- 0) absent
 - 1) present
138. Posterior-most cervical and anterior dorsal bifurcated neural spines, trifold with median tubercle at least as tall as metapophyses
- 0) absent
 - 1) present
139. Cervical ribs, longest shafts are
- 0) elongate and form overlapping bundles
 - 1) short and do not project far beyond the end of the centrum to which they attach
140. Cervical ribs, longest shafts extend beneath
- 0) fewer than three vertebrae
 - 1) three vertebrae or more
141. Middle-posterior dorsal vertebrae, internal tissue texture
- 0) solid
 - 1) camerate
 - 2) camellate
142. Middle posterior dorsal centra, ventral keel
- 0) absent
 - 1) present
143. Dorsal centra, lateral pneumatic foramen
- 0) absent
 - 1) present
144. Dorsal centra, lateral pneumatic foramina are
- 0) shallow fossae or excavations that do not ramify throughout the centrum
 - 1) deep excavations that ramify throughout the centrum and into the base of the neural arch, often leaving only a thin septum on the midline of the centrum
145. Dorsal centra, lateral pneumatic foramina
- 0) have margins that are flush with the lateral surface of the centrum

- 1) are set within a lateral fossa on the lateral surface of the centrum
146. Anterior dorsal centra, lateral pneumatic foramina have
- 0) rounded posterior margins
 - 1) acute posterior margins
147. Middle-posterior dorsal centra, anterior articular face shape
- 0) flat or concave
 - 1) mildly convex, with degree of convexity notably reducing along the dorsal sequence
 - 2) strongly convex, with degree of convexity approximately consistent along the dorsal sequence
148. Middle-posterior dorsal neural arches, posterior centroparapophyseal lamina
- 0) absent
 - 1) present as a single lamina
 - 2) two parallel laminae
149. Middle-posterior dorsal neural arches, hyposphene hypantrum system
- 0) present
 - 1) absent
150. Middle-posterior dorsal neural arches, hyposphene shape
- 0) narrow, ventral end subequal to or only slightly wider than dorsal tip
 - 1) wide, triangular shape, with ventral end at least twice width of dorsal tip
151. Middle-posterior dorsal neural arches, posterior centrodiapophyseal lamina (PCDL)
- 0) has an unexpanded ventral tip
 - 1) expands and bifurcates towards its ventral tip
152. Middle-posterior dorsal neural arches, PODL
- 0) present
 - 1) absent
153. Anterior dorsal diapophyses are
- 0) directed laterally or slightly upwards
 - 1) directed strongly dorsolaterally at approximately 45° to the horizontal
154. Anterior-middle dorsal diapophyses
- 0) short and dorsoventrally tall

- 1) elongate and dorsoventrally narrow
155. Middle-posterior dorsal diapophyses are
- 0) directed strongly dorsolaterally at approximately 45° to the horizontal
 - 1) directed laterally or slightly upwards
156. Middle-posterior dorsal diapophyses, distal end
- 0) curves smoothly into the remaining dorsal surface of the process
 - 1) is set off from the remaining dorsal surface by a lip, forming a distinct area
157. Posterior-most dorsal diapophyses lie
- 0) posterior or posterodorsal to the parapophysis
 - 1) vertically above the parapophysis
158. Dorsal neural spines, height
- 0) anterior dorsal neural spines subequal to or dorsoventrally shorter than posterior dorsal neural spines
 - 1) anterior dorsal neural spines dorsoventrally taller than posterior dorsal neural spines
159. Dorsal neural spines, anteroposterior width
- 0) approximately constant along the height of the spine, with subparallel anterior and posterior margins
 - 1) narrows dorsally to form a triangular shape in lateral view, with the base approximately twice the width of the dorsal tip
160. Anterior dorsal neural spines, orientation
- 0) project dorsally or slightly anterodorsally
 - 1) project posterodorsally
161. Middle dorsal neural spines
- 0) unbifurcated
 - 1) bifurcated (dorsal surface excavated transversely)
162. Middle-posterior dorsal neural spines
- 0) tapering or not flaring distally
 - 1) flared distally with triangular aliform processes projecting laterally from the top [formed primarily from the expansion of the spinopostzygapophyseal laminae (SPOLs)]
163. Middle-posterior dorsal neural spines
- 0) tapering or not flaring distally, or with absent or weakly developed triangular aliform processes

1) strongly developed triangular aliform processes so that the lateral tips of these processes extend further laterally than the postzygapophyses

164. Middle-posterior dorsal neural spines, orientation

0) vertical or slightly posterodorsal

1) strongly posterodorsal, oriented at 45° to the horizontal or greater

165. Middle-posterior dorsal neural spines, SPOL shape

0) single

1) divided into medial and lateral branches

166. Middle-posterior dorsal neural spines, SPDL

0) absent or restricted to posterior dorsals

1) present on middle and posterior dorsals

167. Middle-posterior dorsal neural spines, prespinal and postspinal laminae

0) form mediolaterally wide surfaces, with little anterior relief, infilling the prespinal and postspinal fossae

1) form distinct, mediolaterally narrow ridges or laminae along the midline of the prespinal and postspinal fossae

168. Middle-posterior dorsal neural spines, midline prespinal lamina (forming distinct ridge) along proximal (lower) half of neural spine

0) present

1) absent

169. Middle-posterior dorsal neural spines, postspinal lamina (forming distinct ridge) along proximal (lower) half of neural spine

0) present

1) absent

170. Thoracic (dorsal) ribs, pneumatized (with proximal pneumatocoels)

0) absent

1) present

171. Anterior thoracic ribs, cross-sectional shape

0) subcircular

1) plank-like, anteroposterior breadth more than three times mediolateral breadth

172. Sacral vertebrae, camellate internal tissue structure

0) absent

1) present

173. Sacral centra, lateral pneumatic foramina or very deep depressions

0) absent

1) present

174. Sacral neural spines, dorsal portions of at least sacral vertebrae 1-4 fused, forming a dorsal? platform?

0) absent

1) present

175. Caudal vertebrae, number

0) more than 35

1) 35 or fewer

176. Anterior-most caudal vertebrae, camellate internal tissue structure

0) absent

1) present

177. Anterior caudal centra, posterior articular surface

0) flat or concave throughout series

1) convex in anterior-most caudal vertebrae, changing to flat or concave in more distal anterior caudal vertebrae

2) convex throughout all anterior caudal vertebrae with ribs

178. Anterior caudal centra, lateral pneumatic fossae or foramina

0) absent

1) present

179. Anterior caudal centra, lateral pneumatic fossae or foramina

0) without sharply defined margins

1) with sharply defined margins

180. Anterior? middle caudal centra, small, shallow vascular foramina pierce the lateral and/or ventral surfaces

0) absent

1) present

181. Anterior? middle caudal centra (excluding the anterior-most caudal vertebrae), ventral longitudinal hollow

0) absent

1) present

182. Anterior? middle caudal centra (excluding the anterior-most caudal vertebrae), distinct ventrolateral ridges, extending the full length of the centrum

0) absent

1) present

183. Middle caudal centra, anteroposteriorly elongate ridge situated at approximately two-thirds of the way up the lateral surface

0) absent

1) present

184. Middle-posterior caudal centra (at least some), posterior articular surface

0) flat or concave

1) convex

185. Middle-posterior caudal centra with convex posterior articular surface

0) condylar convexity merges smoothly into the lateral surface of the main body of the centrum

1) distinct rim rings the condyle, separating it from the lateral surface of the main body of the centrum

186. Distal caudal centra, biconvex

0) absent

1) present

187. Anterior caudal neural arches, hyposphenal ridge

0) present

1) absent

188. Anterior caudal neural arches, hyposphenal ridge shape

0) slender ridge

1) block-like hyposphene

189. Anterior caudal neural arches, distinct prezygodiapophyseal lamina

0) absent

1) present

190. Anterior caudal neural arches, sharp-lipped lateral coel (postzygapophyseal centrodiapophyseal fossa of Wilson et al., 2011) bounded by PCDL (or caudal rib itself), CPOL, and PODL

0) absent

1) present

191. Anterior middle caudal neural arches, prezygapophyses switch from projecting anterodorsally, anteriorly, and back to anterodorsally along the sequence

0) absent

1) present

192. Middle caudal neural arches

0) situated over the midpoint of the centrum with approximately subequal amounts of the centrum exposed at either end

1) located on the anterior half of the centrum

193. Middle-posterior caudal neural arches, distance that prezygapophyses extend beyond the anterior margin of the centrum

0) less than 20% of centrum length (excluding ball), short prezygapophyses

1) 20% or greater of centrum length (excluding ball), elongate prezygapophyses

194. Anterior-most caudal neural spines, sharp- lipped lateral coel [spinodiapophyseal fossa (SDF) of Wilson et al. 2011] bounded by spinoprezygapophyseal lamina (SPRL), SPOL, and PODL

0) absent

1) present

195. Anterior caudal neural spines, project

0) posterodorsally

1) dorsally (sometimes with a subtle anterior deflection)

2) anterodorsally, such that the anterodorsal margin of the neural spine projects beyond the anterior margin of the centrum

196. Anterior caudal neural spines, anterodorsal margin of neural spine

0) level with or posterior to posterior margin of postzygapophyses

1) situated anterior to posterior margin of postzygapophyses (usually does not even approach postzygapophyses)

197. Anterior caudal neural spines, prespinal and postspinal lamina

0) absent or form mediolaterally wide surfaces, with little anterior relief, infilling the prespinal and postspinal fossae

1) form distinct, mediolaterally narrow ridges or laminae along the midline of the prespinal and postspinal fossae

198. Anterior caudal neural spines, SPRL SPOL contact

0) absent

- 1) present, forming a prominent lateral lamina on the neural spine
199. Middle caudal neural spines, in lateral view, widen anteroposteriorly (approximately doubling) from their base to their summit
- 0) absent
- 1) present
200. Middle caudal neural spines, extend posteriorly to the midpoint (or beyond) of the proceeding caudal centrum
- 0) present
- 1) absent (usually do not extend beyond the posterior margin of the centrum)
201. Caudal ribs
- 0) present beyond approximately Cd10 (usually at least up to approximately Cd15)
- 1) only present through to approximately Cd10
202. First caudal rib (transverse process), with prominent ventral bulge
- 0) absent
- 1) present
203. First caudal rib, expands anteroposteriorly towards its distal end, forming an anchor shape in dorsal view
- 0) absent
- 1) present
204. Anterior caudal ribs, shape in anterior view
- 0) triangular, tapering distally
- 1) wing-like, with a dorsolaterally orientated dorsal margin
205. Anterior caudal ribs
- 0) curve strongly anterolaterally
- 1) mainly laterally
- 2) curve strongly posterolaterally
206. Anterior caudal ribs
- 0) do not extend beyond posterior end of centrum (excluding posterior ball)
- 1) extend beyond posterior end of centrum (excluding posterior ball)
207. First chevron, morphology
- 0) Y-shaped and does not differ notably from subsequent chevrons
- 1) anteroposteriorly flattened and V-shaped, with dorsoventrally reduced distal blade

208. Anterior chevrons, proximal ends

- 0) open dorsally
- 1) bridged dorsally by a bar of bone

209. Anterior-middle chevrons, lateral bulges close to distal ends of chevron blades

- 0) absent
- 1) present

210. Middle-posterior chevrons, with anterior expansion of distal blade

- 0) present
- 1) absent

211. Middle-posterior chevrons, with posterior expansion of distal blade (excluding the natural posteroventral curvature of many chevrons)

- 0) present
- 1) absent

212. Scapular acromion (proximal plate), area situated posterior to the acromial ridge

- 0) flat or convex
- 1) forms a separate excavated area

213. Scapular glenoid surface, orientation

- 0) faces anteroventrally and/or slightly laterally
- 1) deflected to face anteroventrally and medially

214. Scapula, posterior margin of the dorsal part of the acromion

- 0) straight and orientated vertically, or sloping to face posterodorsally
- 1) concave, posterodorsal corner of acromion overhangs the dorsal surface of the scapular blade

215. Scapular acromion, subtriangular process at posteroventral corner

- 0) absent
- 1) present

216. Scapular blade, subtriangular process at anteroventral corner

- 0) absent
- 1) present

217. Scapular blade, cross-sectional shape at base

- 0) rectangular

- 1) D-shaped (lateral surface is strongly convex dorsoventrally and medial surface flat)
218. Coracoid, anterior and dorsal margins in lateral view
- 0) merge smoothly into each other, giving a rounded profile
 - 1) meet each other at an abrupt angle, making the coracoid quadrangular in outline
219. Coracoid, dorsal margin in lateral view
- 0) lies below the level of the scapular acromion plate (separated from the latter by a V-shaped notch)
 - 1) reaches or surpasses the level of the dorsal margin of the scapular acromion plate
220. Coracoid, ventral margin in lateral view forms a notch anterior to the glenoid, resulting in an infraglenoid lip anterior to the notch
- 0) absent
 - 1) present
221. Sternal plate, shape in dorsal view
- 0) subcircular or oval
 - 1) triangular (created by an acute anterolateral projection)
 - 2) elliptical with a mildly or strongly concave lateral margin
222. Sternal plate, prominent posterolateral expansion produces a kidney shaped profile in dorsal view
- 0) absent
 - 1) present
223. Humeral proximolateral corner, shape
- 0) rounded, surfaces merge smoothly into each other to produce a transversely rounded proximal end, with the proximal-most point of the lateral margin at a lower level than the remaining lateral half of the proximal surface
 - 1) square, surfaces meet each other at an abrupt angle to produce a squared proximal end in anterior view, with the proximal-most point of the lateral margin level with the remaining lateral half of the proximal surface
224. Humerus, shape of lateral margin of diaphysis (approximately the middle third of the humerus) in anterior view
- 0) concave
 - 1) straight
225. Humeral deltopectoral crest, projection
- 0) anteriorly or anterolaterally

- 1) anteromedially, extending across the anterior face of the humerus

226. Humerus, strong bulge or tuberosity (site for M. latissimus dorsi) close to the lateral margin of the posterior surface, at approximately the level of the distal tip of the deltopectoral crest

- 0) absent
1) present

227. Humerus, anterior surface of distal lateral condyle

- 0) divided by a notch, forming two ridges
1) undivided

228. Humerus, distal-most part of the posterior surface (supracondylar fossa) is

- 0) flat or shallowly concave
1) deeply concave between prominent lateral and medial vertical condylar ridges

229. Humeral distal condyles, articular surface

- 0) flat anteroposteriorly and restricted to distal portion of humerus
1) anteroposteriorly convex so that it curves up onto the anterior and posterior faces of the humerus

230. Humeral distal articular surface, condyles

- 0) undivided
1) divided

231. Radius, strong twist in axis, such that the long axes of the proximal and distal ends are not oriented in the same plane

- 0) absent
1) present

232. Radius, well-developed interosseous ridge that extends along most of the radius length (at least along the distal two-thirds)

- 0) absent
1) present

233. Ulnar olecranon process, development

- 0) absent or only rudimentary, i.e., projecting just above the proximal articulation
1) prominent, projecting well above proximal articulation

234. Ulna, articular surface of anteromedial process is

- 0) flat

- 1) concave along its length
235. Ulna, orientation of anteromedial process
- 0) flat or sloping downwards less than 40°
- 1) sloping downwards at an angle of at least 40° to the horizontal
236. Ulna, distal end
- 0) prominently expanded posteriorly
- 1) unexpanded
237. Carpal bones, number
- 0) three or more
- 1) fewer than three
238. Carpal bones
- 0) at least one carpa present
- 1) absent
239. Metacarpals, distal articular surfaces
- 0) extend onto dorsal/anterior surface of metacarpal
- 1) restricted to distal surface (except sometimes in metacarpal IV)
240. Metacarpals, metacarpal I distal end mediolateral axis orientation
- 0) approximately perpendicular (or only gently bevelled) to long axis of shaft
- 1) bevelled approximately 20° proximo- distally with respect to axis of shaft
241. Metacarpals, metacarpal IV has a prominent proximolateral projection that wraps around the dorsal (anterior) face of metacarpal V (metacarpal IV often forms a chevron shape in proximal end view)
- 0) absent
- 1) present
242. Manual digits
- 0) possess at least some phalanges
- 1) have lost the phalanges
243. Manual phalanx I.1, shape in dorsal view
- 0) rectangular
- 1) wedge-shaped
244. Ilium, preacetabular process in dorsal view

- 0) projects anteriorly
 - 1) projects anterolaterally
245. Ilium, preacetabular process orientation
- 0) lies in approximately vertical plane
 - 1) turns laterally towards its ventral tip to form a horizontal portion
246. Ilium, preacetabular process shape
- 0) dorsoventrally tapers anteriorly to a point
 - 1) semicircular, or rounded outline, such that it does not continue to taper along its anterior-most portion
247. Ilium, preacetabular process, bulge or kink on ventral margin
- 0) absent
 - 1) present
248. Ilium, highest point on the dorsal margin
- 0) occurs level with or posterior to the anterior margin of the base of the pubic process
 - 1) occurs anterior to the anterior margin of the base of the pubic process
249. Ilium, pneumatized
- 0) absent
 - 1) present
250. Pubis, obturator foramen, in lateral view is
- 0) subcircular
 - 1) oval or elliptical, with long axis orientated in same plane as long axis of pubis
251. Pubis, anterior margin of distal end strongly concave in lateral view, such that the distal end forms a prominent, anteriorly expanded boot
- 0) absent
 - 1) present
252. Ischium, acetabular margin, in lateral view
- 0) flat or mildly concave
 - 1) strongly concave, such that the pubic articular surface forms an anterodorsal projection
253. Ischium, symphysis between the ischia

0) terminates at the base of the proximal plates (emarginate distal to pubic articulation)

1) extends along the ventral edges of the proximal plates as well as the distal shafts, so that there is no V-shaped gap between the anterior ends of the ischia in dorsal view (no emargination distal to pubic articulation)

254. Ischium, long axis of shaft, if projected upwards

0) passes through the lower part of the acetabular margin or the upper part of the pubic articular surface (i.e. it is approximately 60° to the horizontal in lateral view)

1) passes through the upper part of the acetabular margin or even approaches the rim of the iliac articulation (i.e. the shaft is at approximately 80° to the horizontal)

255. Femur, proximolateral margin, above the lateral bulge

0) level with or lateral to the lateral margin of the distal half of the shaft

1) medial to the lateral margin of the distal half of the shaft

256. Femur, anteroposterior thickness of lateral margin of proximal third

0) relatively constant with main body of femur

1) narrows to form a flange-like trochanteric shelf, forming a medially bounding vertical ridge along the posterior surface

257. Femur, proximodistally elongate midline ridge (linea intermuscularis cranialis) on anterior face, extending along most of shaft length

0) absent

1) present

258. Femur, fourth trochanter

0) not visible in anterior view

1) visible in anterior view

259. Femoral distal condyles, orientation relative to long axis of femoral shaft

0) bevelled dorsolaterally approximately 10° (tibial condyle extends further distally than fibular condyle)

1) perpendicular (tibial and fibular condyles extend approximately the same distance distally)

2) bevelled dorsomedially approximately 10° (fibular condyle extends further distally than tibial condyle)

260. Tibia, cnemial crest projects

0) laterally

1) anteriorly or anterolaterally

261. Tibia, lateral edge of proximal end forms a pinched out projection, posterior to cnemial crest (the second cnemial crest of Bonaparte et al., 2000)

0) present

1) absent

262. Fibula, proximal end with anteromedially directed crest extending into a notch behind the cnemial crest of the tibia

0) absent

1) present

263. Fibula, lateral muscle scar is

0) oval in outline

1) formed from two vertically elongate, parallel ridges

264. Fibula, shaft in lateral view

0) straight

1) sigmoidal

265. Astragalus, in dorsal (or proximal) view

0) rectangular, with anteroposterior lengths of medial and lateral margins subequal (or medial margin greater)

1) wedge-shaped, narrowing antero- posteriorly towards its medial end, such that it has a reduced anteromedial corner

266. Astragalus, ascending process

0) does not extend to the posterior margin of the astragalus (usually limited to anterior two-thirds of astragalus)

1) extends to the posterior margin of the astragalus

267. Astragalus, laterally directed ventral shelf underlies the distal end of the fibula

0) present

1) absent

268. Astragalus

0) caps most, or all, of the distal end of the tibia

1) reduced so that medial edge of tibia is uncapped

269. Astragalus, posterior margin bears a tongue- like projection posteromedial to the ascending process, which is separated from the latter by a groove

0) present

1) absent

270. Calcaneum

- 0) present
- 1) absent

271. Calcaneum, shape in proximal view

- 0) subcircular
- 1) subrectangular

272. Metatarsals, metatarsal I with a prominent ventrolateral expansion along its distal half, such that the distal end expands further laterally than the proximal end

- 0) absent
- 1) present

273. Metatarsals, lateral margin of metatarsal II in proximal view

- 0) concave
- 1) straight

274. Metatarsals, metatarsal II distal articular surface extends up on to the dorsal surface (extending proximally approximately 25% of metatarsal length and most prominently along medial half)

- 0) absent
- 1) present

275. Metatarsals, medial surface of the proximal portion of metatarsal IV concave (for reception of metatarsal III)

- 0) absent
- 1) present

276. Metatarsals, distal end orientation of metatarsal IV

- 0) perpendicular to long axis of bone
- 1) bevelled to face medially

277. Pedal digit IV

- 0) has at least three phalanges
- 1) has two phalanges or fewer

278. Pedal unguals, tuberosity on the ventral margin, along distal half

- 0) absent
- 1) present

279. Osteoderms

0) absent

1) present

280. Humerus, strong bulge or tuberosity (site for M. scapulohumeralis anterior) on the lateral margin of the posterior surface (usually visible in anterior view), approximately level with the most prominently developed portion of the deltopectoral crest

0) absent or weakly developed, and not visible in anterior view

1) present, forms a distinct lateral bulge that interrupts the line of the lateral humeral margin in anterior view

281. Ulna, posterior process of proximal end

0) weakly developed, so that the proximal profile of the ulna is V-shaped (formed by the anteromedial and anterolateral processes)

1) strongly developed, so that the proximal profile of the ulna is T or Y-shaped, and there is a deep fossa between the anteromedial and posterior processes, rivalling the radial fossa in depth

282. Ulna, shape of the distal end

0) comma-shaped, with tapering curved anterior process associated with an anteromedial fossa for reception of the radius

1) elliptical or oval in outline, with the anteromedial fossa strongly reduced or absent

283. Radius, profile of proximal end

0) D-shaped or elliptical

1) oval or subtriangular, with marked tapering towards the medial process

284. Radius, ridge or flange on medial margin, near proximal end, for attachment of the M. biceps brachii and M. brachialis inferior

0) absent or very weakly developed

1) present, projecting beyond the medial margin of the main radial shaft

285. Radius, posterior margin of distal end

0) lacks condylar-like processes and fossa

1) forms two low rounded processes (posteromedial and posterolateral), with a shallow fossa between them

286. Snout, shape in dorsal view, Premaxillary-Maxillary Index (PMI)

0) 60% or less

1) >60% to 75%

2) greater than 75%

287. Premaxilla, shape of ascending process in lateral view

0) convex

1) concave, with a large dorsal projection

2) sub-rectilinear and directed posterodorsally

288. Maxilla, anterior (dentigerous) portion of lateral surface excavated by dorsoventrally elongate, deep vascular groove

0) absent

1) present

289. Maxilla, foramen anterior to the preantorbital fenestra

0) absent

1) present

290. Maxilla, position of external opening of the preantorbital fenestra

0) lies below antorbital fenestra

1) lies anterior to antorbital fenestra, with the posterior margin of the preantorbital fenestra lying entirely anterior to the anterior margin of the antorbital fenestra

291. Maxilla, preantorbital fenestra development

0) weakly developed, shallow fossa (difficult to distinguish from posterior maxillary foramen)

1) deep, sharp-lipped fossa

292. Maxilla, posterior extent of dorsal (ascending) process

0) anterior to, or level with, posterior end of main body

1) extending posterior to posterior end of main body

293. Maxilla, ventral margin of jugal process

0) reduced in dorsoventral height, such that the ventral margin is strongly emarginated relative to the remainder of the ventral margin of the maxilla

1) continuous with ventral margin of remainder of maxilla, or very gently emarginated

294. Maxilla, contact with quadratojugal

0) absent or small (i.e. no more than a point contact)

1) extensive

295. Jugal, dorsal process

0) present

1) absent

296. Jugal, contact with ectopterygoid

- 0) present
- 1) absent

297. Frontal, anteroposterior length to transverse width ratio

- 0) 1.0 or greater
- 1) less than 1.0

298. Frontal, lateral margin

- 0) expands posteriorly, orbital margin concave in dorsal view
- 1) unexpanded posteriorly, orbital margin straight or convex in dorsal view

299. Frontal, contribution to margin of supratemporal fenestra

- 0) present
- 1) absent, frontal excluded from anterior margin of fenestra by a postorbital-parietal contact

300. Orbit, anterior-most point

- 0) anterior to the anterior extremity of lateral temporal fenestra
- 1) approximately level with or posterior to anterior extent of lateral temporal fenestra

301. Lateral temporal fenestra, shape in lateral view

- 0) taller than wide anteroposteriorly and subtriangular (anteroposteriorly broader ventral margin and narrower dorsal apex)
- 1) linear, slit-like, crescentic (longer anteroposteriorly than high dorsoventrally)

302. Postorbital, posterior (squamosal) process

- 0) present as a distinct process
- 1) absent

303. Parietal, relative height of suture with frontal

- 0) lies level with or above the dorsal surfaces of the frontals and parietals
- 1) lies below the dorsal surfaces of the parietals and frontals (i.e. in a deep transverse trough)

304. Parietal, elevation of anterior margin creates a step-like curving crest transversely, where the parietal meets the frontal

- 0) absent
- 1) present

305. Pterygoid, morphology

- 0) robust element
 - 1) plate-like, with its three processes coplanar
306. Pterygoid, sutural contact with ectopterygoid
- 0) anteroposteriorly elongate, along the medial or lateral surface
 - 1) anteroposteriorly short, restricted to the anterior tip of the pterygoid
307. Pterygoid, palatobasal contact for basipterygoid articulation with a convex, rocker-like articular surface
- 0) absent
 - 1) present
308. Supraoccipital, longitudinal groove along posterodorsal surface
- 0) absent
 - 1) present (i.e. sagittal crest divided into two subparallel parasagittal crests with central groove)
309. Supraoccipital-exoccipital-opisthotic, paired facets for articulation with the proatlas
- 0) absent
 - 1) present
310. Parasphenoid rostrum, cross-sectional shape
- 0) triangular
 - 1) transversely thin, sheet-like
311. Basipterygoid processes, shape
- 0) widely diverging at 30° or more
 - 1) narrowly diverging at less than 30°
312. Basipterygoid processes, orientation in lateral view
- 0) directed 80° or more to skull roof (normally perpendicular)
 - 1) angled less than 80° to skull roof (anteroventrally directed)
313. Basioccipital, orientation of occipital condyle relative to the horizontal plane (in lateral view with supraoccipital held in a vertical plane)
- 0) 60° or less
 - 1) greater than 60°
314. Basal tubera, angle of divergence in posterior view
- 0) less than 50°
 - 1) more than or equal to 50°

315. Basisphenoid, relative position of the external opening for cranial nerve VI

- 0) lies ventral, and generally close, to the opening for cranial nerve III
- 1) lies anteroventral to, and more distant from, the opening for cranial nerve III

316. Basisphenoid, opening for cranial nerve VI

- 0) penetrates the pituitary fossa
- 1) does not penetrate the pituitary fossa

317. Basisoccipital+exoccipital-opisthotic, number of exits for cranial nerve XII

- 0) 2

318. Basisphenoid, position of the external foramen of the internal carotid artery

- 0) lateral to basipterygoid process
- 1) medial to basipterygoid process

319. Dentary, angle between the long-axis of the anterior margin (mandibular symphysis) and the long-axis of the main body of the dentary, in lateral view

- 0) greater than 90°, with the dorsal margin of the dentary extending further anteriorly than the ventral margin
- 1) approximately 90°, with the dorsal and ventral margins extending an equal distance anteriorly

320. Tooth crowns, longitudinal groove paralleling mesial and distal margins on the labial surface

- 0) labial grooves present
- 1) absent

321. Atlantal intercentrum, ventral margin of posterior surface

- 0) straight or convex
- 1) concave, forming ventrolateral projections

322. Axis, aEI (average elongation index: anteroposterior length of centrum (excluding articular ball if present) divided by mean average value of the mediolateral width and dorsoventral height of posterior articular surface of centrum)

- 0) 2.0 or greater
- 1) less than 2.0

323. Postaxial cervical centra, pneumatization of lateral surface

- 0) lateral pneumatic opening occupies approximately anterior two-thirds of centrum or more
- 1) reduced and restricted to less than the anterior two-thirds of the centrum

324. Postaxial cervical centra, midline notch on the dorsal margin of the posterior articular surface

0) absent

1) present

325. Postaxial anterior cervical vertebrae, prezygapophyses

0) extend anterior to the anterior tip of the condyle

1) terminate level with or posterior to the anterior tip of the condyle

326. Postaxial anterior cervical neural spines, orientation of posterior margin in lateral view

0) dorsal (vertical) or anterodorsal

1) posterodorsal

327. Middle cervical neural spines, height to arch height ratio

0) 2.0 or lower

1) greater than 2.0

328. Posterior (usually just the posterior-most) cervical neural arches, postzygapophyses

0) terminate at or beyond the posterior edge of the centrum

1) terminate in front of the posterior edge of the centrum

329. Posterior cervical neural spines, horizontal, rugose ridge immediately below spine summit on lateral surface

0) absent, spinodiapophyseal fossa fades out gradually dorsally

1) present, serves as distinct dorsal edge of the spinodiapophyseal fossa

330. Posteriormost cervical and anteriormost dorsal neural spines, shape in anterior/posterior view

0) taper dorsally, or mediolateral width remains constant along length

1) expand dorsally, with a strongly convex dorsal margin (paddle-shaped)

331. Cervical ribs, dorsal surface of proximal portion of shaft

0) excavated, forming a longitudinal groove

1) unexcavated

332. Anterior dorsal centra, ventral keel on midline

0) absent

1) present

333. Middle posterior dorsal centra, ventral surface

0) flat or transversely convex

- 1) transversely concave, between ventrolateral ridges
334. Middle posterior dorsal centra, lateral pneumatic foramina divided by internal ridge/s
- 0) absent
- 1) present
335. Anterior dorsal neural arches, shape of anterior neural canal opening
- 0) height greater than or equal to width
- 1) height is less than width
336. Anterior middle dorsal neural arches, vertical midline ridge (median infrapostzygapophyseal lamina) extending from roof of neural canal to ventral midpoint of postzygapophyses/ intrapostzygapophyseal lamina (TPOL)
- 0) absent
- 1) present
337. Anterior middle dorsal neural arches, zygapophyseal articulation angle
- 0) between horizontal and less than 40° to the horizontal
- 1) strongly dorsomedially oriented (40° or more)
338. Middle posterior dorsal neural arches, neural canal in anterior view
- 0) entirely surrounded by the neural arch
- 1) enclosed in a deep fossa in the dorsal surface of the centrum (i.e. much of the canal is enclosed laterally by pedicels that are part of the centrum rather than the neural arch)
339. Middle posterior dorsal neural arches, position of parapophysis
- 0) posterior to the vertical plane defined by the anterior margin of the centrum (excluding any convex articular condyle)
- 1) level with, or anterior to, the vertical plane defined by the margin of the centrum (excluding any convex articular condyle)
340. Middle posterior dorsal neural arches, anterior centradiapophyseal lamina (ACDL)
- 0) absent
- 1) present
341. Posterior dorsal neural arches, zygapophyseal articulation angle relative to horizontal line
- 0) less than 30° , usually close to horizontal
- 1) steeply oriented, 30° or greater
342. Middle posterior dorsal neural spines (single, not bifid), SPRLs

0) remain separate or converge at about spine midheight (or above) to form a dorsally restricted median composite lamina (SPRF well-developed and occupies the ventral half of the anterior spine surface)

1) SPRLs, if present, are short and merge into the PRSL close to the base of the spine (the PRSL may extend between the bases of the SPRLs to the top of the TPRL)

343. Middle posterior dorsal neural spines, postspinal lamina

0) does not extend ventral to the neural spine

1) extends ventral to the neural spine, beyond the postzygapophyseal articular surfaces

344. Middle posterior dorsal neural spines, anterior spinodiapophyseal lamina (aSPDL)

0) absent

1) present

345. Middle posterior dorsal neural spines, SPDL bifurcates at its dorsal end to create a SPDL-F

0) absent

1) present

346. Sacrum, ratio of mediolateral width across sacral vertebrae and ribs (taken at midlength on the coossified sacrum) to average length of a sacral centrum

0) less than 4.0

1) 4.0 or higher

347. Sacral centra, ratio of mediolateral width of middle sacral centra to first and last sacral centra

0) approximately constant, ratio less than 1.3

1) 1.3 or greater

348. Sacral neural spines, all fused, forming a dorsal platform

0) absent

1) present

349. First caudal centrum, anterior articular face shape

0) flat or concave

1) convex

350. Anterior?middle caudal centra (excluding Cd1), comparison of anterior and posterior articular faces

0) anterior face more concave than posterior one, or these two faces are equally concave

1) posterior face more deeply concave than anterior face

351. Middle caudal centra with convex posterior articular surface, condyle dorsally displaced

0) absent

1) present

352. Anteriormost caudal neural arches, prezygapophyses curve downwards (droop) at their distal ends

0) absent

1) present

353. Anterior caudal neural spines, anterior expansion of lower portion of spinoprezygapophyseal lamina (SPRL)

0) absent

1) present

354. First caudal rib, subtriangular process projects posteriorly at approximately midlength

0) absent

1) present

355. Anteriormost caudal ribs, tubercle on dorsal surface at approximately midlength

0) absent

1) present

356. Anterior?middle chevrons, articular facet surface

0) flat or anteroposteriorly convex

1) divided into anterior and posterior facets by a furrow

357. Anterior middle chevrons, posteroventrally directed ridge or bulge on lateral surface of distal half of proximal ramus

0) absent

1) present

358. Scapula, ventrolateral margin of acromion, anteroposteriorly concave region posterior to glenoid, followed by a flattened area

0) absent

1) present

359. Scapular blade, ridge on medial surface, close to junction with acromial plate and near dorsal margin

0) absent

1) present

360. Scapular blade, orientation of blade long-axis with respect to coracoid articulation

0) more than 70° (usually approximately perpendicular)

1) 70° or less

361. Coracoid, glenoid

0) does not expand strongly laterally relative to the lateral surface of the coracoid

1) expands prominently laterally and curves dorsolaterally so that part of the glenoid articular surface can be seen in lateral view

362. Sternal plate, shape of posterior margin in dorsal/ventral view

0) convex

1) straight

363. Sternal plate, anteroposteriorly directed ridge on ventral surface, at the anterior end

0) absent

1) present

364. Humerus, proximal margin in anterior/posterior view

0) straight or convex

1) sinuous, as a result of a prominently developed process (attachment site for M. supracoracoideus) on the lateral margin of the proximal end

365. Humerus, proximal end

0) expands laterally relative to the shaft, giving the humerus an hourglass outline in anterior view

1) asymmetrical, with no expansion of lateral margin relative to shaft

366. Humerus, humeral head forms a prominent subcircular process on the posterior surface of the proximal end

0) absent

1) present

367. Humerus, prominent vertical ridge extends along the lateral margin of the posterior surface, from the proximolateral corner to approximately the level of the deltopectoral crest (this ridge defines the lateral margin of the lateral triceps fossa and causes this fossa to be much deeper than the medial one)

0) absent

1) present

368. Humerus, tuberosity for attachment of the M. coracobrachialis on the anterior surface of the proximal third

- 0) absent
- 1) present

369. Humerus, deltopectoral crest, mediolateral thickness of anterior attachment surface

- 0) approximately constant along length
- 1) distal half mediolaterally expanded relative to proximal half (often doubling in thickness)

370. Humerus, ratio of maximum mediolateral width of distal end to proximodistal length

- 0) 0.30 or greater
- 1) less than 0.30

371. Radius, beveling of distal end relative to long axis of shaft

- 0) restricted to lateral half
- 1) extends across the entire distal end

372. Ulna, angle between long axes of anteromedial and anterolateral processes in proximal end view

- 0) 80° or greater (usually approximately a right angle)
- 1) less than 80° (acute)

373. Metacarpals, longest metacarpal to radius proximodistal length ratio

- 0) less than 0.50
- 1) 0.50 or greater

374. Metacarpals, metacarpal II, ratio of minimum transverse width of shaft to metacarpal length

- 0) 0.2 or higher
- 1) less than 0.2

375. Metacarpals, metacarpal III

- 0) longest metacarpal
- 1) shorter than at least one other metacarpal

376. Metacarpals, metacarpal IV, distal end profile

- 0) subrectangular
- 1) possesses small pointed lateral and medial projections such that the dorsal margin is longer than the ventral margin, producing a dorsoventrally compressed hexagonal or trapezoidal outline

377. Metacarpals, metacarpal V, ratio of proximal end long axis diameter to that of metacarpal I

- 0) less than 1.0
- 1) 1.0 or greater

378. Metacarpals, metacarpal V, ratio of proximal end long axis diameter to that of metacarpal IV

- 0) equal or smaller
- 1) larger than that for metacarpal IV

379. Metacarpals, metacarpal V with a medially biased flange-like swelling along proximal half of ventral surface

- 0) absent
- 1) present

380. Ilium, ratio of dorsoventral height of iliac blade above pubic peduncle to anteroposterior length of ilium

- 0) less than 0.35
- 1) 0.35 or greater

381. Ilium, projected line (chord) connecting articular surfaces of ischiadic and pubic processes

- 0) passes ventral to ventral margin of postacetabular portion of ilium
- 1) passes through or dorsal to ventral edge of postacetabular portion of ilium

382. Ilium, orientation of the pubic peduncle with respect to the long axis of the ilium

- 0) anteriorly deflected
- 1) perpendicular

383. Ilium, protuberance on the lateral surface of the ischiadic articulation

- 0) absent
- 1) present

384. Pubis, proximodistally oriented ridge on lateral surface of blade, separated from the anterior margin of the pubis by a longitudinal groove

- 0) absent
- 1) present

385. Pubis, distal end transversely expanded along lateral surface relative to shaft

- 0) present
- 1) absent

386. Ischium, iliac articular surface, anteroposterior length to mediolateral width ratio

- 0) 1.0 or greater
- 1) less than 1.0

387. Ischium, ridge (for attachment of M. flexor tibialis internus III) on lateral surface of the lower part of the proximal plate/proximal portion of shaft, close to the posterior/dorsal margin of ischium

- 0) associated with parallel groove, posterior/dorsal to ridge
- 1) groove absent

388. Femur, femoral head, projection

- 0) directed medially
- 1) directed dorsomedially

389. Femur, ratio of mediolateral breadth of tibial condyle to breadth of fibular condyle

- 0) greater than 0.8
- 1) 0.8 or less

390. Femur, shape of distal condyles

- 0) articular surface restricted to distal portion of femur
- 1) expanded onto anterior portion of femoral shaft

391. Tibia to femur length ratio

- 0) less than 0.6
- 1) 0.6 or greater

392. Fibula, articular surface of lateral trochanter

- 0) not visible in anterior view
- 1) visible in anterior view

393. Fibula, distal end mediolateral width to anteroposterior width ratio

- 0) 0.8 or less
- 1) greater than 0.8

394. Fibula, distal end profile

- 0) elliptical or semicircular (with a straight medial margin)
- 1) subtriangular (with a rounded or sharper apex projecting laterally or anterolaterally where flattened anterolateral and posterolateral margins meet)

395. Metatarsals, metatarsal V, proximal end

- 0) dorsoventrally expanded relative to shaft, with a domed dorsal margin

1) not expanded relative to shaft

396. Metatarsals, metatarsal V, tubercle or ridge on ventral surface, at approximately midlength, equidistant from the medial and lateral margins

0) absent

1) present

397. Pedal digit I, proximal articular surface of ungual (phalanx I-2)

0) perpendicular to long axis of ungual

1) bevelled so that the proximal articular surface faces proximolaterally and thus lies at a distinct angle to the long axis of the ungual

398. Basioccipital, fossa on lateral surface, extending from base of occipital condyle to base of basal tubera

0) absent

1) present

399. Basicranium, cranial nerve opening II (opticforamen)

0) single opening

1) medially divided to form two foramina

400. Surangular, anterior foramen

0) absent

1) present

401. Splenial, position of anterior end relative to mandibular symphysis

0) posterir to symphysis

1) participates in symphysis

402. Teeth, D-shaped crown morphology in labial/lingual view

0) narrows mesiodistally along its apical third

1) narrows mesiodistally along its apical half, giving it a heart-shaped outline

403. Middle posterior cervical neural arches, vertical midline lamina (part of the interprezygapophyseal lamina [TPRL]) divides the centroprezygapophyseal fossa (CPRF) into two fossae

0) absent

1) present

404. Middle posterior cervical neural arches, vertical midline lamina (part of the interpostzygapophyseal lamina [TPOL]) divides the centropostzygapophyseal fossa (CPOF) into two fossae

0) absent

1) present

405. Middle cervical neural spines, lateral fossa at the base of the prezygapophyseal process bounded by SPRL, PRDL and PODL

0) absent

1) present

406. Middle and posterior cervical neural spines, lateral surface between PRDL, PODL, SPOL (i.e., the spinodiapophyseal fossa [SDF]), has 3 or more coels separated from each other by low ridges

0) absent

1) present

407. Cervical ribs, anterior projection extends beyond anterior margin of centrum (including condyle)

0) present

1) absent

408. Sacral ribs, Sv2 ribs

0) emanate solely from Sv2

1) emanate from Sv2, with a contribution from Sv1

409. Antermost caudal centra, ACDL

0) absent, or represented by no more than a faint ridge

1) present, well defined or sheet-like

410. Anterior middle caudal neural arches, spinopostzygapophyseal lamina (SPOL) shape: SPOL grades smoothly toward postzygapophyses

0) SPOL grades smoothly toward postzygapophyses

1) SPOL abruptly ends near the anterior margin of the postzygapophyseal facet, and postzygapophyses sharply set off from neural spine, often projecting as distinct processes

411. Anterior middle caudal neural arches, anteroposteriorly oriented ridge and fossa (shoulder) between prezygapophyses and postzygapophyses

0) absent

1) present

412. Radius, proximal to distal end anteroposterior length ratio

0) 0.5 or greater

1) less than 0.5

413. Manus, arc of a circle covered by the proximal ends of the metacarpals in articulation

- 0) $<180^\circ$
- 1) $>180^\circ$ (usually close to 270°), forming a tubular manus

414. Carpal bones, distal carpal mediolateral width to anteroposterior length ratio

- 0) less than 1.4
- 1) 1.4 or greater

415. Metacarpal III, maximum mediolateral width to dorsoventral height of the proximal end ratio

- 0) less than 1.3
- 1) 1.3 or greater

416. Tibia, tubercle (tuberculum fibularis) on posterior (internal) face of cnemial crest

- 0) absent
- 1) present

417. Posterior cervical neural arches, spinodiapophyseal fossa, at the base of lateral surface of neural spine

- 0) absent or shallow fossa
- 1) deep fossa

418. Posterior cervical neural spines, dorsal half laterally expanded as a result of expansion of the lateral lamina (spinodiapophyseal lamina)

- 0) absent
- 1) present

419. Anteriormost caudal neural spines, medial spinoprezygapophyseal laminae (mSPRLs) merge into the prespinal lamina (PRSL) close to the base of the spine

- 0) absent
- 1) present

420. Metacarpals, metacarpal V, dorsomedial margin of distal third forms a prominent ridge or flange

- 0) absent
- 1) present

421. Metatarsals, ratio of metatarsal III to metatarsal I proximodistal length

- 0) 1.3 or greater
- 1) less than 1.3

422. Metatarsals, ratio of metatarsal III to metatarsal IV proximodistal length

- 0) 1.0 or greater
- 1) less than 1.0

423. Pedal digit III, number of phalanges

- 0) three or more
- 1) two or fewer

424. Maxilla, preantorbital opening, size

- 0) small, subequal or only slightly larger than other neurovascular foramina on the lateral surface of the maxilla
- 1) large, a widely open fenestra that is dramatically larger than other neurovascular foramina

425. Maxilla, preantorbital opening, connectivity

- 0) lacking obvious communication to the antorbital cavity
- 1) with obvious communication with the antorbital cavity dorsal to the palatine shelf

426. Frontal, deep orbital rim

- 0) 0.8
- 1) present, ratio of transverse width of nasal+prefrontal suture to maximum transverse width of the dorsal surface of the frontal in dorsal view < 0.8

427. Frontoparietal, midline fenestra

- 0) absent
- 1) present

428. Endocranial surface of parietal, anterior dural impression separated from posterior dural impression by a transverse ridge (producing a transverse divot in an endocast)

- 0) absent, endocranial surface of parietal bears an uninterrupted fossa along the midline
- 1) present

429. Tooth crown, distinct lingual boss on distolingual surface

- 0) absent
- 1) present

430. Cervical vertebrae, number (where first dorsal is that which shows parapophyseal migration)

- 0) 13 or fewer
- 1) 14

- 2) 15
- 3) 16
- 4) 17
- 5) 18

431. Postaxial cervical centra, lateral surfaces

- 0) lack an excavation or have a shallow fossa without subdivision
- 1) shallow fossa in which a single (or occasionally more than one) oblique septum partially divides fossa
- 2) possess a deep foramen that is not divided into portions by accessory laminae
- 3) have a deep foramen that is divided into separate portions by one prominent and occasionally several smaller accessory laminae

432. Cervical vertebrae 2 and 3, centrum length

- 0) moderate length increase, $CV3 < 1.3 \times CV2$
- 1) length increases considerably, $CV3 1.3-1.55 \times CV2$
- 2) significant length increase, $CV3 1.55 \times CV2$ or greater

433. Posterior middle and posterior cervical vertebrae, morphology of the centroprezygapophyseal lamina (CPRL)

- 0) single
- 1) dorsally divided, with a laterally positioned bifurcation comprising a vertical medial arm that undergirds medial aspect of prezygapophysis and a lateral arm that meets PRDL
- 2) dorsally divided, resulting in a lateral and medial lamina, with the medial lamina (mdCPRL) linked with the intraprezygapophyseal lamina (TRPL) and not with the prezygapophysis
- 3) divided, resulting in the presence of a true divided centroprezygapophyseal lamina, which is dorsally connected to the prezygapophysis

434. Middle and posterior cervical vertebrae, form of PRDL in lateral view

- 0) sublinear or weakly concave
- 1) convex or with distinct bulging interruption

435. Middle and posterior cervical vertebrae, rugose muscle scar extends anteriorly from epipophysis to invade the posterior margin of the spinodiapophyseal fossa (SDF), producing a scalloped posterodorsal margin of the fossa

- 0) absent
- 1) present

436. Middle to posterior cervical neural arches, a raised ridge of rugose striations extends posteriorly from the preepiphysis to a point nearly subequal with or posterior to the anterior margin of the spinodiapophyseal fossa (SDF)

0) absent

1) present

437. Cervicodorsal vertebrae, ventrally bifurcated postzygodiapophyseal lamina (PODL)

0) absent

1) present

438. Number of dorsal vertebrae (where first dorsal is that which shows parapophyseal migration)

0) 14 or more

1) 13

2) 12

3) 11

4) 10

439. Middle and posterior dorsal centra, form of lateral fossa surrounding lateral pneumatic foramen

0) strongly asymmetric, such that the lateral pneumatic foramen is emplaced near the ventral margin of a dorsally expansive fossa

1) more nearly symmetrical position of pneumatic foramen

440. Middle and posterior dorsal vertebrae neural spine, anterior margin is level with or posterior to the posterior margin of the neural arch

0) absent

1) present in at least some vertebrae

441. Astragalus, fibular facet

0) faces laterally

1) faces posterolaterally, anterior margin visible in posterior view

442. Middle posterior cervical and anteriormost dorsal neural arches, prezygapophyseal articular surfaces

0) flat or gently concave

1) strongly convex mediolaterally

443. Manual phalanx I-2 (ungual), proximal articular surface

0) approximately perpendicular to the long axis of the ungual

- 1) bevelled so that it faces proximolaterally
444. Manual digit IV, number of phalanges
- 0) two or more
- 1) one or fewer
445. Pterygoid, transverse process
- 0) arcuate, with a gently hooked distal end
- 1) straight and rod-like
446. Surangular, relative size of anterior surangular foramen
- 0) maximum diameter of the anterior surangular foramen is subequal to or not substantially larger than that of the posterior surangular foramen
- 1) maximum diameter of the anterior surangular foramen is at least twice as large as that of the posterior surangular foramen
447. Axis, anteriorly directed prong at the anteroventral end of the spinoprezygapophyseal lamina (SPRL)
- 0) absent
- 1) present
448. Cervical ribs, anterior process
- 0) single
- 1) bifurcate
449. Femur, position of fourth trochanter
- 0) On or near the midline
- 1) Medial margin, but not visible in anterior view
- 2) Medial margin, and visible in anterior view

Appendix 2. Bone measurements

พหุ ประถมศึกษา

Appendix table 1. Measurements of the cervical vertebrae of PRC & SM Mamenchisauridae (mm)

| Pos | No. | Centrum | | | | | | | Neural arch & Spine | | | | Total | | |
|---------------|-----------|---------|-------|-------|-------|------|-------|-------|---------------------|-------|-------|-------|-------|-------|------|
| | | FL | CL | ACH | ACW | MLW | PCH | PCW | NAH | NAW | NSH | NSL | NSW | H | EI |
| Ant - Mid. CV | PN17-47 | 10.47 | 12.86 | 2.64 | 4.11 | 3.2 | 4.16 | 5.39 | - | - | - | - | - | 4.16 | 2.52 |
| Mid. CV | PN 14-131 | 27.16 | 33.9 | 9.9 | 10.21 | 7.47 | 10.21 | 11.47 | - | - | - | - | - | 10.21 | 2.66 |
| Mid. CV | PN 14-98 | 32.61 | 37.61 | 8.74 | 8.95 | 9.26 | 12 | 14.63 | - | - | - | - | - | 12 | 2.72 |
| Mid. CV | - | - | - | - | - | - | - | - | 10.53 | - | 5.68 | 13.37 | - | 5.68 | - |
| Mid. CV | - | 26.84 | 31.76 | 10.74 | - | - | 12.84 | - | - | - | - | - | - | 12.84 | 2.09 |
| Mid. CV | PN602 | 15.52 | 23.2 | - | 13.86 | 9.64 | - | 11.83 | 3.83 | 14.63 | 3.83 | - | 6.52 | 12.98 | - |
| Mid. CV | KS34-3806 | 38.46 | 42.89 | 7.28 | - | - | 9.88 | - | 9.38 | - | 11.3 | 14.38 | - | 30.37 | 3.89 |
| Pos. CV | PN 15-123 | 22.26 | 25.49 | 9.36 | - | - | 10.74 | - | 19.56 | - | 10.93 | 11.28 | - | 41.08 | 2.07 |
| Pos. CV | - | - | - | - | - | - | - | - | 13.71 | - | 7.52 | 5.77 | - | 20.49 | - |
| Pos. CV | PN 17-X | - | - | - | - | - | - | - | 24.95 | - | 12.26 | 11.4 | - | 44.73 | - |
| Pos. CV | PN 138 | 36.78 | 30.48 | 12.1 | - | - | 14.67 | - | 11.94 | - | 10.88 | 10.16 | - | 34.84 | 2.51 |
| Pos. CV | PN 139 | 27.91 | 33.15 | 12.42 | - | - | 14.84 | - | 13.88 | - | 12.75 | 7.67 | - | 40.96 | 1.88 |

Abbreviations: ACH, anterior centrum height; ACW, anterior centrum width; CL, centrum length; EL, elongation index; FL, functional length (length of centrum excluding condyle); H, height; MLW, centrum middle least width; NAH, neural arch height; NAW, neural arch width; NSH, neural spine height; NSL, neural spine anteroposterior length; NSW, neural spine width; PCH, Posterior centrum height; PCW, Posterior centrum width.

Appendix table 2. Measurements of the cervical ribs of PRC Mamenchisauridae (cm)

| No. | Pos. of Rib | L | AL | PL | CW | H | TuL |
|-------------|--------------------|-------|------|-------|----|-------|------|
| KS34-1970 | Middle | 45.4 | 10.6 | 22.6 | - | 15.2 | 11.8 |
| KS34-2746 | Middle | 43.3 | 11.7 | 25.4 | - | 22.2 | 6 |
| PN15-74 | Middle | 41.2 | 8.9 | 24.3 | - | 13.4 | 8 |
| J No number | Middle | 31.51 | 5.95 | 20.2 | - | 17.53 | 8.77 |
| K PN14-115 | Middle | 44.8 | 10.7 | 23.6 | - | 18.1 | 9 |
| L PN15-200 | Middle | 45.25 | - | 32.79 | - | 14.81 | 8.73 |
| M PN18-26 | Anterior to middle | 18.2 | 4.9 | 3.8 | - | 10 | 5.4 |
| O PN9-49 | Anterior to middle | 14.2 | 4.8 | 3.8 | - | 9.2 | 5.4 |

Abbreviations: AL, anterior process length; CW, transverse width from capitulum to lateral surface of the rib; L, anteroposterior length; PL, posterior process length; H, dorsoventral height; TuL, anteroposterior length of tuberculum.

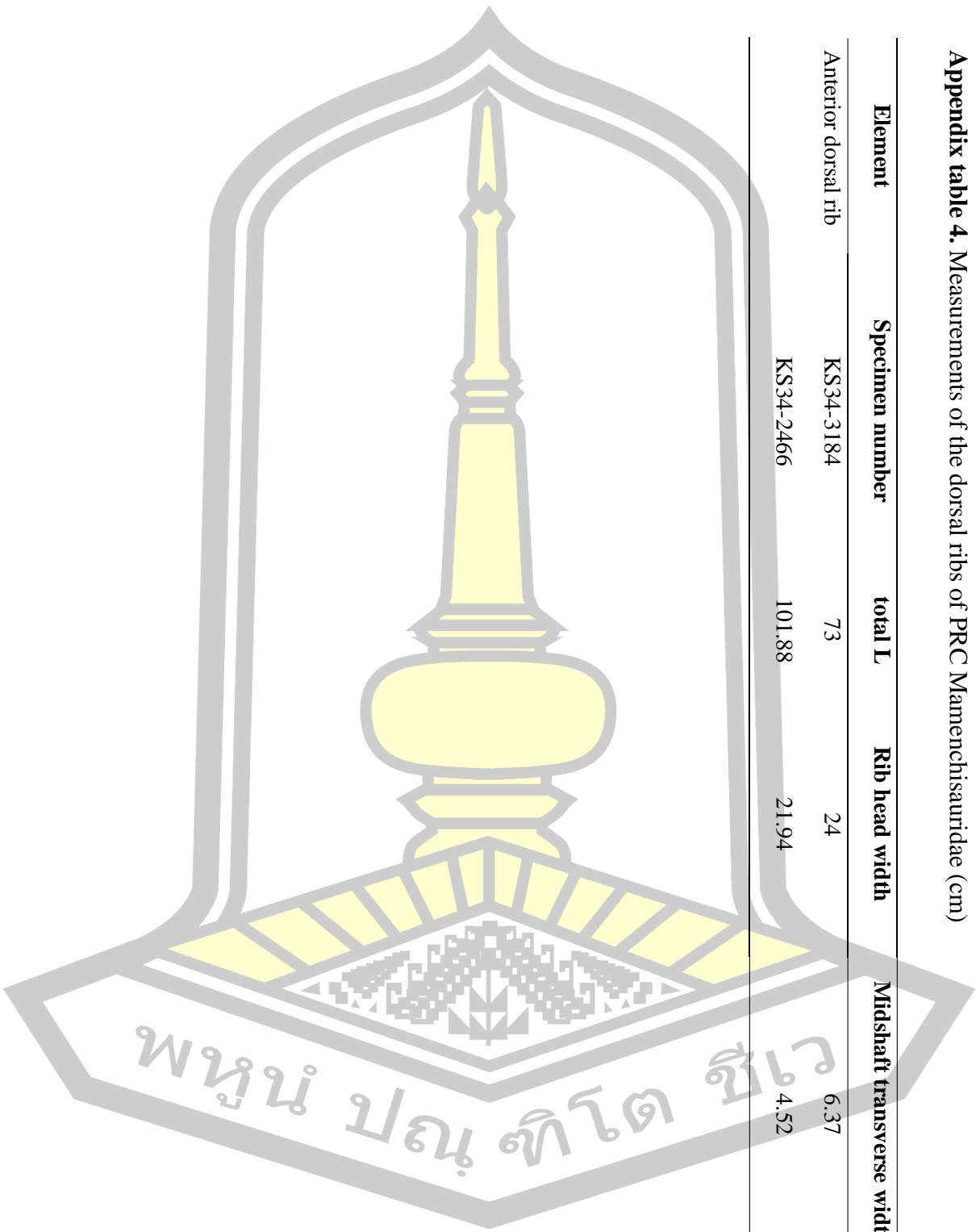
Appendix table 3. Measurements of the dorsal vertebrae of PRC Mamenchisauridae (cm)

| Centrum | | | | | | | | | | Neural arch & Spine | | | | | Total |
|---------------|-----------|-------|-------|-------|-------|-------|-------|-------|-------|---------------------|-------|-------|-------|------|-------|
| Pos | No. | FL | CL | ACH | ACW | PCH | PCW | NAH | NAW | NSH | NSL | NSW | H | El | |
| Ant. DV | PN15-16 | - | - | - | - | - | - | 19.17 | 46.09 | 11.28 | - | 27.9 | 28.61 | - | |
| Ant. DV | PN581 | - | - | 18.23 | 23.16 | 16.62 | 21.89 | 18.35 | 69.87 | 17.14 | - | 32.03 | 54.89 | - | |
| Ant. DV | PN582 | - | - | - | - | - | - | 26.02 | 47.07 | 17.74 | - | 22.56 | 42.33 | - | |
| Mid. DV | PN692 | - | - | 23.91 | 22.34 | 23.58 | 23.58 | 25.01 | 45.82 | 22.82 | - | 20.81 | 62.91 | - | |
| Mid. DV | PN15-49 | - | - | - | - | - | - | 25.7 | 44.42 | 19.38 | - | 21.21 | 41.43 | - | |
| Pos. DV | PN17-147 | - | - | 21.67 | 20.33 | 22.91 | 20.05 | 23.25 | 37.71 | 23.48 | - | 18.52 | 63.39 | - | |
| Pos. DV | PN13-23 | 24.61 | 34.9 | 26.86 | 15.1 | 27.65 | 15.69 | 33.53 | 34.12 | 24.71 | 12.39 | 15.5 | 83.33 | 0.89 | |
| Pos. DV (Art) | No number | 21.33 | 33.65 | 23.05 | - | 20.95 | - | 35.33 | - | 29.24 | 16.73 | - | 87.43 | 1.02 | |
| Pos. DV (Art) | No number | 15.62 | - | - | - | 25.65 | - | 37.57 | - | 30.1 | 13.48 | - | 90 | 0.61 | |

Abbreviations: ACH, anterior centrum height; ACW, anterior centrum width; CL, centrum length; El, elongation index; FL, functional length (length of centrum excluding condyle); H, height; NAH, neural arch height; NAW, neural arch width; NSH, neural spine height; NSL, neural spine anteroposterior length; NSW, neural spine width; PCH, Posterior centrum height; PCW, Posterior centrum width.

Appendix table 4. Measurements of the dorsal ribs of PRC Mamenchisauridae (cm)

| Element | Specimen number | total L | Rib head width | Midshaft transverse width |
|---------------------|-----------------|---------|----------------|---------------------------|
| Anterior dorsal rib | KS34-3184 | 73 | 24 | 6.37 |
| | KS34-2466 | 101.88 | 21.94 | 4.52 |



Appendix table 5. Measurements of caudal vertebrae of PRC Mamenchisauridae (mm)

| No. | Centrum | | | Neural arch & Spine | | | Total |
|-----------|---------|--------|--------|---------------------|--------|--------|--------|
| | FL | ACH | PCH | NAH | NSH | NSW | |
| PN14-146 | 108.00 | 252.52 | 211.49 | 360.00 | 278.52 | 118.21 | 612.52 |
| PN14-212A | 53.70 | 215.93 | 235.77 | 344.00 | 215.38 | 61.90 | 555.00 |
| PN14-212B | 200.37 | 197.58 | 183.89 | 262.60 | 196.08 | 28.22 | 467.00 |
| PN14-212C | 127.68 | 214.44 | - | 253.32 | 210.00 | 21.69 | 475.00 |
| PN14-212D | 109.93 | - | 161.93 | 226.37 | 186.00 | 18.95 | 465.00 |
| PN14-212E | 147.01 | 178.15 | 144.04 | 288.00 | 213.28 | 28.00 | 423.00 |
| PN14-212F | 135.86 | 161.68 | 109.95 | 295.00 | 215.90 | 27.07 | 430.00 |

Abbreviations: ACH, anterior centrum height; FL, functional length (length of centrum excluding condyle); H, height; NAH, neural arch height; NSH, neural spine height; NSW, neural spine width.

Appendix table 6. Measurements of the chevrons of PRC Mamenchisauridae (cm)

| Specimen No. | PDH | PW | HCH | HCW | DH | DW |
|--------------|------|------|-----|-----|------|-----|
| A PN15-186 | 19.6 | 6.9 | 4 | 2.9 | 13.1 | 1.5 |
| B PN14-24 | 20.9 | 6.5 | 5.1 | 1.2 | 13.6 | 1.8 |
| C PN15-151 | 21.2 | 8.2 | 6.3 | 2.1 | 11.8 | 2.6 |
| D PN13-11 | 27.7 | 6 | 2.4 | 1.7 | 21 | 0.9 |
| E KS34-631 | 28.6 | 5 | 4 | 1.5 | 20 | 1.4 |
| F KS34-1004 | 25.3 | 10.6 | 3.9 | 3.5 | 18.3 | 1.3 |
| G PN638 | 28.4 | 9.5 | 4.4 | 2.3 | 19.9 | 2.3 |

Abbreviations: PDH = proximodistal height along the midline, PW = proximal transverse width, PL = proximal anteroposterior length, HCH = haemal canal height, HCW = haemal canal width, DH = distal blade height, DL = distal blade anteroposterior length, DW = distal blade transverse width.

Appendix table 7. Measurements of the middle and posterior chevrons of PRC Mamenchisauridae (cm)

| Specimen No. | PDH | PW | HCH | HCW | ant. DH | ant. DL | ant. DW | pos. DH | pos. DL | pos. DW |
|--------------|-------|------|------------|------|---------|---------|---------|---------|---------|---------|
| KS34-2240 | 18.79 | 9.91 | 5.48 | 3.18 | 10.17 | 3.64 | 0.83 | 9.95 | 2.31 | 1.3 |
| KS34-2797 | 14.19 | 3.68 | 2.33 | 0.58 | 8.29 | 2.31 | 0.43 | 7.34 | 2.21 | 1.13 |
| KS34-1166 | 7.58 | - | HCL = 5.74 | 1.49 | - | 2.15 | - | - | 2.97 | - |
| KS34-2244 | 4.9 | 7.21 | HCL = 9.87 | 1.81 | - | 7.16 | 2.76 | - | 6 | 2.89 |
| KS34-2311 | 6.26 | 3.32 | HCL = - | 0.34 | - | 5.1 | 2.58 | - | 5.99 | 2.33 |

Abbreviations: PDH = proximodistal height along the midline, PW = proximal transverse width, PL = proximal anteroposterior length, HCH = haemal canal height, HCL = haemal canal length, HCW = haemal canal width, DH = distal blade height, DL = distal blade anteroposterior length, DW = distal blade transverse width

Appendix table 8. Measurements of the pectoral girdle of PRC Mamenchisauridae (cm) following Mannion et al., 2017; Moore et al., 2020

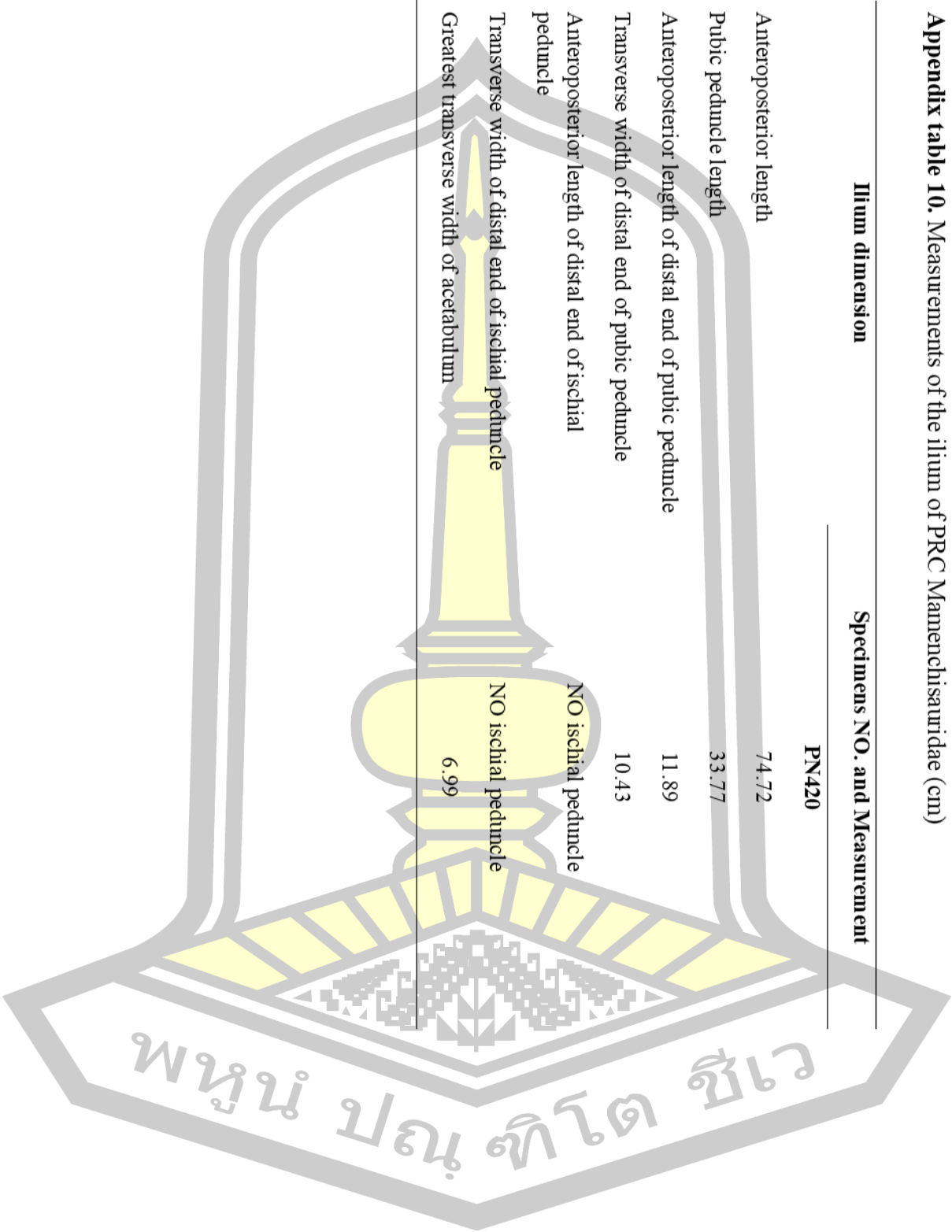
| Scapula dimension | Specimens NO. and Measurement | | | | | |
|---|-------------------------------|----------------|----------------|----------------|---------|-------|
| | PN65 | SM no number 1 | SM no number 2 | SM no number 3 | PN15-36 | PN781 |
| Minimum breadth of blade proximally | 32.18 | 28.98 | 22.89 | 23.1 | 20.43 | 18.74 |
| Acromion dorsoventral height, perpendicular to the blade, measured between horizontal lines extending through dorsal and ventralmost points of acromion | 91.4 | 72.61 | 76.27 | 60.65 | 65.71 | 61.36 |
| Angle of blade with respect to coracoid articulation | 90.55 | 77.52 | - | 87.08 | 78.05 | 87.02 |
| Anteroposterior length of scapular blade, from posterior margin of distal end to anterodorsal corner, where it meets the coracoid | 117.99 | 104.53 | 119.96 | 80.13 | 89.92 | 82.89 |
| Length of glenoid | - | 21.89 | - | - | 19.77 | 14.39 |
| Maximum width of glenoid | - | - | - | - | - | - |

Appendix table 9. Measurements of the humerus of PRC Mamenchisauridae (cm)

| Humerus dimension | Specimens NO. and Measurement (cm) | | | | | |
|--|------------------------------------|-----------|-----------|---------|----------|----------|
| | No NO (L) | No NO (R) | No NO (L) | PN13-15 | PN17-104 | PN17-142 |
| 1) Proximodistal length | 115.7 | 114.2 | 94.2 | 114.1 | 98.2 | 68.7 |
| 2) Transverse width of proximal end | 44.8 | 39.9 | 36 | 44.6 | 33.9 | 27.1 |
| Anteroposterior width across humeral head | - | - | - | - | - | - |
| 3) Midshaft transverse width | 18.8 | 14 | 16.1 | 19 | 16 | 11.8 |
| Midshaft anteroposterior width | - | - | - | - | - | - |
| 4) Transverse width of distal end | 38.1 | 27.3 | 31.4 | 39.3 | 35.5 | 17.8 |
| 5) Distance from proximal end to most prominent point of deltopectoral crest | - | - | - | 48.9 | 36.6 | 27 |

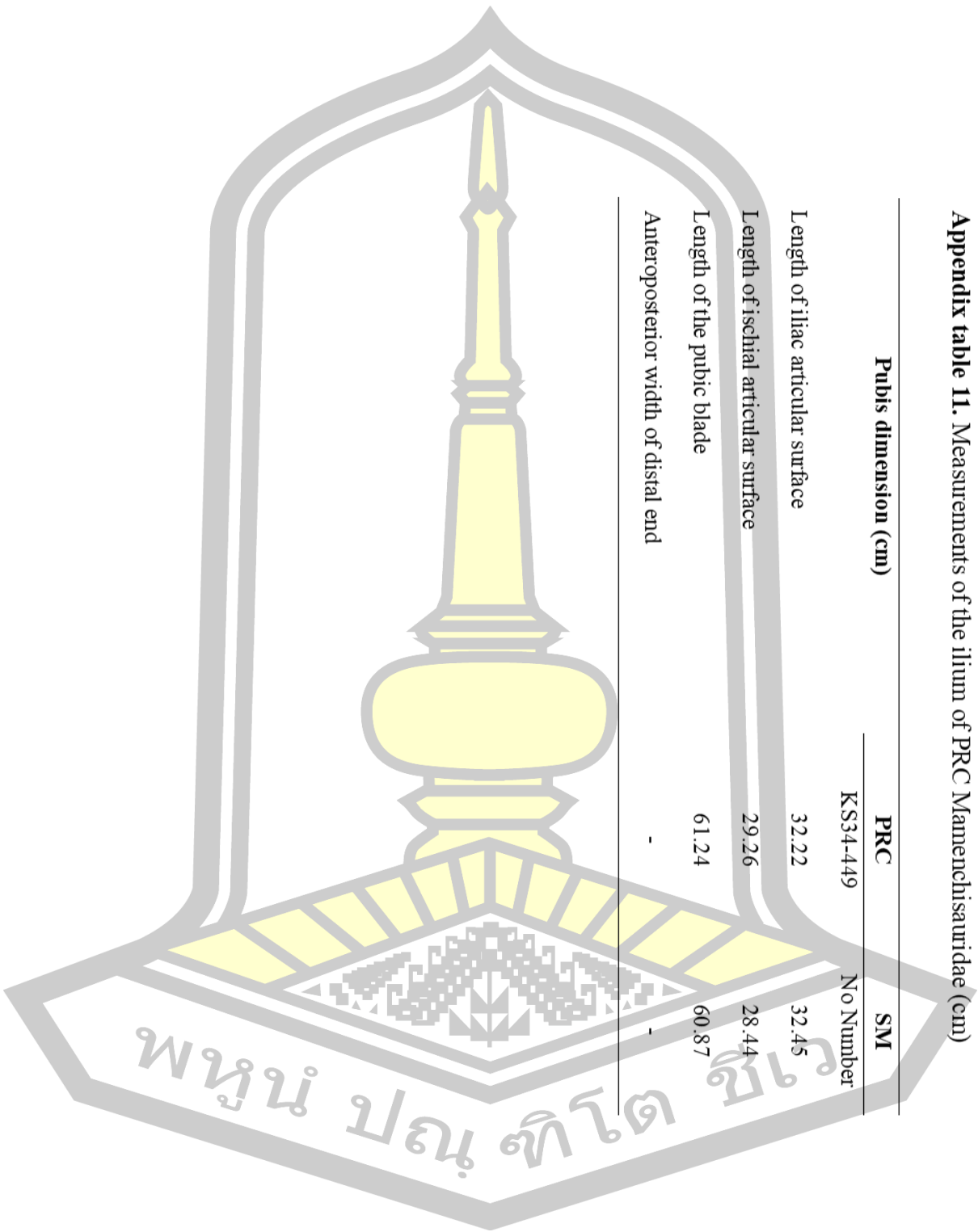
Appendix table 10. Measurements of the ilium of PRC Mamenchisauridae (cm)

| Ilium dimension | Specimens NO. and Measurement |
|--|-------------------------------|
| | PN420 |
| Anteroposterior length | 74.72 |
| Pubic peduncle length | 33.77 |
| Anteroposterior length of distal end of pubic peduncle | 11.89 |
| Transverse width of distal end of pubic peduncle | 10.43 |
| Anteroposterior length of distal end of ischial peduncle | NO ischial peduncle |
| Transverse width of distal end of ischial peduncle | NO ischial peduncle |
| Greatest transverse width of acetabulum | 6.99 |



Appendix table 11. Measurements of the ilium of PRC Mamenchisauridae (cm)

| Pubis dimension (cm) | PRC | SM |
|-------------------------------------|----------|-----------|
| | KS34-449 | No Number |
| Length of iliac articular surface | 32.22 | 32.45 |
| Length of ischial articular surface | 29.26 | 28.44 |
| Length of the pubic blade | 61.24 | 60.87 |
| Anteroposterior width of distal end | - | - |



BIOGRAPHY

| | |
|--------------------------|--|
| NAME | Apirut Nilpanapan |
| DATE OF BIRTH | 05/12/1990 |
| PLACE OF BIRTH | Bang Rak, Bangkok, Thailand |
| ADDRESS | 143/228 Soi Santinakhon, Theparak road, Bangpla sub-district, Bangphli district, Samut prakan province, Zip code 10540. |
| EDUCATION | 2012 Bachelor's Degree - Department of Biology, Faculty of Science, Silpakorn University 2016 Master's Degree - Department of Marine Science, Faculty of Science, Chulalongkorn University 2024 Doctoral's Degree - Department of Biology, Faculty of Science, Mahasarakham University |
| Research grants & awards | Development and Promotion of Science and Technology Talents Project (Royal Government of Thailand scholarship). |

